Title

Determining 4D Nuclear Architecture Dynamics of Ligand-Dependent Transcription Activation Using Live Imaging Techniques

Author

Wang, Susan

Publication Date

2021

Peer reviewed|Thesis/dissertation

UNIVERSITY OF CALIFORNIA SAN DIEGO

Determining 4D Nuclear Architecture Dynamics of Ligand-Dependent Transcription Activation Using Live Imaging Techniques

A dissertation submitted in partial satisfaction of the requirements for the degree

Doctor of Philosophy

in

Biomedical Sciences

by

Susan Shubai Wang

Committee in charge:

Professor Michael Geoff Rosenfeld, Chair
Professor Christopher Glass
Professor Cornelis Murre
Professor Elizabeth Villa
Professor Jin Zhang

2021

The dissertation of Susan Shubai Wang is approved, and it is acceptable in quality and form for publication on microfilm and electronically.

University of California San Diego

2021

TABLE OF CONTENTS

LIST OF FIGURES

ACKNOWLEDGEMENTS

I would like to thank my advisor Michael Geoff Rosenfeld for his extensive mentorship in scientific research and communication. I would like to thank my committee members for their advice and support. Furthermore, I would like to thank all my past and present colleagues in the Rosenfeld Lab. In particular, I would like to thank Thomas Suter for his close collaboration and dedicated efforts to make single cell live imaging techniques possible. Lastly, I would like to thank my family and friends for their never-ending support throughout my graduate career.

Chapter 2, in full, has been submitted for publication in *Nature Reviews Molecular Cell Biology*, 2021, and is currently under peer review. “Enhancers in space and time: cell biological and biophysical strategies of transcriptional regulation.” Sree Nair, Thomas Suter, Susan Wang, Lu Yang, Feng Yang, and Michael Rosenfeld. The dissertation author is a coauthor of this paper.

Chapter 3 is currently being prepared for submission, with the assistance of Thomas Suter and Michael Rosenfeld. The dissertation author is a coauthor of this paper.

Chapter 4, in full, has been published in *Nature Structural and Molecular Biology*, 2019. “Phase separation of ligand-activated enhancers licenses cooperative chromosomal enhancer assembly.” Sree Nair, Lu Yang, Dario Meluzzi, Soohwan Oh, Feng Yang, Meyer Friedman, Susan Wang, Thomas Suter, Ibraheem Alshareedah, Amir Gamliel, Qi Ma, Jie Zhang, Yiren Hu, Yuliang Tan, Kenneth Ohgi, Ranveer Singh Jayani, Priya Banerjee, Aneel Aggarwal, and Michael Rosenfeld. The dissertation author is a coauthor of this paper.

VITA

2013 Bachelor of Arts, University of California Berkeley

2013-2014 Research Technician, University of California San Francisco

2021 Doctor of Philosophy, University of California San Diego

PUBLICATIONS

Nair S, Suter T, **Wang S**, Yang L, Yang F, Rosenfeld M. Enhancers in space and time: cell biological and biophysical strategies of transcriptional regulation. Nature Reviews Molecular Cell Biology. 2021 (In Peer Review)

Nair S, Yang L, Meluzzi D, Oh S, Yang F, Friedman M, **Wang S**, Suter T, Alshareedah I, Gamliel A, Ma Q, Zhang J, Hu Y, Tan Y, Ohgi K, Singh Jayani R, Banerjeey P, Aggarwal A, Rosenfeld M. Phase separation of ligand-activated enhancers licenses cooperative chromosomal enhancer assembly. Nature Structural and Molecular Biology. 2019 Mar 4;26(3):193-203.

Lau J, Ilkhanizadeh S, **Wang S**, Miroshnikova YA, Salvatierra NA, Wong RA, Schmidt C, Weaver VM, Weiss WA, Persson AI. STAT3 blockade inhibits radiation-induced malignant progression in glioma. Cancer Research. 2015 Oct 15;75(20):4302-11.

Ilkanizadeh S, Lau J, Huang M, Foster DJ, Wong R, Frantz A, **Wang S**, Weiss WA, Persson AI. Glial progenitors as targets for transformation in glioma. Advances in Cancer Research. 2014;121:1-65.

ABSTRACT OF THE DISSERTATION

Determining 4D Nuclear Architecture Dynamics of Ligand-Dependent Transcription Activation Using Live Imaging Techniques

by

Susan Shubai Wang

Doctor of Philosophy in Biomedical Sciences

University of California San Diego, 2021

Professor Michael Geoff Rosenfeld, Chair

This dissertation discusses the 4D chromosomal dynamics relative to subnuclear organelles and transcription hubs during transcription activation, in an estrogen-dependent system. The phenomenon of transcriptional bursting has been observed across numerous model organisms, where gene transcription does not occur continuously over time but rather in periods of high levels followed by periods of inactivity. I aim to explore such phenomenon in our estrogen inducible model and attempt to decipher the spatial and temporal dynamics associated with transcription

burst by using RNA and DNA live cell imaging techniques. In the first chapter, I introduce the concept of burst transcription and relevant literature associated with bursting and transcription regulation. In the second chapter, I have included a review I co-authored on enhancers and its biological and biophysical properties that impact transcription regulation. Chapter 3 is where I present the core of my graduate research work involving live cell visualization techniques. Lastly, Chapter 4 is another paper I assisted on, where we examined how acute E_2 enhancer activation results in eRNA-mediated phase-separated condensates that allow for cooperative activation of the most robust ERα enhancers.

Chapter 1: Introduction to burst transcription and regulation

1.1 Bursting model

Gene transcription does not occur at continuous and even levels over time, but rather in acute periods of high levels of transcription followed by periods of inactivity, in a process called burst transcription. The phenomenon of transcriptional bursting has been observed across the full spectrum of model organisms, including prokaryotes, yeast, drosophila, c. elegans, mice and humans (Suter et al., 2011), and thus appears to be the fundamental mechanism through which transcription occurs. Bursting has thus been shown to facilitate dynamic transcriptional responses to various stimuli, inducing precisely regulated responses to developmental or environmental signals (Berrocal et al., 2020; Bothma et al., 2014; Falo-Sanjuan et al., 2019; Lee et al., 2019). Furthermore, cellular transcriptional heterogeneity, which is promoted by bursting due to the stochastic nature of bursts between cells, has been shown to be key in several developmental processes that include the development of drosophila photoreceptors (Wernet et al., 2006), zebrafish retinal neurons (Boije et al., 2015), and lineage segregation in mouse embryonic stem cells (Simon et al., 2018). Importantly, the bursting model of transcription implies a distinct set of regulatory components when compared with the outdated model of continuous transcription, and recent evidence has shown that transcriptional bursting is regulated through precise spatiotemporal coordination of genes, enhancers, and nuclear-body-forming coactivators.

While burst transcription refers to the rather simple concept of an acute period of transcription followed by a period of inactivity, the modeling and characterization of

bursting have explored multiple properties. At a simpler level, bursts be characterized by a burst frequency, or the rate at which a burst is initiated; and burst size, or the amount of transcript produced by each burst. Burst size can be further broken down into burst duration, or the time period in which the transcript is bursting; and burst amplitude, or the amount of transcript produced at any one point of the burst. Burst frequency can additionally be characterized by monitoring the duration of the off period, which can be used to determine the K_{ON}, or the frequency at which an inactive locus can transition to an active state. These properties have in turn been used to extrapolate components of transcription that include rates of transcription initiation, polymerase loading, and elongation.

1.2 Methods of burst detection

Data on bursting using methods that include single-cell RNA-seq (scRNA), single-molecule RNA FISH (smFISH), destabilized reporters, or MS2/PP7-fluorescent tagging of nascent transcripts.

Destabilized reporter systems involve the fusion of a protein reporter, typically a luciferase or fluorescent protein, to a single bursting gene of interest in either an endogenous, randomly integrated, or extrachromosomal context. Upon transcriptional bursting, the reporter will be transcribed, translated, and will then provide a read-out of burst activity. Importantly, this reporter peptide has destabilizing sequences or mutations that will reduce the half-life of the reporter to produce a more direct read-out of the transcriptional burst. Destabilized reporters typically continue to produce signal up to several hours after transcriptional bursting, which makes them poorly suited to determine the precise kinetics of most studied active bursting

genes, whose burst frequency of less than 1 hour would be obscured by the long half-life of the reporter. Furthermore, unlike smFISH and MS2/PP7-reporter methods, destabilized reporters do not provide spatial information regarding the burst, making destabilized reporters poorly suited for associating transcriptional bursting with other nuclear elements. Regardless, destabilized reporters do provide a relatively easy to generate and clear readout of bursting in low burst frequency genes, which can be useful when testing a large number of genes and conditions, or screening for burst related phenotypes.

smFISH involves the *in situ* labeling of RNA transcripts with multiple, short, fluorescently-labelled oligonucleotides, which have the sensitivity to detect single transcript molecules with high 3D spatial resolution when imaged. Bursting events are thus detected by smFISH as clear punctate fluorescent foci, whose fluorescent intensity can be used to precisely calculate the exact number of transcripts composing each burst at that point in time. While smFISH experiments involve cellular fixation and are thus unable to follow a single cell or burst event over time, precise bursting kinetics for a gene can be modeled and extrapolated through analysis of smFISH bursting data over a population of cells or at different points in time relative to a signal. Furthermore, smFISH can be combined with immunofluorescence, DNA-FISH, or other smFISH targets to determine spatial relationships between bursting and other nuclear elements.

scRNA approaches make use of single-cell quantitation of transcripts to extrapolate bursting kinetics in a high-throughput, open-ended, whole-genome manner, which stands in contrast to the aforementioned methods that only provide

bursting information on a single targeted transcript. As each scRNA-seq experiment can capture only a single moment in time, like smFISH, scRNA-seq experiments extrapolate bursting kinetics based upon each transcripts' distribution over a population of cells. These experiments typically make use of SNPs to distinguish transcripts between alleles and thus more accurately quantify bursting. While scRNA-seq experiments are unable to provide any 3D context to bursting, their high-throughput nature allows for the informatics extrapolation of general bursting properties, as well as the correlation of bursting properties with genomic and epigenomic features.

MS2/PP7-tagging of transcripts involves the introduction of a series of MS2 or PP7 repeats into the transcript of interest, which, upon the bursting of the transcript, will recruit fluorescently tagged MS2 or PP7 recognizing coat proteins to the transcript of interest and produce punctate foci correlating to the burst of transcription. MS2/PP7 tagging of transcripts provides a very direct readout of bursting, allowing resolution of bursting dynamics at minute resolution, rather than the hour-resolution timescale of destabilized reporter systems. The ability of the MS2/PP7 system to distinguish individual bursts can be compromised, however, in cases of very high burst frequency results in individual bursts merging together into single larger extended bursts. Often observed is cases of close enhancer-promoter genomic proximity as seen in drosophila eve reporter systems (Falo-Sanjuan et al., 2019; Fukaya et al., 2016; Lammers et al., 2020), these partially overlapping bursts can still be modeled to extrapolate high confidence bursting kinetics. However, careful controls are needed to ensure that a higher amplitude resulting from peak

merging due to increased bursting frequency is not mistaken for increased burst size. Furthermore, because MS2/PP7 signal produces clear focus at the locus from which it is transcribed, this system can also provide precise 3D spatial quantitation of bursting kinetics relative to other nuclear regulatory entities, similar to smFISH.

Use of these reporter systems has allowed for an understanding of the role of burst transcription in various biological contexts, as well as the role of enhancers in regulation of bursting.

1.3 Burst size and frequency

While considerable evidence has affirmed burst frequency as the primary bursting kinetic parameter responsible for transcriptional changes in response to certain signaling or developmental stimuli, regulation on burst size has still played a considerable role in many signaling contexts. An MS2-tagged reporter of the Notch responsive *sygl-1* gene showed a dramatic change in burst duration that directly correlated with a clear spatial gradient Notch signaling activity in c. elegans, while burst frequency and intensity amplitude showed minimal correlation (Lee et al., 2019). Furthermore, use of a mutant that inhibited notch signaling caused a 3-fold reduction in burst duration, a 2-fold reduction in burst amplitude, and only a 1.5-fold reduction in burst frequency. The role of bursting in the mediation of Notch signaling was explored further in an independent study in drosophila, where changes in expression levels of the intracellular domain of Notch (NICD) directly correlated to the burst size (both burst amplitude and duration) of 2 genes regulated by 2 distinct Notch-activated enhancers (Falo-Sanjuan et al., 2019). In addition to NICD levels, manipulation of transcription factor motifs in the Notch regulated enhancers, including

optimization of CSL motif spacing or mutation of the Twist and Dorsal in motifs, resulted in further alteration of target gene bursting kinetics, again primarily through an impact on burst size. Similarly, activation of Wnt /β-catenin signaling in HEK293 cells caused a dramatic increase in burst size of a MS2-tagged Cyclin D1 reporter gene through both an approximate 3-fold increase in burst duration and a ~1.5 fold increase in burst intensity, though changes in metrics relating to burst frequency were also observed (Kafri et al.). Taken together, these three studies clearly show that burst size can contribute to regulation of transcriptional response to stimuli.

While the aforementioned studies showing examples of Wnt and Notch regulating transcription through modulation of burst size all make use of reporter systems where the signal responsive element is within 2-3kb of the reporter gene transcription start site (TSS), some examples of promoter-based regulation of burst frequency have been shown (Nicolas et al., 2018; Senecal et al., 2014; Stavreva et al., 2019). In a study that will be discussed in greater depth later, Stavreva et al. made use of an MS2-tagged reporter that showed clear and definitive changes in both burst frequency and size in response to promoter-based activation by Glococorticoid Receptor. In a separate study by Nicolas et al. that made use of both smFISH and a destabilized luciferase reporter to determine bursting of a circadian regulated reporter gene, it was observed that promoter H3K27ac levels correlated with burst frequency and not burst size. This analysis was supported by dCas9 recruitment of acetyltransferases to the reporter promoter resulting in smFISH determined increases in burst frequency, as well as smFISH confirmed correlations in burst frequency of 38 mESC genes with H3K27ac and H3K9ac levels in a 5kb

window around each genes' TSS. Some caution should be given when assessing these results, as no mention was given to distinguishing burst duration (a component of burst size) from burst frequency, components that could be misidentified without proper experimental or analytic control in smFISH data. Regardless, while the study at least suggests an example of promoter control of bursting, it also makes the mechanistic observation of the sufficiency of promoter histone acetylation levels in regulating burst kinetic parameters.

In addition to providing more clear evidence of promoter regulation of burst frequency, a 2014 study by Senecal et al. provided insight into the types of molecular events that could control the different kinetic parameters of bursting. Using smFISH, it was observed that c-Fos stimulation by serum and Zinc result in increased foci number with no change in burst intensity in a manner consistent with regulation through burst frequency (Senecal et al., 2014). By combining this stimulation data with results obtained by recruiting TALE-targeted activation domains of various strengths to the c-Fos loci, the authors were able to model and dissect how different transcription factor properties related to changes in specific bursting kinetic parameters. The authors thus concluded that burst amplitude correlated to activator domain strength, burst duration corresponded to the duration of transcription factor binding, and burst frequency showed dependence upon transcription factor concentration.

1.4 Bursting in a ligand-dependent system

Further insight into the mechanism by which enhancer and promoter elements regulate burst transcription was provided by three independent studies that each

made use of nuclear receptor activated transcription. In the study by Stavreva et al., the bursting of the PP7-tagged reporter gene MMTV was modelled in response to activation by hormone stimulated Glococorticoid Recepter (GR), which regulated the reporter gene through a promoter element (Stavreva et al., 2019). In Fritzsch et al. and Rodriguez et al., the bursting of endogenously tagged gene loci (PP7-tagged GREB1 and MS2-tagged TFF1, respectively) was monitored in response to hormone stimulated Estrogen Receptor (ER) (Fritzsch et al., 2018; Rodriguez et al., 2019), which regulates both genes in large part through the activity of enhancers (Deschênes et al., 2007; Nair et al., 2019). Interestingly, all three studies showed relatively similar ranges of bursting parameters, with the GR-promoter regulated MMTV having ~5-10 minute bursts with ~30-60 minute off periods, the ER-enhancer regulated GREB1 showing ~7-13 minute bursts with ~25-80 minute off periods, and the ER-enhancer regulated TFF1 showing ~5-20 minute bursts with ~30+ minute off periods.

While broadly similar in their bursting kinetics, the studies different in terms of how manipulations of each system affected burst size and frequency. In Stavreva et al., GR regulated bursting kinetics were altered by changing the hormone used to stimulate GR (corticosterone vs dexamethasone) and by different durations of hormone stimulation (0-6 hours vs 6-12 hours). In each set of manipulations, both burst frequency and burst duration were significantly altered to relatively similar degrees. To further explore the mechanism behind GR regulation of burst size and frequency, the study performed single molecule tracking (SMT) of Halo-tagged GR in conjunction with burst tracing of GR stimulated MMTV. It was then observed that

burst frequency corresponded closely to clustered GR binding. In contrast, the total fraction of GR in the bound state in a particular condition correlated with the duration of bursting, though it remains unclear exactly how this phenomenon directly contributes to a longer burst duration at a given locus. Taken together, this study indicates not only that nuclear receptors are able to differentially regulate burst size and frequency in response to different stimuli, but that the regulation of burst size and frequency by nuclear receptors may occur through distinct mechanisms.

In both Fritzsch et al. and Rodriguez et al., bursting kinetics of ER-enhancer regulated endogenous reporter genes were altered with different concentrations of the ER stimulating hormone estradiol (E2). Fritzsch et al found changes in E2 concentration to have the largest bursting kinetic impact on burst frequency, with a 184 minute OFF-duration in 0 pM E2 decreasing to a 78 minute OFF-duration at 5 pM E2 decreasing further to a 26 minute OFF-duration at 1000 pM E2. However, burst size was still very significantly regulated by E2 concentration, with 4.9 extrapolated RNAs/burst at 0 pM E2 increasing to 7.1 RNAs/burst in 5 pM E2 increasing further to 15.4 RNAs/burst at 1000 pM E2. In contrast, Rodriguez et al. detected no change in burst size at different E2 concentrations, attributing E2 dependent changes in bursting kinetics entirely to changes in burst frequency, with a 86 minute OFF-duration at 500 pM E2 compared to a 185 minute OFF-duration at 50 pM E2. While the reason for this discrepancy between these studies remains unclear it is possible that the higher doses of E2 used in Rodriguez et al. obscured the burst-size differences observed in E2 regulation by Fritzsch et al. While Fritzsch et al. did not test the 50 pM E2 dose used by Rodriguez, the 20 pM and 100 pM E2 doses

used by Fritzsch et al. gave burst sizes of 11.3 and 16.7 RNAs/burst, respectively, suggesting that a 50 pM E2 dose may not have appeared significant compared with 500 pM E2 in terms of change in burst size.

Taken together, these results strongly suggest that burst frequency and burst size, while possibly regulated through different molecular mechanisms, can be regulated by both enhancer and promoter elements. Furthermore, while there were some differences in the relative contributions of burst frequence and size in the Stavreva GR-promoter model to the Fritzsch ER-enhancer model, the overall similarities in bursting patterns and changes in bursting kinetic parameters also suggest that the TSS-proximal positioning of a regulatory elemental does not fundamentally change the nature of the element from a “burst frequency regulating element” to a “burst size regulating element”.

1.5 Enhancer vs. promoter mediated bursting

Clear evidence of enhancer control of gene burst frequency was shown in a seminal study tracing changes in MS2-visualized gene bursting patterns in response to series of enhancer manipulations (Fukaya et al., 2016). Fukaya et al. made use of an MS2-tagged reporter gene controlled by different sets of single or combined enhancers that would activate in nc14 of drosophila development. Different enhancers resulted in considerably different levels of total burst transcription output, and it was shown that burst frequency accounted for a far greater portion of these differences than burst amplitude. It should be noted, however, that a very consistent, though relatively minor, trend was observed of lower burst amplitude being produced

by reporters with enhancers that produced less frequent gene bursting, suggesting that enhancers may have some degree of control of burst size.

In a study that modelled MS2 bursting data of the even-skipped gene during drosophila stripe development, it was again shown that burst frequency, driven by the eve stripe 2 enhancer, accounted for differences in gene expression to a greater extent than did burst size (Lammers et al., 2020). Interestingly, the authors found that total duration of the high frequency bursting period varied in a partially independent manner from burst frequency, and was similarly important as burst frequency in accounting for differences in total transcription levels between cells. Using modeling of transcription factor levels to account for independent regulation of burst frequency and the duration of the high burst frequency period, the study highlights the window of bursting as an additional feature that can be regulated by enhancers.

To complement the extensively studied enhancer control of eve gene bursting regulation by the stripe 2 enhancer, a recent study explored eve gene bursting in seven stripes controlled by 5 independent enhancers (Berrocal et al., 2020). The study found bursting in all 7 stripes to be controlled in a similar regulatory manner, and while the study did find that burst amplitude (but not burst duration) was a significant contributor to increased eve expression, burst frequency was once again the kinetic parameter most strongly associated with enhancer related increases in transcription.

The role of enhancers and promoters in regulating burst frequency and burst size was further examined in a genome wide scale in several scRNA-seq papers.

Using allele specific scRNA-seq in mESCs, it was shown that 425 of 7486 biallelic bursting genes were shown to have significant differences in burst frequency between alleles, while only 2 showed differences in burst size. The same study then performed allele specific scRNA-seq in human primary fibroblasts, and found that 26 of 2277 biallelic bursting genes showed burst frequency differences, against only 1 gene showing burst size difference. While the mutations in cis-regulatory elements responsible for these allele specific changes in transcription could associated with either enhancers or promoters, the study's clear association of allele specific differences in transcription to burst frequency rather than burst size strongly suggests the regulation of burst frequency by cis-regulatory factors may be the more common strategy for regulating transcriptional response to developmental and environmental stimuli.

The role of enhancers in this cis-regulation of burst frequency was elucidated by a subsequent study linking changes in bursting kinetics to genomic and epigenetic regulatory elements (Larsson et al., 2019). This study found that differences in expression between cell types correlated more strongly with burst frequency, echoing the earlier study's implication that burst frequency is a more significant contributor to changes in gene expression. These changes in burst frequency were correlated with changes in regulatory enhancers, as shown by differences in enhancer H3K27ac tag density correlating with burst frequency. Additionally, enhancer, but not promoter SNPs correlated with these changes in burst frequency and expression. Conversely, the study did find that promoter composition, particularly the presence of TATA and initiator elements, did correlate with burst size. These findings provide further

support for the paradigm that, while promoters can impact transcription through regulation of burst size, transcription is primarily regulated through burst frequency, which is in turn controlled largely by enhancers.

An attempt was made to identify additional factors and pathways implicated in the control of bursting kinetics, implicating elongation machinery with regulation of bursting kinetics (Ochiai et al., 2020). While the relative contributions of burst size and frequency to overall differences in transcript levels were not thoroughly explored, the promoter binding of many key transcriptional regulators, including EP300, ELL2, and MED12, was found to correlate strongly with burst size, while binding of other regulatory factors, including BRD9 and AFF4, to enhancers was found to correlate more strongly to changes in burst frequency. Interestingly, while the enhancer/factor bursting correlations were considerably weaker than those of the promoters, gene body enrichment of several elongation-related factors, including AFF4, BRD4 and H3K36me3, were strikingly enriched with burst frequency. This result was strikingly consistent with an earlier study again associating H3K36me3 gene body enrichment to bursting frequency (Kim and Marioni, 2013). However, as inhibition of elongation showed varying gene- and context-specific effects on burst frequency and size, the relationship of elongation to bursting regulation remains an unclear but promising avenue for further exploration. Taken in concert with the context-specific findings of the study, including inhibition of PRC2, mTOR, Akt, and MAPK pathways resulting in opposing effects on bursting kinetics on different genes, the regulation of bursting kinetics in response to various signaling stimuli is likely to be highly complex.

One key question raised by such analysis of enhancer and promoter regulation of burst transcription is whether a fundamental difference truly exists between a promoter or an enhancer in their regulation of burst transcription, or whether the differences between the two elements arises only as a function of the distance of the regulatory element to the TSS. Given that promoter-based regulation was able to regulate both burst duration (as seen in the Notch and Wnt studies) as well as burst frequency (as seen in the c-Fos and GR systems), and that promoter-based regulation by GR follows incredibly similar mechanics as enhancer-based regulation by ER, it doesn't appear that promoter and enhancer based regulation of transcriptional bursting is categorically fundamentally different, though trends may exist. Furthermore, data from the 2016 study by Fukaya et al. strongly suggests that distance of the regulatory element to the TSS can have a substantial but not fundamental impact on transcription bursting. When the sna shadow enhancer was placed 1.5kb from its MS2-tagged reporter gene, transcription occurred in a long, single, continuous bursts that lasted the entirety of the drosophila nc14 developmental stage in which the shadow enhancer was active. However, when the enhancer was moved 7.5 kb from the reporter's TSS, clear and distinct bursts were instead observed over this same period. As burst amplitude remained the same in both the TSS-distal and proximal arrangements of the enhancer, this change in distance thus resulted in either an increase in burst duration or burst frequency, with burst frequency appearing somewhat more likely as careful examination of burst traces seems to show a periodicity consistent with the original burst duration. This result thus provides evidence that enhancers and promoters may not be

fundamentally different in their impact on bursting parameters, but that their placement relative to a TSS can have a significant impact on burst transcription.

1.6 Simultaneous bursting of multiple alleles

In addition to presenting clear evidence of the ability of enhancers to regulate gene bursting frequency, Fukaya et al. also provides data suggesting an enhancer can simultaneously activate the bursting of 2 alleles (Fukaya et al., 2016). This determined by placing two different reporter genes, one tagged with MS2 and the other with PP7, under control of a single enhancer that was 7.5kb from the TSS of each reporter. The resulting burst traces were highly significantly non-random, showed a clear pattern of co-bursting of the two reporters. Interestingly, while insertion of an insulator sequence between one reporter and the enhancer greatly diminished the burst frequency of that reporter alone, the infrequent bursts of the insulated promoter still showed coordinated bursting with the non-insulated reporter. Additionally, co-bursting genes showed competition, as placement of one enhancer closer to the promoter resulted in diminishing of burst frequency of the more distal promoter while increasing the frequency of the proximal reporter.

This observation was echoed and expanded upon by transvection studies in drosophila, whereby insulator-dependent association of 2 alleles allowed the enhancer on one allele to regulate burst transcription of MS2/PP7 labeled reporter genes on both alleles (Lim et al., 2018). In addition to allowing trans-chromosomal regulation of burst transcription, bursting of the two alleles was again shown to be coordinated in a significantly co-bursting manner and detected competition between the enhancer-sharing reporters. However, where Fukaya et al.'s exhibited that

competing promoters showed alterations primarily in burst frequency, Lim et al. determined that competition between reporters resulted in reduction in burst amplitude and a delay in onset of bursting without any detectable difference in burst frequency. Also of note was the relatively equivalent bursting of the cis and trans reporters, contrasting with the traditional model of enhancer:promoter relationships where the nearest promoter to an enhancer would be strongly favored, and instead suggesting a model of dynamic 3-dimensional interaction between enhancer and promoter. The mechanistic reason for the difference between these results remains unclear, though, as both systems utilized reporters under control of the same sna shadow enhancer, the clearest difference between the studies lies in Lim et al. using a transvection system while Fukaya et al. made use of promoters on the same molecule of DNA and <7.5kb from the shared enhancer.

Co-bursting data from transvection experiments was then expanded upon to support a model of enhancer-promoter interaction that is fundamentally different from the traditional “looping” based model: namely, that enhancers could regulate promoters without coming into direct contact as is required by the “looping” model (Heist et al., 2019). Not only were co-bursting MS2-tagged reporter genes an average of 200-300nm apart throughout their co-bursting periods, but clear examples were identified where bursting reporters were >200nm apart throughout their entire burst durations. These examples suggest that at least one of the co-bursting alleles was at least 100nm from the enhancer at its time of bursting, which is a greater distance than would be suggested by traditional enhancer:promoter looping models. Additionally, it was shown that reporter arrangements producing more spatial distant

bursts (~270nm vs ~200nm) actually resulted in higher burst size, raising the possibility not only that direct interaction between enhancers and promoter is not necessary for bursting, but that greater 3-dimensional space between elements within certain limits can actually facilitate bursting. One caveat behind the latter observation, however, is that the larger distance between bursts was observed in a reporter construct where 2 co-bursting promoters were placed ~1.5kb on either side of an enhancer and in a divergent orientation, while the construct showing smaller distances between bursts placed constructs ~8kb on either side of an enhancer and in a convergent orientation. Thus, the differences in intensity between these constructs' bursts could potentially be explained not by the distance between the bursts, but by other phenomena including stronger activation due to closer enhancer promoter proximity or by interference from converging RNA polymerase complexes. Regardless of these remaining questions, this study provides support for a model where an enhancer can exert its regulatory impact on a promoter without the two elements coming into direct contact.

Further support for this model of bursting in the absence of direct promoter-enhancer looping was provided by a study that meticulously characterized the impact that the distance between an enhancer and promoter played upon the bursting of the promoter (Alexander et al., 2019). The study made use of tetO/TetR and cuO/CymR systems to create a persistent fluorescent genomic label of the *Sox2* promoter and its enhancer ~100kb away. Additionally, *Sox2* itself was MS2 tagged, allowing for the quantitation of bursting relative to the spatiotemporal dynamics of the gene's enhancer and promoter. While the Sox2 enhancer and promoter persistently

remained relatively close to one another, with a mean distance of 339nm and only 2.1% of measured distances greater than 750nm, no spatiotemporal relationship was observed between enhancer-promoter association and Sox2 bursting. Not only was there no observable difference in enhancer:promoter proximity at the time of promoter bursting, but alignment of burst traces showed no significant increase in enhancer:promoter association up to 25 minutes prior to bursting, and , like in Heist et al., examples were shown where bursting occurred when the promoter and enhancer were >300 um apart for ~30 minutes preceding and during the burst. While these results cannot entirely exclude the possibility that direct enhancer:promoter interaction occurred 30+ minutes prior to bursting, this study provides strong support for the model whereby enhancers can regulate gene bursting without direction promoter interaction.

While the data from Alexander et al. indicated that spatial proximity between enhancer promoter at distances that averaged 339nm did not seem to affect bursting, a complementary study indicated that reaching an ~350nm distance threshold between enhancer and promoter was key for activation of burst transcription (Chen et al., 2018). A three part tagging system was developed in Drosophila to monitor the distances between an enhancer and a distal activated gene: a PP7-tagged reporter gene was placed 142kb from the eve enhancer and linked to the eve enhancer via the homie insulator; the endogenous eve gene proximal to and regulated by the eve enhancer was tagged with MS2 to function as a proxy for the enhancer position during the gene's active period in nc14; and the parb system was integrated nearby the distal enhancer to determine the distal gene's location in the absence of its

bursting. The authors observe that, upon activation, the distal gene transitions from an average distance of ~600nm from the enhancer in the OFF state to an average distance of ~350nm in the ON state. Conversely, the distal promoter transitions from an average distance of ~350nm to a distance of ~600nm as it transitions from ON to OFF. Further modeling of the relationship between enhancer:distal-promoter proximity and distal-promoter bursting suggested a 3 state model of an OFF state with low proximity of >700nm, transitioning to an OFF state with high proximity of ~385nm, transitioning to an on state of high proximity of ~331nm.

Taken together, these studies suggest that while enhancer activated bursting of a gene requires a general proximity of the two of ~350nm, the direct interaction between the two elements does not appear necessary for bursting. This ability of an enhancer to regulate a promoter through proximity can in turn explain the ability of an enhancer to regulate multiple genes simultaneously, as has been observed in the co-bursting of genes regulated by the same promoter.

1.7 Bursting at transcription hubs

A possible explanation for the ability of enhancers to regulate burst transcription of one or multiple genes without direct looping lie in the ability of enhancers to influence the formation and activity of transcriptional hubs, or small and transient subnuclear bodies consisting of localized enrichments of transcriptional co-activators (Cho et al., 2016, 2018; Hnisz et al., 2017; Monahan et al., 2019; Sabari et al., 2018).

Using a methodology that functions like a combination of live-PALM/STORM and single molecule tracking (SMT), transient (~5 and ~8 second average lifetimes in

human and mouse cells, respectively) 100-200nm clusters of RNA PolII were observed throughout the nucleus. Furthermore, bursting MS2-tagged β-actin was shown to associate with these transient clusters, though thorough statistical analysis of the significance of the association between the bursts and hubs was not performed. The lifetime of hubs also increased considerably upon stimulation of cells with serum, in a manner coinciding with the bursting of serum-responsive β-actin and possibly coinciding with a change in burst kinetics that has previously been observed upon serum stimulation (Molina et al., 2013; Senecal et al., 2014). Additionally, the authors suggested these transient PolII clusters were implicated in transcription initiation rather than elongation given the duration and kinetics of the hubs, as well as their insensitivity to elongation inhibitors DRB and flavopiridol. These small and transient hubs thus represent a potential component of burst regulation machinery and could also represent a sort of transcriptional hub by which enhancers and promoters could associate and interact without direct and sustained looping.

RNA polymerase II and Mediator are two fundamental factors involved in transcription activation, and both have been reported in numerous publications to be capable of condensate formation. Mediator is known to contain a large intrinsically disordered region (IDR) involved in homotypic protein-protein and heterotypic protein-RNA interactions responsible for phase separated nuclear compartments(Boija et al., 2018; Kagey et al., 2010; Manteiga et al., 2019; Shrinivas et al., 2019). Fluorescence Recovery After Photobleaching (FRAP) effectively illustrates liquid phase separated properties of both Mediator and RNA polymerase II, where 60% of Mediator and 90% of RNA polymerase II are exchanged within 10 seconds within clusters(Cho et al.,

2018). Moreover, 1-6-hexandiol treatment results in a gradual dissolution of both Mediator and RNA polymerase II clusters, suggesting that these hubs are condensates comprised of Mediator and RNA polymerase II(Cho et al., 2018; Manteiga et al., 2019; Shrinivas et al., 2019). Specifically, it has been reported that the hypophosphorylated C-terminal domain of RNA polymerase II is interacting with the Mediator condensates, and these clusters are concentrated and localized to enhancers and promoter regions involved in transcription initiation(Manteiga et al., 2019).

Using both live imaging of the MS2 tagging system(Larson et al., 2011; Qin et al., 2017; Wang, Su, Zhang, et al., 2016) and intronic FISH, only a fraction of target loci is shown to be in direct contact (less than the diffraction limited 300nm) with RNA polymerase II and Mediator clusters, though majority are in proximity to these condensates (<1um)(Cho et al., 2018). While in proximity, it is possible that the density of factors at a particular enhancer locus is what drives compartmentalization and that decrease in distance during colocalization, where a threshold of the number of cooperative binding events at a particular locus need to occur before robust recruitment and assembly of transcription machinery required for activation(Shrinivas et al., 2019). It is proposed that, distal clusters may colocalize and “kiss” the enhancer-regulated active gene transiently at certain points in time(Cho et al., 2018). In support of this model, a study records using single molecule tracking that protein-protein LCD-dependent interactions between transcription factors only lasts between 5-20 seconds, and rarely exceed 1 minute, indicating that these transient hubs concentrate transcription machinery in an extremely dynamic, multivalent way(Chong

et al., 2018). Live visualization via the CARGO system further demonstrates how transcription activation may increase enhancer-promoter contact frequencies by increasing the probability of stochastic encounters within a chromatin domain rather than through the formation of stable enhancer-promoter loops(Gu et al., 2018).

Given the size of the hubs, data suggests the lack of direct enhancer-promoter contact required for transcription activation, and such distances between enhancers and promoters may be explained by RNA polymerase II, Mediator, and other factors that help bridge that gap. It is also suspected that the presence of larger clusters at enhancers may allow these condensates to simultaneously contact multiple transcription factories at different enhancers and promoters in a cooperative network(Alexander et al., 2019; Cho et al., 2018; Chong et al., 2018; Manteiga et al., 2019). Compaction of chromatin to allow not only genomic interactions within the same domain but also merging of multiple chromatin domains has been reported during IgH locus rearrangement in B cell development(Khanna et al., 2019; Lin et al., 2012; Lucas et al., 2014). During pre-B cell to pro-B cell VDJ recombination, distal and proximal V regions in two separate domains merge into a single cloud before recruiting DJ and regulatory elements(Jung et al., 2006). Data proposes that coding VDJ regions and enhancer-promoter regulatory elements within the newly rearranged compartment of proteins and chromatin fibers bounce back and forth in a spring-like manner (fractional Langevin motion) to establish genomic interactions. Simulations demonstrate that increasing the diffusion coefficient 2-fold only results in a 4-fold increase in interaction frequency; however, decreasing the confinement radius during chromatin compaction 2-fold results in a 16-fold increase in interaction frequency,

suggesting that the size of confinement of the hub largely determines the frequency of interactions between regulatory and coding elements(Khanna et al., 2019; Lucas et al., 2014).

We have established that RNA polymerase II, Mediator, and various transcription factors with IDRs are capable of forming individual condensates localized to enhancer and promoter regions to facilitate transcription activation. However, evidence suggests that these clusters may be part of a higher-order level of organization and interaction where genomic regions across chromosomes may colocalize around non-membrane bound nuclear organelles to shape the global genomic organization(Berry et al., 2015; Feric et al., 2016; Mao et al., 2011; Quinodoz et al., 2018; Skowronska-Krawczyk et al., 2014; Spector & Lamond, 2011). Within the nucleus, only two higher-order inter-chromosomal hubs are found via SPRITE, and they are preferentially organized around the nucleolus and nuclear speckles. Organization around these two nuclear bodies results in closer spatial organization between different chromosomes, and DNA regions within the same hub are found to simultaneously colocalize to the same nuclear body to form higher-order interactions which is confirmed via DNA-FISH. Gene-dense and actively transcribed regions are reported to organize around nuclear speckles whereas gene-poor and transcriptionally inactive regions organize around the nucleolus, and colocalization to either the nuclear speckle or nucleolus is found to be arranged non-linearly(Quinodoz et al., 2018). Though not directly examining the relationship of global genomic organization relative to subnuclear structures, numerous reports found that spatial organization of chromosomes is functionally important in transcription

regulation(Bintu et al., 2018; Gibson et al., 2019; Wang, Su, Beliveau, et al., 2016). Super resolution imaging via STORM illustrates that active, inactive, and repressed domains have varied levels of intermixing and overlap, suggesting that the degree of spatial separation between different domains is highly dependent on the epigenetic state(Wang, Su, Beliveau, et al., 2016). These domains may further be categorized into A, active, and B, inactive, compartments where they are organized in a spatially divided manner, similar to the model proposed by SPRITE. These compartments may serve to locally enrich for factors and cofactors that enhance the efficiency of molecular processes, and concentration of transcriptional machinery may directly cross-link multiple chromatin domains belonging to the same compartment(Bintu et al., 2018).

To further elaborate on the phenomenon of hubs involved in higher-order global genomic organization, several studies have argued that, at least in certain systems, enhancer-promoter localization to non-membrane bound nuclear bodies is necessary for transcription regulation(Khanna et al., 2014; Manteiga et al., 2019; Sharma et al., 2007; Skowronska-Krawczyk et al., 2014). In an estrogen-regulated system, the most robustly ERα-bound enhancers are found to recruit an array of ERα-dependent transcription factors and cofactors, referred to as the MegaTrans complex, where many proteins within this complex, such as ERα and GATA3, harbor IDRs(Liu et al., 2014). These proteins with IDRs are shown to undergo phase separation and form condensates at ERα-regulated enhancers both in vitro and in vivo via droplet and FRAP assays using confocal microscopy. Interestingly, estradiol treatment results in a decrease in spatial distance between several robustly active

ERα-bound enhancers on Chromosome 21, some separated by distances as far as 27MB apart, again suggesting a level of organization where recruitment of loci spread among different chromatin domains are capable of colocalization to the same hub. Confocal microscopy analysis reveal that around 80% of ERα condensates are located within 400nm of a nuclear speckle, and 1-6-hexandiol effectively attenuates the E2-induced proximity of ERα-dependent enhancer loci visualized through FISH, indicating that the spatial proximity between MegaTrans bound enhancers require the formation of phase-separated condensates through cooperative interactions. It is found via intronic RNA-FISH that that two robustly transcribed ERα-dependent alleles, *TFF1* and *NRIP1,* 27MB apart are associated with the nuclear speckle and are roughly three times more active than alleles not localized to the speckle. Moreover, disruption of the nuclear speckle through either 1-6-hexandiol or knockdown of splicing components SRSF1 or U2AF1 results in dampened transcription of ERα-dependent enhancers that are localized to the speckle, suggesting the functional importance of higher-order colocalization and arrangement of enhancer condensates to a nuclear body to facilitate robust transcription(Nair et al., 2019). It is no surprise that gene active, RNA polymerase II dense regions organize around nuclear speckles as several other reports have supported this claim(Khanna et al., 2014; Manteiga et al., 2019). Specifically, hyperphosphorylated C-terminal domain of RNA polymerase II preferentially interacts with splicing factors, forming higher-order hubs. Co-transcriptional RNA splicing can occur, and it makes sense that serine2phosphorylated C-terminal domain of RNA polymerase II involved in transcriptional elongation may be concentrated and partitioned into condensates

formed by splicing factors(Manteiga et al., 2019). A functional transcription enhancement of the Hsp70 transgene is also shown when traveled into proximity of speckles post heat shock(Khanna et al., 2014). Proteomics reveal more than 150 different proteins compose the speckle, and is thought to have a core acting as the storage granule for RNA processing components. Surrounding that core is a network of perichromatin fibrils where localization of condensates at that periphery is suspected to occur to facilitate transcription activation(Mao et al., 2011; Spector & Lamond, 2011).

The matrin3 network is another non-membrane bound nuclear compartment shown to serve functional importance in transcription regulation upon colocalization with target regions. Pit1, the POU-homeodomain transcription factor necessary for differentiation of three cell types in the anterior pituitary in mice and humans, binds many enhancers and is found to interact with the matrin3 network via mass spectrometry. DNA-FISH shows more than 65% colocalization of Pit1-bound regulatory elements occupying the same compartments as matrin3. When Pit1 associated factors β-catenin and SATB1 are knocked down, only 35% colocalization exists between target locus and matrin3. GRO-seq of double knockdown of these two factors surprisingly shows that all 991 Pit1-enhancer bound target genes are downregulated, indicating the role of β-catenin and SATB1 in facilitating the association of Pit1 with the matrin3 network that allows for transcription robustness. A naturally occurring mutant of Pit1, R271W, is fully expressed at similar levels as WT-Pit1 and capable of binding its cognate enhancers yet results in failed differentiation of the three cell lineages during pituitary development. The R271W mutation

specifically fails to bind β-catenin and SATB1, which in turn disrupts the ability of Pit1 to interact with the matrin3 network. Interestingly, the addition of a protein domain responsible for association with matrin3 can rescue matrin3 colocalization, and thus restore target gene expression(Skowronska-Krawczyk et al., 2014). This study is in further support of the model where higher-order organization and colocalization to a subnuclear compartment may be essential for transcription activation.

While the functional relationship between enhancers and transcription hubs remains unclear, there are various lines of evidence that suggesting these hubs may play a key role in enhancer activation of bursting, and raise the question of whether enhancers may play a causal role in the formation of these hubs. At a circumstantial level, the observation that the distance of enhancer-gene proximity needed for bursting is very similar to the approximate radius of observed transcription hubs, is highly suggestive of a functional association between the two elements, especially when considering the high degree of correlation between these hubs and enhancer produced RNA bursts. A computational study which suggested that clustering of enhancers in a superenhancer would greatly facilitate recruitment of sufficient localized concentration of transcription co-activators as to induce liquid-liquid phase separation of the clustered activators and promote bursting (Hnisz et al., 2017), and the observation that disruption of enhancer recruited OCT4 disrupts MED1 cluster (Boijja et al., 2018) or observance of nuclear receptors to form clusters at hormone stimulated bursts (Stavreva et al., 2019) further implicates enhancers as having a causal role in the formation of transcriptional coactivators. The transient nature of the

PolII clusters observed by Cho et al., 2016, is also consistent with the transient nature of bursting.

Also compelling, though entirely theoretical, is the potential of an enhancer induced transcriptional hub to explain the model of enhancer regulation of gene bursting in the absence of direct enhancer promoter looping. By initializing or activating transcription within a ~300-400nm transcriptional hub through recruitment and locally concentrating transcriptional co-activators, an enhancer would be thus able to induce transcription without coming into direct contact with a regulated gene. Furthermore, this model would explain several observed co-bursting phenomena, as multiple promoters could be burst from a single transcriptional hub without the steric hindrance that would be expected to occur from a single enhancer coming into direct contact with 2 promoters simultaneously.

Ultimately, however, this potential relationship between enhancers, bursting, and transcriptional hubs needs to be examined experimentally. Fortunately, the monitoring of bursting kinetics with high spatiotemporal resolution through MS2/PP7 tagging should allow for the modeling of gene bursting relative to transcriptional hub formation to determine what sort of relationship between the two exists. Furthermore, these MS2/PP7 tagging approaches can theoretically be applied to enhancers directly so as to directly determine the relationship between enhancer bursting, hub formation and composition, and target gene bursting.

1.8 References

1. Alexander, J.M., Guan, J., Li, B., Maliskova, L., Song, M., Shen, Y., Huang, B., Lomvardas, S., and Weiner, O.D. (2019). Live-cell imaging reveals enhancer-

dependent Sox2 transcription in the absence of enhancer proximity. ELife 8, e41769.

2. Banani, S. F., Lee, H. O., Hyman, A. A., & Rosen, M. K. (2017). Biomolecular condensates: organizers of cellular biochemistry. Nature Reviews Molecular Cell Biology, 18(5), 285–298. https://doi.org/10.1038/nrm.2017.7

3. Berrocal, A., Lammers, N., Garcia, H.G., and Eisen, M.B. (2020). Kinetic sculpting of the seven stripes of the Drosophila even-skipped gene. BioRxiv 335901.

4. Berry, J., Weber, S. C., Vaidya, N., Haataja, M., Brangwynne, C. P., & Weitz, D. A. (2015). RNA transcription modulates phase transition-driven nuclear body assembly. Proceedings of the National Academy of Sciences of the United States of America, 112(38), E5237–E5245. https://doi.org/10.1073/pnas.1509317112

5. Bintu, B., Mateo, L. J., Su, J. H., Sinnott-Armstrong, N. A., Parker, M., Kinrot, S., Yamaya, K., Boettiger, A. N., & Zhuang, X. (2018). Super-resolution chromatin tracing reveals domains and cooperative interactions in single cells. Science, 362(6413). https://doi.org/10.1126/science.aau1783

6. Boija, A., Klein, I. A., Sabari, B. R., Dall'Agnese, A., Coffey, E. L., Zamudio, A. V., Li, C. H., Shrinivas, K., Manteiga, J. C., Hannett, N. M., Abraham, B. J., Afeyan, L. K., Guo, Y. E., Rimel, J. K., Fant, C. B., Schuijers, J., Lee, T. I., Taatjes, D. J., & Young, R. A. (2018). Transcription Factors Activate Genes through the Phase-Separation Capacity of Their Activation Domains. Cell, 175(7), 1842-1855.e16. https://doi.org/10.1016/j.cell.2018.10.042

7. Boije, H., Rulands, S., Dudczig, S., Simons, B.D., and Harris, W.A. (2015). The Independent Probabilistic Firing of Transcription Factors: A Paradigm for Clonal Variability in the Zebrafish Retina. Dev. Cell 34, 532–543.

8. Boijja, A., Klein, I.A., Sabari, B.R., Dall'Agnese, A., Coffey, E.L., Zamudio, A.V., Li, C.H., Shrinivas, K., Manteiga, J.C., Hannett, N.M., et al. (2018). Transcription factors activate genes through the phase separation capacity of their activation domains. Cell 175, 1842.

9. Bothma, J.P., Garcia, H.G., Esposito, E., Schlissel, G., Gregor, T., and Levine, M. (2014). Dynamic regulation of eve stripe 2 expression reveals transcriptional bursts in living Drosophila embryos. Proc. Natl. Acad. Sci. 111, 10598–10603.

10. Chen, H., Levo, M., Barinov, L., Fujioka, M., Jaynes, J.B., and Gregor, T. (2018). Dynamic interplay between enhancer-promoter topology and gene activity. Nat. Genet. 50, 1296–1303.

11. Cho, W.-K., Jayanth, N., English, B.P., Inoue, T., Andrews, J.O., Conway, W., Grimm, J.B., Spille, J.-H., Lavis, L.D., Lionnet, T., et al. (2016). RNA Polymerase II cluster dynamics predict mRNA output in living cells. ELife 5, e13617.

12. Cho, W.-K., Spille, J.-H., Hecht, M., Lee, C., Li, C., Grube, V., and Cisse, I.I. (2018). Mediator and RNA polymerase II clusters associate in transcription-dependent condensates. Science 361, 412–415.

13. Chong, S., Dugast-Darzacq, C., Liu, Z., Dong, P., Dailey, G. M., Cattoglio, C., Heckert, A., Banala, S., Lavis, L., Darzacq, X., & Tjian, R. (2018). Imaging dynamic and selective low-complexity domain interactions that control gene transcription. Science, 361(6400), 1–25. https://doi.org/10.1126/science.aar2555

14. Deschênes, J., Bourdeau, V., White, J.H., and Mader, S. (2007). Regulation of GREB1 transcription by estrogen receptor alpha through a multipartite enhancer spread over 20 kb of upstream flanking sequences. J. Biol. Chem. 282, 17335–17339.

15. Falo-Sanjuan, J., Lammers, N.C., Garcia, H.G., and Bray, S.J. (2019). Enhancer Priming Enables Fast and Sustained Transcriptional Responses to Notch Signaling. Dev. Cell 50, 411-425.e8.

16. Feric, M., Vaidya, N., Harmon, T. S., Mitrea, D. M., Zhu, L., Richardson, T. M., Kriwacki, R. W., Pappu, R. V., & Brangwynne, C. P. (2016). Coexisting Liquid Phases Underlie Nucleolar Subcompartments. Cell, 165(7), 1686–1697. https://doi.org/10.1016/j.cell.2016.04.047

17. Fritzsch, C., Baumgärtner, S., Kuban, M., Steinshorn, D., Reid, G., and Legewie, S. (2018). Estrogen-dependent control and cell-to-cell variability of transcriptional bursting. Mol. Syst. Biol. 14, e7678.

18. Fukaya, T., Lim, B., and Levine, M. (2016). Enhancer Control of Transcriptional Bursting. Cell 166, 358–368.

19. Gibson, B. A., Doolittle, L. K., Schneider, M. W. G., Jensen, L. E., Gamarra, N., Henry, L., Gerlich, D. W., Redding, S., & Rosen, M. K. (2019). Organization of

Chromatin by Intrinsic and Regulated Phase Separation. Cell, 179(2), 470-484.e21. https://doi.org/10.1016/j.cell.2019.08.037

20. Gu, B., Swigut, T., Spencley, A., Bauer, M. R., Chung, M., Meyer, T., & Wysocka, J. (2018). Transcription-coupled changes in nuclear mobility of mammalian cis-regulatory elements. Science, 359(6379), 1050–1055. https://doi.org/10.1126/science.aao3136

21. Guo, Y.E., Manteiga, J.C., Henninger, J.E., Sabari, B.R., Dall'Agnese, A., Hannett, N.M., Spille, J.-H., Afeyan, L.K., Zamudio, A.V., Shrinivas, K., et al. (2019). Pol II phosphorylation regulates a switch between transcriptional and splicing condensates. Nature 572, 543.

22. Harrison, M. M., Li, X.-Y., Kaplan, T., Botchan, M. R., & Eisen, M. B. (2011). Zelda binding in the early Drosophila melanogaster embryo marks regions subsequently activated at the maternal-to-zygotic transition. PLoS Genetics, 7.

23. Heist, T., Fukaya, T., and Levine, M. (2019). Large distances separate coregulated genes in living Drosophila embryos. Proc. Natl. Acad. Sci. 116, 15062–15067.

24. Hnisz, D., Shrinivas, K., Young, R.A., Chakraborty, A.K., and Sharp, P.A. (2017). A phase separation model predicts key features of transcriptional control. Cell 169, 13–23.

25. Jiang, Y., Zhang, N.R., and Li, M. (2017). SCALE: modeling allele-specific gene expression by single-cell RNA sequencing. Genome Biol. 18, 74.

26. Jung, D., Giallourakis, C., Mostoslavsky, R., & Alt, F. W. (2006). Mechanism and control of V(D)J recombination at the immunoglobulin heavy chain locus. Annual Review of Immunology, 24, 541–570.

27. Kafri, P., Hasenson, S.E., Kanter, I., Sheinberger, J., Kinor, N., Yunger, S., and Shav-Tal, Y. Quantifying β-catenin subcellular dynamics and cyclin D1 mRNA transcription during Wnt signaling in single living cells. ELife 5.

28. Kagey, M. H., Newman, J. J., Bilodeau, S., Zhan, Y., Orlando, D. a, van Berkum, N. L., Ebmeier, C. C., Goossens, J., Rahl, P. B., Levine, S. S., Taatjes, D. J., Dekker, J., & Young, R. a. (2010). Mediator and cohesin connect gene expression and chromatin architecture. Nature, 467(7314), 430–435. https://doi.org/10.1038/nature09380

29. Khanna, N., Hu, Y., & Belmont, A. S. (2014). HSP70 transgene directed motion to nuclear speckles facilitates heat shock activation. Current Biology, 24(10), 1138–1144. https://doi.org/10.1016/j.cub.2014.03.053

30. Khanna, N., Zhang, Y., Lucas, J. S., Dudko, O. K., & Murre, C. (2019). Chromosome dynamics near the sol-gel phase transition dictate the timing of remote genomic interactions. Nature Communications, 10(1), 1–13. https://doi.org/10.1038/s41467-019-10628-9

31. Kim, J.K., and Marioni, J.C. (2013). Inferring the kinetics of stochastic gene expression from single-cell RNA-sequencing data. Genome Biol. 14, R7.

32. Lammers, N.C., Galstyan, V., Reimer, A., Medin, S.A., Wiggins, C.H., and Garcia, H.G. (2020). Multimodal transcriptional control of pattern formation in embryonic development. Proc. Natl. Acad. Sci. 117, 836–847.

33. Larson, D. R., Zenklusen, D., Wu, B., Chao, J. A., & Singer, R. H. (2011). Real-Time Observation of Transcription Initiation and Elongation on an Endogenous Yeast Gene. Science, 332.

34. Larsson, A.J.M., Johnsson, P., Hagemann-Jensen, M., Hartmanis, L., Faridani, O.R., Reinius, B., Segerstolpe, Å., Rivera, C.M., Ren, B., and Sandberg, R. (2019). Genomic encoding of transcriptional burst kinetics. Nature 565, 251–254.

35. Lee, C., Shin, H., and Kimble, J. (2019). Dynamics of Notch-Dependent Transcriptional Bursting in Its Native Context. Dev. Cell 50, 426-435.e4.

36. Li, X.-Y., Harrison, M. M., Villalta, J. E., Kaplan, T., & Eisen, M. B. (2014). Establishment of regions of genomic activity during the Drosophila maternal to zygotic transition. ELife.

37. Lim, B., Heist, T., Levine, M., and Fukaya, T. (2018). Visualization of Transvection in Living Drosophila Embryos. Mol. Cell 70, 287-296.e6.

38. Lin, Y. C., Benner, C., Mansson, R., Heinz, S., Miyazaki, K., Miyazaki, M., Chandra, V., Bossen, C., Glass, C. K., & Murre, C. (2012). Global changes in the nuclear positioning of genes and intra-and interdomain genomic interactions that orchestrate B cell fate. Nature Immunology, 13(12), 1196–1204. https://doi.org/10.1038/ni.2432

39. Liu, Z., Merkurjev, D., Yang, F., Li, W., Oh, S., Friedman, M. J., Song, X., Zhang, F., Ma, Q., Ohgi, K. a, Krones, A., & Rosenfeld, M. G. (2014). Enhancer activation requires trans-recruitment of a mega transcription factor complex. Cell, 159(2), 358–373. https://doi.org/10.1016/j.cell.2014.08.027

40. Lucas, J. S., Zhang, Y., Dudko, O. K., & Murre, C. (2014). 3D trajectories adopted by coding and regulatory DNA elements: First-passage times for genomic interactions. Cell, 158(2), 339–352. https://doi.org/10.1016/j.cell.2014.05.036

41. Manteiga, J. C., Henninger, J. E., Sabari, B. R., Shrinivas, K., Abraham, B. J., Hannett, N. M., Spille, J., Afeyan, L. K., Boija, A., Decker, T., Rimel, J. K., Fant, C. B., Lee, T. I., Cisse, I. I., Sharp, P. A., Taatjes, D. J., & Young, R. A. (2019). Pol II phosphorylation regulates a switch between transcriptional and splicing condensates. Nature, 572, 543.

42. Mao, Y. S., Zhang, B., & Spector, D. L. (2011). Biogenesis and function of nuclear bodies. Trends in Genetics : TIG, 27(8), 295–306. https://doi.org/10.1016/j.tig.2011.05.006

43. Mir, M., Reimer, A., Haines, J. E., Li, X. Y., Stadler, M., Garcia, H., Eisen, M. B., & Darzacq, X. (2017). Dense bicoid hubs accentuate binding along the morphogen gradient. Genes and Development, 31(17), 1784–1794. https://doi.org/10.1101/gad.305078.117

44. Mir, M., Stadler, M. R., Ortiz, S. A., Hannon, C. E., Harrison, M. M., Darzacq, X., & Eisen, M. B. (2018). Dynamic multifactor hubs interact transiently with sites of active transcription in drosophila embryos. ELife, 7(Dv), 1–27. https://doi.org/10.7554/eLife.40497

45. Molina, N., Suter, D.M., Cannavo, R., Zoller, B., Gotic, I., and Naef, F. (2013). Stimulus-induced modulation of transcriptional bursting in a single mammalian gene. Proc. Natl. Acad. Sci. 110, 20563–20568.

46. Monahan, K., Horta, A., and Lomvardas, S. (2019). LHX2- and LDB1-mediated trans interactions regulate olfactory receptor choice. Nature 565, 448–453.

47. Nair, S.J., Yang, L., Meluzzi, D., Oh, S., Yang, F., Friedman, M.J., Wang, S., Suter, T., Alshareedah, I., Gamliel, A., et al. (2019). Phase separation of ligand-activated enhancers licenses cooperative chromosomal enhancer assembly. Nat. Struct. Mol. Biol. 26, 193–203.

48. Nicolas, D., Zoller, B., Suter, D.M., and Naef, F. (2018). Modulation of transcriptional burst frequency by histone acetylation. Proc. Natl. Acad. Sci. 115, 7153–7158.

49. Nien, C.-Y., Liang, H.-L., Butcher, S., Sun, Y., Fu, S., Gocha, T., Kirov, N., Manak, J. R., & Rushlow, C. (2011). Temporal Coordination of Gene Networks by Zelda in the Early Drosophila Embryo. PLoS Genetics.

50. Ochiai, H., Hayashi, T., Umeda, M., Yoshimura, M., Harada, A., Shimizu, Y., Nakano, K., Saitoh, N., Liu, Z., Yamamoto, T., et al. (2020). Genome-wide kinetic properties of transcriptional bursting in mouse embryonic stem cells. Sci. Adv. 6, eaaz6699.

51. Qin, P., Parlak, M., Kuscu, C., Bandaria, J., Mir, M., Szlachta, K., Singh, R., Darzacq, X., Yildiz, A., & Adli, M. (2017). Live cell imaging of low- and non-repetitive chromosome loci using CRISPR-Cas9. Nature Communications, 8, 14725. https://doi.org/10.1038/ncomms14725

52. Quinodoz, S. A., Ollikainen, N., Tabak, B., Palla, A., Schmidt, J. M., Detmar, E., Lai, M. M., Shishkin, A. A., Bhat, P., Takei, Y., Trinh, V., Aznauryan, E., Russell, P., Cheng, C., Jovanovic, M., Chow, A., Cai, L., McDonel, P., Garber, M., & Guttman, M. (2018). Higher-Order Inter-chromosomal Hubs Shape 3D Genome Organization in the Nucleus. Cell, 174(3), 744-757.e24. https://doi.org/10.1016/j.cell.2018.05.024

53. Rodriguez, J., Ren, G., Day, C.R., Zhao, K., Chow, C.C., and Larson, D.R. (2019). Intrinsic Dynamics of a Human Gene Reveal the Basis of Expression Heterogeneity. Cell 176, 213-226.e18.

54. Sabari, B.R., Dall'Agnese, A., Boija, A., Klein, I.A., Coffey, E.L., Shrinivas, K., Abraham, B.J., Hannett, N.M., Zamudio, A.V., Manteiga, J.C., et al. (2018). Coactivator condensation at super-enhancers links phase separation and gene control. Science 361.

55. Schultz, K. N., Bondra, E. R., Moshe, A., Villalta, J. E., Lieb, J. D., Kaplan, T., McKay, D. J., & Harrison, M. M. (2015). Zelda is differentially required for chromatin accessibility, transcription factor binding, and gene expression in the early Drosophila embryo. Genome Research, 25, 1715–1726.

56. Senecal, A., Munsky, B., Proux, F., Ly, N., Braye, F.E., Zimmer, C., Mueller, F., and Darzacq, X. (2014). Transcription Factors Modulate c-Fos Transcriptional Bursts. Cell Rep. 8, 75–83.

57. Sharma, S. V, Bell, D. W., Settleman, J., & Haber, D. A. (2007). Epidermal growth factor receptor mutations in lung cancer. Nature Reviews. Cancer, 7(3), 169–181. https://doi.org/10.1038/nrc2088

58. Shrinivas, K., Sabari, B. R., Coffey, E. L., Klein, I. A., Boija, A., Zamudio, A. V., Schuijers, J., Hannett, N. M., Sharp, P. A., Young, R. A., & Chakraborty, A. K. (2019). Enhancer Features that Drive Formation of Transcriptional Condensates. Molecular Cell, 75(3), 549-561.e7. https://doi.org/10.1016/j.molcel.2019.07.009

59. Simon, C.S., Hadjantonakis, A.-K., and Schröter, C. (2018). Making lineage decisions with biological noise: Lessons from the early mouse embryo. Wiley Interdiscip. Rev. Dev. Biol. 7, e319.

60. Skowronska-Krawczyk, D., Ma, Q., Schwartz, M., Scully, K., Li, W., Liu, Z., Taylor, H., Tollkuhn, J., Ohgi, K. A., Notani, D., Kohwi, Y., Kohwi-Shigematsu, T., & Rosenfeld, M. G. (2014). Required enhancer-matrin-3 network interactions for a homeodomain transcription program. Nature, 514(7521), 257–261. https://doi.org/10.1038/nature13573

61. Spector, D. L., & Lamond, A. I. (2011). Nuclear speckles. Cold Spring Harbor Perspectives in Biology, 3(2), 1–12. https://doi.org/10.1101/cshperspect.a000646

62. Stavreva, D.A., Garcia, D.A., Fettweis, G., Gudla, P.R., Zaki, G.F., Soni, V., McGowan, A., Williams, G., Huynh, A., Palangat, M., et al. (2019). Transcriptional Bursting and Co-bursting Regulation by Steroid Hormone Release Pattern and Transcription Factor Mobility. Mol. Cell 75, 1161-1177.e11.

63. Suter, D.M., Molina, N., Naef, F., and Schibler, U. (2011). Origins and consequences of transcriptional discontinuity. Curr. Opin. Cell Biol. 23, 657–662.

64. Wang, S., Su, J., Beliveau, B. J., Bintu, B., Moffitt, J. R., Wu, C., & Zhuang, X. (2016). Spatial organization of chromatin domains and compartments in single chromosomes. Science, 544(2011), 2955–2960.

65. Wang, S., Su, J., Zhang, F., Zhuang, X., Misteli, T., Misteli, T., Hübner, M. R., Spector, D. L., Robinett, C. C., Miyanari, Y., Ziegler-Birling, C., Torres-Padilla, M.-E., Chen, B., Ma, H., Chen, B., Esvelt, K. M., Ran, F. A., Hocine, S., Raymond, P., … Zhuang, X. (2016). An RNA-aptamer-based two-color CRISPR labeling system. Scientific Reports, 6, 26857. https://doi.org/10.1038/srep26857

66. Wernet, M.F., Mazzoni, E.O., Çelik, A., Duncan, D.M., Duncan, I., and Desplan, C. (2006). Stochastic spineless expression creates the retinal mosaic for colour vision. Nature 440, 174–180.

67. Zaret, K. S., & Mango, S. E. (2016). Pioneer transcription factors, chromatin dynamics, and cell fate control. Current Opinion in Genetics & Development.

68. Zoller, B., Little, S.C., and Gregor, T. (2018). Diverse Spatial Expression Patterns Emerge from Unified Kinetics of Transcriptional Bursting. Cell 175, 835-847.e25.

Chapter 2: An enhancer's tale: cell biological and biophysical strategies of transcriptional regulation

2.1 Abstract

Gene control by transcriptional enhancers is one of the dominant mechanisms behind the cell-type and signal-specific transcriptional diversity in metazoans. Intense research over the past four decades has not only provided surprising insights into the ever-increasing complexity of eukaryotic gene regulatory programmatic networks but has also revealed important principles underlying cell-type specification, tissue homeostasis, and the genetic basis of disease conditions. Multidisciplinary efforts in the past decade have provided novel insights into enhancer-mediated gene control. Real-time imaging and genetic approaches shed light on the role of RNAs and intrinsically disordered regions of proteins in enhancer complex assembly and the molecular basis of *in vivo* functions of enhancers. Biophysical experiments reveal the role of biomolecular condensate and the cell biological basis of enhancer activation. Here we review the outcome of these efforts, which challenges several conventional paradigms of enhancer functions. We will also outline major challenges that need to be tackled next.

2.2 Introduction

Spatio-temporal control of gene expression is crucial for precise developmental programs, cell-type specification, and cellular responses to the environment. Transcription regulators predominantly interact with regulatory genomic elements like promoters and enhancers to precisely orchestrate gene activation and repression in response to signaling cues. Promoters flank the transcription start sites

of all genes, both in unicellular and multicellular organisms and recruit general transcription machinery to facilitate basal activation of the genes[1,2]. Enhancers recruit cell-type specific or signal-activated transcription factors and co-factors to activate transcription from promoters from distant genomic regions[3,4].

Even after four decades since the initial discovery[5], and with extensive research, our understanding of enhancer biology is far from complete. For instance, there is still no clear consensus on how many functional enhancers exist in different cell types in metazoans. Numerous next-generation sequencing based efforts have provided invaluable insights into the genetic and epigenetic features of enhancer elements[6,7]. Elevated levels of H3K27ac, H3K4me1/2[8-10], and higher levels of chromatin binding of proteins such as p300 acetyl transferase[11] and the mediator complex[12] are some of the commonly used epigenetic features to define putative enhancer elements. Most of these regions with enhancer-like features also tend to be nucleosome free open chromatin[13,14]. Based on these criteria, the human genome is reported to have close to a million regulatory elements[15]. How many of these elements have in vivo regulatory activity is not yet known. Epigenetically defined enhancers do not always exhibit *in vivo* enhancer activity[16], and conversely, genomic regions with no known enhancer-like feature may have regulatory potential[17,18]. The lack of robust assays to test the context-specific *in vivo* enhancer activity limit the accurate estimation and validation of functionally active enhancers in the biological context. For the purpose of this review, we use the term enhancers to refer to cis-regulatory elements that have epigenetic features of the putative enhancers. We also interchangeably use the terms “enhancer strength” or “enhancer robustness” to refer

to the regulatory potential of the enhancers based on the level of eRNA transcription from these loci or in the case of signal-activated enhancers, the fold-induction of mRNA from the closest putative target genes.

Another area of active debate is how meaningful are the epigenetic features used to define the putative enhancers. For example, from the analysis of thousands of genomics data sets, we appreciate several commonalities between enhancers and promoters. High throughput chromatin conformation capture studies and genome perturbation analyses reveal that promoters, in addition to controlling the downstream target genes, also engage in long-distance interaction with other promoters[19] and behave as enhancers by activating transcription of neighboring genes[17,20,21]. On the other hand, like gene promoters, enhancers are also found to be active transcription units producing a class of non-coding RNA known as enhancer RNA (eRNA)[22,23]. As a result of these findings, genomic regions with regulatory activities are now commonly being referred to as cis-regulatory elements (CRE). Interestingly, many signal-regulated DNA binding transcription factors bind preferentially oy enhancers, casing their activation temporally preceding the subsequent activation of their cognate gene promoter.

The overall objective of this review is to highlight the aspects of enhancer biology for which we have yet to find answers, and how some emerging concepts help to potentially fill this gap. Advances in real-time imaging, genome editing, and biophysical techniques have expanded the availability of tools to better understand the physical and thermodynamic principles driving three-dimensional gene regulation. We will discuss the outcome of these multidisciplinary efforts that challenge several

conventional paradigms of enhancer functions and shed light on the cell biology of *in vivo* enhancer function. Finally, we give a brief overview of the aspects of enhancer biology that need immediate attention and will propose strategies to address these questions.

2.3 Enhancer-promoter communication

How enhancers control gene expression from far away genomic loci is still largely an enigma. In recent years, the gene regulation field has made use of advancements in super-resolution microscopy and live cell imaging tools to study transcription factor dynamics and visualization of enhancer-promoter (E-P) communication in live cells [24]. Single molecular tracking (SMT) of transcription regulators and the real-time imaging of genomic loci have been used to study the dynamics of transcription complex assembly and genomic interactions. Here we will review the key insights gained from these experiments.

Enhancer control of gene bursting kinetics: Transcription does not occur at constant levels over time, but rather in acute bursts, a phenomenon that has been observed across the full spectrum of model organisms, including prokaryotes, yeast, Drosophila species, C. elegans, mice and humans[25-27]. Bursting has been shown to facilitate precisely regulated responses to developmental or environmental signals[28-31]. Both live imaging and RNA-FISH experiment data indicate that enhancers can increase transcription rate either by increasing the frequency of the gene bursting (Burst frequency)[28,32-35] or by increasing the amount of nascent transcript through the high concentration of the transcription machinery (burst size)[30,3638] (Fig. 2.1 a, b). For example, the dynamics of enhancer-regulated burst transcription activity were directly

examined by a study that imaged the mRNA of a gene (*TFF1*) induced by the hormone estrogen in a human breast cancer cell line[35]. *TFF1* exhibits minimal activation in the absence of estrogen, but hormonal stimulation significantly increases the frequency of transcriptional bursts to a rate of approximately one burst every hour. The role of an estrogen receptor-regulated enhancer in activating burst transcription was then confirmed, as deletion of the cognate enhancer led to a reduction in the burst frequency from ~66 minutes to ~126 minutes. These studies establish enhancer regulation of gene transcription through bursting, suggesting that the interaction between enhancers and gene promoters is a highly dynamic process. Consistent with this, live visualization of E-P dynamics demonstrates a positive correlation between transcription bursting and enhancer mobility[39], lead to the proposal that increased enhancer and promoter mobility may facilitate enhancer activation of gene burst transcription by increasing the stochastic frequency of E-P interactions. In contrast, underscoring the uncertainty regarding the precise mechanism of E-P communication, several studies that predominantly used conformation capture-based approaches in developmental model systems suggest that E-P interactions are preestablished[40,41]. The genes and corresponding enhancers are present in close spatial proximity early in the developmental program. We speculate that at the mechanistic level both the developmental and the signalactivated enhancers would operate with similar kinetics with increased activity-dependent mobility and interaction. In both developmental and signal-induced gene programs, gene regulation occurs primarily through RNA PolII pause release[42-44] and several enhancers activate gene expression by PolII pause release[44,45].

Communication through looping: The current models of spatial gene regulation is mostly based on the data obtained from high throughput derivatives of chromatin conformation capture (3C) technologies[46]. These data together suggest that enhancers and promoters exhibit complex one-to-many or many-to-many looping patterns and that the majority of enhancers are functionally linked to a single target promoter [47,48]. In contrast to these results, live-cell imaging studies indicate that an active enhancer in a topologically associated domain (TAD) has an opportunity to contact many promoters inside the domain, presumably due to the Brownian motion of the enhancer DNA[49]. Although multiple studies using the genomics and statistical approaches have helped in the identification of enhancers and their target genes[50-52], the precise mechanism behind the specificity of E-P communication is largely unknown.

Several models have been proposed to explain the mode of communication between enhancers and their cognate promoters[53] (Fig. 2.1 c, d). According to the looping model, the enhancers loop over to the promoter regions as a result of extrusion of the intervening sequence. A number of proteins have been shown to facilitate E-P contacts:

CTCF and Cohesin: The cohesin complex, a ring-shaped protein complex involved in chromosomal architecture[54], has been shown to associate with transcription co-factors such as Mediator complex, to establish cell-type specific E-P contacts[55,56] (Fig. 2.1c). Cohesin co-occupy the chromatin with another architectural Zn-finger protein CTCF, suggesting a co-operative role for these proteins in chromatin architecture through a mechanism that involves loop extrusion[57,58]. The

cohesin complex is loaded as a ring on the chromatin and extrudes the DNA through its ATP-dependent motor activity until it collides with CTCF[59]. Although CTCF is predominantly associated with the formation of large chromatin domains through its insulation property, a number of studies also suggest its role in E-P looping through binding at convergent sites[60,61]. According to one study, approximately 60% of the most active gene promoters in a given cell type are typically occupied by CTCF[62], although at a much lower level compared to TAD boundaries. In the case of estrogen hormone-induced gene activation, mutation of the CTCF sites in the preferred target promoter resulted in the re-targeting of the enhancer to the next best CTCF-bound promoter located in the same contact domain, even though it was not the closest with respect to linear distance. A CTCF mutant (Y226A/F228A) defective for cohesin interaction failed to promote such enhancer retargeting, thus clearly indicating a role of CTCF-cohesion complex in signal-dependent E-P contact[62]. However, while the near-complete depletion of cohesin and CTCF has a huge impact on the 3D organization of the genome, its impact on enhancer-promoter looping and gene transcription varies depending on the cell types, depletion strategies, and assays used to map the interaction[63-65]. It is also possible that the cohesin complex may function beyond its role in chromatin looping, for example as a molecular platform to assemble transcription machinery[66].

LDB1 and YY1: One mechanism of E-P contact through looping is achieved by molecular bridging through protein homodimerization. LDB1 is one such protein that is suggested to enable E-P looping through homodimerization of molecules bound to enhancer and promoter regions (Fig. 2.1c). In support of this model, forced looping of

beta-globin locus control region to the fetal β-globin promoter, using the selfassociation domain of LDB1, in primary human erythroblasts increases the bursting frequency for the β-globin gene[67,68]. Chromatin occupancy data suggest that in a large fraction of erythroid genes known to engage in enhancer contact through LDB1 do not recruit cohesin to these sites suggesting that cohesin is not required for LDB1 anchored E-P contacts[69]. YY1 is another example of a protein that facilitates E-P contact through homodimerization[70]. It is possible that the ubiquitously expressed proteins like cohesin and YY1 facilitate tissue-specific E-P interaction through their association with cell type-specific transcription regulators[69,71]. Studies have also indicated the role of RNA in oligomerization of chromatinbound architectural proteins such as CTCF[72,73] and transcription factor YY1 (Fig. 2.1d)[74]. Deletion of RNA-binding domain of CTCF disrupted the expression of ~500 genes and a subset of topological boundaries[75]. It is not clear whether this gene regulatory effect is mediated through transcriptional enhancers, although the deregulated genes tend to be located closer to the disrupted chromatin loop. Similarly, the enhancer-binding of YY1 is mediated through local RNA interaction[74]. Taken together, these findings strongly suggest a role for RNA in concentrating transcription machinery at enhancers and sites of active transcription (Figure.1d).

Approximately 40% of enhancer elements skip intervening gene loci to interact with preferred target promoters[19,76]. This suggests a high degree of specificity in E-P interactions. Further, there are several examples for pre-existing E-P loops, and a significant fraction of these promoters contain a paused RNA Pol II [40,77]. In these instances, the promoters are already primed for activation, potentially through their

association with the enhancers. A secondary event, such as signal activation or change in topology, is needed for the full activation of the gene[46]. Together, these results support the view that direct E-P interaction, possibly mediated by chromatin-bound proteins, is needed for transcriptional activation. Although several proteins and mechanisms have been implicated in the E-P communication, it is likely to be a cell-type and context-dependent event. Using a novel nucleosome-resolution chromatin conformation strategy[78,79], a study showed minimal roles for proteins such CTCF, cohesin complex, and YY1 in the short-term maintenance of E-P interaction that is already established[66]. This suggests the involvement of distinct machinery in the establishment and maintenance of the E-P interactions. However, as discussed below, emerging evidence from imaging studies indicates that physical E-P contact may not be a universal requirement for enhancer action.

Gene activation without looping: While stable E-P looping is the conventional model explaining enhancer-promoter interactions, many recent live-imaging studies produce a more complex picture of enhancer-promoter communication. Simultaneous visualization of two different reporter genes tagged with either MS2 or PP7 viral RNA hairpins in Drosophila embryos [33] shows a high frequency of coordinated bursting of the reporter genes linked to the same enhancer, thus providing evidence that one enhancer can simultaneously target multiple target genes. Using a similar approach, another study reveals that during the process of interchromosomal regulation of homologous genes (transvection), a shared enhancer co-activates homologues genes in both *cis* and *trans*-chromosomes[37]. Further studies using this transvection system reveal that although enhancer and promoter come into relative spatial

proximity in an activity-dependent manner, relatively large distances (300-400nm) separate the co-activated genes and the enhancers[36]. Live-imaging of transcriptional activation of a reporter gene by the endogenous evenskipped enhancers, separated by a genomic distance of 150 kb, shows that the reporter gene transitions from an average distance of ~600nm from the enhancer in the “off” state to an average distance of ~350nm in the “on” state. While this study indicates that the enhancer and promoter come in closer proximity during activation, the 350nm proximity needed for E-P activation is a distance far exceeding that which would be expected by the looping model (Fig. 2.1f) [80]. Furthermore, this interaction was on average maintained for the duration of gene activation, which in this system was approximately 40 minutes.

A meticulous visualization effort examining the spatial dynamics of *Sox2* enhancer and promoter reports gene bursting in the absence of direct promoter-enhancer looping [81]. This study uses tetO–TetR and cuO– CymR systems (Supplementary Table 1) to create a persistent fluorescent genomic label of the Sox2 promoter and its enhancer. Additionally, the *Sox2* transcript itself is MS2 tagged, allowing for the simultaneous visualization of bursting and E-P movement. While the *Sox2* enhancer and promoter persistently remain relatively close to one another (mean distance of 339nm), no spatiotemporal relationship was observed between *Sox2* transcription and E-P proximity. Along the same lines, DNAFISH based measurement of spatial distance between Shh and its neural enhancers suggests that during transcription the enhancer and the target gene move farther away [82]. The ability of an enhancer to regulate a promoter without physical contact can, in turn,

explain the ability of an enhancer to regulate multiple genes simultaneously, as has been observed in the co-bursting of genes regulated by the same enhancer[33]. These data from live-cell imaging, together with a number of studies using genome-wide approaches, strongly suggest complex multi-way enhancer mediated gene control without direct E-P contact[83-85]. This could be an appealing model for the regulation of a large number of genes that need to be coordinately regulated in various developmental programs (Fig. 2.1f).

While several molecular studies and 3C based analysis support a looping mechanism for E-P communication, live-cell imaging studies largely favor gene activation without stable E-P loops. The major reason for this discrepancy could be the technical differences between 3C technologies and microscopy approaches[86-88]. As almost all 3C based tools rely on proximity ligation and are thus limited to detecting very close genomic interactions that can be tethered with the crosslinking agents, these methodologies are largely agnostic to the >200nm E-P proximities observed in the FISH and live imaging studies[33,80-82]. On the other hand, live-imaging approaches are generally low throughput with the examination of one or two alleles at a time. Therefore, the generalization of the observations in microscopy is challenging.

Even with considerable evidence supporting the idea that E-P regulation can occur without direct looping, there remain several questions regarding the mechanism by which this regulation occurs. What are the molecular events underlying transcription bursting? How do enhancers regulate promoter bursting at proximities greater than 200nm? Many upcoming technologies such as single-cell Hi-C methodologies [89,90], non- proximity ligation approaches for studying genome

organization[91,92], high throughput microscopy [93,94], and super-resolution live cell microscopy[95] will need to come together to better understand the mechanism of E-P interactions (Supplementary Table 1).

2.4 Assembly and architecture of enhancers

The majority of the cell-type specific and signal-specific transcription programs are controlled by a relatively small fraction of enhancers with superior regulatory potential, characterized by higher transcriptional activation in reporter assay increased expression levels of proximal genes, and high eRNA transcription[96-98]. We will discuss two conceptually related strategies to explain such elevated regulatory function of these enhancer elements. It is also important to note that the most active configurations of the enhancers are not necessarily the optimal configuration for the biological functions[99] and we will discuss the organization features of enhancers that help to maintain transcription at biologically optimum levels.

Enhancer strength through spatial clustering: Informatics analysis suggesting that clustered transcription factor binding sites are indicators of cis-regulatory elements[100,101] has previously been experimentally validated in the β-globin Locus control region (LCR) and other similar enhancer elements [102,103]. Genome-wide studies further illustrate that the clustered enhancer pattern is a common feature of most of the key cell-type-specification genes that are master regulators of gene expression programs both in ESCs and differentiated cells [97,104,105]. Such enhancer clusters, typically spanning approximately 820kb, are occupied by DNA-binding transcription factors, and are referred to as super enhancers or stretch enhancers[105,97]. These enhancer domains have an unusually high composite density

of cell type specific master regulators and mediator proteins and can engage in cooperative spatial association[85,106]. In certain instances, mutations in one of the constituent enhancers result in the deactivation of the entire super enhancer domain [107-109]. Conversely, nucleotide polymorphisms or disease mutations creating a novel transcription factor binding can be sufficient to create a super enhancer de novo [110]. These studies suggest the role of cooperative interactions in super enhancer formation[111] (Fig. 2.2 a,b). The co-operative interactions could be either additive or synergistic in nature[112]. An additive response refers to a linear relationship between the transcriptional activation of target genes and the number of the interacting enhancers. The additive regulation is observed when the enhancers function independently of each other and can contribute to target gene transcription individually[107,113,114](Fig. 2.2a). These enhancers can tolerate the loss of individual elements and typically regulate the genes expressed in a cell type specific, and the developmental stage independent manner[112,114-116]. Synergistic enhancers on the other hand depend on each other to elicit a switch-like response in the target gene expression[107,109,111] (Fig. 2.2b). Genes that need to be regulated with a rapid “on” or “off” kinetics, such as those regulated in response to acute signaling programs or those expressed in cell-type specific manner during differentiation would benefit from a synergistic mode of enhancer regulation[112]. One possible mechanism of enhancer synergism could be transcriptional complex condensation that facilitates multi-enhancer association (discussed below). However, the precise kinetics of the transcriptional synergy from enhancers are not fully understood. Together, these

results demonstrate that spatial clustering of enhancer elements facilitates the superior regulatory potential of the super enhancers.

Enhancer strength without spatial clustering: It is likely that cooperative spatial clustering of individual enhancers is not the only mechanism for achieving higher regulatory potential. For instance, even among super enhancers, there is ample evidence showing that the deletion of individual enhancers in a super enhancer domain does not always impact the regulatory potential of the super enhancers[107,113,114] which indicates that bioinformatically declared super-enhancers do not always possess superior regulatory potential. In addition, ~15% of bioinformatically defined super enhancers in mESCs are not clustered but contain only a single strong enhancer elements[117]. There are many examples of enhancers with high regulatory potential containing a single enhancer element. For example, in breast cancer cells, β-estradiol stimulation results in the activation of hundreds of non-clustered enhancers with very high levels of eRNA transcription and higher recruitment of chromatin regulators[96]. However, based on the bioinformatic criteria used for defining super enhancers, such as high H3K27Ac modification, or MED1 recruitment[97], only <30% of these enhancers overlap with super enhancers[118]. In addition to the typical transcription machinery recruited on the enhancers, these enhancers also feature binding by a large protein complex, called Megatrans complex, that is mostly composed of other transcription factors such as, GATA3, AP2ɣ, RARα, YAP/TEAD, and the architectural protein complex of condensins (Fig. 2.2c)[118-120]. Interestingly, many of these transcription factors can still be recruited to these regions even with the deletion of their DNA-binding domains, suggesting that

these factors are recruited through protein-protein interactions rather than protein-DNA interactions. Thus, a significant fraction of Megatrans-bound enhancers represent a cohort of functional enhancers that accomplish superior regulatory potential by bringing together a large ribonucleoprotein complex as a result of high-affinity binding of a single transcription factor[118,121]. Such enhancers that are mostly activated in response to ligand stimulation or cell differentiation also elicit a switch-like response shown by synergistic clustered enhancers[122-124] (Fig. 2.2 b, c). There are many important questions that remain to be answered. How do certain enhancers acquire superior regulatory potential with the initial binding of a single transcription factor? How does such a large multidomain complex assemble within minutes, if not seconds, of initiation of ligand-induced signaling program? One possibility is that the high-affinity binding of a single TF might lead to increased chromatin resident time and eventual recruitment of a large transcription factor complex. Super resolution live cell imaging studies might provide an answer with regard to this phenomenon.

Grammar of functional enhancers: While the above-mentioned mechanisms explain how enhancers can recruit large transcriptional complexes to elevate the target gene expression, an important role of enhancers is the optimized gene expression in a larger dynamic range in a cell-type specific manner. Sequence features of enhancer elements referred to as “enhancer grammar[125]”, such as the affinity, number, spacing, and orientation of the transcription factor binding sites within the regulatory elements, play a crucial role in gene activation at the biological level. Based on the features of transcription factor binding motifs two main models have emerged[126]. The “enhanceosome model” refers to the specific sequence and

orientation of transcription factor binding site[127,128]. The “billboard model” on the other hand is refers to the flexible sequence, but just requires the specific combination of the transcription factors binding to the enhancer[129].

It is very likely that enhancers follow diverse organizational and grammatical rules that are adopted over the course of evolution. The rigid enhanceosome model, mostly based on the IFN-β enhancer[127], requires precise arrangements and orientations of their composite transcription factor binding sites for the proper activity. In contrast, genome-wide analysis of conserved cis-regulatory sites in mouse and human embryonic stem cells (ESCs) reveals that on average these sites contain 12.6 conserved transcription factor binding motifs[130]. Functional validation of these sites indicates that a more relevant feature that determines the enhancer activity would be the diversity of the transcription factors recruited to the enhancer loci[131]. These findings together favor a billboard model for a large fraction of developmental enhancers. While flexibility and less rigid grammatical rules favor organismal evolution, the rigid grammar may be a favorable feature for precise and predictable gene control in response to signaling events or during the developmental transition.

The importance of “grammar” in developing organisms is demonstrated by a study on fibroblast growth factor (FGF) responsive enhancer for the gene *Otx-a* in the invertebrate chordate *Ciona intestinalis* embryos[99]. The optimal *in vivo* expression of *Otx-a* in the neural plate is dependent on the low-affinity binding sites for GATA and ETS transcription factors (Fig. 2.2d). A 3 bp insertion between GATA and ETS amplifies the *Otx-a* expression but results in aberrant expression of *Otx-a* in ectopic tissues. Almost all other spacing modifications significantly reduce the *Otx-a*

expression. Similarly, clustered low-affinity binding sites for the hox family protein Ultrabithorax are required for the tissue-specific expression of the target gene *shavenbody* in the *Drosophila* embryo[132]. These studies together indicate the 'suboptimal' organization of the enhancers are evolutionarily selected for the restrictive expression of genes at biologically optimum levels. In addition to the primary DNA sequence, the chromatin context such as distance to the cognate promoter, the surrounding chromatin state, association with nuclear microenvironments such as membraneless nuclear compartments[133], and the trans-recruitment of transcription factors to the enhancer regions [118,134] should also be considered in defining the enhancer grammar. However, so far there are only a handful of studies that have been able to predict and experimentally validate enhancer function based on such expanded enhancer grammar definition. The increasing breadth and depth of genome-wide functional assays and computational approaches will lead to significant advances in our understanding of enhancer grammar.

In summary, data from imaging and genomics studies reveal a complex picture of enhancer-mediated gene regulation. In order to unravel the underlying principles of the rapid kinetics of transcription complex assembly and the spatial organization of multi-way gene regulatory programs, we need to reconsider the current paradigms of enhancer activation. These questions insinuate the role of a complex nuclear environment in dictating genome organization and gene regulation and call for further examination of the cell biological basis of gene regulation and nuclear organization.

2.5 Enhancers as membraneless organelles

Compartmentalization of biomolecules is required to carry out intracellular biochemical processes. While membrane-bound organelles such as the endoplasmic reticulum and Golgi apparatus have been prototypical examples for cellular compartments, recent findings indicate that macromolecules involved in specialized cellular functions can be partitioned into mesoscale assemblies called “biomolecular condensates” without being confined by lipid bilayers[135]. Studies over the past few years have shown that many of these membraneless organelles are assembled through the physical process of liquid-liquid phase separation (LLPS). In this thermodynamically driven process, in response to changes in physical parameters, a homogenous mixture of macromolecules spontaneously “demixes” into two distinct compartments of high concentration and low concentration [136]. Emerging data indicate a crucial role of this thermodynamic process in gene regulation and enhancer functions (Supplementary File1).

Compartmentalization of enhancer apparatus: Early nascent RNA labeling and visualization experiments reveal that active transcription sites form distinct foci that are enriched for the elongating form of RNA Pol II[137,138]. These “transcription factories” are found to co-localize the co-expressed genes[139,140]. *In vivo* visualization of transcription factors and cofactors also reveal an activity-dependent spatial clustering of transcription regulators [141-144]. As described above, most active enhancers are characterized by high densities of transcription factors, co-factors, RNA PolII complex, and RNA molecules. Based on these *in vitro* results and the other puzzling features of enhancer biology described earlier, it is proposed that the

super enhancers are assembled following the principles of phase separation[145]. *In vivo* evidence in support of this model comes from live-cell imaging and biophysical experiments revealing that fluorescently labeled endogenous MED1, BRD4, various transcription factors, and RNA PolII subunit form structures that exhibit the physical properties of biomolecular condensates such as rapid exchange kinetics, fusion, and wetting properties[146-148]. *In vivo,* real-time imaging studies reveal that MED1 clusters colocalized with PolII clusters, and these structures are sensitive to the inhibition of transcription and also to aliphatic alcohol 1,6-hexanediol[146], which dissolves several membraneless compartments in a transient manner[149]. Further studies showed that several other transcription regulators also form 'transcriptional condensates' in the nucleus, which include signal-activated transcription complexes[148,150-153], RNA PolII[154,155], and PolII pause release machinery [156,157]. Altogether these *in vitro* and *in vivo* data suggest that the previously described transcription factories correspond to the phase-separated compartments at the enhancer and promoter loci[158]. An important question is what are the molecular features and biophysical forces driving the assembly of transcriptional condensates?

IDRs and RNAs in enhancer complex assembly: In addition to the well-structured DNA binding domains (DBDs), TFs also harbor activation domains that are mostly composed of low complexity domains (LCD) characterized by over-representation of one or few selected amino acids (ADs)[159-161]. The cellular events leading up to full enhancer activation in response signaling events involve a plethora of chemical reactions and molecular interactions. The initial phase of transcription factor-DNA interaction is highly dynamic with very low resident time on DNA. Pioneer

factors gain initial access to the nucleosome-bound DNA and facilitate the sequence-specific binding of the transcription factor. The direct transcription factor-DNA interactions mostly involve electrostatic interactions and van der Waals forces [162] (Fig. 2.3a). The precise molecular events leading to megadalton-sized enhancer complex observed in super enhancers or signal-induced enhancers is not clear. Here, we speculate that assembly of large transcriptional complexes involves several more steps in addition to transcription factor-DNA interaction. Chromatin-bound transcription factors recruit classic transcription machinery composed of RNA Pol II and various co-factors to initiate eRNA transcription. This stage involves low-affinity multivalent interaction between IDR regions of transcription factors and co-factors and is mediated through several types of chemical bonding[163] (Fig. 2.3b). In those enhancers with high-affinity binding of transcription factors or clustered super enhancers, elevated local eRNA act as a scaffold to interact with transcription complex to further stabilize it into dynamic biomolecule condensates (Fig. 2.3c) (Also see Box.1). In condensates, the component disordered domains engage in relatively non-specific transient interaction and exist in a fuzzy interface[164,165]. The alternate view is that the LCDs are engaged in specific structured interactions with certain LCDs even forming labile, reversible cross-β polymers [166-168]. It is likely that the condensates are assembled through a combination of both high-affinity and low-affinity interactions.

RNA molecules can also promote condensate assembly by intermolecular RNA-RNA interactions or by acting as a scaffold to enrich the local concentration of multivalent RNA-binding proteins [169,170]. RNAs can enhance the phase separation

potential of proteins with IDRs by direct binding[171,172]. Sites of active transcription might provide the proper milieu for the condensate assembly through this process due to the high local concentration of RNA and several proteins harboring extended Serine/Arginine repeats such as splicing factors SRSF family of proteins[173,174]. There are several well-documented examples where longnoncoding RNAs (lncRNA) interacting directly with canonical and non-canonical RNA binding proteins to influence gene regulation and genome organization[175-178]. Consistent with these findings, a growing number of examples demonstrate that RNAs are not only a product of transcription but also play active regulatory roles. For example, several DNA binding transcription factors and co-regulators also efficiently bind to RNAs[179]. Transcription factors such as FUS[180], YY1[74,181,182], CTCF[72,73,75], BRD3[183], and transcriptional cofactor MED1[184] directly interact with RNA. This interaction enhances their chromatin recruitment and transcriptional activation. eRNAs can also bind directly to transcription regulators and act as a condensate scaffold at the enhancers[74,185] (Box.1). In addition, the roles of chromatin-associated RNAs and retrotransposon repeat RNAs in enhancer activity, gene regulation and chromatin architecture are just beginning to be unraveled[176,186,187].

2.6 Puzzles, solutions, and new concepts

An important feature of the enhancers that has come into focus recently is the rapid kinetics of assembly of mega-Dalton-sized transcription complexes on signal-activated super enhancers [118,120,123,188]. How do transcription factors and cofactors search and find the target sites with rapid kinetics? How do enhancers control gene expression even while separated by a spatial distance of ~300nm[81,82]? These

important and fundamental questions still largely remain unanswered. Based on imaging and biophysical findings discussed here we take significant liberty to speculate and propose few models to answer some of these questions. These models can be tested with the available and emerging technologies.

Mechanisms of long-distance genomic interactions: In those cases where there is no evidence of looping, how does the E-P communication works? How E-P specificity is achieved? Super-resolution live cell imaging revealed that PolII and mediators form stable clusters with a mean size of 300nm, [146] raising the possibility that transcription factories or condensates, may act as nuclear platforms mediating longdistance genomic interaction[139,189], and therefore, E-P contacts (Fig. 2.4a). Surface tension driven movement and fusion of artificially created condensates have been predicted to contribute to the chromatin architecture[190]. Due to the similarities in the functional activity of enhancers and promoters[98,191], particularly those activated in response to a signaling program, we speculate that complexes assembled at enhancers and cognate promoters would be compositionally, not quantitatively, similar to facilitate droplet fusion, as seen in the case of *in vitro* and *in vivo* homogenous condensates[192](Fig. 2.4a). E-P condensate fusion increases the concentration of transcription machinery at the promoter and increase transcription.

Although the vast majority of enhancers and their cognate genes are located in the same genomic domains (TADs or insulated neighborhoods) [193,194], there are many instances of long-distance genomic interactions beyond the confines of the TADs. Genes, that are even located on different chromosomes, that are coregulated by signaling programs such as TNFα and β-Estradiol, have shown to engage in

signal-induced spatial associations [96,153,195-199]. Similarly, super enhancers activated in a cell-type specific manner also can engage in long-distance interactions [83,84,200,201]. The mechanism of inter-TAD or inter-chromosomal interactions is not easily explainable by conventional models. In olfactory receptor neurons, the cooperative inter-chromosomal interaction of the olfactory receptor enhancers is mediated through looping factor LDB1 recruitment by transcription regulators Ebf and Lhx2[202,203] (Fig. 2.4b). Enhancers are also found to form extensive networks during mesenchymal differentiation and seem to stabilize the TF binding of interacting enhancers, suggestive of high-density clustering of gene regulatory machinery[201].

The ligand-induced spatial proximity of enhancer is abolished by eRNA depletion[96,153,199], and the aliphatic alcohol 1,6-Hexanediol, which is known to disrupt the assembly of several phase separated membraneless organelles[153]. These studies together suggest a possible role of RNP condensates in the establishment of enhancer networks and the genome-wide coordination of transcriptional programs. Similar to the condensate coalescence model proposed above for the E-P interactions, the enhancers activated by the same signaling programs are also likely to assemble compositionally transcriptional condensates and would be able to interact with each other in a surface tension-driven manner[190]. (Fig. 2.4b). Ongoing efforts on SMT approaches aimed towards simultaneous visualization of the *in vivo* labeled eRNA, mRNA, and transcription factors would help answer this question.

Multitasking by nuclear organelles: The eukaryotic cell nucleus contains a large number of membraneless compartments with diverse biological functions[163,204]. Several studies have demonstrated that actively transcribed genes and enhancers

are known to engage in cooperative interaction on nuclear speckles[153,205-208]. Techniques such as SPRITE[92] and TSA-seq[91], that probe the genome organization without proximity ligation reveal that the human genome is compartmentalized around nuclear speckles and nucleolus in an activity-dependent manner[209]. The actively transcribed genomic regions are segregated near nuclear speckles, while the majority of the transcriptionally inactive regions are associated with nucleoli. Other studies have found that disruption of the nuclear speckle through either 1-6-hexanediol or knockdown of splicing components SRSF1 or U2AF1 results in dampened transcription of genes and enhancers that are localized to the speckle. A poorly characterized nuclear assembly built around matrin3 protein, a DNA-RNA binding protein with diverse biological function[210], is another such non-membrane bound nuclear compartment shown to contribute to transcription regulation upon colocalization with target enhancers[211] (Fig. 2.4c). Pit1, the POU-homeodomain transcription factor necessary for the differentiation of progenitor cells in the anterior pituitary, binds many enhancers and recruits them to the matrin3 network through interaction with protein partners, SATB1 and β-catenin. A point mutation in Pit1 blocks its interaction with β-catenin and SATB1, which prevents the activation of Pit1 target enhancers due to failure to recruit to Matrin3 (Fig. 2.4c). Artificial tethering of the transcription machinery to matrin3 network by fusion of mutant Pit1 with matrix attachment regions such as SAF/SAP domains resulted in the rescue of the enhancer activation and gene expression, suggesting the critical role of subnuclear localization in gene expression and alternate functions of membraneless compartments[211]. While nuclear speckles are generally considered to be storage

factories for splicing machinery[212] and the nucleolus is primarily responsible for ribosomal RNA transcription and ribosomal assembly[213,214], these and several other studies[215-218] together support the model that subnuclear compartments and nuclear proteins may be playing multiple roles for transcription activation programs.

Another example of molecular multitasking is the case of transcription factors functioning as co-regulators on enhancers in a DNA-binding independent manner. (Fig. 2.4c). Transcription factors can be recruited to enhancer complex indirectly through tethering mechanisms. Indirect binding is defined by open chromatin conformation and ChIP-seq signal for the transcription factor of interest but without the consensus motif features[118,219-221]. It is also difficult to distinguish the possibility of indirect co-operative binding of transcription factors on the enhancer sites where they also bind directly. Single molecular imaging of LCD from transcription factor FET and another transcription factor Sp1 provide many insights into the dynamics and specificity of IDR in transcription complex assembly and also transcription factor tethering[222]. The transcription factor- LCDs form distinct nuclear puncti that recruit RNA-PolII machinery and exhibit dynamic internal molecular exchange. While the FET LCDs engage in self-interaction, they did not interact with Sp1 LCD, indicating the sequence specificity in disordered domain interaction. Interestingly, the pathogenic proteins formed through the fusion of DNA binding domain of FLI and IDR of another transcription factor EWS are retargeted to microsatellite repeats, which is distinct from the endogenous targets recognized by wildtype FLI protein[223]. This, and a number of other pieces of data support the role of IDRs in genomic targeting of transcription factors by DNA-binding independent mechanisms[150,153,224,225]. The

structural and motif features in the IDR that give the specificity to such interactions are still not clear.

Regulatory roles of enhancer-bound condensates: In addition to establishing biophysical and thermodynamic principles of transcription complex assembly, do transcriptional condensate offer any new gene regulatory mechanisms? A number of findings suggest that enhancer-bound condensates might be involved in gene regulation in previously unappreciated ways. For instance, RNA can act as negative modulators of transcription as a result of electrostatic repulsive forces[226]. In this scenario, in contrast to complex coacervation that results in electrostatically driven assembly of the condensates[174], an electrostatic repulsive mechanism, known as reentrant phase transition, would drive condensate disassembly[226]. While complex coacervation is mediated through positively charged protein domains and RNAs drive condensate assembly, higher RNA concentration has been shown to drive condensate disassembly and vacuole formation through a charge inversion mechanism[227]. It is possible that reentrant phase transition could be the underlying biophysical principle for transcriptional bursting, where-in increased transcription, as observed as bursting, is mediated through condensate assembly (Fig. 2.5a). This high transcriptional activity is abrogated as a result of condensate dissolution with a high local concentration of RNA, therefore acting as a potential feedback regulatory mechanism. Consistent with this model, both mRNA and eRNA can modulate assembly and disassembly of mediator condensates, with low levels of RNA favoring condensate assembly and higher levels resulting in its dissolution [228]. Simultaneous live-cell super-resolution imaging of endogenously labeled transcription complex and

RNA would be needed for proper in vivo validation of this model. The physical properties of condensates can vary depending on the post-translational modifications[229], disease mutations[230], and local concentration solvent molecules[231,232]. Material properties of transcriptional condensates were also found to correlate with transcriptional activation. With an increase in the duration of stimulation with the hormone estrogen, the physical property of the ER puncti changes from liquid to gel-like consistency with a corresponding decrease in enhancer activation, measured with eRNA transcription level(Fig. 2.5b)[153]. While pathological mutations have been shown to result in maturation and solidification of the condensates[230,233,234], this report suggests that altered material states could also have a regulatory role in ligand-induced enhancer activation.

2.7 Future perspectives

Four decades of research on enhancer biology have provided a wealth of insights into regulatory biology of development, health, and diseases. Advances in genomics tools will continue to identify novel chromatin features of enhancers. CRISPR-based genetic perturbation strategies have already begun to identify functional enhancers in multiple cell types. However, our understanding of the molecular mechanisms of enhancer function is still rather rudimentary. We are listing here four areas where we have major gaps in knowledge and how the emerging technologies would help to close that gap.

Cataloging of functional enhancers: Epigenetic approaches have identified millions of “enhancerlike” cis-regulatory elements. But epigenetics features are only surrogate marks for regulatory activities. There are several questions that remain to

be addressed as part of these cataloging efforts. How many of them have regulatory functions *in vivo*? How do genomic variations in enhancers cause diseases? How to identify the targets of enhancers? There are many exciting technologies that would help to answers these questions at least partially (Supplementary Table 1). Cas9-directed genome editing, the most revolutionary technology of the past decade, helps to manipulate the genome with incredible precision and throughput[235]. High throughput genome and epigenome editing strategies offer great promise towards comprehensive cataloging of regulatory elements[236-238]. Loss of function screen by NHEJ-mediate deletion or dCAS9 fused to inhibitory domains such as KRAB[239], histone demethylase-LSD1[240], and gainof-function studies using VP16, or p300-dCAS9 fusion have been successfully employed to identify regulatory elements in the genomic regions of interest. Assays such as Mosaic-seq[241] and Targeted Perturb-seq[242] that combine epigenome editing with single-cell transcriptomics offers efficient, highconfident mechanisms to detect the regulatory potential of selected enhancers at single-cell resolution. Although still expensive to apply at genomic scales, iterations of such strategies would clearly help to validate functional enhancers identified through epigenome marks.

An equally important problem is the functional validation of disease-associated single nucleotide polymorphism (SNPs) at the enhancer elements. A large fraction of disease associated SNPs is concentrated at the enhancers[243-246]. But only a few of these SNPs were functionally validated to have a phenotypic impact. Cas9-mediated saturation mutagenesis would be a useful high throughput strategy to detect regulatory SNPs in gene regulation[247]. Through genome-wide enhancer networks

(discussed earlier), potentially mediated through transcriptional condensates, it is possible that mutations on a given enhancer could have a much broader impact that might have a subtle but additive effect on disease development and therapy (Box.2). Yet another important area in the cataloging effort should be the identification of the direct enhancer targets. Currently, the enhancer targets are assigned based on an informatically detected correlation between epigenomic and transcriptomic signature between enhancers and neighboring promoters[248,249], a correlation between non-coding variants and gene expression level across population[250], and by overlapping Hi-C loop information with annotated enhancers and promotes[251,252]. Enrichment strategies of Hi-C approaches are being used to obtain deeper sequencing of selected genomic regions such as ChIA-PET[76], Hi-ChIP[253], PLAC-seq[254], Capture-HiC[255], and Micro-C[66].

Imaging transcription to study the thermodynamics of gene regulation: Transcriptional condensates assembled through IDR interaction is an attractive system to study the thermodynamics of gene regulation and genome organization (Supplementary file1) However, this model is in no way beyond any caveats. A vast majority of biophysical studies on condensates are performed on *in vitro* constituted systems with minimal compositional complexity. Complex *in vivo* environments can also influence the physical properties of condensates and the ability of macromolecules to co-partition[256], which can lead to conflicting *in vitro* and *in vivo* observations. Many widely used “condensate diagnostic parameters” are not rigorous and are mostly qualitative in nature (condensate shape, size, fusion, etc.)[257,258]. More rigorous *in vivo* data is needed to better understand the biophysical principles driving

the transcription complex assemblies. Regardless of the underlying physical principles, overwhelming evidence supports the spatial clustering of transcription factors, co-factors, and RNA PolII in actively transcribed loci. There are several important questions that remain to be answered. Do the condensates from different enhancers fuse as liquid droplets or do they maintain their identity? How does the molecular information transfer between condensates? How does the condensate model help to explain E-P specificity? It is clear that the term “disorder” does not equate to a total lack of structures. IDR domains are interspersed with short linear motifs (SLiMs) that can engage in highly specific interactions.

Biophysical and computational approaches have been applied to predict the phase behavior of IDR domains[259]. Such methodologies once applied to characterize and classify the low complexity domains of transcription factors will significantly expand our understandings of the physical principles driving the assembly of unique transcription factor complex. Another exciting possibility is the ability of transcription factor IDRs to specifically interact with cellular metabolites and small molecules. A recent study demonstrates that *in vitro* assembled MED1-IDR condensates concentrate several therapeutic small molecules and target them to enhancer regions[260]. If this phenomenon is relevant in the complex *in vivo* environment, it will render transcription machinery as an effective therapeutic target and also as a direct sensor of cellular metabolic states.

The main tool that would be used to address the mechanism of enhancer activity would be advanced imaging technologies. A high temporal and spatial resolution offered by super-resolution live imaging technologies promises to fill major

gaps in our understudying of E-P communication and biophysical features of transcriptional condensates[24,95]. Improved fluorescent chemistry and new computation tools would be needed for the simultaneous examination of TF dynamics, E-P interactions, and live imaging of transcription. The multiplexed FISH approach combined with super-resolution microscopy has been applied recently to visualize the architecture of an entire human chromosome[94]. Combined with visualization of RNA transcript and live cells, these approaches promise to overcome the low throughput nature and resolution limit of classic DNA FISH method [94,261]. Visualization of transcription is an area of active research that is limited by both the technologies available to label a transcribing locus without affecting transcription and also the live imaging tools at sub-diffraction limits. Our understanding of the transcriptional process and enhancer function will remain as only an approximation until these technologies mature.

2.8 Figures

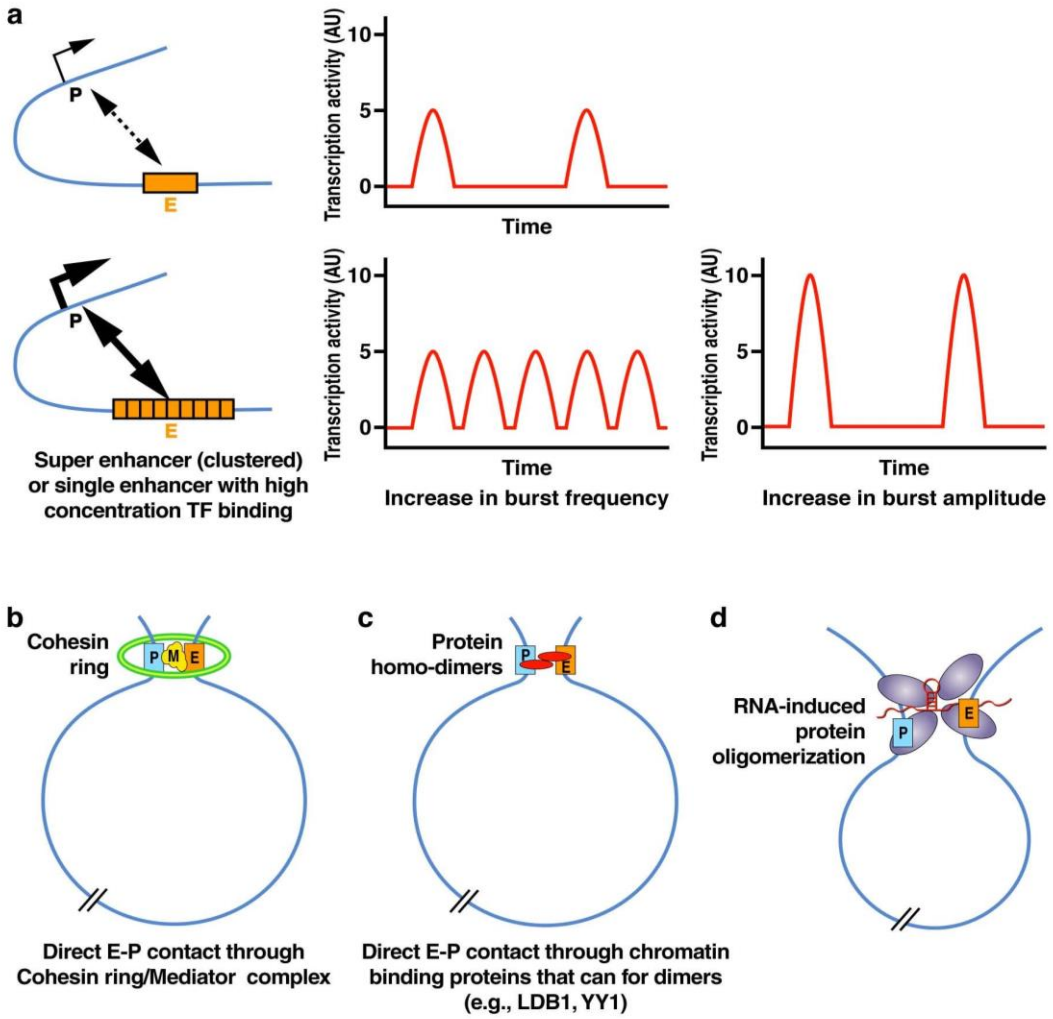

Figure 2.1. Mechanisms of enhancer-promoter interactions and control of gene burst kinetics: (a, b) Enhancers control gene expression through controlling the bursting kinetics. The stronger enhancer clusters or those enhancers recruiting large transcription complex can increase the RNA output of target genes by either increasing the burst frequency or burst amplitude **(c)** Cohesin loading at the enhancers through transcription cofactors (E.g., Mediators) facilitate E-P loop formation that might also involve CTCF (**d**) Proteins such as LDB1 and YY1, known to engage in homo-dimerization also can lead to stable E-P interaction and gene activation in certain genomic loci by associating with enhancers and cognate promoters **(d)** RNA mediated oligomerization of proteins can a facilitate enhancer function. Classic architectural protein CTCF undergoes oligomerization through RNA interaction. CTCF RNA-binding is required for the looping interactions of a fraction of genes. Transcription factor YY1 is tethered to enhancers through interaction with eRNAs.

Figure 2.2. Organizational principles of functional enhancers. Co-operative enhancer interactions could be either additive or synergistic (**a**) In additive interactions, participation of each enhancer element (E1E4) results in a linear increase in transcriptional output. T1, T2, T3 represent target mRNA quantitation. (**b**)In synergistic enhancer interactions, there is a switch-like response in transcriptional output once the number of interacting enhancers (E1-E4) and the interaction frequency crosses a threshold level. This strategy yields a minimal activation below the threshold level interaction and maximal response after the threshold level is reached. T4, T5 and T6 represent the level of transcription with indicated enhancer topologies (**c**) In addition to clustered enhancers, high-affinity binding of a single transcription factor could also populate megadalton-sized enhancer complex assembly. The pioneer factor (E.g., FOXA1) keeps the chromatin open to facilitate rapid signal-induced recruitment of transcription factors. An example of this mechanism is illustrated with a well-studied case of estrogen (E_2)-induced enhancers. In response to E_2, estrogen receptor □ (ER□) bind to a single enhancer and recruit megadalton-sized transcriptional complex potentially through low-affinity multivalent interactions. In addition to the classic co-activators, these enhancers recruit a large cohort of transcription factors potentially through protein domain interaction. At a proteomic level, both the clustered enhancers and non-clustered enhancers are occupied by similar machinery and may exist as ribonucleoprotein complex composed of transcription regulatory proteins and non-coding RNAs such as locally transcribed eRNA. eRNAs can also be modified through methylation which plays a functional role in enhancer activity. The blue hill and valley plot represent histone modification on the active enhancers (**d)** Signal-activated enhancers that nucleate the enhancer complex with ligand-induced binding of a single transcription factor can also elicit a switch-like response to target gene expression with minimal transcription before stimulus and maximal transcription post-stimulus **(e)** In *Ciona* embryos, the neural plate specific minimal enhancer for the gene Otx-1 is 69 base pair sequence composed of three GATA and two ETS binding sites (the 5' GATA-ETS motifs are shown here). The wild-type (WT) sequence is suboptimal for regulatory potential. Mutating transcription motifs for high-affinity binding (indicated by red star) OR addition of 3bp spacing between binding motifs for optimal spacing, alone can significantly elevate the reporter gene expression compared to WT, but this confirmation will result in expression of the reporter gene in the ectopic neural plate. Simultaneous modifications leading to both increase transcription factor binding and optimal spacing amplify the gene expression not only in neural plates but also in several other ectopic tissues. These data demonstrate that suboptimal confirmation of certain enhancers might be evolutionarily favored to restrict the expression of developmental genes to specific tissues.

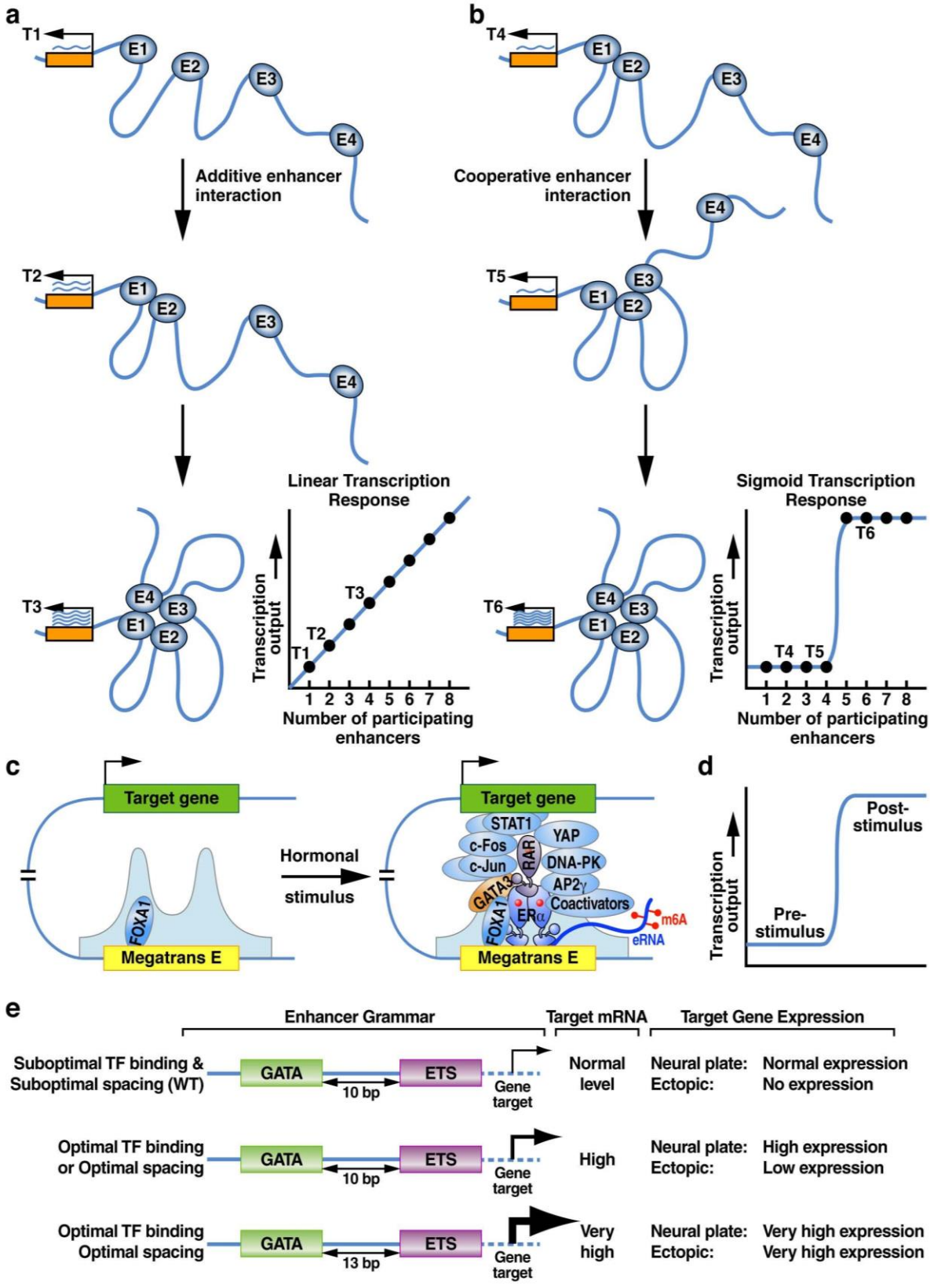
a
T1
E1
E2
E3
E4
Additive enhancer interaction
T2
T3
b
T4
Cooperative enhancer interaction
T5
T6
Linear Transcription Response
Transcription output
Number of participating enhancers
Sigmoid Transcription Response
c
Target gene
FOXA1
Megatrans E
Hormonal stimulus
STAT1
YAP
c-Fos
c-Jun
RAR
DNA-PK
AP2γ
GATA3
Coactivators
ERα
m6A
eRNA
d
Post-stimulus
Pre-stimulus
e
Enhancer Grammar
Target mRNA
Target Gene Expression
Suboptimal TF binding & Suboptimal spacing (WT)
GATA
ETS
10 bp
Gene target
Normal level
Neural plate: Normal expression
Ectopic: No expression
Optimal TF binding or Optimal spacing
High
Neural plate: High expression
Ectopic: Low expression
Optimal TF binding Optimal spacing
13 bp
Very high
Neural plate: Very high expression
Ectopic: Very high expression

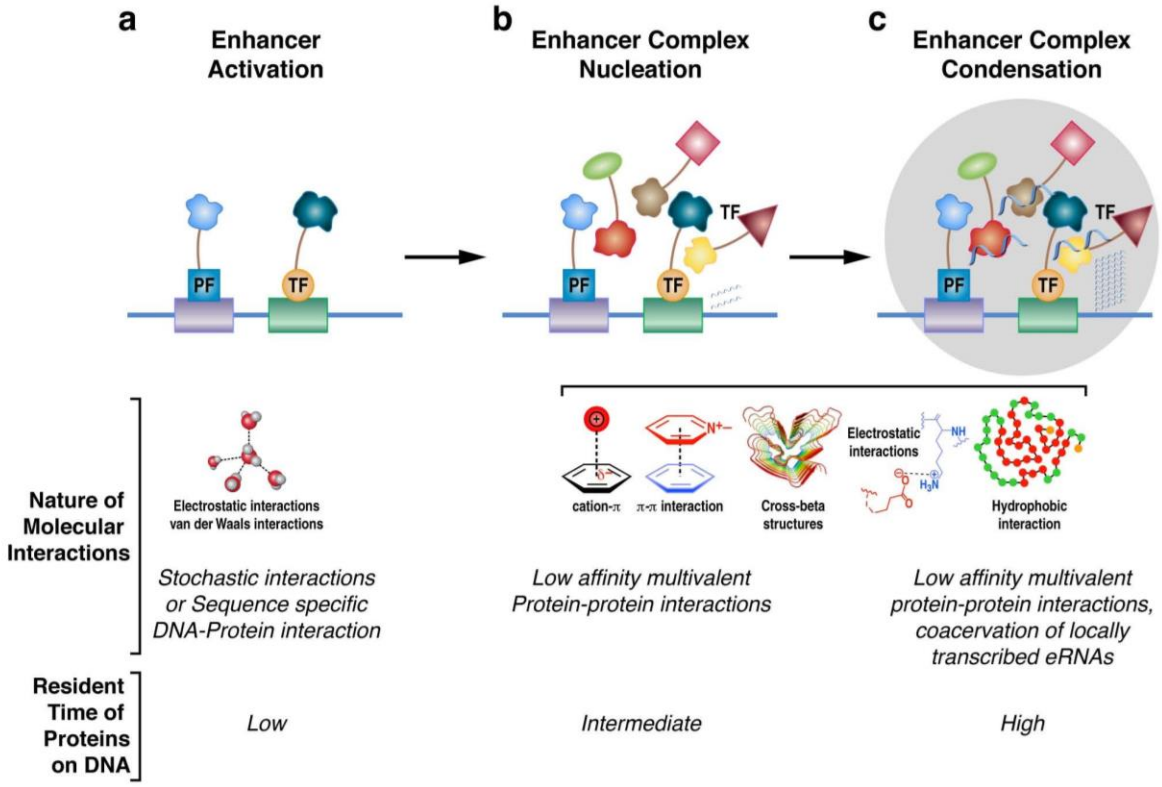

Figure 2.3. Molecular interactions underlying full activation of enhancers: A large number of molecular interaction events have to happen in space and time to activate an enhancer. **(a)** In acute signaling programs, pioneer factors gain access to nucleosome-bound enhancers and the resultant open chromatin is occupied by sequence-specific transcription factors in a ligand-dependent manner. These interactions are largely stochastic and highly dynamic. The resident time of transcription factors on the DNA in this stage is very low. DNA-protein interactions mostly involve electrostatic interactions and van der Waals forces. **(b)** Once the transcription factor binds to the cognate sequences, it will act as a nucleating factor to recruit transcription machinery, which includes co-factors and RNAP PolII, through protein-protein interactions. Emerging data suggest the role of low-affinity multivalent interactions between intrinsically disordered regions of transcription factors and cofactors in this process. Mutational and biophysical studies have revealed the role of cation-pi, pi-pi, hydrophobic interactions, and more structured interactions involving cross-beta structures. We speculate that this complex will initiate the transcription of eRNAs at a lower rate. **(c)** In a subset of enhancers, that are either clustered enhancers or enhancers with high-affinity chromatin binding of transcription factors, elevated local concentration of eRNA would act as a scaffold to bring together multiple components, potentially through complex coacervation and assembly of the enhancer complex as condensates. Post-transcriptional modifications of eRNAs, such as m6A modification, might play a crucial role in this stage.

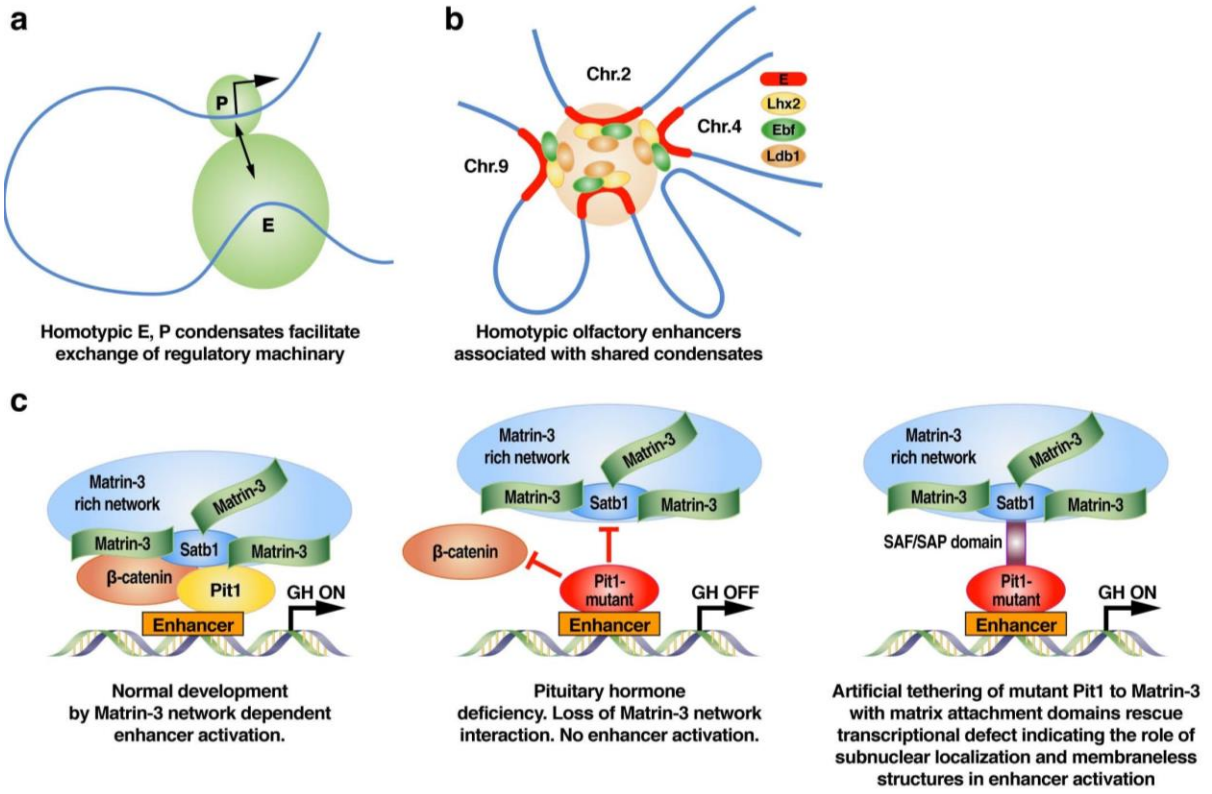

Figure 2.4. Condensates in chromatin interactions. (a) Compositionally similar condensates assembled at the enhancers and promoters (e.g.: transcription complex seeded by same signaling programs) might facilitate fusion between E-P condensates, and potentially the transfer of regulatory molecules from enhancer to promote **(b)** Long-distance intra- and inter-chromosomal enhancer associations might be facilitated by condensate interactions similar to the model proposed for E-P interaction. Olfactory receptor enhancer cooperativity is shown here as an example. The interacting enhancers are bound by transcription factors Lhx2 and Ebf, which in turn recruit Lim Domain Binding protein 1, LDB1, that is known to facilitate E-P contact through dimerization. It is not clear whether LDB1function as s looping protein in these enhancers. Chromatin restructuring through condensates might be driven by surface tension-driven forces. **(c)** The role of nuclear structures in enhancer function is illustrated with the example of Growth Hormone (GH) receptor enhancer bound by the POU-homeodomain transcription factor Pit1. In mouse pituitary, tethering of Pit1-bound enhancers to the nuclear matrin-3 rich network in association with protein Satb1 and β-catenin is requiring for enhancer activation. A naturally occurring point mutation in humans PIT1 (R271W), causing combined pituitary hormone deficiency, prevents Pit1 association with Satb1 and β-catenin, which leads to failure of enhancer activation due to disrupted enhancer association with the matrin-3 network. Fusion of mutant Pit1 with “matrix attachment regions” such as SAF/SAP domains resulted in the rescue of the enhancer activation and gene expression by artificially tethering the enhancer to the subnuclear structures.

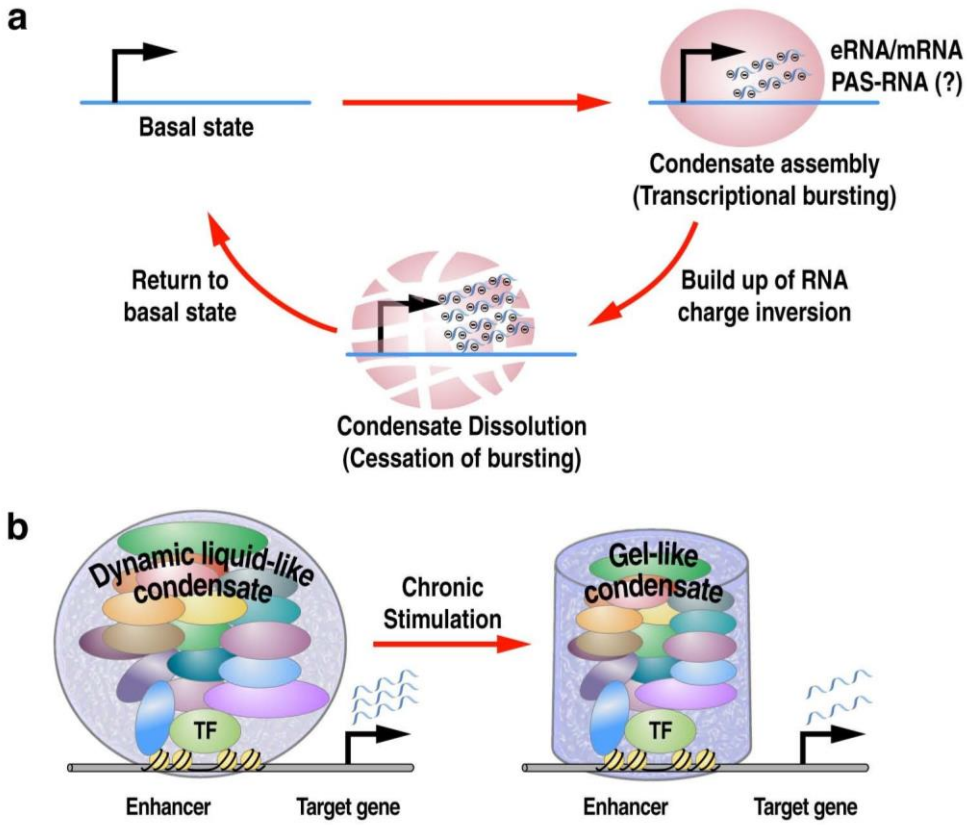

Figure 2.5. Regulatory roles of transcriptional condensates. (a) Condensate assembly and disassembly can be mediated through negative charge build-up correlated with the local concentration of RNA. The eRNAs, even at low concentration serve in the early phase of transcription initiation to favors enhancer complex assembly and condensation. With continued enhancer and target gene activation, the increased concentration eRNAs can result in the dispersion of the transcription complex due to charge repulsion resulting from an accumulation of the negative charge **(b**) The material property of the enhancer condensate varies in relation to the duration of the signal-dependent transcriptional activation. This is illustrated with the example of an enhancer complex assembled with estrogen stimulation in human breast cancer cells. With acute ligand-stimulation, the condensates assembly behaves as dynamic liquid with a rapid exchange of molecules in the condensates, whereas with chronic stimulation the material property of the condensate changes to a gel-like state with a reduced exchange of molecules between transcriptional condensates and the surrounding medium. The molecular basis of this transition in the physical state is not yet understood.

2.9 Acknowledgements

Chapter 2, in full, has been submitted for publication in *Nature Reviews Molecular Cell Biology*, 2021, and is currently under peer review. “Enhancers in space and time: cell biological and biophysical strategies of transcriptional regulation.” Sree Nair, Thomas Suter, Susan Wang, Lu Yang, Feng Yang, and Michael Rosenfeld. The dissertation author is a coauthor of this paper.

2.10 References

1. Haberle, V. & Stark, A. Eukaryotic core promoters and the functional basis of transcription initiation. *Nat Rev Mol Cell Biol* **19**, 621-637, doi:10.1038/s41580-018-0028-8 (2018).

2. Lenhard, B., Sandelin, A. & Carninci, P. Metazoan promoters: emerging characteristics and insights into transcriptional regulation. *Nat Rev Genet* **13**, 233-245, doi:10.1038/nrg3163 (2012).

3. Bulger, M. & Groudine, M. Functional and mechanistic diversity of distal transcription enhancers. *Cell* **144**, 327-339, doi:10.1016/j.cell.2011.01.024 S0092-8674(11)00063-8 [pii] (2011).

4. Levine, M., Cattoglio, C. & Tjian, R. Looping back to leap forward: transcription enters a new era. *Cell* **157**, 13-25, doi:10.1016/j.cell.2014.02.009 (2014).

5. Banerji, J., Rusconi, S. & Schaffner, W. Expression of a beta-globin gene is enhanced by remote SV40 DNA sequences. *Cell* **27**, 299-308 (1981).

6. Consortium, E. P. An integrated encyclopedia of DNA elements in the human genome. *Nature* **489**, 57-74, doi:10.1038/nature11247 (2012).

7. Calo, E. & Wysocka, J. Modification of enhancer chromatin: what, how, and why? *Mol Cell* **49**, 825-837, doi:10.1016/j.molcel.2013.01.038 (2013).

8. Creyghton, M. P., Cheng, A. W., Welstead, G. G., Kooistra, T., Carey, B. W., Steine, E. J., Hanna, J., Lodato, M. A., Frampton, G. M., Sharp, P. A., Boyer, L. A., Young, R. A., & Jaenisch, R. (2010). Histone H3K27ac separates

active from poised enhancers and predicts developmental state. *Proceedings of the National Academy of Sciences*, *107*(50), 21931–21936. https://doi.org/10.1073/pnas.1016071107

9. Heintzman, N. D., Hon, G. C., Hawkins, R. D., Kheradpour, P., Stark, A., Harp, L. F., Ye, Z., Lee, L. K., Stuart, R. K., Ching, C. W., Ching, K. A., Antosiewicz-Bourget, J. E., Liu, H., Zhang, X., Green, R. D., Lobanenkov, V. V., Stewart, R., Thomson, J. A., Crawford, G. E., … Ren, B. (2009). Histone modifications at human enhancers reflect global cell-type-specific gene expression. *Nature*, *459*(7243), 108–112. https://doi.org/10.1038/nature07829

10. Rada-Iglesias, A., Bajpai, R., Swigut, T., Brugmann, S. A., Flynn, R. A., & Wysocka, J. (2011). A unique chromatin signature uncovers early developmental enhancers in humans. Nature, 470(7333), 279–283. https://doi.org/10.1038/nature09692

11. Visel, A., Blow, M. J., Li, Z., Zhang, T., Akiyama, J. A., Holt, A., Plajzer-Frick, I., Shoukry, M., Wright, C., Chen, F., Afzal, V., Ren, B., Rubin, E. M., & Pennacchio, L. A. (2009). ChIP-seq accurately predicts tissue-specific activity of enhancers. Nature, 457(7231), 854–858. https://doi.org/10.1038/nature07730

12. Soutourina, J. Transcription regulation by the Mediator complex. *Nature Reviews Molecular Cell Biology* **19**, 262-274, doi:10.1038/nrm.2017.115 (2018).

13. Boyle, A. P., Davis, S., Shulha, H. P., Meltzer, P., Margulies, E. H., Weng, Z., Furey, T. S., & Crawford, G. E. (2008). High-resolution mapping and characterization of open chromatin across the genome. *Cell*, *132*(2), 311–322. https://doi.org/10.1016/j.cell.2007.12.014

14. Klemm, S. L., Shipony, Z. & Greenleaf, W. J. Chromatin accessibility and the regulatory epigenome. *Nature Reviews Genetics* **20**, 207-220, doi:10.1038/s41576-018-0089-8 (2019).

15. Moore, J. E., Pratt, H. E., Purcaro, M. J., & Weng, Z. (2020). A curated benchmark of enhancer-gene interactions for evaluating enhancer-target gene prediction methods. Genome Biology, 21(1), 17. https://doi.org/10.1186/s13059-019-1924-8

16. Gasperini, M., Tome, J. M. & Shendure, J. Towards a comprehensive catalogue of validated and target-linked human enhancers. *Nat Rev Genet* **21**, 292-310, doi:10.1038/s41576-0190209-0 (2020).

17. Rajagopal, N., Srinivasan, S., Kooshesh, K., Guo, Y., Edwards, M. D., Banerjee, B., Syed, T., Emons, B. J. M., Gifford, D. K., & Sherwood, R. I. (2016). High-throughput mapping of regulatory DNA. Nature Biotechnology, 34(2), 167–174. https://doi.org/10.1038/nbt.3468

18. Tak, Y. G., Hung, Y., Yao, L., Grimmer, M. R., Do, A., Bhakta, M. S., O'Geen, H., Segal, D. J., & Farnham, P. J. (2016). Effects on the transcriptome upon deletion of a distal element cannot be predicted by the size of the H3K27Ac peak in human cells. Nucleic Acids Research, 44(9), 4123–4133. https://doi.org/10.1093/nar/gkv1530

19. Sanyal, A., Lajoie, B. R., Jain, G. & Dekker, J. The long-range interaction landscape of gene promoters. *Nature* **489**, 109-113, doi:10.1038/nature11279 (2012).

20. Dao, L. T. M., Galindo-Albarrán, A. O., Castro-Mondragon, J. A., Andrieu-Soler, C., Medina-Rivera, A., Souaid, C., Charbonnier, G., Griffon, A., Vanhille, L., Stephen, T., Alomairi, J., Martin, D., Torres, M., Fernandez, N., Soler, E., van Helden, J., Puthier, D., & Spicuglia, S. (2017). Genome-wide characterization of mammalian promoters with distal enhancer functions. Nature Genetics, 49(7), 1073–1081. https://doi.org/10.1038/ng.3884

21. Engreitz, J. M., Haines, J. E., Perez, E. M., Munson, G., Chen, J., Kane, M., McDonel, P. E., Guttman, M., & Lander, E. S. (2016). Local regulation of gene expression by lncRNA promoters, transcription and splicing. Nature, 539(7629), 452–455. https://doi.org/10.1038/nature20149

22. De Santa, F., Barozzi, I., Mietton, F., Ghisletti, S., Polletti, S., Tusi, B. K., Muller, H., Ragoussis, J., Wei, C.-L., & Natoli, G. (2010). A large fraction of extragenic rna pol ii transcription sites overlap enhancers. PLoS Biology, 8(5), e1000384. https://doi.org/10.1371/journal.pbio.1000384

23. Kim, T.-K., Hemberg, M., Gray, J. M., Costa, A. M., Bear, D. M., Wu, J., Harmin, D. A., Laptewicz, M., Barbara-Haley, K., Kuersten, S., Markenscoff-Papadimitriou, E., Kuhl, D., Bito, H., Worley, P. F., Kreiman, G., & Greenberg, M. E. (2010). Widespread transcription at neuronal activity-

regulated enhancers. Nature, 465(7295), 182–187. https://doi.org/10.1038/nature09033

24. Liu, Z. & Tjian, R. Visualizing transcription factor dynamics in living cells. *J Cell Biol* **217**, 1181-1191, doi:10.1083/jcb.201710038 (2018).

25. Chen, H. & Larson, D. R. What have single-molecule studies taught us about gene expression? *Genes Dev* **30**, 1796-1810, doi:10.1101/gad.281725.116 (2016).

26. Tunnacliffe, E. & Chubb, J. R. What Is a Transcriptional Burst? *Trends Genet* **36**, 288-297, doi:10.1016/j.tig.2020.01.003 (2020).

27. Suter, D. M., Molina, N., Gatfield, D., Schneider, K., Schibler, U., & Naef, F. (2011). Mammalian genes are transcribed with widely different bursting kinetics. Science, 332(6028), 472–474. https://doi.org/10.1126/science.1198817

28. Berrocal, A., Lammers, N. C., Garcia, H. G. & Eisen, M. B. Kinetic sculpting of the seven stripes of the Drosophila even-skipped gene. *Elife* **9**, doi:10.7554/eLife.61635 (2020).

29. Bothma, J. P., Garcia, H. G., Esposito, E., Schlissel, G., Gregor, T., & Levine, M. (2014). Dynamic regulation of eve stripe 2 expression reveals transcriptional bursts in living Drosophila embryos. *Proceedings of the National Academy of Sciences*, *111*(29), 10598–10603. https://doi.org/10.1073/pnas.1410022111

30. Falo-Sanjuan, J., Lammers, N. C., Garcia, H. G. & Bray, S. J. Enhancer Priming Enables Fast and Sustained Transcriptional Responses to Notch Signaling. *Dev Cell* **50**, 411-425 e418, doi:10.1016/j.devcel.2019.07.002 (2019).

31. Lee, C., Shin, H. & Kimble, J. Dynamics of Notch-Dependent Transcriptional Bursting in Its Native Context. *Dev Cell* **50**, 426-435 e424, doi:10.1016/j.devcel.2019.07.001 (2019).

32. Fritzsch, C., Baumgärtner, S., Kuban, M., Steinshorn, D., Reid, G., & Legewie, S. (2018). Estrogen-dependent control and cell-to-cell variability of

transcriptional bursting. Molecular Systems Biology, 14(2). https://doi.org/10.15252/msb.20177678

33. Fukaya, T., Lim, B. & Levine, M. Enhancer Control of Transcriptional Bursting. *Cell* **166**, 358368, doi:10.1016/j.cell.2016.05.025 (2016).

34. Larsson, A. J. M., Johnsson, P., Hagemann-Jensen, M., Hartmanis, L., Faridani, O. R., Reinius, B., Segerstolpe, Å., Rivera, C. M., Ren, B., & Sandberg, R. (2019). Genomic encoding of transcriptional burst kinetics. Nature, 565(7738), 251–254. https://doi.org/10.1038/s41586-018-0836-1

35. Rodriguez, J., Ren, G., Day, C.R., Zhao, K., Chow, C.C., and Larson, D.R. (2019). Intrinsic Dynamics of a Human Gene Reveal the Basis of Expression Heterogeneity. Cell 176, 213-226.e18.

36. Heist, T., Fukaya, T. & Levine, M. Large distances separate coregulated genes in living Drosophila embryos. *Proc Natl Acad Sci U S A* **116**, 15062-15067, doi:10.1073/pnas.1908962116 (2019).

37. Lim, B., Heist, T., Levine, M. & Fukaya, T. Visualization of Transvection in Living Drosophila Embryos. *Mol Cell* **70**, 287-296 e286, doi:10.1016/j.molcel.2018.02.029 (2018).

38. Stavreva, D.A., Garcia, D.A., Fettweis, G., Gudla, P.R., Zaki, G.F., Soni, V., McGowan, A., Williams, G., Huynh, A., Palangat, M., et al. (2019). Transcriptional Bursting and Co-bursting Regulation by Steroid Hormone Release Pattern and Transcription Factor Mobility. Mol. Cell 75, 1161-1177.e11.

39. Gu, B., Swigut, T., Spencley, A., Bauer, M. R., Chung, M., Meyer, T., & Wysocka, J. (2018). Transcription-coupled changes in nuclear mobility of mammalian cis-regulatory elements. *Science*, *359*(6379), 1050–1055. https://doi.org/10.1126/science.aao3136

40. Ghavi-Helm, Y., Klein, F. A., Pakozdi, T., Ciglar, L., Noordermeer, D., Huber, W., & Furlong, E. E. M. (2014). Enhancer loops appear stable during development and are associated with paused polymerase. Nature, 512(7512), 96–100. https://doi.org/10.1038/nature13417

41. Cruz-Molina, S., Respuela, P., Tebartz, C., Kolovos, P., Nikolic, M., Fueyo, R., van Ijcken, W. F. J., Grosveld, F., Frommolt, P., Bazzi, H., & Rada-

Iglesias, A. (2017). Prc2 facilitates the regulatory topology required for poised enhancer function during pluripotent stem cell differentiation. Cell Stem Cell, 20(5), 689-705.e9. https://doi.org/10.1016/j.stem.2017.02.004

42. Gaertner, B. & Zeitlinger, J. RNA polymerase II pausing during development. *Development (Cambridge, England)* **141**, 1179-1183, doi:10.1242/dev.088492 (2014).

43. Day, D. S., Zhang, B., Stevens, S. M., Ferrari, F., Larschan, E. N., Park, P. J., & Pu, W. T. (2016). Comprehensive analysis of promoter-proximal RNA polymerase II pausing across mammalian cell types. *Genome Biology*, *17*(1), 120. https://doi.org/10.1186/s13059-016-0984-2

44. Liu, X., Kraus, W. L. & Bai, X. Ready, pause, go: regulation of RNA polymerase II pausing and release by cellular signaling pathways. *Trends in biochemical sciences* **40**, 516-525, doi:10.1016/j.tibs.2015.07.003 (2015).

45. Schaukowitch, K., Joo, J.-Y., Liu, X., Watts, J. K., Martinez, C., & Kim, T.-K. (2014). Enhancer rna facilitates nelf release from immediate early genes. Molecular Cell, 56(1), 29–42. https://doi.org/10.1016/j.molcel.2014.08.023

46. Schoenfelder, S. & Fraser, P. Long-range enhancer-promoter contacts in gene expression control. *Nat Rev Genet* **20**, 437-455, doi:10.1038/s41576-019-0128-0 (2019).

47. Gasperini, M., Hill, A. J., McFaline-Figueroa, J. L., Martin, B., Kim, S., Zhang, M. D., Jackson, D., Leith, A., Schreiber, J., Noble, W. S., Trapnell, C., Ahituv, N., & Shendure, J. (2019). A genome-wide framework for mapping gene regulation via cellular genetic screens. Cell, 176(6), 1516. https://doi.org/10.1016/j.cell.2019.02.027

48. Corces, M. R., Granja, J. M., Shams, S., Louie, B. H., Seoane, J. A., Zhou, W., Silva, T. C., Groeneveld, C., Wong, C. K., Cho, S. W., Satpathy, A. T., Mumbach, M. R., Hoadley, K. A., Robertson, A. G., Sheffield, N. C., Felau, I., Castro, M. A. A., Berman, B. P., Staudt, L. M., … Zhu, J. (2018). The chromatin accessibility landscape of primary human cancers. Science, 362(6413), eaav1898. https://doi.org/10.1126/science.aav1898

49. Lucas, J. S., Zhang, Y., Dudko, O. K. & Murre, C. 3D trajectories adopted by coding and regulatory DNA elements: first-passage times for genomic interactions. *Cell* **158**, 339-352, doi:10.1016/j.cell.2014.05.036 (2014).

50. The FANTOM Consortium, Andersson, R., Gebhard, C., Miguel-Escalada, I., Hoof, I., Bornholdt, J., Boyd, M., Chen, Y., Zhao, X., Schmidl, C., Suzuki, T., Ntini, E., Arner, E., Valen, E., Li, K., Schwarzfischer, L., Glatz, D., Raithel, J., Lilje, B., … Sandelin, A. (2014). An atlas of active enhancers across human cell types and tissues. Nature, 507(7493), 455–461. https://doi.org/10.1038/nature12787

51. Fang, R., Yu, M., Li, G., Chee, S., Liu, T., Schmitt, A. D., & Ren, B. (2016). Mapping of long-range chromatin interactions by proximity ligation-assisted ChIP-seq. Cell Research, 26(12), 1345–1348. https://doi.org/10.1038/cr.2016.137

52. Xie, S., Duan, J., Li, B., Zhou, P. & Hon, G. C. Multiplexed Engineering and Analysis of Combinatorial Enhancer Activity in Single Cells. *Mol Cell* **66**, 285-299 e285, doi:10.1016/j.molcel.2017.03.007 (2017).

53. Blackwood, E. M. & Kadonaga, J. T. Going the distance: a current view of enhancer action. *Science* **281**, 60-63 (1998).

54. Yatskevich, S., Rhodes, J. & Nasmyth, K. Organization of Chromosomal DNA by SMC Complexes. *Annual Review of Genetics* **53**, 445-482, doi:10.1146/annurev-genet-112618043633 (2019).

55. Kagey, M. H., Newman, J. J., Bilodeau, S., Zhan, Y., Orlando, D. A., van Berkum, N. L., Ebmeier, C. C., Goossens, J., Rahl, P. B., Levine, S. S., Taatjes, D. J., Dekker, J., & Young, R. A. (2010). Mediator and cohesin connect gene expression and chromatin architecture. Nature, 467(7314), 430–435. https://doi.org/10.1038/nature09380

56. Phillips-Cremins, J. E., Sauria, M. E. G., Sanyal, A., Gerasimova, T. I., Lajoie, B. R., Bell, J. S. K., Ong, C.-T., Hookway, T. A., Guo, C., Sun, Y., Bland, M. J., Wagstaff, W., Dalton, S., McDevitt, T. C., Sen, R., Dekker, J., Taylor, J., & Corces, V. G. (2013). Architectural protein subclasses shape 3d organization of genomes during lineage commitment. Cell, 153(6), 1281–1295. https://doi.org/10.1016/j.cell.2013.04.053

57. Wendt, K. S., Yoshida, K., Itoh, T., Bando, M., Koch, B., Schirghuber, E., Tsutsumi, S., Nagae, G., Ishihara, K., Mishiro, T., Yahata, K., Imamoto, F., Aburatani, H., Nakao, M., Imamoto, N., Maeshima, K., Shirahige, K., & Peters, J.-M. (2008). Cohesin mediates transcriptional insulation by CCCTC-binding factor. Nature, 451(7180), 796–801. https://doi.org/10.1038/nature06634

58. Rubio, E. D., Reiss, D. J., Welcsh, P. L., Disteche, C. M., Filippova, G. N., Baliga, N. S., Aebersold, R., Ranish, J. A., & Krumm, A. (2008). CTCF physically links cohesin to chromatin. Proceedings of the National Academy of Sciences, 105(24), 8309–8314. https://doi.org/10.1073/pnas.0801273105

59. Vian, L., Pękowska, A., Rao, S. S. P., Kieffer-Kwon, K.-R., Jung, S., Baranello, L., Huang, S.-C., El Khattabi, L., Dose, M., Pruett, N., Sanborn, A. L., Canela, A., Maman, Y., Oksanen, A., Resch, W., Li, X., Lee, B., Kovalchuk, A. L., Tang, Z., … Casellas, R. (2018). The energetics and physiological impact of cohesin extrusion. Cell, 173(5), 1165-1178.e20. https://doi.org/10.1016/j.cell.2018.03.072

60. de Wit, E., Vos, E. S. M., Holwerda, S. J. B., Valdes-Quezada, C., Verstegen, M. J. A. M., Teunissen, H., Splinter, E., Wijchers, P. J., Krijger, P. H. L., & de Laat, W. (2015). Ctcf binding polarity determines chromatin looping. Molecular Cell, 60(4), 676–684. https://doi.org/10.1016/j.molcel.2015.09.023

61. Guo, Y., Xu, Q., Canzio, D., Shou, J., Li, J., Gorkin, D. U., Jung, I., Wu, H., Zhai, Y., Tang, Y., Lu, Y., Wu, Y., Jia, Z., Li, W., Zhang, M. Q., Ren, B., Krainer, A. R., Maniatis, T., & Wu, Q. (2015). Crispr inversion of ctcf sites alters genome topology and enhancer/promoter function. Cell, 162(4), 900–910. https://doi.org/10.1016/j.cell.2015.07.038

62. Oh, S., Shao, J., Mitra, J., Xiong, F., D'Antonio, M., Wang, R., Garcia-Bassets, I., Ma, Q., Zhu, X., Lee, J.-H., Nair, S. J., Yang, F., Ohgi, K., Frazer, K. A., Zhang, Z. D., Li, W., & Rosenfeld, M. G. (2021). Enhancer release and retargeting activates disease-susceptibility genes. Nature, 595(7869), 735–740. https://doi.org/10.1038/s41586-021-03577-1

63. Nora, E. P., Goloborodko, A., Valton, A.-L., Gibcus, J. H., Uebersohn, A., Abdennur, N., Dekker, J., Mirny, L. A., & Bruneau, B. G. (2017). Targeted degradation of ctcf decouples local insulation of chromosome domains from

genomic compartmentalization. Cell, 169(5), 930-944.e22. https://doi.org/10.1016/j.cell.2017.05.004

64. Rao, S. S. P., Huang, S.-C., Glenn St Hilaire, B., Engreitz, J. M., Perez, E. M., Kieffer-Kwon, K.-R., Sanborn, A. L., Johnstone, S. E., Bascom, G. D., Bochkov, I. D., Huang, X., Shamim, M. S., Shin, J., Turner, D., Ye, Z., Omer, A. D., Robinson, J. T., Schlick, T., Bernstein, B. E., … Aiden, E. L. (2017). Cohesin loss eliminates all loop domains. Cell, 171(2), 305-320.e24. https://doi.org/10.1016/j.cell.2017.09.026

65. Thiecke, M. J., Wutz, G., Muhar, M., Tang, W., Bevan, S., Malysheva, V., Stocsits, R., Neumann, T., Zuber, J., Fraser, P., Schoenfelder, S., Peters, J.-M., & Spivakov, M. (2020). Cohesin-dependent and -independent mechanisms mediate chromosomal contacts between promoters and enhancers. Cell Reports, 32(3), 107929. https://doi.org/10.1016/j.celrep.2020.107929

66. Hsieh, T.-H. S., Cattoglio, C., Slobodyanyuk, E., Hansen, A. S., Darzacq, X., & Tjian, R. (2021). Enhancer-promoter interactions and transcription are maintained upon acute loss of CTCF, cohesin, WAPL, and YY1 [Preprint]. Molecular Biology. https://doi.org/10.1101/2021.07.14.452365

67. Bartman, C. R., Hsu, S. C., Hsiung, C. C., Raj, A. & Blobel, G. A. Enhancer Regulation of Transcriptional Bursting Parameters Revealed by Forced Chromatin Looping. *Mol Cell* **62**, 237-247, doi:10.1016/j.molcel.2016.03.007 (2016).

68. Deng, W., Rupon, J. W., Krivega, I., Breda, L., Motta, I., Jahn, K. S., Reik, A., Gregory, P. D., Rivella, S., Dean, A., & Blobel, G. A. (2014). Reactivation of developmentally silenced globin genes by forced chromatin looping. Cell, 158(4), 849–860. https://doi.org/10.1016/j.cell.2014.05.050

69. Krivega, I. & Dean, A. LDB1-mediated enhancer looping can be established independent of mediator and cohesin. *Nucleic Acids Res* **45**, 8255-8268, doi:10.1093/nar/gkx433 (2017).

70. Weintraub, A. S., Li, C. H., Zamudio, A. V., Sigova, A. A., Hannett, N. M., Day, D. S., Abraham, B. J., Cohen, M. A., Nabet, B., Buckley, D. L., Guo, Y. E., Hnisz, D., Jaenisch, R., Bradner, J. E., Gray, N. S., & Young, R. A.

(2017). Yy1 is a structural regulator of enhancer-promoter loops. Cell, 171(7), 1573-1588.e28. https://doi.org/10.1016/j.cell.2017.11.008

71. Furlong, E. E. M. & Levine, M. Developmental enhancers and chromosome topology. *Science* **361**, 1341-1345, doi:10.1126/science.aau0320 (2018).

72. Saldana-Meyer, R., Gonzalez-Buendia, E., Guerrero, G., Narendra, V., Bonasio, R., Recillas-Targa, F., & Reinberg, D. (2014). CTCF regulates the human p53 gene through direct interaction with its natural antisense transcript, Wrap53. Genes & Development, 28(7), 723–734. https://doi.org/10.1101/gad.236869.113

73. Saldaña-Meyer, R., Rodriguez-Hernaez, J., Escobar, T., Nishana, M., Jácome-López, K., Nora, E. P., Bruneau, B. G., Tsirigos, A., Furlan-Magaril, M., Skok, J., & Reinberg, D. (2019). Rna interactions are essential for ctcf-mediated genome organization. Molecular Cell, 76(3), 412-422.e5. https://doi.org/10.1016/j.molcel.2019.08.015

74. Sigova, A. A., Abraham, B. J., Ji, X., Molinie, B., Hannett, N. M., Guo, Y. E., Jangi, M., Giallourakis, C. C., Sharp, P. A., & Young, R. A. (2015). Transcription factor trapping by RNA in gene regulatory elements. Science, 350(6263), 978–981. https://doi.org/10.1126/science.aad3346

75. Hansen, A. S., Hsieh, T.-H. S., Cattoglio, C., Pustova, I., Saldaña-Meyer, R., Reinberg, D., Darzacq, X., & Tjian, R. (2019). Distinct classes of chromatin loops revealed by deletion of an rna-binding region in ctcf. Molecular Cell, 76(3), 395-411.e13. https://doi.org/10.1016/j.molcel.2019.07.039

76. Li, G., Ruan, X., Auerbach, R. K., Sandhu, K. S., Zheng, M., Wang, P., Poh, H. M., Goh, Y., Lim, J., Zhang, J., Sim, H. S., Peh, S. Q., Mulawadi, F. H., Ong, C. T., Orlov, Y. L., Hong, S., Zhang, Z., Landt, S., Raha, D., … Ruan, Y. (2012). Extensive promoter-centered chromatin interactions provide a topological basis for transcription regulation. Cell, 148(1–2), 84–98. https://doi.org/10.1016/j.cell.2011.12.014

77. Melo, C. A., Drost, J., Wijchers, P. J., van de Werken, H., de Wit, E., Vrielink, J. A. F. O., Elkon, R., Melo, S. A., Léveillé, N., Kalluri, R., de Laat, W., & Agami, R. (2013). Ernas are required for p53-dependent enhancer activity and gene transcription. Molecular Cell, 49(3), 524–535. https://doi.org/10.1016/j.molcel.2012.11.021

78. Krietenstein, N., Abraham, S., Venev, S. V., Abdennur, N., Gibcus, J., Hsieh, T.-H. S., Parsi, K. M., Yang, L., Maehr, R., Mirny, L. A., Dekker, J., & Rando, O. J. (2020). Ultrastructural details of mammalian chromosome architecture. Molecular Cell, 78(3), 554-565.e7. https://doi.org/10.1016/j.molcel.2020.03.003

79. Hsieh, T.-H. S., Cattoglio, C., Slobodyanyuk, E., Hansen, A. S., Rando, O. J., Tjian, R., & Darzacq, X. (2020). Resolving the 3d landscape of transcription-linked mammalian chromatin folding. Molecular Cell, 78(3), 539-553.e8. https://doi.org/10.1016/j.molcel.2020.03.002

80. Chen, H., Levo, M., Barinov, L., Fujioka, M., Jaynes, J.B., and Gregor, T. (2018). Dynamic interplay between enhancer-promoter topology and gene activity. Nat. Genet. 50, 1296–1303.

81. Alexander, J. M., Guan, J., Li, B., Maliskova, L., Song, M., Shen, Y., Huang, B., Lomvardas, S., & Weiner, O. D. (2019). Live-cell imaging reveals enhancer-dependent Sox2 transcription in the absence of enhancer proximity. ELife, 8, e41769. https://doi.org/10.7554/eLife.41769

82. Benabdallah, N. S., Williamson, I., Illingworth, R. S., Kane, L., Boyle, S., Sengupta, D., Grimes, G. R., Therizols, P., & Bickmore, W. A. (2019). Decreased enhancer-promoter proximity accompanying enhancer activation. Molecular Cell, 76(3), 473-484.e7. https://doi.org/10.1016/j.molcel.2019.07.038

83. Allahyar, A., Vermeulen, C., Bouwman, B. A. M., Krijger, P. H. L., Verstegen, M. J. A. M., Geeven, G., van Kranenburg, M., Pieterse, M., Straver, R., Haarhuis, J. H. I., Jalink, K., Teunissen, H., Renkens, I. J., Kloosterman, W. P., Rowland, B. D., de Wit, E., de Ridder, J., & de Laat, W. (2018). Enhancer hubs and loop collisions identified from single-allele topologies. Nature Genetics, 50(8), 1151–1160. https://doi.org/10.1038/s41588-018-0161-5

84. Beagrie, R. A., Scialdone, A., Schueler, M., Kraemer, D. C. A., Chotalia, M., Xie, S. Q., Barbieri, M., de Santiago, I., Lavitas, L.-M., Branco, M. R., Fraser, J., Dostie, J., Game, L., Dillon, N., Edwards, P. A. W., Nicodemi, M., & Pombo, A. (2017). Complex multi-enhancer contacts captured by genome architecture mapping. Nature, 543(7646), 519–524. https://doi.org/10.1038/nature21411

85. Jiang, T., Raviram, R., Snetkova, V., Rocha, P. P., Proudhon, C., Badri, S., Bonneau, R., Skok, J. A., & Kluger, Y. (2016). Identification of multi-loci hubs from 4C-seq demonstrates the functional importance of simultaneous interactions. Nucleic Acids Research, 44(18), 8714–8725. https://doi.org/10.1093/nar/gkw568

86. Dekker, J. Mapping the 3D genome: Aiming for consilience. *Nat Rev Mol Cell Biol* **17**, 741742, doi:10.1038/nrm.2016.151 (2016).

87. Giorgetti, L. & Heard, E. Closing the loop: 3C versus DNA FISH. *Genome Biol* **17**, 215, doi:10.1186/s13059-016-1081-2 (2016).

88. Fudenberg, G. & Imakaev, M. FISH-ing for captured contacts: towards reconciling FISH and 3C. *Nature Methods* **14**, 673-678, doi:10.1038/nmeth.4329 (2017).

89. Ramani, V., Deng, X., Qiu, R., Gunderson, K. L., Steemers, F. J., Disteche, C. M., Noble, W. S., Duan, Z., & Shendure, J. (2017). Massively multiplex single-cell Hi-C. Nature Methods, 14(3), 263–266. https://doi.org/10.1038/nmeth.4155

90. Nagano, T., Lubling, Y., Várnai, C., Dudley, C., Leung, W., Baran, Y., Mendelson Cohen, N., Wingett, S., Fraser, P., & Tanay, A. (2017). Cell-cycle dynamics of chromosomal organization at single-cell resolution. Nature, 547(7661), 61–67. https://doi.org/10.1038/nature23001

91. Chen, Y., Zhang, Y., Wang, Y., Zhang, L., Brinkman, E. K., Adam, S. A., Goldman, R., van Steensel, B., Ma, J., & Belmont, A. S. (2018). Mapping 3D genome organization relative to nuclear compartments using TSA-Seq as a cytological ruler. Journal of Cell Biology, 217(11), 4025–4048. https://doi.org/10.1083/jcb.201807108

92. Quinodoz, S. A., Ollikainen, N., Tabak, B., Palla, A., Schmidt, J. M., Detmar, E., Lai, M. M., Shishkin, A. A., Bhat, P., Takei, Y., Trinh, V., Aznauryan, E., Russell, P., Cheng, C., Jovanovic, M., Chow, A., Cai, L., McDonel, P., Garber, M., & Guttman, M. (2018). Higher-order inter-chromosomal hubs shape 3d genome organization in the nucleus. Cell, 174(3), 744-757.e24. https://doi.org/10.1016/j.cell.2018.05.024

93. Shachar, S., Voss, T. C., Pegoraro, G., Sciascia, N. & Misteli, T. Identification of Gene Positioning Factors Using High-Throughput Imaging Mapping. *Cell* **162**, 911-923, doi:10.1016/j.cell.2015.07.035 (2015).

94. Wang, S., Su, J.-H., Beliveau, B. J., Bintu, B., Moffitt, J. R., Wu, C., & Zhuang, X. (2016). Spatial organization of chromatin domains and compartments in single chromosomes. Science, 353(6299), 598–602. https://doi.org/10.1126/science.aaf8084

95. Brandão, H. B., Gabriele, M. & Hansen, A. S. Tracking and interpreting long-range chromatin interactions with super-resolution live-cell imaging. *Current Opinion in Cell Biology* **70**, 1826, doi:https://doi.org/10.1016/j.ceb.2020.11.002 (2021).

96. Li, W., Notani, D., Ma, Q., Tanasa, B., Nunez, E., Chen, A. Y., Merkurjev, D., Zhang, J., Ohgi, K., Song, X., Oh, S., Kim, H.-S., Glass, C. K., & Rosenfeld, M. G. (2013). Functional roles of enhancer RNAs for oestrogen-dependent transcriptional activation. Nature, 498(7455), 516–520. https://doi.org/10.1038/nature12210

97. Whyte, W. A., Orlando, D. A., Hnisz, D., Abraham, B. J., Lin, C. Y., Kagey, M. H., Rahl, P. B., Lee, T. I., & Young, R. A. (2013). Master transcription factors and mediator establish super-enhancers at key cell identity genes. Cell, 153(2), 307–319. https://doi.org/10.1016/j.cell.2013.03.035

98. Mikhaylichenko, O., Bondarenko, V., Harnett, D., Schor, I. E., Males, M., Viales, R. R., & Furlong, E. E. M. (2018). The degree of enhancer or promoter activity is reflected by the levels and directionality of eRNA transcription. Genes & Development, 32(1), 42–57. https://doi.org/10.1101/gad.308619.117

99. Farley, E. K., Olson, K. M., Zhang, W., Brandt, A. J., Rokhsar, D. S., & Levine, M. S. (2015). Suboptimization of developmental enhancers. Science, 350(6258), 325–328. https://doi.org/10.1126/science.aac6948

100. Berman, B. P., Nibu, Y., Pfeiffer, B. D., Tomancak, P., Celniker, S. E., Levine, M., Rubin, G. M., & Eisen, M. B. (2002). Exploiting transcription factor binding site clustering to identify cis-regulatory modules involved in pattern formation in the Drosophila genome. Proceedings of the National Academy of Sciences, 99(2), 757–762.

101. Wasserman, W. W. & Fickett, J. W. Identification of regulatory regions which confer musclespecific gene expression. *J Mol Biol* **278**, 167-181, doi:10.1006/jmbi.1998.1700 (1998).

102. Magram, J., Chada, K. & Costantini, F. Developmental regulation of a cloned adult betaglobin gene in transgenic mice. *Nature* **315**, 338-340, doi:10.1038/315338a0 (1985).

103. Li, Q., Harju, S. & Peterson, K. R. Locus control regions: coming of age at a decade plus. *Trends Genet* **15**, 403-408, doi:10.1016/s0168-9525(99)01780-1 (1999).

104. Lovén, J., Hoke, H. A., Lin, C. Y., Lau, A., Orlando, D. A., Vakoc, C. R., Bradner, J. E., Lee, T. I., & Young, R. A. (2013). Selective inhibition of tumor oncogenes by disruption of super-enhancers. Cell, 153(2), 320–334. https://doi.org/10.1016/j.cell.2013.03.036

105. Parker, S. C. J., Stitzel, M. L., Taylor, D. L., Orozco, J. M., Erdos, M. R., Akiyama, J. A., van Bueren, K. L., Chines, P. S., Narisu, N., NISC Comparative Sequencing Program, Black, B. L., Visel, A., Pennacchio, L. A., Collins, F. S., National Institutes of Health Intramural Sequencing Center Comparative Sequencing Program Authors, NISC Comparative Sequencing Program Authors., Becker, J., Benjamin, B., Blakesley, R., … Young, A. (2013). Chromatin stretch enhancer states drive cell-specific gene regulation and harbor human disease risk variants. Proceedings of the National Academy of Sciences, 110(44), 17921–17926. https://doi.org/10.1073/pnas.1317023110

106. Dowen, J. M., Fan, Z. P., Hnisz, D., Ren, G., Abraham, B. J., Zhang, L. N., Weintraub, A. S., Schuijers, J., Lee, T. I., Zhao, K., & Young, R. A. (2014). Control of cell identity genes occurs in insulated neighborhoods in mammalian chromosomes. Cell, 159(2), 374–387. https://doi.org/10.1016/j.cell.2014.09.030

107. Hnisz, D., Schuijers, J., Lin, C. Y., Weintraub, A. S., Abraham, B. J., Lee, T. I., Bradner, J. E., & Young, R. A. (2015). Convergence of developmental and oncogenic signaling pathways at transcriptional super-enhancers. Molecular Cell, 58(2), 362–370. https://doi.org/10.1016/j.molcel.2015.02.014

108. Proudhon, C., Snetkova, V., Raviram, R., Lobry, C., Badri, S., Jiang, T., Hao, B., Trimarchi, T., Kluger, Y., Aifantis, I., Bonneau, R., & Skok, J. A.

(2016). Active and inactive enhancers cooperate to exert localized and long-range control of gene regulation. Cell Reports, 15(10), 2159–2169. https://doi.org/10.1016/j.celrep.2016.04.087

109. Shin, H. Y., Willi, M., Yoo, K. H., Zeng, X., Wang, C., Metser, G., & Hennighausen, L. (2016). Hierarchy within the mammary STAT5-driven Wap super-enhancer. Nature Genetics, 48(8), 904–911. https://doi.org/10.1038/ng.3606

110. Mansour, M. R., Abraham, B. J., Anders, L., Berezovskaya, A., Gutierrez, A., Durbin, A. D., Etchin, J., Lawton, L., Sallan, S. E., Silverman, L. B., Loh, M. L., Hunger, S. P., Sanda, T., Young, R. A., & Look, A. T. (2014). An oncogenic super-enhancer formed through somatic mutation of a noncoding intergenic element. Science, 346(6215), 1373–1377. https://doi.org/10.1126/science.1259037

111. Shrinivas, K., Sabari, B. R., Coffey, E. L., Klein, I. A., Boija, A., Zamudio, A. V., Schuijers, J., Hannett, N. M., Sharp, P. A., Young, R. A., & Chakraborty, A. K. (2019). Enhancer features that drive formation of transcriptional condensates. Molecular Cell, 75(3), 549-561.e7. https://doi.org/10.1016/j.molcel.2019.07.009

112. Choi, J., Lysakovskaia, K., Stik, G., Demel, C., Söding, J., Tian, T. V., Graf, T., & Cramer, P. (2021). Evidence for additive and synergistic action of mammalian enhancers during cell fate determination. ELife, 10, e65381. https://doi.org/10.7554/eLife.65381

113. Hay, D., Hughes, J. R., Babbs, C., Davies, J. O. J., Graham, B. J., Hanssen, L. L. P., Kassouf, M. T., Oudelaar, A. M., Sharpe, J. A., Suciu, M. C., Telenius, J., Williams, R., Rode, C., Li, P.-S., Pennacchio, L. A., Sloane-Stanley, J. A., Ayyub, H., Butler, S., Sauka-Spengler, T., … Higgs, D. R. (2016). Genetic dissection of the α-globin super-enhancer in vivo. Nature Genetics, 48(8), 895–903. https://doi.org/10.1038/ng.3605

114. Moorthy, S. D., Davidson, S., Shchuka, V. M., Singh, G., Malek-Gilani, N., Langroudi, L., Martchenko, A., So, V., Macpherson, N. N., & Mitchell, J. A. (2017). Enhancers and super-enhancers have an equivalent regulatory role in embryonic stem cells through regulation of single or multiple genes. Genome Research, 27(2), 246–258. https://doi.org/10.1101/gr.210930.116

115. Perry, M. W., Boettiger, A. N. & Levine, M. Multiple enhancers ensure precision of gap geneexpression patterns in the Drosophila embryo. *Proc Natl Acad Sci U S A* **108**, 13570-13575, doi:10.1073/pnas.1109873108 (2011).

116. Osterwalder, M., Barozzi, I., Tissières, V., Fukuda-Yuzawa, Y., Mannion, B. J., Afzal, S. Y., Lee, E. A., Zhu, Y., Plajzer-Frick, I., Pickle, C. S., Kato, M., Garvin, T. H., Pham, Q. T., Harrington, A. N., Akiyama, J. A., Afzal, V., Lopez-Rios, J., Dickel, D. E., Visel, A., & Pennacchio, L. A. (2018). Enhancer redundancy provides phenotypic robustness in mammalian development. Nature, 554(7691), 239–243. https://doi.org/10.1038/nature25461

117. Pott, S. & Lieb, J. D. What are super-enhancers? *Nat Genet* **47**, 8-12, doi:10.1038/ng.3167 (2015).

118. Liu, Z., Merkurjev, D., Yang, F., Li, W., Oh, S., Friedman, M. J., Song, X., Zhang, F., Ma, Q., Ohgi, K. A., Krones, A., & Rosenfeld, M. G. (2014). Enhancer activation requires trans-recruitment of a mega transcription factor complex. Cell, 159(2), 358–373. https://doi.org/10.1016/j.cell.2014.08.027

119. Bi, M., Zhang, Z., Jiang, Y.-Z., Xue, P., Wang, H., Lai, Z., Fu, X., De Angelis, C., Gong, Y., Gao, Z., Ruan, J., Jin, V. X., Marangoni, E., Montaudon, E., Glass, C. K., Li, W., Huang, T. H.-M., Shao, Z.-M., Schiff, R., … Liu, Z. (2020). Enhancer reprogramming driven by high-order assemblies of transcription factors promotes phenotypic plasticity and breast cancer endocrine resistance. Nature Cell Biology, 22(6), 701–715. https://doi.org/10.1038/s41556-020-0514-z

120. Li, W., Hu, Y., Oh, S., Ma, Q., Merkurjev, D., Song, X., Zhou, X., Liu, Z., Tanasa, B., He, X., Chen, A. Y., Ohgi, K., Zhang, J., Liu, W., & Rosenfeld, M. G. (2015). Condensin i and ii complexes license full estrogen receptor α-dependent enhancer activation. Molecular Cell, 59(2), 188–202. https://doi.org/10.1016/j.molcel.2015.06.002

121. Yang, F., Ma, Q., Liu, Z., Li, W., Tan, Y., Jin, C., Ma, W., Hu, Y., Shen, J., Ohgi, K. A., Telese, F., Liu, W., & Rosenfeld, M. G. (2017). Glucocorticoid receptor:megatrans switching mediates the repression of an erα-regulated transcriptional program. Molecular Cell, 66(3), 321-331.e6. https://doi.org/10.1016/j.molcel.2017.03.019

122. Hah, N. et al. A rapid, extensive, and transient transcriptional response to estrogen signaling in breast cancer cells. Cell 145, 622-634, doi:10.1016/j.cell.2011.03.042S0092-8674(11)00376-X [pii] (2011).

123. Siersbæk, R., Rabiee, A., Nielsen, R., Sidoli, S., Traynor, S., Loft, A., Poulsen, L. L. C., Rogowska-Wrzesinska, A., Jensen, O. N., & Mandrup, S. (2014). Transcription factor cooperativity in early adipogenic hotspots and super-enhancers. Cell Reports, 7(5), 1443–1455. https://doi.org/10.1016/j.celrep.2014.04.042

124. Michida, H., Imoto, H., Shinohara, H., Yumoto, N., Seki, M., Umeda, M., Hayashi, T., Nikaido, I., Kasukawa, T., Suzuki, Y., & Okada-Hatakeyama, M. (2020). The number of transcription factors at an enhancer determines switch-like gene expression. Cell Reports, 31(9), 107724. https://doi.org/10.1016/j.celrep.2020.107724

125. Farley, E. K., Olson, K. M., Zhang, W., Rokhsar, D. S. & Levine, M. S. Syntax compensates for poor binding sites to encode tissue specificity of developmental enhancers. *Proc Natl Acad Sci U S A* **113**, 6508-6513, doi:10.1073/pnas.1605085113 (2016).

126. Long, H. K., Prescott, S. L. & Wysocka, J. Ever-Changing Landscapes: Transcriptional Enhancers in Development and Evolution. *Cell* **167**, 1170-1187, doi:10.1016/j.cell.2016.09.018 (2016).

127. Panne, D., Maniatis, T. & Harrison, S. C. An atomic model of the interferon-beta enhanceosome. *Cell* **129**, 1111-1123, doi:10.1016/j.cell.2007.05.019 (2007).

128. Thanos, D. & Maniatis, T. Virus induction of human IFN beta gene expression requires the assembly of an enhanceosome. *Cell* **83**, 1091-1100, doi:10.1016/0092-8674(95)90136-1 (1995).

129. Arnosti, D. N. & Kulkarni, M. M. Transcriptional enhancers: Intelligent enhanceosomes or flexible billboards? *Journal of Cellular Biochemistry* **94**, 890-898, doi:https://doi.org/10.1002/jcb.20352 (2005).

130. Singh, G., Mullany, S., Moorthy, S. D., Zhang, R., Mehdi, T., Tian, R., Duncan, A. G., Moses, A. M., & Mitchell, J. A. (2021). A flexible repertoire of transcription factor binding sites and a diversity threshold determines

enhancer activity in embryonic stem cells. Genome Research, 31(4), 564–575. https://doi.org/10.1101/gr.272468.120

131. King, D. M., Hong, C. K. Y., Shepherdson, J. L., Granas, D. M., Maricque, B. B., & Cohen, B. A. (2020). Synthetic and genomic regulatory elements reveal aspects of cis-regulatory grammar in mouse embryonic stem cells. ELife, 9, e41279. https://doi.org/10.7554/eLife.41279

132. Crocker, J., Abe, N., Rinaldi, L., McGregor, A. P., Frankel, N., Wang, S., Alsawadi, A., Valenti, P., Plaza, S., Payre, F., Mann, R. S., & Stern, D. L. (2015). Low affinity binding site clusters confer hox specificity and regulatory robustness. Cell, 160(1–2), 191–203. https://doi.org/10.1016/j.cell.2014.11.041

133. Jindal, G. A. & Farley, E. K. Enhancer grammar in development, evolution, and disease: dependencies and interplay. *Dev Cell* **56**, 575-587, doi:10.1016/j.devcel.2021.02.016 (2021).

134. Junion, G., Spivakov, M., Girardot, C., Braun, M., Gustafson, E. H., Birney, E., & Furlong, E. E. M. (2012). A transcription factor collective defines cardiac cell fate and reflects lineage history. Cell, 148(3), 473–486. https://doi.org/10.1016/j.cell.2012.01.030

135. Banani, S. F., Lee, H. O., Hyman, A. A. & Rosen, M. K. Biomolecular condensates: organizers of cellular biochemistry. *Nat Rev Mol Cell Biol*, doi:10.1038/nrm.2017.7 (2017).

136. Alberti, S. Phase separation in biology. *Curr Biol* **27**, R1097-R1102, doi:10.1016/j.cub.2017.08.069 (2017).

137. Feuerborn, A. & Cook, P. R. Why the activity of a gene depends on its neighbors. *Trends Genet* **31**, 483-490, doi:10.1016/j.tig.2015.07.001 (2015).

138. Iborra, F. J., Pombo, A., Jackson, D. A. & Cook, P. R. Active RNA polymerases are localized within discrete transcription "factories' in human nuclei. *J Cell Sci* **109 (Pt 6)**, 1427-1436 (1996).

139. Osborne, C. S., Chakalova, L., Brown, K. E., Carter, D., Horton, A., Debrand, E., Goyenechea, B., Mitchell, J. A., Lopes, S., Reik, W., & Fraser, P. (2004). Active genes dynamically colocalize to shared sites of ongoing

transcription. Nature Genetics, 36(10), 1065–1071. https://doi.org/10.1038/ng1423

140. Schoenfelder, S., Sexton, T., Chakalova, L., Cope, N. F., Horton, A., Andrews, S., Kurukuti, S., Mitchell, J. A., Umlauf, D., Dimitrova, D. S., Eskiw, C. H., Luo, Y., Wei, C.-L., Ruan, Y., Bieker, J. J., & Fraser, P. (2010). Preferential associations between co-regulated genes reveal a transcriptional interactome in erythroid cells. Nature Genetics, 42(1), 53–61. https://doi.org/10.1038/ng.496

141. McNally, J. G., Muller, W. G., Walker, D., Wolford, R. & Hager, G. L. The glucocorticoid receptor: rapid exchange with regulatory sites in living cells. *Science* **287**, 1262-1265, doi:10.1126/science.287.5456.1262 (2000).

142. Stenoien, D. L., Patel, K., Mancini, M. G., Dutertre, M., Smith, C. L., O'Malley, B. W., & Mancini, M. A. (2001). FRAP reveals that mobility of oestrogen receptor-α is ligand- and proteasome-dependent. Nature Cell Biology, 3(1), 15–23. https://doi.org/10.1038/35050515

143. Kocanova, I., Kuchar, J., Dankovicova, V. & Cernak, J. Redetermination of aqua-(dihydrogen ethyl-enediamine-tetra-acetato-kappaO,O',N,N',O'')nickel(II). *Acta Crystallogr Sect E Struct Rep Online* **66**, m196-197, doi:10.1107/S1600536810002011 (2010).

144. Sharp, Z. D., Mancini, M. G., Hinojos, C. A., Dai, F., Berno, V., Szafran, A. T., Smith, K. P., Lele, T. T., Ingber, D. E., & Mancini, M. A. (2006). Estrogen-receptor-α exchange and chromatin dynamics are ligand- and domain-dependent. Journal of Cell Science, 119(19), 4101–4116. https://doi.org/10.1242/jcs.03161

145. Hnisz, D., Shrinivas, K., Young, R. A., Chakraborty, A. K. & Sharp, P. A. A Phase Separation Model for Transcriptional Control. *Cell* **169**, 13-23, doi:10.1016/j.cell.2017.02.007 (2017).

146. Cho, W.-K., Spille, J.-H., Hecht, M., Lee, C., Li, C., Grube, V., & Cisse, I. I. (2018). Mediator and RNA polymerase II clusters associate in transcription-dependent condensates. Science, 361(6400), 412–415. https://doi.org/10.1126/science.aar4199

147. Sabari, B. R., Dall'Agnese, A., Boija, A., Klein, I. A., Coffey, E. L., Shrinivas, K., Abraham, B. J., Hannett, N. M., Zamudio, A. V., Manteiga, J. C., Li, C.

H., Guo, Y. E., Day, D. S., Schuijers, J., Vasile, E., Malik, S., Hnisz, D., Lee, T. I., Cisse, I. I., … Young, R. A. (2018). Coactivator condensation at super-enhancers links phase separation and gene control. Science, 361(6400), eaar3958. https://doi.org/10.1126/science.aar3958

148. Boija A, Klein IA, Sabari BR, et al. Transcription Factors Activate Genes through the Phase-Separation Capacity of Their Activation Domains. Cell. 2018;175(7):1842-1855.e16. doi:10.1016/j.cell.2018.10.042.

149. Lin, Y. et al. Toxic PR Poly-Dipeptides Encoded by the C9orf72 Repeat Expansion Target LC Domain Polymers. Cell 167, 789-802 e712, doi:10.1016/j.cell.2016.10.003 (2016).

150. Zamudio, A. V., Dall'Agnese, A., Henninger, J. E., Manteiga, J. C., Afeyan, L. K., Hannett, N. M., Coffey, E. L., Li, C. H., Oksuz, O., Sabari, B. R., Boija, A., Klein, I. A., Hawken, S. W., Spille, J.-H., Decker, T.-M., Cisse, I. I., Abraham, B. J., Lee, T. I., Taatjes, D. J., … Young, R. A. (2019). Mediator condensates localize signaling factors to key cell identity genes. Molecular Cell, 76(5), 753-766.e6. https://doi.org/10.1016/j.molcel.2019.08.016

151. Cai, D., Feliciano, D., Dong, P., Flores, E., Gruebele, M., Porat-Shliom, N., Sukenik, S., Liu, Z., & Lippincott-Schwartz, J. (2019). Phase separation of YAP reorganizes genome topology for long-term YAP target gene expression. Nature Cell Biology, 21(12), 1578–1589. https://doi.org/10.1038/s41556-019-0433-z

152. Lu, Y., Wu, T., Gutman, O., Lu, H., Zhou, Q., Henis, Y. I., & Luo, K. (2020). Phase separation of TAZ compartmentalizes the transcription machinery to promote gene expression. Nature Cell Biology, 22(4), 453–464. https://doi.org/10.1038/s41556-020-0485-0

153. Nair, S. J., Yang, L., Meluzzi, D., Oh, S., Yang, F., Friedman, M. J., Wang, S., Suter, T., Alshareedah, I., Gamliel, A., Ma, Q., Zhang, J., Hu, Y., Tan, Y., Ohgi, K. A., Jayani, R. S., Banerjee, P. R., Aggarwal, A. K., & Rosenfeld, M. G. (2019). Phase separation of ligand-activated enhancers licenses cooperative chromosomal enhancer assembly. Nature Structural & Molecular Biology, 26(3), 193–203. https://doi.org/10.1038/s41594-019-0190-5

154. Boehning, M. et al. RNA polymerase II clustering through carboxy-terminal domain phase separation. Nat Struct Mol Biol, doi:10.1038/s41594-018-0112-y (2018).

155. Lu, H., Yu, D., Hansen, A. S., Ganguly, S., Liu, R., Heckert, A., Darzacq, X., & Zhou, Q. (2018). Phase-separation mechanism for C-terminal hyperphosphorylation of RNA polymerase II. Nature, 558(7709), 318–323. https://doi.org/10.1038/s41586-018-0174-3

156. Guo, Y.E., Manteiga, J.C., Henninger, J.E., Sabari, B.R., Dall'Agnese, A., Hannett, N.M., Spille, J.-H., Afeyan, L.K., Zamudio, A.V., Shrinivas, K., et al. (2019). Pol II phosphorylation regulates a switch between transcriptional and splicing condensates. Nature 572, 543.

157. Rawat, P., Boehning, M., Hummel, B., Aprile-Garcia, F., Pandit, A. S., Eisenhardt, N., Khavaran, A., Niskanen, E., Vos, S. M., Palvimo, J. J., Pichler, A., Cramer, P., & Sawarkar, R. (2021). Stress-induced nuclear condensation of NELF drives transcriptional downregulation. Molecular Cell, 81(5), 1013-1026.e11. https://doi.org/10.1016/j.molcel.2021.01.016

158. Sabari, B. R. Biomolecular Condensates and Gene Activation in Development and Disease. *Dev Cell* **55**, 84-96, doi:10.1016/j.devcel.2020.09.005 (2020).

159. Ma, J. & Ptashne, M. A new class of yeast transcriptional activators. *Cell* **51**, 113-119, doi:10.1016/0092-8674(87)90015-8 (1987).

160. Kadonaga, J. T., Courey, A. J., Ladika, J. & Tjian, R. Distinct regions of Sp1 modulate DNA binding and transcriptional activation. *Science* **242**, 1566-1570, doi:10.1126/science.3059495 (1988).

161. Keegan, L., Gill, G. & Ptashne, M. Separation of DNA binding from the transcriptionactivating function of a eukaryotic regulatory protein. *Science* **231**, 699-704, doi:10.1126/science.3080805 (1986).

162. Suter, D. M. Transcription Factors and DNA Play Hide and Seek. *Trends in Cell Biology* **30**, 491-500, doi:10.1016/j.tcb.2020.03.003 (2020).

163. Sabari, B. R., Dall'Agnese, A. & Young, R. A. Biomolecular Condensates in the Nucleus. *Trends Biochem Sci*, doi:10.1016/j.tibs.2020.06.007 (2020).

164. Fuxreiter, M. & Tompa, P. in *Fuzziness: Structural Disorder in Protein Complexes* (eds Monika Fuxreiter & Peter Tompa) 1-14 (Springer US, 2012).

165. Tuttle, L. M., Pacheco, D., Warfield, L., Luo, J., Ranish, J., Hahn, S., & Klevit, R. E. (2018). Gcn4-mediator specificity is mediated by a large and dynamic fuzzy protein-protein complex. Cell Reports, 22(12), 3251–3264. https://doi.org/10.1016/j.celrep.2018.02.097

166. Henley, M. J., Linhares, B. M., Morgan, B. S., Cierpicki, T., Fierke, C. A., & Mapp, A. K. (2020). Unexpected specificity within dynamic transcriptional protein–protein complexes. Proceedings of the National Academy of Sciences, 117(44), 27346–27353. https://doi.org/10.1073/pnas.2013244117

167. Goetz, S. K. & Mahamid, J. Visualizing Molecular Architectures of Cellular Condensates: Hints of Complex Coacervation Scenarios. *Dev Cell* **55**, 97-107, doi:10.1016/j.devcel.2020.09.003 (2020).

168. Kato, M. & McKnight, S. L. Cross-beta Polymerization of Low Complexity Sequence Domains. *Cold Spring Harb Perspect Biol* **9**, doi:10.1101/cshperspect.a023598 (2017).

169. Roden, C. & Gladfelter, A. S. RNA contributions to the form and function of biomolecular condensates. *Nat Rev Mol Cell Biol*, doi:10.1038/s41580-020-0264-6 (2020).

170. Van Treeck, B. & Parker, R. Emerging Roles for Intermolecular RNA-RNA Interactions in RNP Assemblies. *Cell* **174**, 791-802, doi:10.1016/j.cell.2018.07.023 (2018).

171. Lee, C.-Y. S., Putnam, A., Lu, T., He, S., Ouyang, J. P. T., & Seydoux, G. (2020). Recruitment of mRNAs to P granules by condensation with intrinsically-disordered proteins. ELife, 9, e52896.

172. Garcia-Jove Navarro, M., Kashida, S., Chouaib, R., Souquere, S., Pierron, G., Weil, D., & Gueroui, Z. (2019). RNA is a critical element for the sizing

and the composition of phase-separated RNA–protein condensates. Nature Communications, 10(1), 3230. https://doi.org/10.1038/s41467-019-11241-6

173. Zhou, Z. & Fu, X. D. Regulation of splicing by SR proteins and SR protein-specific kinases. *Chromosoma* **122**, 191-207, doi:10.1007/s00412-013-0407-z (2013).

174. Aumiller, W. M., Pir Cakmak, F., Davis, B. W. & Keating, C. D. RNA-Based Coacervates as a Model for Membraneless Organelles: Formation, Properties, and Interfacial Liposome Assembly. *Langmuir* **32**, 10042-10053, doi:10.1021/acs.langmuir.6b02499 (2016).

175. Kopp, F. & Mendell, J. T. Functional Classification and Experimental Dissection of Long Noncoding RNAs. *Cell* **172**, 393-407, doi:10.1016/j.cell.2018.01.011 (2018).

176. Li, X. & Fu, X.-D. Chromatin-associated RNAs as facilitators of functional genomic interactions. *Nature Reviews Genetics* **20**, 503-519, doi:10.1038/s41576-019-0135-1 (2019).

177. Cerase, A., Armaos, A., Neumayer, C., Avner, P., Guttman, M., & Tartaglia, G. G. (2019). Phase separation drives X-chromosome inactivation: A hypothesis. Nature Structural & Molecular Biology, 26(5), 331–334. https://doi.org/10.1038/s41594-019-0223-0

178. Hacisuleyman, E., Goff, L. A., Trapnell, C., Williams, A., Henao-Mejia, J., Sun, L., McClanahan, P., Hendrickson, D. G., Sauvageau, M., Kelley, D. R., Morse, M., Engreitz, J., Lander, E. S., Guttman, M., Lodish, H. F., Flavell, R., Raj, A., & Rinn, J. L. (2014). Topological organization of multichromosomal regions by the long intergenic noncoding RNA Firre. Nature Structural & Molecular Biology, 21(2), 198–206. https://doi.org/10.1038/nsmb.2764

179. Cassiday, L. A. & Maher III, L. J. Having it both ways: transcription factors that bind DNA and RNA. *Nucleic Acids Research* **30**, 4118-4126, doi:10.1093/nar/gkf512 (2002).

180. Schwartz, J. C., Wang, X., Podell, E. R. & Cech, T. R. RNA seeds higher-order assembly of FUS protein. *Cell Rep* **5**, 918-925, doi:10.1016/j.celrep.2013.11.017 (2013).

181. Belak, Z. R. & Ovsenek, N. Assembly of the Yin Yang 1 transcription factor into messenger ribonucleoprotein particles requires direct RNA binding activity. *J Biol Chem* **282**, 3791337920, doi:10.1074/jbc.M708057200 (2007).

182. Jeon, Y. & Lee, J. T. YY1 tethers Xist RNA to the inactive X nucleation center. *Cell* **146**, 119133, doi:10.1016/j.cell.2011.06.026 (2011).

183. Daneshvar, K., Ardehali, M. B., Klein, I. A., Hsieh, F.-K., Kratkiewicz, A. J., Mahpour, A., Cancelliere, S. O. L., Zhou, C., Cook, B. M., Li, W., Pondick, J. V., Gupta, S. K., Moran, S. P., Young, R. A., Kingston, R. E., & Mullen, A. C. (2020). Lncrna digit and brd3 protein form phase-separated condensates to regulate endoderm differentiation. Nature Cell Biology, 22(10), 1211–1222. https://doi.org/10.1038/s41556-020-0572-2

184. Lai, F., Orom, U. A., Cesaroni, M., Beringer, M., Taatjes, D. J., Blobel, G. A., & Shiekhattar, R. (2013). Activating RNAs associate with Mediator to enhance chromatin architecture and transcription. Nature, 494(7438), 497–501. https://doi.org/10.1038/nature11884

185. Lee, J.-H., Wang, R., Xiong, F., Krakowiak, J., Liao, Z., Nguyen, P. T., Moroz-Omori, E. V., Shao, J., Zhu, X., Bolt, M. J., Wu, H., Singh, P. K., Bi, M., Shi, C. J., Jamal, N., Li, G., Mistry, R., Jung, S. Y., Tsai, K.-L., … Li, W. (2021). Enhancer RNA m6A methylation facilitates transcriptional condensate formation and gene activation. Molecular Cell, 81(16), 3368-3385.e9. https://doi.org/10.1016/j.molcel.2021.07.024

186. Zhang, X. O., Gingeras, T. R. & Weng, Z. Genome-wide analysis of polymerase III-transcribed Alu elements suggests cell-type-specific enhancer function. *Genome Res* **29**, 1402-1414, doi:10.1101/gr.249789.119 (2019).

187. Su, M., Han, D., Boyd-Kirkup, J., Yu, X. & Han, J. J. Evolution of Alu elements toward enhancers. *Cell Rep* **7**, 376-385, doi:10.1016/j.celrep.2014.03.011 (2014).

188. Siersbæk, R., Baek, S., Rabiee, A., Nielsen, R., Traynor, S., Clark, N., Sandelin, A., Jensen, O. N., Sung, M.-H., Hager, G. L., & Mandrup, S. (2014). Molecular architecture of transcription factor hotspots in early adipogenesis. Cell Reports, 7(5), 1434–1442. https://doi.org/10.1016/j.celrep.2014.04.043

189. Papantonis, A. & Cook, P. R. Transcription factories: genome organization and gene regulation. *Chem Rev* **113**, 8683-8705, doi:10.1021/cr300513p (2013).

190. Shin, Y. et al. Liquid Nuclear Condensates Mechanically Sense and Restructure the Genome. Cell 175, 1481-1491 e1413, doi:10.1016/j.cell.2018.10.057 (2018).

191. Andersson, R., Sandelin, A. & Danko, C. G. A unified architecture of transcriptional regulatory elements. *Trends in Genetics* **31**, 426-433, doi:10.1016/j.tig.2015.05.007 (2015).

192. Shin, Y. & Brangwynne, C. P. Liquid phase condensation in cell physiology and disease. *Science* **357**, doi:10.1126/science.aaf4382 (2017).

193. Hnisz, D., Day, D. S. & Young, R. A. Insulated Neighborhoods: Structural and Functional Units of Mammalian Gene Control. *Cell* **167**, 1188-1200, doi:10.1016/j.cell.2016.10.024 (2016).

194. Sun, F., Chronis, C., Kronenberg, M., Chen, X.-F., Su, T., Lay, F. D., Plath, K., Kurdistani, S. K., & Carey, M. F. (2019). Promoter-enhancer communication occurs primarily within insulated neighborhoods. Molecular Cell, 73(2), 250-263.e5. https://doi.org/10.1016/j.molcel.2018.10.039

195. Fanucchi, S., Shibayama, Y., Burd, S., Weinberg, M. S. & Mhlanga, M. M. Chromosomal contact permits transcription between coregulated genes. *Cell* **155**, 606-620, doi:10.1016/j.cell.2013.09.051 (2013).

196. Papantonis, A., Kohro, T., Baboo, S., Larkin, J. D., Deng, B., Short, P., Tsutsumi, S., Taylor, S., Kanki, Y., Kobayashi, M., Li, G., Poh, H.-M., Ruan, X., Aburatani, H., Ruan, Y., Kodama, T., Wada, Y., & Cook, P. R. (2012). TNFα signals through specialized factories where responsive coding and miRNA genes are transcribed: Specialized transcription factories. The EMBO Journal, 31(23), 4404–4414. https://doi.org/10.1038/emboj.2012.288

197. Spilianakis, C. G., Lalioti, M. D., Town, T., Lee, G. R. & Flavell, R. A. Interchromosomal associations between alternatively expressed loci. *Nature* **435**, 637-645, doi:10.1038/nature03574 (2005).

198. Mourad, R., Hsu, P.-Y., Juan, L., Shen, C., Koneru, P., Lin, H., Liu, Y., Nephew, K., Huang, T. H., & Li, L. (2014). Estrogen induces global

reorganization of chromatin structure in human breast cancer cells. PLoS ONE, 9(12), e113354. https://doi.org/10.1371/journal.pone.0113354

199. Hsu, P.-Y., Hsu, H.-K., Hsiao, T.-H., Ye, Z., Wang, E., Profit, A. L., Jatoi, I., Chen, Y., Kirma, N. B., Jin, V. X., Sharp, Z. D., & Huang, T. H.-M. (2016). Spatiotemporal control of estrogen-responsive transcription in ERα-positive breast cancer cells. Oncogene, 35(18), 2379–2389. https://doi.org/10.1038/onc.2015.298

200. Markenscoff-Papadimitriou, E., Allen, W. E., Colquitt, B. M., Goh, T., Murphy, K. K., Monahan, K., Mosley, C. P., Ahituv, N., & Lomvardas, S. (2014). Enhancer interaction networks as a means for singular olfactory receptor expression. Cell, 159(3), 543–557. https://doi.org/10.1016/j.cell.2014.09.033

201. Madsen, J. G. S., Madsen, M. S., Rauch, A., Traynor, S., Van Hauwaert, E. L., Haakonsson, A. K., Javierre, B. M., Hyldahl, M., Fraser, P., & Mandrup, S. (2020). Highly interconnected enhancer communities control lineage-determining genes in human mesenchymal stem cells. Nature Genetics, 52(11), 1227–1238. https://doi.org/10.1038/s41588-020-0709-z

202. Monahan, K., Schieren, I., Cheung, J., Mumbey-Wafula, A., Monuki, E. S., & Lomvardas, S. (2017). Cooperative interactions enable singular olfactory receptor expression in mouse olfactory neurons. ELife, 6, e28620. https://doi.org/10.7554/eLife.28620

203. Monahan, K., Horta, A. & Lomvardas, S. LHX2- and LDB1-mediated trans interactions regulate olfactory receptor choice. *Nature* **565**, 448-453, doi:10.1038/s41586-018-0845-0 (2019).

204. Mao, Y. S., Zhang, B. & Spector, D. L. Biogenesis and function of nuclear bodies. *Trends Genet* **27**, 295-306, doi:10.1016/j.tig.2011.05.006 (2011).

205. Brown, J. M. et al. Association between active genes occurs at nuclear speckles and is modulated by chromatin environment. J Cell Biol 182, 1083-1097, doi:10.1083/jcb.200803174 (2008).

206. Khanna, N., Hu, Y. & Belmont, A. S. HSP70 transgene directed motion to nuclear speckles facilitates heat shock activation. *Curr Biol* **24**, 1138-1144, doi:10.1016/j.cub.2014.03.053 (2014).

207. Shopland, L. S., Johnson, C. V., Byron, M., McNeil, J. & Lawrence, J. B. Clustering of multiple specific genes and gene-rich R-bands around SC-35 domains: evidence for local euchromatic neighborhoods. *J Cell Biol* **162**, 981-990, doi:10.1083/jcb.200303131 (2003).

208. Hu, Y., Plutz, M. & Belmont, A. S. Hsp70 gene association with nuclear speckles is Hsp70 promoter specific. *Journal of Cell Biology* **191**, 711-719, doi:10.1083/jcb.201004041 (2010).

209. Bhat, P., Honson, D. & Guttman, M. Nuclear compartmentalization as a mechanism of quantitative control of gene expression. *Nat Rev Mol Cell Biol*, doi:10.1038/s41580-02100387-1 (2021).

210. Coelho, M. B., Attig, J., Bellora, N., König, J., Hallegger, M., Kayikci, M., Eyras, E., Ule, J., & Smith, C. W. (2015). Nuclear matrix protein Matrin3 regulates alternative splicing and forms overlapping regulatory networks with PTB. The EMBO Journal, 34(5), 653–668. https://doi.org/10.15252/embj.201489852

211. Skowronska-Krawczyk, D. et al. Required enhancer-matrin-3 network interactions for a homeodomain transcription program. Nature 514, 257-261, doi:10.1038/nature13573 (2014).

212. Spector, D. L. & Lamond, A. I. Nuclear speckles. *Cold Spring Harb Perspect Biol* **3**, doi:10.1101/cshperspect.a000646 (2011).

213. Boisvert, F.-M., van Koningsbruggen, S., Navascués, J. & Lamond, A. I. The multifunctional nucleolus. *Nature Reviews Molecular Cell Biology* **8**, 574-585, doi:10.1038/nrm2184 (2007).

214. Pederson, T. The nucleolus. *Cold Spring Harbor perspectives in biology* **3**, a000638, doi:10.1101/cshperspect.a000638 (2011).

215. Lindström, M. S., Jurada, D., Bursac, S., Orsolic, I., Bartek, J., & Volarevic, S. (2018). Nucleolus as an emerging hub in maintenance of genome stability and cancer pathogenesis. Oncogene, 37(18), 2351–2366. https://doi.org/10.1038/s41388-017-0121-z

216. Frottin, F., Schueder, F., Tiwary, S., Gupta, R., Körner, R., Schlichthaerle, T., Cox, J., Jungmann, R., Hartl, F. U., & Hipp, M. S. (2019). The nucleolus

functions as a phase-separated protein quality control compartment. Science, 365(6451), 342–347. https://doi.org/10.1126/science.aaw9157

217. Lafontaine, D. L. J., Riback, J. A., Bascetin, R. & Brangwynne, C. P. The nucleolus as a multiphase liquid condensate. *Nature Reviews Molecular Cell Biology* **22**, 165-182, doi:10.1038/s41580-020-0272-6 (2021).

218. Kim, J., Venkata, N. C., Hernandez Gonzalez, G. A., Khanna, N. & Belmont, A. S. Gene expression amplification by nuclear speckle association. *J Cell Biol* **219**, doi:10.1083/jcb.201904046 (2020).

219. 2 Chromatin patterns at transcription factor binding sites. *Nature*, doi:10.1038/nature28171 (2019).

220. Ratman, D., Vanden Berghe, W., Dejager, L., Libert, C., Tavernier, J., Beck, I. M., & De Bosscher, K. (2013). How glucocorticoid receptors modulate the activity of other transcription factors: A scope beyond tethering. Molecular and Cellular Endocrinology, 380(1–2), 41–54.

221. Stender, J. D., Kim, K., Charn, T. H., Komm, B., Chang, K. C. N., Kraus, W. L., Benner, C., Glass, C. K., & Katzenellenbogen, B. S. (2010). Genome-wide analysis of estrogen receptor α dna binding and tethering mechanisms identifies runx1 as a novel tethering factor in receptor-mediated transcriptional activation. Molecular and Cellular Biology, 30(16), 3943–3955. https://doi.org/10.1128/MCB.00118-10

222. Chong, S. et al. Imaging dynamic and selective low-complexity domain interactions that control gene transcription. Science, doi:10.1126/science.aar2555 (2018).

223. Boulay, G. et al. Cancer-Specific Retargeting of BAF Complexes by a Prion-like Domain. Cell 171, 163-178 e119, doi:10.1016/j.cell.2017.07.036 (2017).

224. Brodsky, S., Jana, T., Mittelman, K., Chapal, M., Kumar, D. K., Carmi, M., & Barkai, N. (2020). Intrinsically disordered regions direct transcription factor in vivo binding specificity. Molecular Cell, 79(3), 459-471.e4. https://doi.org/10.1016/j.molcel.2020.05.032

225. Garcia, D. A., Johnson, T. A., Presman, D. M., Fettweis, G., Wagh, K., Rinaldi, L., Stavreva, D. A., Paakinaho, V., Jensen, R. A. M., Mandrup, S., Upadhyaya, A., & Hager, G. L. (2021). An intrinsically disordered region-

mediated confinement state contributes to the dynamics and function of transcription factors. Molecular Cell, 81(7), 1484-1498.e6. https://doi.org/10.1016/j.molcel.2021.01.013

226. Milin, A. N. & Deniz, A. A. Reentrant Phase Transitions and Non-Equilibrium Dynamics in Membraneless Organelles. *Biochemistry* **57**, 2470-2477, doi:10.1021/acs.biochem.8b00001 (2018).

227. Banerjee, P. R., Milin, A. N., Moosa, M. M., Onuchic, P. L. & Deniz, A. A. Reentrant Phase Transition Drives Dynamic Substructure Formation in Ribonucleoprotein Droplets. *Angew Chem Int Ed Engl* **56**, 11354-11359, doi:10.1002/anie.201703191 (2017).

228. Henninger, J. E., Oksuz, O., Shrinivas, K., Sagi, I., LeRoy, G., Zheng, M. M., Andrews, J. O., Zamudio, A. V., Lazaris, C., Hannett, N. M., Lee, T. I., Sharp, P. A., Cissé, I. I., Chakraborty, A. K., & Young, R. A. (2021). Rna-mediated feedback control of transcriptional condensates. Cell, 184(1), 207-225.e24. https://doi.org/10.1016/j.cell.2020.11.030

229. Snead, W. T. & Gladfelter, A. S. The Control Centers of Biomolecular Phase Separation: How Membrane Surfaces, PTMs, and Active Processes Regulate Condensation. *Molecular cell* **76**, 295-305, doi:10.1016/j.molcel.2019.09.016 (2019).

230. Patel, A., Lee, H. O., Jawerth, L., Maharana, S., Jahnel, M., Hein, M. Y., Stoynov, S., Mahamid, J., Saha, S., Franzmann, T. M., Pozniakovski, A., Poser, I., Maghelli, N., Royer, L. A., Weigert, M., Myers, E. W., Grill, S., Drechsel, D., Hyman, A. A., & Alberti, S. (2015). A liquid-to-solid phase transition of the als protein fus accelerated by disease mutation. Cell, 162(5), 1066–1077. https://doi.org/10.1016/j.cell.2015.07.047

231. Maharana, S., Wang, J., Papadopoulos, D. K., Richter, D., Pozniakovsky, A., Poser, I., Bickle, M., Rizk, S., Guillén-Boixet, J., Franzmann, T. M., Jahnel, M., Marrone, L., Chang, Y.-T., Sterneckert, J., Tomancak, P., Hyman, A. A., & Alberti, S. (2018). RNA buffers the phase separation behavior of prion-like RNA binding proteins. Science, 360(6391), 918–921. https://doi.org/10.1126/science.aar7366

232. Patel, A., Malinovska, L., Saha, S., Wang, J., Alberti, S., Krishnan, Y., & Hyman, A. A. (2017). ATP as a biological hydrotrope. Science, 356(6339), 753–756. https://doi.org/10.1126/science.aaf6846

233. Lin, Y., Protter, D. S., Rosen, M. K. & Parker, R. Formation and Maturation of PhaseSeparated Liquid Droplets by RNA-Binding Proteins. *Mol Cell* **60**, 208-219, doi:10.1016/j.molcel.2015.08.018 (2015).

234. Molliex, A. et al. Phase separation by low complexity domains promotes stress granule assembly and drives pathological fibrillization. Cell 163, 123-133, doi:10.1016/j.cell.2015.09.015 (2015).

235. Canver, M. C., Haeussler, M., Bauer, D. E., Orkin, S. H., Sanjana, N. E., Shalem, O., Yuan, G.-C., Zhang, F., Concordet, J.-P., & Pinello, L. (2018). Integrated design, execution, and analysis of arrayed and pooled CRISPR genome-editing experiments. Nature Protocols, 13(5), 946–986. https://doi.org/10.1038/nprot.2018.005

236. Montalbano, A., Canver, M. C. & Sanjana, N. E. High-Throughput Approaches to Pinpoint Function within the Noncoding Genome. *Mol Cell* **68**, 44-59, doi:10.1016/j.molcel.2017.09.017 (2017).

237. Li, K., Liu, Y., Cao, H., Zhang, Y., Gu, Z., Liu, X., Yu, A., Kaphle, P., Dickerson, K. E., Ni, M., & Xu, J. (2020). Interrogation of enhancer function by enhancer-targeting CRISPR epigenetic editing. Nature Communications, 11(1), 485. https://doi.org/10.1038/s41467-020-14362-5

238. Canver, M. C., Bauer, D. E. & Orkin, S. H. Functional interrogation of non-coding DNA through CRISPR genome editing. *Methods* **121-122**, 118-129, doi:https://doi.org/10.1016/j.ymeth.2017.03.008 (2017).

239. Gilbert, L. A., Larson, M. H., Morsut, L., Liu, Z., Brar, G. A., Torres, S. E., Stern-Ginossar, N., Brandman, O., Whitehead, E. H., Doudna, J. A., Lim, W. A., Weissman, J. S., & Qi, L. S. (2013). Crispr-mediated modular rna-guided regulation of transcription in eukaryotes. Cell, 154(2), 442–451. https://doi.org/10.1016/j.cell.2013.06.044

240. Kearns, N. A., Pham, H., Tabak, B., Genga, R. M., Silverstein, N. J., Garber, M., & Maehr, R. (2015). Functional annotation of native enhancers with a

Cas9–histone demethylase fusion. *Nature Methods*, *12*(5), 401–403. https://doi.org/10.1038/nmeth.3325

241. Xie, S., Duan, J., Li, B., Zhou, P. & Hon, G. C. Multiplexed Engineering and Analysis of Combinatorial Enhancer Activity in Single Cells. *Molecular Cell* **66**, 285-299.e285, doi:https://doi.org/10.1016/j.molcel.2017.03.007 (2017).

242. Schraivogel, D., Gschwind, A. R., Milbank, J. H., Leonce, D. R., Jakob, P., Mathur, L., Korbel, J. O., Merten, C. A., Velten, L., & Steinmetz, L. M. (2020). Targeted Perturb-seq enables genome-scale genetic screens in single cells. Nature Methods, 17(6), 629–635. https://doi.org/10.1038/s41592-020-0837-5

243. Rickels, R. & Shilatifard, A. Enhancer Logic and Mechanics in Development and Disease. *Trends Cell Biol* **28**, 608-630, doi:10.1016/j.tcb.2018.04.003 (2018).

244. Ernst, J., Kheradpour, P., Mikkelsen, T. S., Shoresh, N., Ward, L. D., Epstein, C. B., Zhang, X., Wang, L., Issner, R., Coyne, M., Ku, M., Durham, T., Kellis, M., & Bernstein, B. E. (2011). Mapping and analysis of chromatin state dynamics in nine human cell types. Nature, 473(7345), 43–49. https://doi.org/10.1038/nature09906

245. Hnisz, D., Abraham, B. J., Lee, T. I., Lau, A., Saint-André, V., Sigova, A. A., Hoke, H. A., & Young, R. A. (2013). Super-enhancers in the control of cell identity and disease. Cell, 155(4), 934–947. https://doi.org/10.1016/j.cell.2013.09.053

246. Corradin, O. & Scacheri, P. C. Enhancer variants: evaluating functions in common disease. *Genome Med* **6**, 85, doi:10.1186/s13073-014-0085-3 (2014).

247. Kircher, M., Xiong, C., Martin, B., Schubach, M., Inoue, F., Bell, R. J. A., Costello, J. F., Shendure, J., & Ahituv, N. (2019). Saturation mutagenesis of twenty disease-associated regulatory elements at single base-pair resolution. Nature Communications, 10(1), 3583. https://doi.org/10.1038/s41467-019-11526-w

248. Sheffield, N. C., Thurman, R. E., Song, L., Safi, A., Stamatoyannopoulos, J. A., Lenhard, B., Crawford, G. E., & Furey, T. S. (2013). Patterns of regulatory activity across diverse human cell types predict tissue identity,

transcription factor binding, and long-range interactions. Genome Research, 23(5), 777–788. https://doi.org/10.1101/gr.152140.112

249. Thurman, R. E., Rynes, E., Humbert, R., Vierstra, J., Maurano, M. T., Haugen, E., Sheffield, N. C., Stergachis, A. B., Wang, H., Vernot, B., Garg, K., John, S., Sandstrom, R., Bates, D., Boatman, L., Canfield, T. K., Diegel, M., Dunn, D., Ebersol, A. K., … Stamatoyannopoulos, J. A. (2012). The accessible chromatin landscape of the human genome. Nature, 489(7414), 75–82. https://doi.org/10.1038/nature11232

250. The Geuvadis Consortium, Lappalainen, T., Sammeth, M., Friedländer, M. R., ‘t Hoen, P. A. C., Monlong, J., Rivas, M. A., Gonzàlez-Porta, M., Kurbatova, N., Griebel, T., Ferreira, P. G., Barann, M., Wieland, T., Greger, L., van Iterson, M., Almlöf, J., Ribeca, P., Pulyakhina, I., Esser, D., … Dermitzakis, E. T. (2013). Transcriptome and genome sequencing uncovers functional variation in humans. Nature, 501(7468), 506–511. https://doi.org/10.1038/nature12531

251. Moore, J. E., Pratt, H. E., Purcaro, M. J. & Weng, Z. A curated benchmark of enhancer-gene interactions for evaluating enhancer-target gene prediction methods. *Genome Biology* **21**, 17, doi:10.1186/s13059-019-1924-8 (2020).

252. Rao, S. S. P., Huntley, M. H., Durand, N. C., Stamenova, E. K., Bochkov, I. D., Robinson, J. T., Sanborn, A. L., Machol, I., Omer, A. D., Lander, E. S., & Aiden, E. L. (2014). A 3d map of the human genome at kilobase resolution reveals principles of chromatin looping. Cell, 159(7), 1665–1680. https://doi.org/10.1016/j.cell.2014.11.021

253. Mumbach, M. R., Satpathy, A. T., Boyle, E. A., Dai, C., Gowen, B. G., Cho, S. W., Nguyen, M. L., Rubin, A. J., Granja, J. M., Kazane, K. R., Wei, Y., Nguyen, T., Greenside, P. G., Corces, M. R., Tycko, J., Simeonov, D. R., Suliman, N., Li, R., Xu, J., … Chang, H. Y. (2017). Enhancer connectome in primary human cells identifies target genes of disease-associated DNA elements. Nature Genetics, 49(11), 1602–1612. https://doi.org/10.1038/ng.3963

254. Nott, A., Holtman, I. R., Coufal, N. G., Schlachetzki, J. C. M., Yu, M., Hu, R., Han, C. Z., Pena, M., Xiao, J., Wu, Y., Keulen, Z., Pasillas, M. P., O’Connor, C., Nickl, C. K., Schafer, S. T., Shen, Z., Rissman, R. A., Brewer, J. B., Gosselin, D., … Glass, C. K. (2019). Brain cell type–specific enhancer–

promoter interactome maps and disease - risk association. Science, 366(6469), 1134–1139. https://doi.org/10.1126/science.aay0793

255. Javierre, B. M., Burren, O. S., Wilder, S. P., Kreuzhuber, R., Hill, S. M., Sewitz, S., Cairns, J., Wingett, S. W., Várnai, C., Thiecke, M. J., Burden, F., Farrow, S., Cutler, A. J., Rehnström, K., Downes, K., Grassi, L., Kostadima, M., Freire-Pritchett, P., Wang, F., … Flicek, P. (2016). Lineage-specific genome architecture links enhancers and non-coding disease variants to target gene promoters. Cell, 167(5), 1369-1384.e19. https://doi.org/10.1016/j.cell.2016.09.037

256. Riback, J. A., Zhu, L., Ferrolino, M. C., Tolbert, M., Mitrea, D. M., Sanders, D. W., Wei, M.-T., Kriwacki, R. W., & Brangwynne, C. P. (2020). Composition-dependent thermodynamics of intracellular phase separation. Nature, 581(7807), 209–214. https://doi.org/10.1038/s41586-020-2256-2

257. McSwiggen, D. T., Mir, M., Darzacq, X. & Tjian, R. Evaluating phase separation in live cells: diagnosis, caveats, and functional consequences. *Genes Dev* **33**, 1619-1634, doi:10.1101/gad.331520.119 (2019).

258. Wheeler, J. R., Matheny, T., Jain, S., Abrisch, R. & Parker, R. Distinct stages in stress granule assembly and disassembly. *Elife* **5**, doi:10.7554/eLife.18413 (2016).

259. Martin, E. W., Holehouse, A. S., Peran, I., Farag, M., Incicco, J. J., Bremer, A., Grace, C. R., Soranno, A., Pappu, R. V., & Mittag, T. (2020). Valence and patterning of aromatic residues determine the phase behavior of prion-like domains. Science, 367(6478), 694–699.

260. Klein, I. A., Boija, A., Afeyan, L. K., Hawken, S. W., Fan, M., Dall'Agnese, A., Oksuz, O., Henninger, J. E., Shrinivas, K., Sabari, B. R., Sagi, I., Clark, V. E., Platt, J. M., Kar, M., McCall, P. M., Zamudio, A. V., Manteiga, J. C., Coffey, E. L., Li, C. H., … Young, R. A. (2020). Partitioning of cancer therapeutics in nuclear condensates. Science, 368(6497), 1386–1392. https://doi.org/10.1126/science.aaz4427

261. Boettiger, A. N., Bintu, B., Moffitt, J. R., Wang, S., Beliveau, B. J., Fudenberg, G., Imakaev, M., Mirny, L. A., Wu, C., & Zhuang, X. (2016). Super-resolution imaging reveals distinct chromatin folding for different

epigenetic states. Nature, 529(7586), 418–422. https://doi.org/10.1038/nature16496

262. Tsai, P.-F., Dell'Orso, S., Rodriguez, J., Vivanco, K. O., Ko, K.-D., Jiang, K., Juan, A. H., Sarshad, A. A., Vian, L., Tran, M., Wangsa, D., Wang, A. H., Perovanovic, J., Anastasakis, D., Ralston, E., Ried, T., Sun, H.-W., Hafner, M., Larson, D. R., & Sartorelli, V. (2018a). A muscle-specific enhancer rna mediates cohesin recruitment and regulates transcription in trans. Molecular Cell, 71(1), 129-141.e8. https://doi.org/10.1016/j.molcel.2018.06.008

263. Wang, D., Garcia-Bassets, I., Benner, C., Li, W., Su, X., Zhou, Y., Qiu, J., Liu, W., Kaikkonen, M. U., Ohgi, K. A., Glass, C. K., Rosenfeld, M. G., & Fu, X.-D. (2011). Reprogramming transcription by distinct classes of enhancers functionally defined by eRNA. Nature, 474(7351), 390–394. https://doi.org/10.1038/nature10006

264. Lam, M. T. Y., Cho, H., Lesch, H. P., Gosselin, D., Heinz, S., Tanaka-Oishi, Y., Benner, C., Kaikkonen, M. U., Kim, A. S., Kosaka, M., Lee, C. Y., Watt, A., Grossman, T. R., Rosenfeld, M. G., Evans, R. M., & Glass, C. K. (2013). Rev-Erbs repress macrophage gene expression by inhibiting enhancer-directed transcription. Nature, 498(7455), 511–515. https://doi.org/10.1038/nature12209

265. Michel, M., Demel, C., Zacher, B., Schwalb, B., Krebs, S., Blum, H., Gagneur, J., & Cramer, P. (2017). TT-seq captures enhancer landscapes immediately after T-cell stimulation. Molecular Systems Biology, 13(3), 920. https://doi.org/10.15252/msb.20167507

266. Wu, T., Lyu, R., You, Q. & He, C. Kethoxal-assisted single-stranded DNA sequencing captures global transcription dynamics and enhancer activity in situ. *Nat Methods* **17**, 515-523, doi:10.1038/s41592-020-0797-9 (2020).

267. Wissink, E. M., Vihervaara, A., Tippens, N. D. & Lis, J. T. Nascent RNA analyses: tracking transcription and its regulation. *Nature Reviews Genetics* **20**, 705-723, doi:10.1038/s41576-019-0159-6 (2019).

268. Hirabayashi, S., Bhagat, S., Matsuki, Y., Takegami, Y., Uehata, T., Kanemaru, A., Itoh, M., Shirakawa, K., Takaori-Kondo, A., Takeuchi, O., Carninci, P., Katayama, S., Hayashizaki, Y., Kere, J., Kawaji, H., & Murakawa, Y. (2019). NET-CAGE characterizes the dynamics and topology

of human transcribed cis-regulatory elements. Nature Genetics, 51(9), 1369–1379. https://doi.org/10.1038/s41588-019-0485-9

269. Arner, E., Daub, C. O., Vitting-Seerup, K., Andersson, R., Lilje, B., Drabløs, F., Lennartsson, A., Rönnerblad, M., Hrydziuszko, O., Vitezic, M., Freeman, T. C., M. N. Alhendi, A., Arner, P., Axton, R., Baillie, J. K., Beckhouse, A., Bodega, B., Briggs, J., Brombacher, F., … Hayashizaki, Y. (2015). Transcribed enhancers lead waves of coordinated transcription in transitioning mammalian cells. Science, 347(6225), 1010–1014. https://doi.org/10.1126/science.1259418

270. Meers, M. P., Adelman, K., Duronio, R. J., Strahl, B. D., McKay, D. J., & Matera, A. G. (2018). Transcription start site profiling uncovers divergent transcription and enhancer-associated RNAs in Drosophila melanogaster. BMC Genomics, 19(1), 157. https://doi.org/10.1186/s12864-018-4510-7

271. Henriques, T., Scruggs, B. S., Inouye, M. O., Muse, G. W., Williams, L. H., Burkholder, A. B., Lavender, C. A., Fargo, D. C., & Adelman, K. (2018). Widespread transcriptional pausing and elongation control at enhancers. Genes & Development, 32(1), 26–41. https://doi.org/10.1101/gad.309351.117

272. Chen, R. A.-J., Down, T. A., Stempor, P., Chen, Q. B., Egelhofer, T. A., Hillier, L. W., Jeffers, T. E., & Ahringer, J. (2013). The landscape of RNA polymerase II transcription initiation in C. elegans reveals promoter and enhancer architectures. Genome Research, 23(8), 1339–1347. https://doi.org/10.1101/gr.153668.112

273. Struhl, K. Transcriptional noise and the fidelity of initiation by RNA polymerase II. *Nature Structural & Molecular Biology* **14**, 103-105, doi:10.1038/nsmb0207-103 (2007).

274. Yoo, E. J., Cooke, N. E. & Liebhaber, S. A. An RNA-independent linkage of noncoding transcription to long-range enhancer function. *Mol Cell Biol* **32**, 2020-2029, doi:10.1128/mcb.06650-11 (2012).

275. Lee, J. S. & Mendell, J. T. Antisense-Mediated Transcript Knockdown Triggers Premature Transcription Termination. *Mol Cell* **77**, 1044-1054.e1043, doi:10.1016/j.molcel.2019.12.011 (2020).

276. Lai, F., Damle, S. S., Ling, K. K. & Rigo, F. Directed RNase H Cleavage of Nascent Transcripts Causes Transcription Termination. *Molecular Cell* **77**, 1032-1043.e1034, doi:10.1016/j.molcel.2019.12.029 (2020).

277. Arnold, P. R., Wells, A. D. & Li, X. C. Diversity and Emerging Roles of Enhancer RNA in Regulation of Gene Expression and Cell Fate. *Frontiers in Cell and Developmental Biology* **7**, doi:10.3389/fcell.2019.00377 (2020).

278. Sartorelli, V. & Lauberth, S. M. Enhancer RNAs are an important regulatory layer of the epigenome. *Nat Struct Mol Biol* **27**, 521-528, doi:10.1038/s41594-020-0446-0 (2020).

279. Blinka, S., Reimer, M. H., Jr., Pulakanti, K. & Rao, S. Super-Enhancers at the Nanog Locus Differentially Regulate Neighboring Pluripotency-Associated Genes. *Cell Rep* **17**, 19-28, doi:10.1016/j.celrep.2016.09.002 (2016).

280. Pnueli, L., Rudnizky, S., Yosefzon, Y. & Melamed, P. RNA transcribed from a distal enhancer is required for activating the chromatin at the promoter of the gonadotropin α-subunit gene. *Proceedings of the National Academy of Sciences* **112**, 4369-4374, doi:10.1073/pnas.1414841112 (2015).

281. Tsai, P.-F., Dell'Orso, S., Rodriguez, J., Vivanco, K. O., Ko, K.-D., Jiang, K., Juan, A. H., Sarshad, A. A., Vian, L., Tran, M., Wangsa, D., Wang, A. H., Perovanovic, J., Anastasakis, D., Ralston, E., Ried, T., Sun, H.-W., Hafner, M., Larson, D. R., & Sartorelli, V. (2018a). A muscle-specific enhancer rna mediates cohesin recruitment and regulates transcription in trans. Molecular Cell, 71(1), 129-141.e8. https://doi.org/10.1016/j.molcel.2018.06.008

282. Lai, F., Gardini, A., Zhang, A. & Shiekhattar, R. Integrator mediates the biogenesis of enhancer RNAs. *Nature* **525**, 399-403, doi:10.1038/nature14906 (2015).

283. Hsieh, C.-L., Fei, T., Chen, Y., Li, T., Gao, Y., Wang, X., Sun, T., Sweeney, C. J., Lee, G.-S. M., Chen, S., Balk, S. P., Liu, X. S., Brown, M., & Kantoff, P. W. (2014). Enhancer RNAs participate in androgen receptor-driven looping that selectively enhances gene activation. Proceedings of the National Academy of Sciences, 111(20), 7319–7324. https://doi.org/10.1073/pnas.1324151111

284. Pezone, A., Zuchegna, C., Tramontano, A., Romano, A., Russo, G., de Rosa, M., Vinciguerra, M., Porcellini, A., Gottesman, M. E., & Avvedimento, E. V. (2019). Rna stabilizes transcription-dependent chromatin loops induced by nuclear hormones. Scientific Reports, 9(1), 3925. https://doi.org/10.1038/s41598-019-40123-6

285. Tan, Y., Jin, C., Ma, W., Hu, Y., Tanasa, B., Oh, S., Gamliel, A., Ma, Q., Yao, L., Zhang, J., Ohgi, K., Liu, W., Aggarwal, A. K., & Rosenfeld, M. G. (2018). Dismissal of rna polymerase ii underlies a large ligand-induced enhancer decommissioning program. Molecular Cell, 71(4), 526-539.e8. https://doi.org/10.1016/j.molcel.2018.07.039

286. Bose, D. A., Donahue, G., Reinberg, D., Shiekhattar, R., Bonasio, R., & Berger, S. L. (2017). Rna binding to cbp stimulates histone acetylation and transcription. Cell, 168(1–2), 135-149.e22. https://doi.org/10.1016/j.cell.2016.12.020

287. Rahnamoun, H., Lee, J., Sun, Z., Lu, H., Ramsey, K. M., Komives, E. A., & Lauberth, S. M. (2018). RNAs interact with BRD4 to promote enhanced chromatin engagement and transcription activation. Nature Structural & Molecular Biology, 25(8), 687–697. https://doi.org/10.1038/s41594-018-0102-0

288. Bai, X., Li, F. & Zhang, Z. Evidences for functional trans-acting eRNA-promoter R-loops at Alu sequences. *bioRxiv*, 2021.2002.2017.431596, doi:10.1101/2021.02.17.431596 (2021).

289. Zhao, Y., Wang, L., Ren, S., Wang, L., Blackburn, P. R., McNulty, M. S., Gao, X., Qiao, M., Vessella, R. L., Kohli, M., Zhang, J., Karnes, R. J., Tindall, D. J., Kim, Y., MacLeod, R., Ekker, S. C., Kang, T., Sun, Y., & Huang, H. (2016). Activation of p-tefb by androgen receptor-regulated enhancer rnas in castration-resistant prostate cancer. Cell Reports, 15(3), 599–610. https://doi.org/10.1016/j.celrep.2016.03.038

290. Pagano, J. M., Kwak, H., Waters, C. T., Sprouse, R. O., White, B. S., Ozer, A., Szeto, K., Shalloway, D., Craighead, H. G., & Lis, J. T. (2014). Defining nelf-e rna binding in hiv-1 and promoter-proximal pause regions. PLoS Genetics, 10(1), e1004090. https://doi.org/10.1371/journal.pgen.1004090

291. Ren, C., Liu, F., Ouyang, Z., An, G., Zhao, C., Shuai, J., Cai, S., Bo, X., & Shu, W. (2017). Functional annotation of structural ncRNAs within enhancer

RNAs in the human genome: Implications for human disease. Scientific Reports, 7(1), 15518. https://doi.org/10.1038/s41598-017-15822-7

292. Gorbovytska, V., Kim, S.-K., Kuybu, F., Götze, M., Um, D., Kang, K., Pittroff, A., Schneider, L.-M., Leitner, A., Kim, T.-K., & Kuhn, C.-D. (2021). Enhancer RNAs stimulate Pol II pause release by harnessing multivalent interactions to NELF [Preprint]. Biochemistry. https://doi.org/10.1101/2021.04.25.441328

293. Aguilo, F., Li, S., Balasubramaniyan, N., Sancho, A., Benko, S., Zhang, F., Vashisht, A., Rengasamy, M., Andino, B., Chen, C., Zhou, F., Qian, C., Zhou, M.-M., Wohlschlegel, J. A., Zhang, W., Suchy, F. J., & Walsh, M. J. (2016). Deposition of 5-methylcytosine on enhancer rnas enables the coactivator function of pgc-1α. Cell Reports, 14(3), 479–492. https://doi.org/10.1016/j.celrep.2015.12.043

294. Maurano, M. T., Humbert, R., Rynes, E., Thurman, R. E., Haugen, E., Wang, H., Reynolds, A. P., Sandstrom, R., Qu, H., Brody, J., Shafer, A., Neri, F., Lee, K., Kutyavin, T., Stehling-Sun, S., Johnson, A. K., Canfield, T. K., Giste, E., Diegel, M., … Stamatoyannopoulos, J. A. (2012). Systematic localization of common disease-associated variation in regulatory dna. Science, 337(6099), 1190–1195. https://doi.org/10.1126/science.1222794

295. Welter, D., MacArthur, J., Morales, J., Burdett, T., Hall, P., Junkins, H., Klemm, A., Flicek, P., Manolio, T., Hindorff, L., & Parkinson, H. (2014). The NHGRI GWAS Catalog, a curated resource of SNP-trait associations. Nucleic Acids Research, 42(D1), D1001–D1006.

296. Pasquali, L., Gaulton, K. J., Rodríguez-Seguí, S. A., Mularoni, L., Miguel-Escalada, I., Akerman, İ., Tena, J. J., Morán, I., Gómez-Marín, C., van de Bunt, M., Ponsa-Cobas, J., Castro, N., Nammo, T., Cebola, I., García-Hurtado, J., Maestro, M. A., Pattou, F., Piemonti, L., Berney, T., … Ferrer, J. (2014). Pancreatic islet enhancer clusters enriched in type 2 diabetes risk-associated variants. Nature Genetics, 46(2), 136–143. https://doi.org/10.1038/ng.2870

297. Sur, I. & Taipale, J. The role of enhancers in cancer. *Nature Reviews Cancer* **16**, 483-493, doi:10.1038/nrc.2016.62 (2016).

298. Findlay, G. M., Boyle, E. A., Hause, R. J., Klein, J. C. & Shendure, J. Saturation editing of genomic regions by multiplex homology-directed repair. *Nature* **513**, 120-123, doi:10.1038/nature13695 (2014).

299. Taub, R., Kirsch, I., Morton, C., Lenoir, G., Swan, D., Tronick, S., Aaronson, S., & Leder, P. (1982). Translocation of the c-myc gene into the immunoglobulin heavy chain locus in human Burkitt lymphoma and murine plasmacytoma cells. Proceedings of the National Academy of Sciences, 79(24), 7837–7841. https://doi.org/10.1073/pnas.79.24.7837

300. Zhang, X., Choi, P. S., Francis, J. M., Imielinski, M., Watanabe, H., Cherniack, A. D., & Meyerson, M. (2016). Identification of focally amplified lineage-specific super-enhancers in human epithelial cancers. Nature Genetics, 48(2), 176–182. https://doi.org/10.1038/ng.3470

301. Abraham, B. J., Hnisz, D., Weintraub, A. S., Kwiatkowski, N., Li, C. H., Li, Z., Weichert-Leahey, N., Rahman, S., Liu, Y., Etchin, J., Li, B., Shen, S., Lee, T. I., Zhang, J., Look, A. T., Mansour, M. R., & Young, R. A. (2017). Small genomic insertions form enhancers that misregulate oncogenes. Nature Communications, 8(1), 14385. https://doi.org/10.1038/ncomms14385

302. Puente, X. S., Beà, S., Valdés-Mas, R., Villamor, N., Gutiérrez-Abril, J., Martín-Subero, J. I., Munar, M., Rubio-Pérez, C., Jares, P., Aymerich, M., Baumann, T., Beekman, R., Belver, L., Carrio, A., Castellano, G., Clot, G., Colado, E., Colomer, D., Costa, D., … Campo, E. (2015). Non-coding recurrent mutations in chronic lymphocytic leukaemia. Nature, 526(7574), 519–524. https://doi.org/10.1038/nature14666

303. Zhou, S., Hawley, J. R., Soares, F., Grillo, G., Teng, M., Madani Tonekaboni, S. A., Hua, J. T., Kron, K. J., Mazrooei, P., Ahmed, M., Arlidge, C., Yun, H. Y., Livingstone, J., Huang, V., Yamaguchi, T. N., Espiritu, S. M. G., Zhu, Y., Severson, T. M., Murison, A., Lupien, M. (2020). Noncoding mutations target cis-regulatory elements of the FOXA1 plexus in prostate cancer. Nature Communications, 11(1), 441. https://doi.org/10.1038/s41467-020-14318-9

304. Bailey, S. D., Desai, K., Kron, K. J., Mazrooei, P., Sinnott-Armstrong, N. A., Treloar, A. E., Dowar, M., Thu, K. L., Cescon, D. W., Silvester, J., Yang, S. Y. C., Wu, X., Pezo, R. C., Haibe-Kains, B., Mak, T. W., Bedard, P. L., Pugh, T. J., Sallari, R. C., & Lupien, M. (2016). Noncoding somatic and inherited single-nucleotide variants converge to promote ESR1 expression in breast

cancer. Nature Genetics, 48(10), 1260–1266. https://doi.org/10.1038/ng.3650

305. Cowper-Sal·lari, R., Zhang, X., Wright, J. B., Bailey, S. D., Cole, M. D., Eeckhoute, J., Moore, J. H., & Lupien, M. (2012). Breast cancer risk–associated SNPs modulate the affinity of chromatin for FOXA1 and alter gene expression. Nature Genetics, 44(11), 1191–1198. https://doi.org/10.1038/ng.2416

306. Wu, S., Turner, K. M., Nguyen, N., Raviram, R., Erb, M., Santini, J., Luebeck, J., Rajkumar, U., Diao, Y., Li, B., Zhang, W., Jameson, N., Corces, M. R., Granja, J. M., Chen, X., Coruh, C., Abnousi, A., Houston, J., Ye, Z., … Mischel, P. S. (2019). Circular ecDNA promotes accessible chromatin and high oncogene expression. Nature, 575(7784), 699–703. https://doi.org/10.1038/s41586-019-1763-5

307. Morton, A. R., Dogan-Artun, N., Faber, Z. J., MacLeod, G., Bartels, C. F., Piazza, M. S., Allan, K. C., Mack, S. C., Wang, X., Gimple, R. C., Wu, Q., Rubin, B. P., Shetty, S., Angers, S., Dirks, P. B., Sallari, R. C., Lupien, M., Rich, J. N., & Scacheri, P. C. (2019). Functional enhancers shape extrachromosomal oncogene amplifications. Cell, 179(6), 1330-1341.e13. https://doi.org/10.1016/j.cell.2019.10.039

308. Zhu, Y., Gujar, A. D., Wong, C.-H., Tjong, H., Ngan, C. Y., Gong, L., Chen, Y.-A., Kim, H., Liu, J., Li, M., Mil-Homens, A., Maurya, R., Kuhlberg, C., Sun, F., Yi, E., deCarvalho, A. C., Ruan, Y., Verhaak, R. G. W., & Wei, C.-L. (2021). Oncogenic extrachromosomal DNA functions as mobile enhancers to globally amplify chromosomal transcription. Cancer Cell, 39(5), 694-707.e7. https://doi.org/10.1016/j.ccell.2021.03.006

309. Karnuta, J. M. & Scacheri, P. C. Enhancers: bridging the gap between gene control and human disease. *Hum Mol Genet* **27**, R219-R227, doi:10.1093/hmg/ddy167 (2018).

310. Murata, T. (2001). Defect of histone acetyltransferase activity of the nuclear transcriptional coactivator CBP in Rubinstein-Taybi syndrome. Human Molecular Genetics, 10(10), 1071–1076.

311. Tsang, B., Pritišanac, I., Scherer, S. W., Moses, A. M. & Forman-Kay, J. D. Phase Separation as a Missing Mechanism for Interpretation of Disease Mutations. *Cell* **183**, 1742-1756, doi:10.1016/j.cell.2020.11.050 (2020).

312. Gryder, B. E., Pomella, S., Sayers, C., Wu, X. S., Song, Y., Chiarella, A. M., Bagchi, S., Chou, H.-C., Sinniah, R. S., Walton, A., Wen, X., Rota, R., Hathaway, N. A., Zhao, K., Chen, J., Vakoc, C. R., Shern, J. F., Stanton, B. Z., & Khan, J. (2019). Histone hyperacetylation disrupts core gene regulatory architecture in rhabdomyosarcoma. Nature Genetics, 51(12), 1714–1722. https://doi.org/10.1038/s41588-019-0534-4

313. Wan, L., Chong, S., Xuan, F., Liang, A., Cui, X., Gates, L., Carroll, T. S., Li, Y., Feng, L., Chen, G., Wang, S.-P., Ortiz, M. V., Daley, S. K., Wang, X., Xuan, H., Kentsis, A., Muir, T. W., Roeder, R. G., Li, H., … Allis, C. D. (2020). Impaired cell fate through gain-of-function mutations in a chromatin reader. Nature, 577(7788), 121–126. https://doi.org/10.1038/s41586-019-1842-7

314. Bushweller, J. H. Targeting transcription factors in cancer - from undruggable to reality. *Nat Rev Cancer* **19**, 611-624, doi:10.1038/s41568-019-0196-7 (2019).

315. Tsafou, K., Tiwari, P. B., Forman-Kay, J. D., Metallo, S. J. & Toretsky, J. A. Targeting Intrinsically Disordered Transcription Factors: Changing the Paradigm. *J Mol Biol* **430**, 2321-2341, doi:10.1016/j.jmb.2018.04.008 (2018).

316. Kwiatkowski, N., Zhang, T., Rahl, P. B., Abraham, B. J., Reddy, J., Ficarro, S. B., Dastur, A., Amzallag, A., Ramaswamy, S., Tesar, B., Jenkins, C. E., Hannett, N. M., McMillin, D., Sanda, T., Sim, T., Kim, N. D., Look, T., Mitsiades, C. S., Weng, A. P., … Gray, N. S. (2014). Targeting transcription regulation in cancer with a covalent CDK7 inhibitor. Nature, 511(7511), 616–620. https://doi.org/10.1038/nature13393

317. Jeselsohn, R., Bergholz, J. S., Pun, M., Cornwell, M., Liu, W., Nardone, A., Xiao, T., Li, W., Qiu, X., Buchwalter, G., Feiglin, A., Abell-Hart, K., Fei, T., Rao, P., Long, H., Kwiatkowski, N., Zhang, T., Gray, N., Melchers, D., … Brown, M. (2018). Allele-specific chromatin recruitment and therapeutic vulnerabilities of esr1 activating mutations. Cancer Cell, 33(2), 173-186.e5. https://doi.org/10.1016/j.ccell.2018.01.004

318. Roe, J.-S., Hwang, C.-I., Somerville, T. D. D., Milazzo, J. P., Lee, E. J., Da Silva, B., Maiorino, L., Tiriac, H., Young, C. M., Miyabayashi, K., Filippini, D., Creighton, B., Burkhart, R. A., Buscaglia, J. M., Kim, E. J., Grem, J. L., Lazenby, A. J., Grunkemeyer, J. A., Hollingsworth, M. A., … Vakoc, C. R. (2017). Enhancer reprogramming promotes pancreatic cancer metastasis. Cell, 170(5), 875-888.e20. https://doi.org/10.1016/j.cell.2017.07.007

319. Magnani, L., Stoeck, A., Zhang, X., Lanczky, A., Mirabella, A. C., Wang, T.-L., Gyorffy, B., & Lupien, M. (2013). Genome-wide reprogramming of the chromatin landscape underlies endocrine therapy resistance in breast cancer. Proceedings of the National Academy of Sciences, 110(16), E1490–E1499. https://doi.org/10.1073/pnas.1219992110

320. Ma, Q., Yang, F., Mackintosh, C., Jayani, R. S., Oh, S., Jin, C., Nair, S. J., Merkurjev, D., Ma, W., Allen, S., Wang, D., Almenar-Queralt, A., & Garcia-Bassets, I. (2020). Super-enhancer redistribution as a mechanism of broad gene dysregulation in repeatedly drug-treated cancer cells. Cell Reports, 31(3), 107532. https://doi.org/10.1016/j.celrep.2020.107532

321. Li, P., Marshall, L., Oh, G., Jakubowski, J. L., Groot, D., He, Y., Wang, T., Petronis, A., & Labrie, V. (2019). Epigenetic dysregulation of enhancers in neurons is associated with Alzheimer's disease pathology and cognitive symptoms. Nature Communications, 10(1), 2246. https://doi.org/10.1038/s41467-019-10101-7

322. Cebola, I. Pancreatic Islet Transcriptional Enhancers and Diabetes. *Curr Diab Rep* **19**, 145, doi:10.1007/s11892-019-1230-6 (2019).

323. Wamstad, J. A., Wang, X., Demuren, O. O. & Boyer, L. A. Distal enhancers: new insights into heart development and disease. *Trends in Cell Biology* **24**, 294-302, doi:10.1016/j.tcb.2013.10.008 (2014).

Chapter 3: Single cell live imaging: visualizing 4D nuclear architectural dynamics of ligand-dependent transcription activation

3.1 Background

Nuclear receptors have been widely established as regulators of gene transcriptional programs critical for development and physiological functions. The precise program of gene expression underlying these functions is dictated by *cis* genomic regulatory elements known as enhancers. The dominant model for their mechanism of action on promoters and transcriptional activation involves the concept of “looping” of enhancer and proximal-promoter sites through cooperative clustering of transcription factors (TF) and coactivators. Estrogen receptor α (ERα) functions by translocating to the nucleus upon ligand binding by 17β-estradiol (E_2), leading to the activation of its bound enhancers and the activation of their associated target genes, and thus impacting chromosomal conformation in 3D nuclear space[1-22].

ChIP-seq data of ERα upon E_2 stimulation in MCF7 human breast cancer cells reveals ~31,000 ERα binding sites genome wide. Of these sites, ERα binds to ~8500 EREs located in enhancers[1-5], of which the ~1300 most robust enhancers adjacent to E_2-upregulated coding genes cause increased enhancer-promoter looping in mammary cell regulatory transcriptional programs[5-21]. To focus the investigation on any potential functional relationships between robust ERα-bound enhancers located at great linear genomic distances within a chromosome, preliminary experiments initially focused on the landscape of ERα enhancers and coding target genes located on Chr21 in MCF7 breast cancer cells as a model. Chr21 harbors 132 ERα-bound, H3K27Ac, H3K4me1-marked enhancers amongst the total of 479 enhancers. Of

these enhancers, 39 showed the signature of particularly robust, E_2-dependent enhancers, including recruitment of ERα and p300, a key protein associated with active enhancers, in comparison to the remaining 93. There is an apparent complex of additional DNA-binding transcription factors and coactivators selectively recruited in *trans* required for activation of these most functionally active estrogen-regulated enhancers and subsequent target gene activation, referred to as the MegaTrans complex[22]. ChIP-seq data revealed that only these 39 enhancers strongly recruit MegaTrans factors GATA3 and AP2γ upon E_2 treatment, as well as pioneer factor FOXA1, RNA Polymerase II (RNA PolII), MED1, BRD4, and condensin. These data correspond to the idea that some enhancers act as “hotspots” to recruit factors that coordinate downstream transcription, with *TFF1e1* and *NRIP1e3* enhancers being the most robust and thus have been selected as candidates for live cell imaging to help determine the dynamics and spatiotemporal kinetics of 4D nuclear architecture upon estrogen-induced transcription activation.

It has been widely reported that gene transcription does not occur continuously over time, but rather in acute periods of high levels followed by periods of inactivity[23]. That process of bursting is now the predominant model of transcription activation. With our live imaging techniques, we aim to answer several questions: 1. Do we see transcriptional bursting in our model system? 2. If we do observe transcription bursting, how do the DNA motions and associations correspond to that burst activation? 3. Are there various phases in estrogen receptor signaling, and thus changes in transcription activation kinetics, in response to nuclear receptor

activation? 4. Lastly, what are the spatial and temporal dynamics of gene activation relative to its associations with subnuclear organelles and transcription factors?

3.2 Results

RNA live visualization reveals burst transcription dynamics during acute versus chronic phase post estrogen stimulation. To truly understand the mechanisms underlying acute enhancer activation, we require a technique that allows for visualizing functional spatiotemporal kinetics at the level of single cell nuclei in real time. We have established microscopy platforms for tagging endogenous gene transcripts with 24xMS2 repeat sequences. The MS2 tagging system consists of transcribed MS2 sequences, which fold into RNA hairpin structures that bind MS2 coat proteins (MCP) with high specificity and affinity[24-27]. The ideal gene loci for MS2 cassette integration must have high transcriptional levels and targeted regions must be removed from known regulatory features to prevent disruption of gene regulation upon integration of the cassette. To increase the efficiency of CRISPR-based insertion of these repeats into the 3' UTR of ERα-induced genes *TFF1* and *NRIP1*, our HDR donor construct includes either a Puromycin tag or a sortable Halo tag immediately upstream of the stop codon and the repeats (Fig. 3.1a), permitting an ~80% positive rate for correct insertion. Subsequent selection of single clonal lines containing stable integration of MCP fused to YFP (MCP-YFP) is done via flow cytometry to gate for an ideal, homogeneous expression level with minimal background to achieve a high signal to noise ratio. For validation of correct MS2 integration at target loci, we have performed sequential imaging of the E_2-induced RNA transcript and DNA FISH, employing a

gridded slide overlay for alignment. We see a >90% overlap of *NRIP1* and *TFF1* DNA FISH dots to their respective transcribed MS2 signal (Fig. 3.1b). For the remainder of this chapter, we will focus on the *NRIP1* loci.

Using the Zeiss 880 Airyscan confocal microscope, we are able to obtain super-resolution (~130nm) movies of the dynamics of ERα-regulated gene loci *NRIP1* in real time, acquiring every 2 minutes to visualize the time of initial response to E_2, the duration of the sustained burst, the time at which the signal dissipates, burst frequency, and the interval preceding another burst. We note an “immediate” onset of bursting upon E_2 treatment, with a median burst length of 9.2 minutes (Fig. 3.2a). We observe a statistically significant increase in burst frequency in the time window of 20min-140min that we will refer to as the acute phase, followed by a lower, sustained burst frequency for the subsequent 8 hours which we will refer to as the chronic phase (140min+) (Fig. 3.2b). We have classified the initial 20 minutes of the movie as the “pre-acute” phase, as we notice a lag in response to estrogen stimulation following treatment. Moreover, we see a statistically significant increase in the interval between bursts (OFF period) during the chronic phase in comparison to the acute phase (Fig. 3.2c). Taken together, these observations indicate that acute estrogen stimulation increases the burst frequency of estrogen-inducible target loci. The burst frequency reaches a lower, sustained steady state once the cell enters the chronic phase of estrogen stimulation.

High temporal resolution of live DNA kinetics reveals increased mobility following estrogen treatment. To further elucidate the spatial and temporal kinetics of the target *NRIP1* loci, we proceed to generate an endogenously tagged DNA

visualization stable cell line with a 144xCuO repeat array. To do so, we have acquired a more stable, mutant version of the CuO array which is effectively knocked-in to the region of interest via integrase integration technology[28]. We first stably integrate 60bp of a Bxb1 landing pad at target loci via CRISPR-cas9. After successful screening of the landing pad insertion, we co-transfect the donor plasmid containing the CuO array along with the Bxb1 integrase that will recognize, cut, and integrate the array at the site of the landing pad (Fig. 3.3a). Subsequent stable integration of the CymR repressor fused to either a fluorescent protein (mTurquoise2 or mKate2) or Halo-tag shows clean and robust signal of tagged DNA loci in all cells within a single clonal population (Fig. 3.3b).

Timelapses with rapid acquisition (12s) of DNA dynamics are again achieved using the Zeiss 880 Airyscan microscope. We have divided each timelapse into three phases, using the parameters defined previously via RNA visualization: 0-20min for pre-acute, 20-140min for acute, and 140min+ for chronic. Interestingly, we not only observe that the mobility of *NRIP1* DNA locus increases following estrogen treatment (Fig. 3.3c), but that mobility continues to increase as the cell transitions from the acute to the chronic phase (Fig. 3.3d). We wonder if this change in DNA mobility upon estrogen stimulation is linked to the change in burst frequency during acute versus chronic transcription activation. One hypothesis would be that the change in burst frequency would explain why we see differential DNA mobility during different phases post E_2 treatment. However, we do not expect the gene to be predominantly bursting so transcription activation alone would not explain the increase in mobility following estrogen stimulation. If the transcription activation is not occurring at a high

level, then any motion associated with bursting would be masked by the motion during the OFF period. Thus, another possibility would be that the increase in DNA mobility we witness is reflective of the overall activation the cell undergoes post estrogen stimulation. This hypothesis would be consistent with previous findings in the field, where activation triggered by developmental signals results in a higher DNA mobility that would account for both bursting during an ON period and scanning during an OFF period[29]. Current findings, however, have not been able to further characterize DNA dynamics to distinguish motion in response to transcriptional activation versus general activation throughout the cell. To fully investigate this question, we need to generate clonal lines that allow for dual DNA and RNA visualization.

Simultaneous RNA and DNA live visualization gives insight into spatiotemporal dynamics of DNA motions corresponding to burst transcription. To establish clonal lines that allow for dual RNA and DNA visualization, we need to knock-in the 24xMS2 repeat cassette into the 3' UTR of *NRIP1* that already contains a 144xCuO array, using the CRISPR-based HDR donor technique as previously described. We are able to successfully build these dual DNA+RNA clonal lines in the 144xCuO *NRIP1* DNA line that retains the CymR-Halo signal. We have noticed that the Halo-tag is less likely to form artefactual aggregates when combined with the MCP-YFP. Additionally, we are able to visualize the Halo-tag using JF647 ligand, which minimizes bleed-through into the YFP channel in comparison to a red fluorescent protein or dye. We use the preestablished DNA visualization signal of our *NRIP1* locus to screen for clonal lines that have integrated

the 24xMS2 repeats into the same allele to allow for dual visualization of DNA + RNA at the target locus.

We are able to acquire 4-hour timelapses with a high temporal resolution (12s) that simultaneous track RNA bursts with MCP-YFP and DNA motion with CymRHalo-JF647, using the Zeiss 880 Airyscan microscope. Strikingly, our analysis shows that the mobility of *NRIP1* is slower during a burst, and that there is a statistically significant increase in displacement of *NRIP1* in the period following a burst (Fig. 3.3e). In other words, we are able to distinguish a difference in DNA dynamics during a burst when the locus is ON and transcriptionally active versus post-burst when the locus is OFF. This evidence suggests that the change in DNA mobility previously discussed is not just representative of the overall activation induced by E_2, but rather directly reflects the change in burst frequency we witness during RNA visualization. The increase in burst frequency and thus transcription activity during the acute phase from our RNA visualization data corresponds to longer periods of DNA maintained in the less mobile state. This explains why we not only see an overall increase in displacement upon estrogen stimulation from DNA visualization, but we observe the highest mobility of *NRIP1* during the chronic phase when bursting frequency is maintained at a lower sustained state.

That restricted motion during a burst may be due to interactions with transcription factors, coactivators, and/or subnuclear organelles within a condensate and/or at a transcriptional hub. Current findings have reported that there is a radius of confinement of around 300-400nm where enhancers, genes, and factors that concentrate within that bubble are able to interact and regulate transcription through

proximity rather than direct contact[30-36]. When the locus is no longer transcriptionally ON, the DNA may be scanning in space to recruit a new set of factors for its next burst event, and thus less restricted in motion.

Acute versus chronic estrogen-stimulated effects relative to subnuclear organelles. Repositioning of specific chromosomal loci with respect to nuclear structures has been correlated with their transcriptional activity in some cases. Several nuclear sub-structures such as the nucleoli, PML bodies, SC35 granules, matrin3 network, and the polycomb complex have been reported to have functional impacts on nuclear organization and dynamics[37-41]. Multiple publications have examined preferential interaction and colocalization of various factors involved in transcription regulation, such as RNA polymerase II, around subnuclear organelles such as the nucleolus and SC35 granules. To screen for subnuclear organelles that may have a functional impact on our DNA and RNA dynamics, we have performed immuno-DNA of both *TFF1* and *NRIP1* relative to subnuclear structures (Fig. 3.4a) and noticed a significant increase in proximity of both genes to the periphery of both SC35 and Matrin3 upon E_2 induction. For all immuno-DNA and RNA FISH data, the observed phenomenon is a composite of all analyzable *TFF1* and *NRIP1* alleles, with more than 400 cells per condition. Interestingly, we find the biggest increase in proximity to SC35 to occur in the acute phase, whereas that biggest shift towards Matrin3, especially for *NRIP1*, to occur during the chronic phase (Fig. 3.4 b, c). The SC35 data is further supported by immuno-RNA FISH of *TFF1* (Fig. 3.4d), which convinced us to further examine whether localization at SC35 granules has a functional impact on transcription activation.

In line with immuno-DNA and RNA FISH data, live cell RNA visualization of tagged *NRIP1* allele via 24xMS2 in conjunction with virally transduced SC35 shows a significant shift away from the periphery of SC35 during the chronic phase of estrogen induction (Fig. 3.4e). That increase in distance away from the periphery of SC35 correlates with the decrease in burst frequency observed during the chronic phase, suggesting that induced proximity to SC35 during the acute phase may be mechanistically important for that increase in gene activation and thus burst frequency. Moreover, SC35 is non-membrane bound and has been reported to be a phase separated structure. Perhaps recruitment to a SC35 hub would allow for retention and stability of associations required for transcriptional activation. To further explore the concept of retention and stability, possibly through phase separation and condensate formation, we require single molecule tracking (SMT).

Single molecule tracking of estrogen receptor examines the differential biophysical properties of transcriptional states of a gene. To complement our DNA and RNA-tagging studies, we have performed SMT of wild-type ERα to test the hypothesis that the majority of ERα binding at the strongest, acutely activated, MegaTrans enhancers such as *NRIP1* primary occurs in a phase separated condensate. We have used Halo-tag to label both endogenous and virally transducible ERα, and have performed 5ms exposure HILO imaging using the Nikon Sterling microscope to determine different clusters of bound and unbound ERα molecules in response to acute and chronic ligand treatment, all consistent with literature (Fig. 3.5a).

By using two different forms of clustering approaches, Gaussian Mixture Models (GMM) and Agglomerative Hierarchical, we are able to group ER molecules into six clusters based on diffusion coefficient, sub-diffusivity (or alpha value), radial diffusion coefficient, radius of confinement, average displacement, and duration of binding within a 250nm radius. Interestingly, both clustering algorithms identified a similar cluster of ER molecules as being most enriched in the acute E_2 condition, and this cluster is characterized by having the lowest diffusion coefficient of all the clusters (Fig. 3.5b). We suspect that this fraction of ER molecules reflects the RNA and DNA visualization data where we see increased burst frequency during acute activation and thus lower mobility relative to that of chronic activation.

Recent findings in the field have reported two distinct states with limited mobility. There is the chromatin bound state and a confined state[42]. For the bound state, there will be heterogeneity in residence times due to variation in response elements with different motif strengths. On the other hand, the confined state will contain heterogeneity in effective binding affinities due to IDR-mediated protein-protein interactions. Hence, both follow a power law distribution in their dwell times. The difference is that the dwell time of components in the confined population is much longer than that of the bound population because of the high local concentration of transcription factors at specific genomic sites that results in a greater number of interacting partners. ER is known to have an intrinsically disordered region (IDR), and capable of forming phase-separated protein-protein interactions. If the acute-specific ER cluster reflects the DNA bound fraction, it should be the most restricted in motion while bound and then be freed when unbound. However, our

SMT data shows that although that population of molecules has the lowest diffusion coefficient, it varies in sub-diffusivity as reflected by the range in alpha we observe. Instead, we propose that this fraction of ER molecules is retained in a phase separated condensate localized at ER-dependent genomic sites, and that lowest diffusion we witness is an indication of a densely concentrated condensate.

To further test the hypothesis that our acute-specific ER cluster is held in a condensate at specific genomic loci during transcription activation, we have treated our endogenously tagged ER cell lines with 1,6-hexandiol, a compound known to disrupt phase-separated structures. Strikingly, we observe that we have a loss in our restricted fraction of ER molecules during 1,6-hexandiol treatment that is only observed during acute E_2 treatment (Fig. 3.5c). This would suggest that the 1,6-hexandiol effectively disrupted our hypothesized condensate at ER-dependent genomic sites, which has resulted in our acute-specific ER cluster to no longer be restricted in motion. Together, our data suggests that during a transcriptional burst, the DNA along with its associated factors are restricted and stabilized in a condensate to allow for activation. That phenomenon is especially evident in the acute phase following estrogen stimulation, where we observe an increase in burst frequency as well as an enrichment in the confined fraction of ER molecules.

3.3 Discussion

The phenomenon of burst transcription has been previously witnessed and reported in various model systems ranging from *Drosophila* to mammalian cells. Insight into DNA motion and dynamics during transcription activation has also been discussed. However, very little has been reported and is known regarding the precise

kinetics of DNA motion relative to transcriptional bursting. Here, we provide evidence that DNA motion is restricted during a transcriptional burst, and that restriction is released following transcription activation.

A previous publication found that activation of a gene or enhancer resulted in increased mobility of DNA. Unfortunately, that article only performed DNA visualization and thus is not able to further examine and distinguish the kinetics of DNA movement in response to a general activation following a developmental signal versus transcription activation. When examining DNA kinetics alone, we also observe that same phenomenon of increased mobility upon transcription activation, when induced by estrogen treatment. Of course, without pairing DNA visualization with live RNA bursting, it is reasonable to conclude that transcription activation results in increased DNA mobility. However, when we do dual visualization of DNA + RNA of our estrogen dependent *NRIP1* locus, we are able to find that mobility is increased following a burst, and that while the gene is transcriptionally bursting, the DNA is actually less mobile. One may suspect that difference in mobility between burst and post-burst intervals to be easily masked by the greater difference one may expect in mobility between overall active versus inactive states of a cell. And that is exactly what we notice in our DNA visualization data, where we see a significant increase in displacement following estrogen stimulation in general. However, what is not expected is that further increase in mobility during the chronic phase of estrogen treatment. The DNA + RNA dual visualization data helps elucidate that phenomenon. We know from our RNA burst data that burst frequency significantly increases during the acute phase immediately following estrogen treatment. That would suggest that

the DNA is maintained in that low mobility state for longer periods of time compared to the DNA that is in the chronic phase when bursting is sustained at a lower frequency. Together, we find that not only is burst frequency higher during the acute phase of estrogen stimulation, but that frequency is reflected in the DNA dynamics.

We propose that the restricted mobility in DNA we witness during burst activation may be explained by its retention in a condensate or transcriptional hub. The existence of a condensate or transcription hub at the gene-enhancer locus is not foreign to the field. Recent findings have reported that homotypic and heterotypic interactions exist between low complexity domains (LCDs), and such interactions are suspected to transiently enrich transcription factors, possibly in the vicinity of target enhancers, to increase factor occupancy at target loci. This transient concentration of factors at a hub locally may play a critical role in the coordination of gene activation in defined spatiotemporal patterns. Various subnuclear organelles have been reported to functionally impact transcriptional activity, and SC35 in particular show striking DNA and RNA immuno-FISH results that suggest colocalization to its periphery upon estrogen stimulation. We are able to replicate that result live through RNA visualization, where we see an induced proximity to SC35 in the acute phase relative to the chronic condition. We suspect that increase in proximity to SC35 is functionally important in the transient retention of our DNA during burst activation, to allow for concentration of essential transcription factors and coactivators for transcription to occur. Once the burst is over, the DNA is free to scan for its next burst event. That induced proximity during the acute phase in particular helps explain the higher burst frequency we witness in our RNA visualization data and the decreased mobility of

DNA in the acute phase relative to the chronic phase. Though, this model relative to SC35 granules does not completely explain the conclusions in current literature where it has been reported that the concentration of factors required for transcription regulation occurs in a hub of around 300-400nm. SC35 granules are too big to fit that profile. Thus, we suspect there to be multiple orders of organization and restriction. We propose that although we have localization of our gene loci to SC35 granules, that localization may still be less restrictive than, for example, retention in a *de novo* condensate comprised of transcription factors and coactivators such as MED1, BRD4, P300, and Pol II, all of which have been reported to exist in phase-separated structures[36,43-46].

Finally, we are able to identify a unique cluster of ER molecules specific to the acute phase of ER activation via SMT to further support the hypothesis of retention in a condensate during transcription regulation. ER is known to have an intrinsically disordered region (IDR), and capable of forming phase-separated protein-protein interactions. If this cluster of ER molecules is the bound fraction resulting in transcription activation, then we should observe the highest restriction due to direct binding to DNA. Instead, we see variable restricted motion with the lowest diffusion coefficient, suggesting that this fraction of acute-specific ER molecules is in a confined state interacting with a high concentration of factors, thus resulting in its low mobility. Thus, we suspect that cluster of ER molecules to be the molecules retained in a condensate during transcription activation and are confined to the DNA locus to trigger burst activation. This fraction of ER molecules is immediately lost upon 1,6-hexandiol treatment, a compound known to disrupt phase-separated condensates.

This evidence supports the notion that the DNA is restricted in mobility during transcription activation and is retained in a phase-separated condensate that allows for recruitment and concentration of essential factors that trigger a burst.

3.4 Future directions

Because we propose that transcription activation occurs in a condensate where the DNA motion is restricted and that essential transcription factors and coactivators are retained and concentrated within the hub, we are curious to find whether there are various levels of organization and hub formation. We currently observe a shift towards SC35 during acute activation relative to chronic induction. Because we do not have three color visualization of DNA + RNA + SC35, we are unable to determine if the DNA is still at an induced proximity when the gene is off. If that induced proximity is retained, then that would suggest that a shift towards the periphery of SC35 is only a general trend during estrogen stimulation. Even when the target locus is off and scanning for its next burst activation, it remains close to SC35. That would indicate that retention at a SC35 granule is a higher level of organization than, for example, retention at a hub specific to the burst event.

Evidence for the interaction of multiple transcriptional regulatory and responsive elements at hubs of clustered transcriptional activators is observed by several additional studies, which showed the formation of nuclear puncta consisting of transcriptional co-activators such as BRD4 and MED1[36,46-47]. In our endogenously tagged MED1 cell lines, we too witness punctate foci consistent with what has been reported in literature. Our next step will be to develop three color visualization of not only our DNA + RNA + SC35 but also DNA + RNA + MED1 and any other potential

transcription factors such as BRD4 and P300 that could functionally be involved in the formation of a condensate at gene locus *de novo* to orchestrate transcription activation.

3.4 Figures

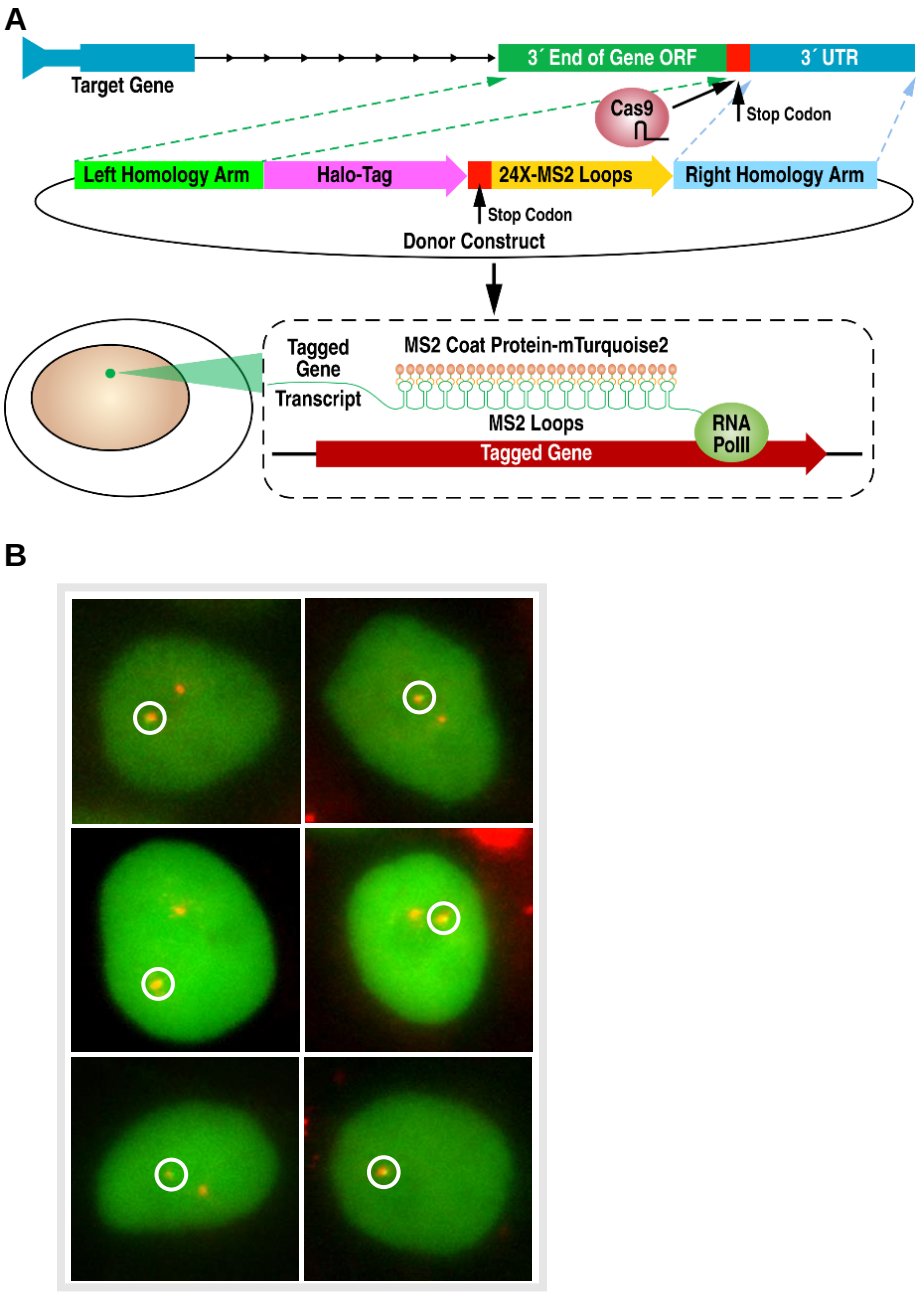

Figure 3.1. Schematic of RNA visualization technique. a. RNA visualization via stable integration of 24xMS2 hairpin repeats at target locus using HDR donor plasmid integration strategy for efficient tagging of gene transcript 3' UTR region. **b.** DNA-FISH validation of E_2-induced *NRIP1* 24xMS2 tagged RNA transcript using a gridded slide alignment and overlay technique.

Figure 3.2.

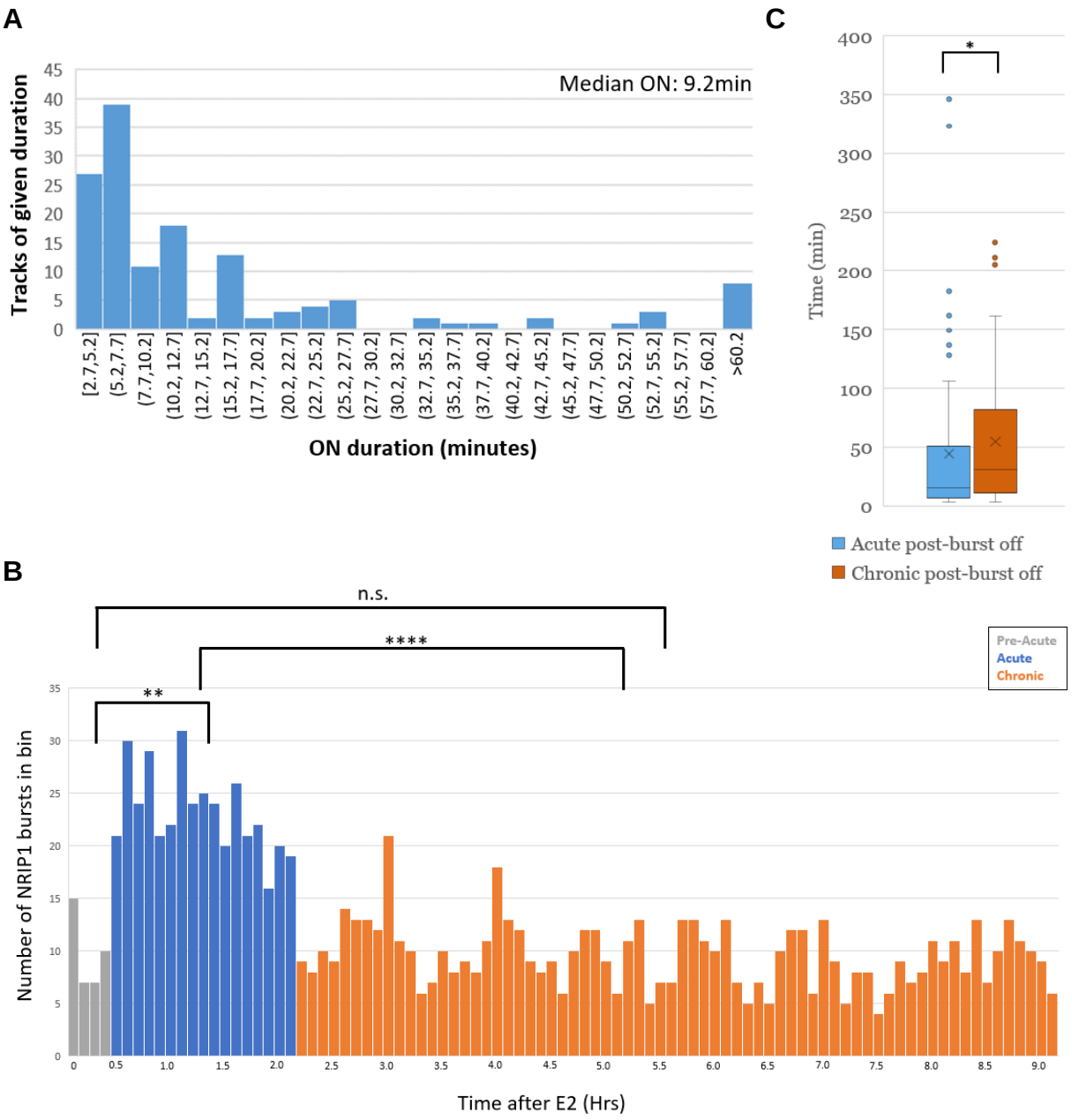

Figure 2.1. RNA visualization of transcriptional bursting. a. RNA visualization of *NRIP1* locus reveals median ON duration of transcription bursts to be 9.2minutes. **b.** Long-term overnight timelapses reveal 3 phases of burst dynamics: 0-20min for pre-acute, 20-140min for acute, and 140min+ for chronic. We observe an increased burst frequency during the acute phase, and a sustained lower frequency in the chronic. **c.** There is an increase in OFF duration during the chronic phase relative to the acute phase. (* = p<0.05, ** = p<0.01, *** = p<0.001, **** = p<0.0001)

Figure 3.3. DNA RNA dual visualization of mobility relative to transcriptional bursting. a. Schematic of DNA visualization of *NRIP1* locus via 144xCuO array knock-in at target loci using integrase technology. **b.** Single clonal lines with stable CymR expression in either mTurquoise2, mKate2, or Halo, demonstrating homogenous, robust punctate signal of DNA-tagged *NRIP1* locus. **c.** Displacement of *NRIP1* tracks of minus E_2 versus plus E_2 treated MCF7 cells imaged at 12s intervals. We observe a statical significant increase in mobility following estrogen stimulation, evaluated with a paired T-test. **d.** 12s movies reveal an increase in mobility not only from minus to plus E_2, but a further increase in mobility in the chronic state, when divided into defined minus, 20-140min acute, and 140min+ chronic intervals. **e.** DNA and RNA dual visualization, taken at 12s intervals, show a statistically significant decrease in mobility during transcriptional bursting. (* = $p<0.05$, ** = $p<0.01$, *** = $p<0.001$, **** = $p<0.0001$)

Figure 3.3

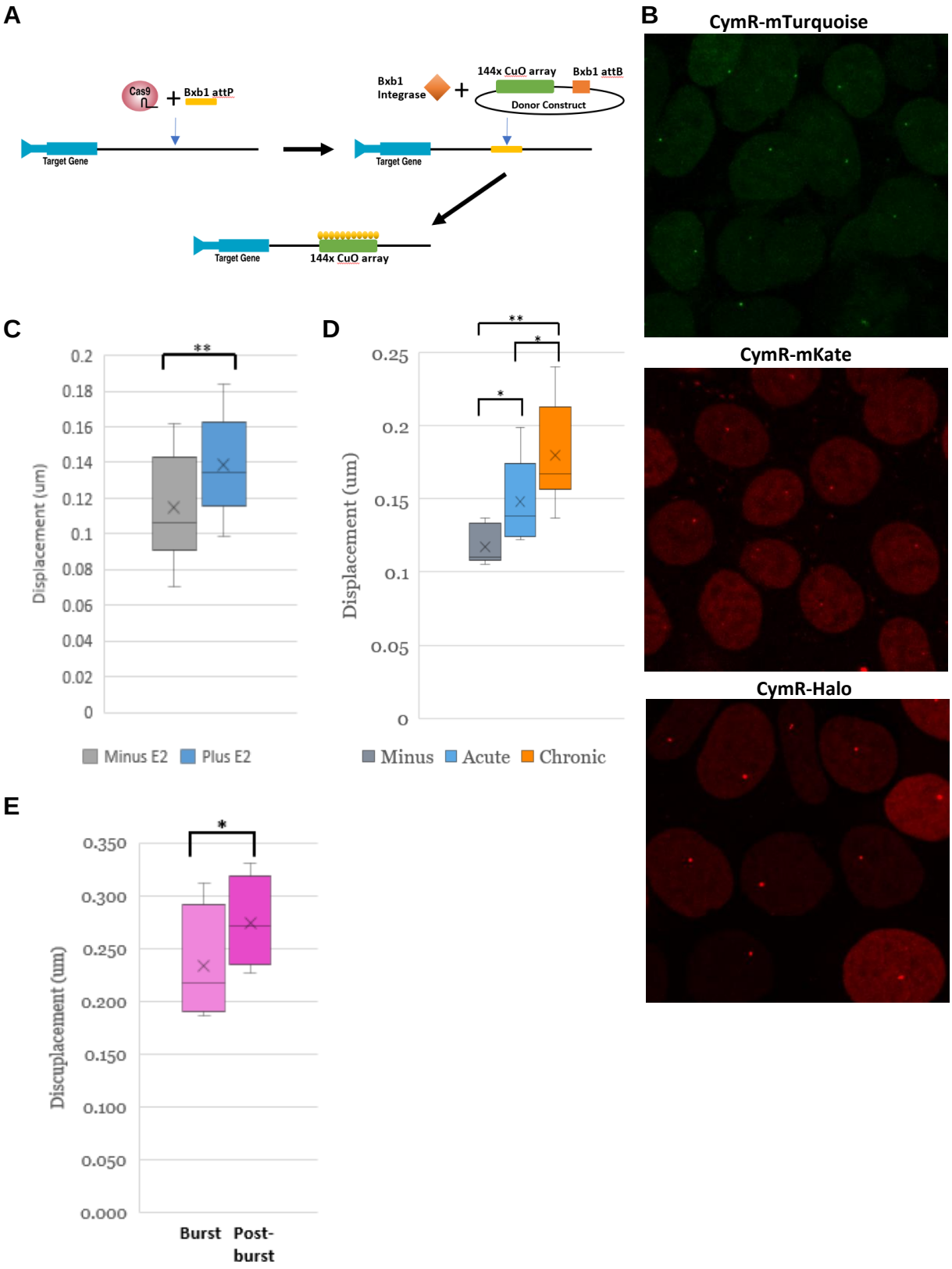
A
Cas9
Bxb1 attP
Target Gene
Bxb1 Integrase
144x CuO array
Bxb1 attB
Donor Construct
Target Gene
Target Gene
144x CuO array
B
CymR-mTurquoise
CymR-mKate
CymR-Halo
C
Displacement (um)
0.2
0.18
0.16
0.14
0.12
0.1
0.08
0.06
0.04
0.02
0
**
Minus E2
Plus E2
D
Displacement (um)
0.25
0.2
0.15
0.1
0.05
0
**
*
*
Minus
Acute
Chronic
E
Discuplacement (um)
0.350
0.300
0.250
0.200
0.150
0.100
0.050
0.000
*
Burst
Post-burst

Figure 3.4. Acute versus chronic dynamics localized at subnuclear structures. **a.** Three-color immuno-DNA FISH of *TFF1* relative to SC35 and Matrin3 network show colocalization. **b.** Cumulative distribution of the distance of *TFF1* to the periphery of SC35 and Matrin during minus E_2, acute E_2, and chronic E_2 states, based on immuno-DNA FISH. **c.** Cumulative distribution of the distance of *NRIP1* to the periphery of SC35 and Matrin during acute E_2 and chronic E_2 states, based on immuno-DNA FISH. **d.** Cumulative distribution of the distance of *TFF1* to the periphery of SC35 during acute E_2 and chronic E_2 states, based on immuno-RNA FISH. **e.** Three-color, live cell RNA visualization of 24xMS2 tagged *NRIP1* locus relative to SC35 during acute and chronic phase post estrogen treatment reveals induced proximity to SC35 during the acute phase.

Figure 3.4.

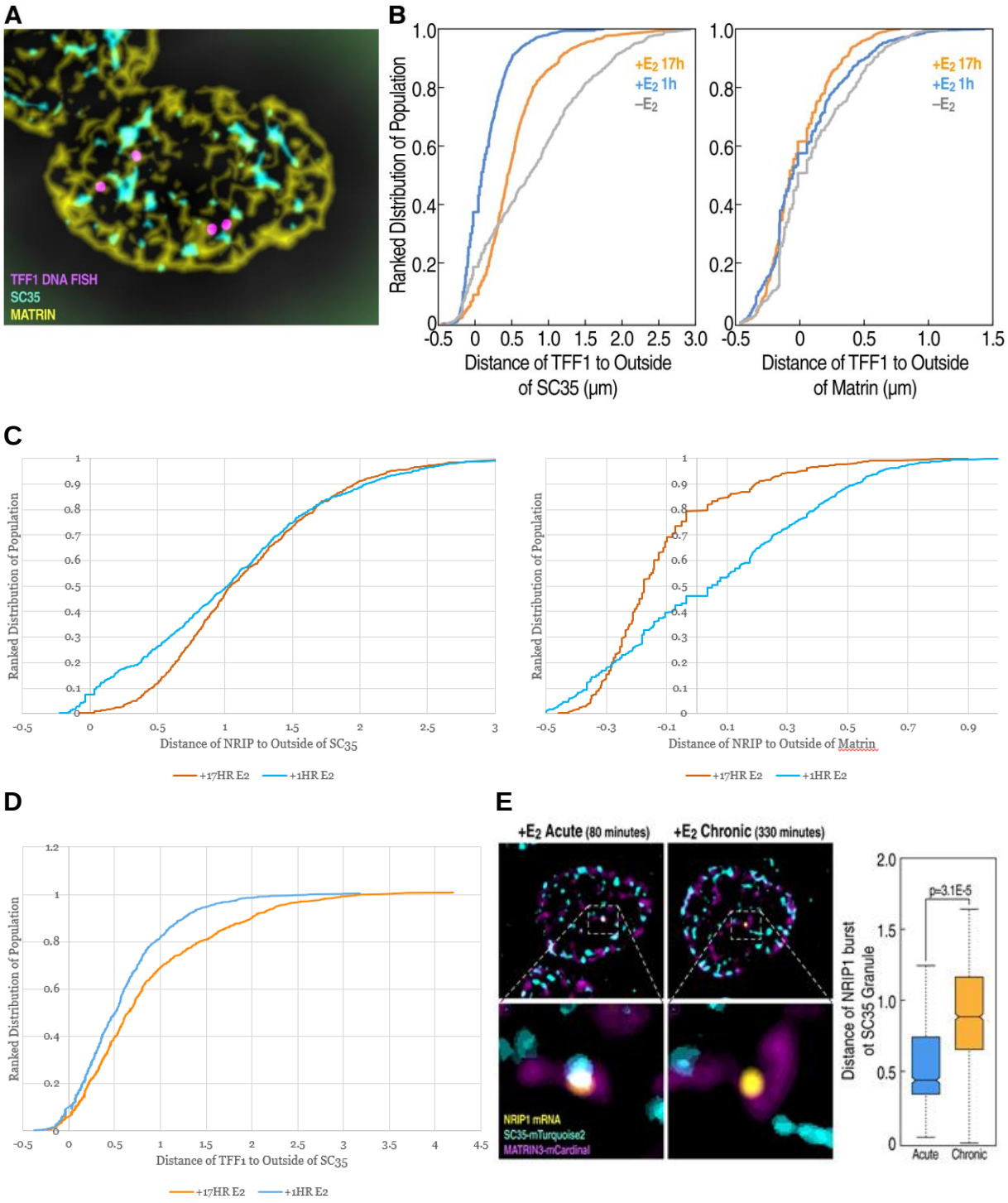
A
TFF1 DNA FISH
SC35
MATRIN
B
Ranked Distribution of Population
+E2 17h
+E2 1h
–E2
Distance of TFF1 to Outside of SC35 (μm)
Distance of TFF1 to Outside of Matrin (μm)
C
Ranked Distribution of Population
Distance of NRIP to Outside of SC35
Distance of NRIP to Outside of Matrin
+17HR E2
+1HR E2
D
Ranked Distribution of Population
Distance of TFF1 to Outside of SC35
+17HR E2
+1HR E2
E
+E2 Acute (80 minutes)
+E2 Chronic (330 minutes)
NRIP1 mRNA
SC35-mTurquoise2
MATRIN3-mCardinal
Distance of NRIP1 burst ot SC35 Granule
p=3.1E-5
Acute
Chronic

Figure 3.5. Biophysical insight into transcription dynamics via single molecule tracking. a. Still frame of a single molecule tracking movie acquired at 5ms exposures of endogenously Halo-tagged ERα. **b.** Gaussian Mixture Models (GMM) and Agglomerative Hierarchical clustering methodologies to help group ER molecules into six clusters based on defined parameters. Both algorithems identified a similar cluster of acute-specific ER molecules characterized by the lowest diffusion coefficient of all the clusters. **c.** 1,6-hexandiol treatment shows loss of acute-specific E2 population of restricted molecules.

Figure 3.5.

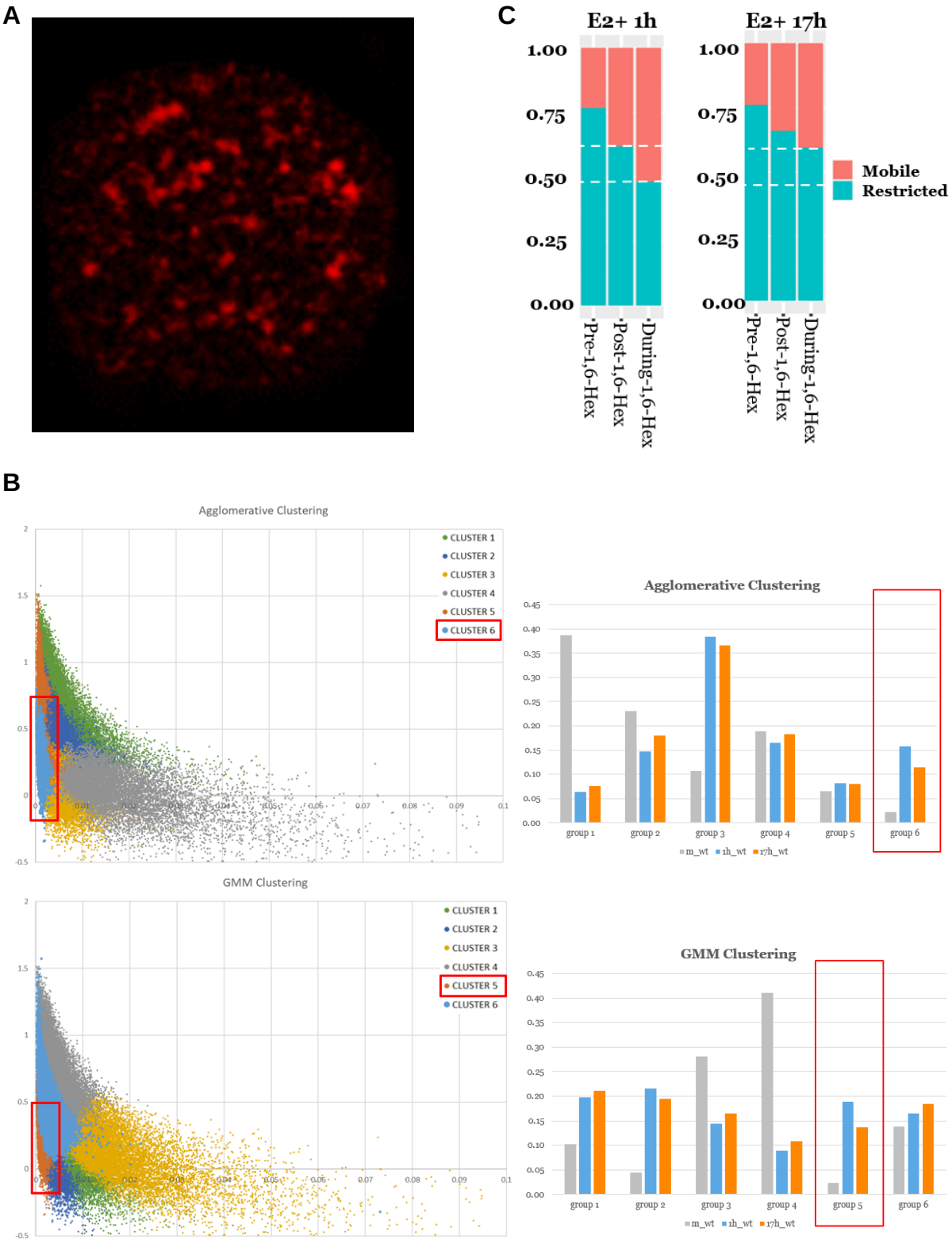
A
C
E2+ 1h
E2+ 17h
1.00
0.75
0.50
0.25
0.00
Mobile
Restricted
Pre-1,6-Hex
Post-1,6-Hex
During-1,6-Hex
B
Agglomerative Clustering
CLUSTER 1
CLUSTER 2
CLUSTER 3
CLUSTER 4
CLUSTER 5
CLUSTER 6
Agglomerative Clustering
group 1
group 2
group 3
group 4
group 5
group 6
m_wt
1h_wt
17h_wt
GMM Clustering
GMM Clustering

3.6 Acknowledgements

Chapter 3 is currently being prepared for submission, with the assistance of Thomas Suter and Michael Rosenfeld. The dissertation author is a coauthor of this paper.

3.7 References

1. Li, W., Notani, D., Ma, Q., Tanasa, B., Nunez, E., Chen, A.Y., Merkurjev, D., Zhang, J., Ohgi, K., Song, X., et al. (2013). Functional roles of enhancer RNAs for oestrogen-dependent transcriptional activation. *Nature* 498: 516-520.

2. Carroll, J.S., Meyer, C.A., Song, J., Li, W., Geistlinger, T.R., Eeckhoute, J., Brodsky, A.S., Keeton, E.K., Fertuck, K.C., Hall, G.F., et al. (2006). Genome-wide analysis of estrogen receptor binding sites. *Nat Genet* 38, 1289-1297.

3. Klinge, C.M. (2001). Estrogen receptor interaction with estrogen response elements. *Nucleic Acids Res* 29, 2905-2919.

4. Lin, C.Y., Vega, V.B., Thomsen, J.S., Zhang, T., Kong, S.L., Xie, M., Chiu, K.P., Lipovich, L., Barnett, D.H., Stossi, F., et al. (2007). Whole-genome cartography of estrogen receptor alpha binding sites. *PLoS Genet* 3, e87.

5. Vega, V.B., Lin, C.Y., Lai, K.S., Kong, S.L., Xie, M., Su, X., Teh, H.F., Thomsen, J.S., Yeo, A.L., Sung, W.K., et al. (2006). Multiplatform genome-wide identification and modeling of functional human estrogen receptor binding sites. *Genome Biol* 7, R82.

6. Hanstein, B., Djahansouzi, S., Dall, P., Beckmann, M.W., and Bender, H.G. (2004). Insights into the molecular biology of the estrogen receptor define novel therapeutic targets for breast cancer. *Eur J Endocrinol* 150, 243-255.

7. Kumar, R., Zakharov, M.N., Khan, S.H., Miki, R., Jang, H., Toraldo, G., Singh, R., Bhasin, S., and Jasuja, R. (2011). The dynamic structure of the estrogen receptor. *J Amino Acids* 2011, 812540.

8. Lin, C.Y., Strom, A., Vega, V.B., Kong, S.L., Yeo, A.L., Thomsen, J.S., Chan, W.C., Doray, B., Bangarusamy, D.K., Ramasamy, A., et al. (2004). Discovery

of estrogen receptor alpha target genes and response elements in breast tumor cells. *Genome Biol* 5, R66.

9. Osborne, C.K., and Schiff, R. (2005). Estrogen-receptor biology: continuing progress and therapeutic implications. *J Clin Oncol* 23, 1616-1622.

10. Balfe, P., McCann, A., McGoldrick, A., McAllister, K., Kennedy, M., Dervan, P., and Kerin, M.J. (2004). Estrogen receptor alpha and beta profiling in human breast cancer. *Eur J Surg Oncol* 30, 469-474.

11. Thomas, C., and Gustafsson, J.A. (2011). The different roles of ER subtypes in cancer biology and therapy. *Nat Rev Cancer* 11, 597-608.

12. Ong, C.T. and V.G. Corces, Enhancer function: new insights into the regulation of tissue-specific gene expression. *Nat Rev Genet*, 2011. 12(4): p. 283-93.

13. Kim, T.K., Hemberg, M., and Gray, J.M. (2015). Enhancer RNAs: a class of long noncoding RNAs synthesized at enhancers. *Cold Spring Harb Perspect Biol* 7, a018622.

14. Shlyueva, D., Stampfel, G., and Stark, A. (2014). Transcriptional enhancers: from properties to genome-wide predictions. *Nat Rev Genet* 15, 272-286.

15. Smith, E., and Shilatifard, A. (2014). Enhancer biology and enhanceropathies. *Nat Struct Mol Biol* 21, 210-219.

16. Freedman, L.P. (1999). Multimeric Coactivator Complexes for Steroid/Nuclear Receptors. *Trends Endocrinol Metab* 10, 403-407.

17. McKenna, N.J., Xu, J., Nawaz, Z., Tsai, S.Y., Tsai, M.J., and O'Malley, B.W. (1999). Nuclear receptor coactivators: multiple enzymes, multiple complexes, multiple functions. *J Steroid Biochem Mol Biol* 69, 3-12.

18. Shang, Y., Myers, M., and Brown, M. (2002). Formation of the androgen receptor transcription complex. *Mol Cell* 9, 601-610.

19. Wang D, Garcia-Bassets I, Benner C, Li W, Su X, Zhou Y, Qiu J, Liu W, Kaikkonen MU, Ohgi KA, Glass CK, Rosenfeld MG, Fu XD. (2011).

Reprogramming transcription by distinct classes of enhancers functionally defined by eRNA. *Nature*. 474:390-394.

20. Torchia, J., Glass, C., and Rosenfeld, M.G. (1998). Co-activators and co-repressors in the integration of transcriptional responses. *Curr Opin Cell Biol* 10, 373-383.

21. Glass CK, Saijo K. Nuclear receptor transrepression pathways that regulate inflammation in macrophages and T cells. *Nat Rev Immunol*. 2010 May;10(5):365-76.

22. Liu, Z., Merkurjev, D., Yang, F., Li, W., Oh, S., Friedman, M. J., Song, X., Zhang, F., Ma, Q., Ohgi, K. A., Krones, A., & Rosenfeld, M. G. (2014). Enhancer activation requires trans-recruitment of a mega transcription factor complex. Cell, 159(2), 358–373. https://doi.org/10.1016/j.cell.2014.08.027

23. Suter, D.M., Molina, N., Naef, F., and Schibler, U. (2011). Origins and consequences of transcriptional discontinuity. Curr. Opin. Cell Biol. 23, 657–662.

24. Larson, D. R., Zenklusen, D., Wu, B., Chao, J. A. & Singer, R. H. Real-Time Observation of Transcription Initiation and Elongation on an Endogenous Yeast Gene.

25. Buxbaum, A. R., Haimovich, G. & Singer, R. H. In the right place at the right time: visualizing and understanding mRNA localization. *Nat. Rev. Mol. Cell Biol.* (2014). doi:10.1038/nrm3918

26. Coulon, A., Chow, C. C., Singer, R. H. & Larson, D. R. Eukaryotic transcriptional dynamics: from single molecules to cell populations. *Nat. Rev. Genet.* 14, 572–84 (2013).

27. Coulon, A. *et al.* Kinetic competition during the transcription cycle results in stochastic RNA processing. *Elife* 3, 1–22 (2014).

28. Alexander, J. M., Guan, J., Li, B., Maliskova, L., Song, M., Shen, Y., Huang, B., Lomvardas, S., & Weiner, O. D. (2019). Live-cell imaging reveals enhancer-dependent Sox2 transcription in the absence of enhancer proximity. ELife, 8, e41769. https://doi.org/10.7554/eLife.41769

29. Gu, B., Swigut, T., Spencley, A., Bauer, M. R., Chung, M., Meyer, T., & Wysocka, J. (2018). Transcription-coupled changes in nuclear mobility of mammalian cis-regulatory elements. *Science*, *359*(6379), 1050–1055. https://doi.org/10.1126/science.aao3136

30. Boijja A, Klein IA, Sabari BR, et al. Separation Capacity of Their Activation Domains. 2019;175(7):1842-1855. doi:10.1016/j.cell.2018.10.042.Transcription

31. Chong S, Dugast-Darzacq C, Liu Z, et al. Imaging dynamic and selective low-complexity domain interactions that control gene transcription. *Science (80-)*. 2018;361(6400):1-25. doi:10.1126/science.aar2555

32. Berry J, Weber SC, Vaidya N, Haataja M, Brangwynne CP, Weitz DA. RNA transcription modulates phase transition-driven nuclear body assembly. *Proc Natl Acad Sci U S A*. 2015;112(38):E5237-E5245.

33. Feric M, Vaidya N, Harmon TS, et al. Coexisting Liquid Phases Underlie Nucleolar Subcompartments. *Cell*. 2016;165(7):1686-1697. doi:10.1016/j.cell.2016.04.047

34. Banani SF, Lee HO, Hyman AA, Rosen MK. Biomolecular condensates: organizers of cellular biochemistry. *Nat Rev Mol Cell Biol*. 2017;18(5):285-298. doi:10.1038/nrm.2017.7

35. Sabari BR, Agnese AD, Young RA. Biomolecular condensates in the nucleus. *Trends Biochem Sci*. Published online 2020.

36. Cho WK, Spille JH, Hecht M, et al. Mediator and RNA polymerase II clusters associate in transcription-dependent condensates. *Science (80-)*. 2018;361(6400):412-415. doi:10.1126/science.aar4199

37. Skowronska-Krawczyk D, Ma Q, Schwartz M, et al. Required enhancer-matrin-3 network interactions for a homeodomain transcription program. *Nature*. 2014;514(7521):257-261. doi:10.1038/nature13573

38. Nair SJ, Yang L, Meluzzi D, et al. Phase separation of ligand-activated enhancers licenses cooperative chromosomal enhancer assembly. *Nat Struct Mol Biol*. 2019;26(3):193-203. doi:10.1038/s41594-019-0190-5

39. Mao YS, Zhang B, Spector DL. Biogenesis and function of nuclear bodies. *Trends Genet*. 2011;27(8):295-306. doi:10.1016/j.tig.2011.05.006

40. Spector DL, Lamond AI. Nuclear speckles. *Cold Spring Harb Perspect Biol*. 2011;3(2):1-12. doi:10.1101/cshperspect.a000646

41. Quinodoz SA, Ollikainen N, Tabak B, et al. Higher-Order Inter-chromosomal Hubs Shape 3D Genome Organization in the Nucleus. *Cell*. 2018;174(3):744-757.e24. doi:10.1016/j.cell.2018.05.024

42. Garcia, D. A., Johnson, T. A., Presman, D. M., Fettweis, G., Wagh, K., Rinaldi, L., Stavreva, D. A., Paakinaho, V., Jensen, R. A. M., Mandrup, S., Upadhyaya, A., & Hager, G. L. (2021). An intrinsically disordered region-mediated confinement state contributes to the dynamics and function of transcription factors. *Molecular Cell*, *81*(7), 1484-1498.e6. https://doi.org/10.1016/j.molcel.2021.01.013

43. Shrinivas K, Sabari BR, Coffey EL, et al. Enhancer Features that Drive Formation of Transcriptional Condensates. *Mol Cell*. 2019;75(3):549-561.e7. doi:10.1016/j.molcel.2019.07.009

44. Kagey MH, Newman JJ, Bilodeau S, et al. Mediator and cohesin connect gene expression and chromatin architecture. *Nature*. 2010;467(7314):430-435. doi:10.1038/nature09380

45. Manteiga JC, Henninger JE, Sabari BR, et al. Pol II phosphorylation regulates a switch between transcriptional and splicing condensates. *Nature*. 2019;572:543.

46. Boija A, Klein IA, Sabari BR, et al. Transcription Factors Activate Genes through the Phase-Separation Capacity of Their Activation Domains. *Cell*. 2018;175(7):1842-1855.e16. doi:10.1016/j.cell.2018.10.042

47. Sabari, B. R., Dall'Agnese, A., Boija, A., Klein, I. A., Coffey, E. L., Shrinivas, K., Abraham, B. J., Hannett, N. M., Zamudio, A. V., Manteiga, J. C., Li, C. H., Guo, Y. E., Day, D. S., Schuijers, J., Vasile, E., Malik, S., Hnisz, D., Lee, T. I., Cisse, I. I., … Young, R. A. (2018). Coactivator condensation at super-enhancers links phase separation and gene control. *Science*, *361*(6400), eaar3958. https://doi.org/10.1126/science.aar3958

Chapter 4: Phase separation of ligand-activated enhancers licenses cooperative chromosomal enhancer assembly

4.1 Abstract

A crucial feature of differentiated cells is the rapid activation of enhancer driven transcriptional programs in response to signals. The potential contributions of physicochemical properties of enhancer assembly in signaling events remain poorly understood. Here, we report that in human breast cancer cells, the acute 17β-estradiol (E_2)-dependent activation of functional enhancers requires assembly of an eRNA-dependent ribonucleoprotein (eRNP) complex exhibiting properties of phase separated condensates. Unexpectedly, while acute ligand-dependent assembly of eRNPs resulted in enhancer activation sensitive to chemical disruption of phase separation, chronically activated enhancers proved resistant to such disruption, with progressive maturation of eRNPs to a more gel-like state. Acute, but not chronic, stimulation resulted in ligand-induced, condensin-dependent changes in spatial chromatin conformation based on homotypic enhancer association, resulting in cooperative enhancer activation events. Thus, distinct physicochemical properties of eRNP condensates on enhancers serve as determinants of rapid ligand-dependent alterations in chromosomal architecture and cooperative enhancer activation.

4.2 Background

Enhancers serve as critical regulatory elements for transcriptional programs by directing development, homeostasis, and disease states[1,2]. Clusters of enhancers located within a relatively small genomic region, known as super-enhancers[3,4] or stretch enhancers[5], exhibit more regulatory potential than individual enhancers by

acting in a cooperative fashion[6-8]. The underlying mechanism for the enhancer function and cooperativity of super-enhancers has been proposed to be the physical process of liquid-liquid phase separation (LLPS)[9,10]. LLPS is characterized by spontaneous demixing of a homogenous solution into two phases of high and low concentrations, and has been attributed to the assembly of several membraneless organelles[11-13]. In support of this model, intrinsically disordered regions (IDR) of transcriptional cofactors associated with clustered enhancers in embryonic stem cells (ESC) are capable of liquid phase condensation at active super-enhancers[14,15]. Key tissue-specific transcription factors also undergo phase separation *in vitro* and condensate formation *in vivo* on super enhancers[16]. Recent studies have also linked low complexity (LC) activation domains of transcription factors, co-factors, and RNA Polymerase II, with gene regulation[17-21].

Other characteristics of enhancers that may be explained by LLPS model of enhancer assembly are the extent and rapidity of their response to specific signals. For example, 17β-estradiol (E_2) can coordinate genome-wide transcriptional programs through acute, signal-induced activation of enhancers that exhibit minimal basal activity[22,23]. In response to E_2, robust enhancers bound to estrogen receptor α (ERα) transcribe high levels of enhancer-RNAs (eRNAs)[23-26], which are a class of long noncoding RNA transcribed from the core of functionally active enhancers[27,28]. A key feature of the most robust E_2 responsive enhancers is the recruitment of an ERα-dependent, megadaltonscale protein complex, referred to as the MegaTrans complex[25]. This complex is characterized by trans-recruitment of DNA-binding transcription factors such as GATA3, RARα/γ, AP2γ, c-Jun, cFos, STAT1, FOXA1;

and enzymatic machinery including DNA-Dependent Protein Kinase (DNAPK). Interestingly, many components of this complex harbor IDRs, consistent with the overrepresentation of low complexity sequences in the activation domains of transcription factors[29,30]. The resulting high local concentration of eRNA together with a complex composed of several transcription factors would appear to provide a conducive microenvironment for the assembly of eRNA-dependent ribonucleoprotein (eRNP) condensates that effectively regulate signal inducible transcription.

Assembly of transcription machinery as biomolecular condensates on most active enhancers raises several interesting questions. For example, is there a distinction in the biophysical properties of the transcription complex condensates assembled at enhancers with respect to the duration of ligand and/or signal activation? Do phase-separated condensates facilitate alterations of 3dimensional chromosomal architecture? What is the functional implication of this process in signal induced transcriptional programs? Here, we report that the most robust E_2-responsive enhancers recruit several proteins harboring IDRs that can undergo LLPS both *in vitro* and *in vivo*. Unexpectedly, the acutely activated enhancers, but not those exposed to chronic stimulation by ligand or constitutively activated enhancers, exhibit assembly of eRNP condensates with physicochemical properties of dynamic liquid droplets. The dynamic nature of eRNPs is linked to signal-induced proximity and cooperative activation of enhancers separated by vast genomic distances.

4.3 Results

MegaTrans enhancer proteins form phase-separated liquid droplets.

Estrogen signaling activates 7,000-8,000 enhancers genome-wide, out of which 1248

are exceptionally active, based on eRNA transcription and regulatory potential[23,25,31]. These exceptionally active enhancers are characterized by E_2-dependent recruitment of high levels of ERα, RNA PolII, MegaTrans components (e.g. GATA3, FOXA1, and AP2γ) [25,31,32], MED1 and P300 (schematics in Fig. 4.1a, Supplementary Fig. 1a, Supplementary Table 1), and by higher induced chromatin openness when compared to weak ERα-bound enhancers (Supplementary Fig. 1b). These robustly E_2-activated enhancers are referred to here as MegaTrans enhancers. Sequence analysis of protein components of the complex bound to MegaTrans enhancers (termed MegaTrans complex) revealed that several (namely GATA3, ERα, RARA, FOXA1, AP2γ, SMC4), contain stretches of amino acids predicted to form intrinsically disordered regions (IDRs) (Supplementary Fig. 4.2a). Consistently, these MegaTrans components were precipitated from nuclear lysates in the presence of biotinylated isoxazole (b-isox), a compound known to precipitate proteins containing LC domains or IDRs[33] (Fig. 1b). GATA3, a central component in the assembly of the MegaTrans complex[25], harbors the highest percentage of disorder among the analyzed proteins (Supplementary Fig. 2a) and was consistently precipitated with the lowest concentration of b-isox (Fig. 4.1b).

The presence of IDRs in MegaTrans components suggests that they may form phase-separated condensates. To investigate this possibility using prototypic MegaTrans components, we purified ERα and GATA3 as holoproteins fused to MBP and mixed each protein with 5% PEG, a crowding agent. Confocal microscopy imaging of these mixtures revealed the formation of micron-sized droplets (Supplementary Fig. 2b). In contrast, such droplets were not observed with MBP

alone under identical experimental conditions. Both GATA3 and ERα condensates exhibited typical characteristics of phase-separated liquid droplets, such as spherical aspect ratio (Supplementary Fig. 2c) and propensity to coalesce (Supplementary Video 1, 2).

To further probe the fluid properties of the condensates, we employed fluorescence recovery after photobleaching (FRAP)[34] as a tool to study protein diffusion within droplets. For FRAP experiments, we used a total protein concentration of 7-10 μM, ~1% of which were labeled with fluorescent dyes[35]. Both GATA3-MBP and ERα-MBP droplets showed almost full recovery (≥ 90%) of bleached fluorescence within 100-400s, suggesting that the condensed protein phases are viscous liquids[36] (Fig. 4.1 c, d). The difference in recovery kinetics between GATA3-MBP and ERα-MBP droplets ($t_{1/2}$ of 100 ± 6s vs. 24 ± 2) is likely due to the distinct nature and strength of weak multivalent interactions[37], as the two proteins possess very different amino acid sequences and structures. Additionally, when GATA3-MBP and ERα-MBP were mixed together *in vitro,* two-color confocal microscopy analysis revealed that they are enriched and coexist in a single, phase-separated condensate, with the concentration of ERα considerably higher in the interior of the GATA3 droplet than at the dispersed phase (Supplementary Fig. 2d).

In order to examine the *in vivo* phase separation capability of the IDRs of GATA3 and ERα, we employed the optodroplet assay, a light activated system to study IDR mediated condensation in cells[38]. IDRs of both GATA3 and ERα fused to mCherry-Cry2 demonstrated efficient clustering and droplet formation upon blue light stimulation and exhibited liquid droplet fusion behavior in HEK293 cells

(Supplementary Fig. 2e-g and Supplementary Video 3, 4). Cry2-mCherry alone showed no clustering activity under the same exposure settings (Supplementary Fig. 2e, Supplementary Video 5). These results support the notion that the IDRs of GATA3 and ERα are capable of forming phase separated droplets *in vivo*.

Because GATA3 and ERα are robustly recruited to MegaTrans enhancers upon stimulation by E_2, we asked whether enhancer-bound MegaTrans holoproteins could also undergo clustering *in vivo*. To visualize such clusters, we fused ERα with monomeric-mCherry at the N-terminus and expressed the fluorescently labeled protein in MCF7 cells. Live-cell imaging revealed acute assembly of nuclear ERα foci within 1 min after E_2 treatment in ~80% of the cells (Fig. 4.1e and Supplementary Video 6), with an average of 121±25 distinct foci per nucleus, whereas no ERα foci were observed before E_2 treatment. We obtained identical results using ERα labeled with mTurquoise, a different monomeric fluorophore (Supplementary Video 6). To examine the physical association of these E_2-dependent ERα condensates with MegaTrans enhancer targets, we performed RNA FISH experiments on cells displaying ERα-mCherry foci. RNA FISH using probes targeting *TFF1* introns, which is ~9 kb from the corresponding MegaTrans enhancer, appeared in close proximity to ERα foci (Supplementary Fig. 3.a, b). In contrast, the transcribing loci of *DYRK1A*, which does not depend on E_2, appeared at a much greater distance from ERα foci (Supplementary Fig. 3.a, b). These data support the hypothesis that at least a subset of ERα foci develops in proximity to MegaTrans enhancers. We next examined the physical properties of ERα foci that formed after 1 h E_2 treatment, with a median radius of ~0.96 μm. FRAP experiments revealed fluorescence recovery with half-life

of 15.6 ± 1.07s (Fig. 4.1f, Supplementary Fig. 3c) and apparent diffusion coefficient D_{app} of ~0.04 $\mu m^2/s$. The D_{app} value is an order of magnitude lower comparable to previously reported *in vivo* FRAP data on transcription related proteins that form biomolecular condensates[15,39], potentially reflecting the difference in the dynamics with which ERα binds directly to consensus motifs in chromatin.

We next explored the possible involvement of IDRs in the function of MegaTrans enhancers in vivo. To probe the role of the IDR in GATA3, we expressed either the wild type protein or a mutant form lacking the IDR (a.a 2-250, a length characteristic of transcription factor IDRs) in MCF7 cells where endogenous *GATA3* had been depleted by targeting its 3'UTR with shRNA (Supplementary Fig. 4.3d, e). The E_2-dependent activation of MegaTrans enhancers was then observed by measuring the expression of their eRNAs by qRT-PCR. We found that the loss of E_2-mediated activation of MegaTrans enhancers and their target genes was effectively rescued by expression of WT GATA3, but not by the mutant protein lacking the IDR (Fig. 4.1g, Supplementary Fig. 3f).

Together, our data demonstrate that GATA3 and ERα, two key components recruited to the MegaTrans enhancers, are capable of phase separating *in vitro* and *in vivo*, forming functional condensates with distinct fluid dynamics at MegaTrans enhancer loci.

Phase separation underlies enhanceosome assembly at acutely induced enhancers. The association of MegaTrans enhancers with functional phase-separated condensates led us to wonder whether such condensates play a role in enhanceosome assembly and thus enhancer activity. To address this question, we

first examined eRNA transcription in the presence of 1,6-hexanediol (1,6-HD), an aliphatic alcohol that disassembles phase-separated ribonucleoprotein (RNP) granules and membraneless structures by disrupting weak hydrophobic interactions[40,41]. qRT-PCR analysis revealed that 1,6-HD considerably reduced E_2-induced eRNA expression from selected MegaTrans enhancers, while no effect was observed by the similar aliphatic alcohols 2,5-hexanediol (2,5-HD) or 1,4-butanediol (1,4-BD), which have minimal impact on the phase behavior of disordered proteins[40,41] (Supplementary Fig. 4a).

To gather genome-wide data, we performed GRO-seq analysis on MCF7 cells that were treated first with 1,6-HD or 2,5-HD for 5 min and then with E_2 for 30 min. The inhibitory effect of 1,6-HD on eRNA transcription was almost exclusively limited to the MegaTrans enhancers, with no effects on transcription from weak ERα enhancers or non-ERα-bound enhancers (Fig. 4.2a), in agreement with MegaTrans enhancers ranking amongst the most active enhancers in E_2-treated cells[23,24]. These results suggest that 1,6-HD inhibited the functional assembly of the MegaTrans complex. To examine whether 1,6-HD could also disrupt the function of preassembled MegaTrans complex, the cells were treated first with E_2 for 1 hr, thus ensuring MegaTrans assembly[25], and then with 1,6-HD for 5 minutes. This experimental design also resulted in specific suppression of MegaTrans-bound enhancer transcription (Supplementary Fig. 4b), suggesting that 1,6-HD may disrupt the function of fully assembled MegaTrans complex. Suppression of E_2-activated transcription was also evident at target coding genes of MegaTrans enhancers (Supplementary Fig. 4c).

In order to examine the impact of 1,6-HD on assembly of MegaTrans on chromatin, we performed ChIP-seq experiments. While ERα was still effectively recruited to MegaTrans enhancers following 1,6-HD treatment (Fig. 4.2b), other MegaTrans component assembly was significantly disrupted, as evidenced by impairment of GATA3 and AP2γ recruitment to the complex (Fig. 4.2 c,d). Therefore, 1,6-HD specifically disrupted the assembly of the trans-recruited complex. Similar results were also observed for RARα on two examined MegaTrans enhancers (Supplementary Fig. 4d). Western blot analysis on control and 1,6-HD-treated samples, both stimulated with E_2, revealed no impact of these treatments on cellular levels of ERα, GATA3 or AP2γ (Supplementary Fig. 4e). Exposure to 1,6HD for 5 min also resulted in dramatic reduction in the number and signal intensity of induced ERα mTurquoise foci (Fig. 4.2e), suggesting that these assemblies are also disrupted in parallel with transcriptional impact. These results indicate that phase separation dependent on hydrophobic interactions plays a role in the assembly of the MegaTrans complex and in acute activation of E_2stimulated enhancers.

The inferred involvement of phase separation with MegaTrans enhancers suggests the possibility that 1,6-HD sensitivity and LLPS are general properties of rapidly induced, signal-dependent enhancers. To test this hypothesis, we examined two other signaling programs that induce rapid activation of enhancers upon stimulation: TNFα-mediated activation of NF-kB–bound enhancers in MCF7 cells[42] and Kdo2-lipid A (KLA)–stimulated Tlr-4 enhancers in mouse macrophage RAW264.7 cells[43]. TNFα-induced activation of NF-kB–dependent enhancers in MCF7 cells was sensitive to 1,6-HD, which affected only the most active NF-kB–dependent

enhancers, with no effects on other enhancers, including those regulated by E_2-stimulation (Fig. 4.2f). Similarly, the rapid, KLA-mediated activation of potent enhancers in mouse macrophage RAW264.7 cells was abrogated by treatment with 1,6-HD (Fig. 4.2g). Interestingly, eRNA transcription from other robust enhancers that are basally active was actually elevated in response to 1,6-HD (Fig. 2a, f, g and Supplementary Fig. 4b, third group in each panel). Together, these data reveal that the initial, signal-dependent nucleation of enhanceosome complexes on potent, acutely activated enhancers, but not on basally active enhancers, represents an assembly process that is sensitive to 1,6-HD and thus likely driven by phase separation.

Phase separation underlies long-distance interactions and cooperative activation of acutely induced enhancers. Since phase-separated condensates are prone to interacting through coalescence[44,45], we asked whether the putative phase separation events affecting MegaTrans enhancers might promote spatial interactions between those enhancers. We investigated E_2-induced changes in chromosomal architecture by examining potential long-range intra-chromosomal interactions of enhancers located on human chromosome 21 (Chr.21), which harbors multiple MegaTrans enhancers (Fig. 4.3a). We first performed Hi-C on ERα-positive MCF7 cells. Contact maps at 1Mb resolution with ~500 M assignable sequence reads revealed no effect of E_2 on A/B compartments or boundaries of topologically associated domains (TADs) (Supplementary Fig. 5a), but suggested an enrichment of interactions between broad and genomically distant regions on Chr.21 (Supplementary Fig. 5b). To study enhancer interactions with greater precision, we

performed 4C-seq experiments using a viewpoint on *TFF1e.* These experiments revealed E_2-induced interaction between the *TFF1* and the *DSCAM-AS* enhancer regions, which are separated by 1.9 Mb and located in two different TADs (Supplementary Fig. 5c), suggesting that homotypic long-distance interactions may be a feature of MegaTrans enhancers.

We systematically examined other E_2-induced changes in chromosome conformation along Chr.21 using DNA-FISH to quantitate pairwise distances between multiple enhancer regions. E_2 treatment for 50 min resulted in subtle (5–17%) but consistent decrease in median spatial distances between several MegaTrans enhancer loci on Chr.21, separated by 1.9–27 Mb, as evidenced by comparing cumulative distance distributions and median spatial distances (Fig. 4.3 b,c, Supplementary Fig. 6a,b, c and Supplementary Table 2). In contrast, no E_2-induced proximity was observed between MegaTrans enhancers and genomic regions devoid of ERα binding (*CP26* and *TFF1*, *CP26* and *NRIP1*, in Supplementary Fig. 6c), suggesting that E_2 specifically affects the spatial proximity of MegaTrans enhancers.

To examine the kinetics of such changes, we assessed the proximity of two regions by comparing their spatial distance to a cutoff value that depends on the genomic separation of those regions (Supplementary Fig. 6d and Supplementary Note). There was ~3 fold increase in the fraction of *TFF1* and *NRIP1* enhancer regions, separated by a genomic distance of 27Mb, reaching spatial proximity (<600 nm) within 5 min of E_2 stimulation (Fig. 4.3d). The rapid kinetics observed for E_2-induced proximity of specific ERα enhancers separated by vast genomic distances suggests a model of homotypic enhancer association driven by coalescence of

ligand-induced enhancer condensates. Our experiments also revealed an asynchrony of transcriptional responses within 15 min of E_2 treatment, as RNA FISH data using intronic and exonic probes of *TFF1* and *NRIP1* demonstrated that only 20-30% of cells have active transcription (intronic probe) of these genes at a given time point, but ~55-75% of cells showed mature transcript (exonic probe) over the 15-minute period of stimulation (Supplementary Fig. 7a–c). This supports the notion that the small changes in spatial proximity could be functionally relevant and is consistent with the relatively lower frequency of active transcriptional events observed.

Functional consequences of E_2-induced proximity of MegaTrans enhancers. In order to assess the functional consequences of the E_2-induced proximity between MegaTrans enhancers, we investigated the relationship between spatial proximity and transcriptional activity of their targets. The transcriptional activation of *NRIP1*, as quantified by measuring the fluorescence signal intensity of intronic RNA-FISH probes, was inversely related to its spatial distance from *TFF1* (Fig. 4.3e, f). A similar relationship was observed for other ERα target pairs, such as *NRIP1DSCAM-AS1* and *DOPEY2-TFF1* (Fig. 4.3f, Supplementary Fig. 7d, e and Supplementary Table 3), suggesting that E_2-induced proximity of MegaTrans enhancers is correlated with cooperative activation of coding targets. To explore whether this induced proximity might require LLPS at the enhancers, we tested the impact of 1,6-HD on their spatial proximity. Indeed, 1,6-HD effectively attenuated the E_2-induced proximity of *NRIP1* and *TFF1* enhancer regions (Fig. 4.3g), suggesting that the spatial proximity between MegaTrans enhancers depends on cooperative

homotypic interactions requiring eRNP complexes with the properties of phase separated condensates.

Previous observations have suggested that such functionally important interactions between loci might involve their colocalization in subnuclear structures[46,47]. For example, enhancer and gene activation in cell lineage determination require interaction of a POU domain lineage-determining factor with the Matrin3 network[48] and possibly with the interchromatin granule (ICG)[46,47,49], which is also a phase-separated RNP condensate[50,51]. Accordingly, we investigated the relation between ICGs and MegaTrans enhancers. RNA-FISH using intronic probes revealed that the actively transcribed *NRIP1* and *TFF1* alleles associated with ICGs were ~3 times more active than the alleles not associated with ICGs (Supplementary Fig. 8a, b). Moreover, the transcriptional robustness of *NRIP1* was significantly higher when both *NRIP1* and *TFF1* were associated with the same ICG (Supplementary Fig. 8c, d), suggesting that association through ICGs may facilitate the cooperative activation of MegaTrans enhancers. Interestingly, knockdown of *SRSF1 or U2AF1* (Supplementary Fig. 8e), two ICG-associated splicing proteins[52,53], resulted in attenuated transcription of eRNAs from MegaTrans enhancers (Supplementary Fig. 8f, g). Next, we evaluated the association of E_2induced ERα foci with ICGs by co-expressing SC35 (SRSF2)-RFP and ERα-mTurquoise in MCF7 cells and inducing the formation of ERα foci by E_2 stimulation. Microscopic analysis revealed that, among the observed ERα condensates, ~80% were located within 400nm of an ICG (Fig. 4.3h and Supplementary Fig. 8h), providing evidence for the spatial proximity of E_2 induced ERα foci and MegaTrans enhancers with ICGs.

These results indicate that phase separation events at enhancers, coupled with proximity to ICG condensates, underlie E_2-induced alterations to chromosomal architecture and cooperative activation of distant MegaTrans enhancer loci.

eRNA and condensin recruitment are required for E_2-induced MegaTrans enhancer proximity. A key feature of active regulatory enhancers, as exemplified by E_2-stimulated enhancers, is production of eRNAs that are functionally important for target gene regulation[23,28,54,55]. Because a large proportion of phase separated biomolecular condensates are assembled as RNP complexes[13,51,56], we asked whether the observed phase separation events at MegaTrans enhancers involve the formation of eRNA-containing RNPs. To test whether MegaTrans eRNAs affect the assembly of MegaTrans components, we performed ChIP experiments in E_2-treated cells after knocking down *TFF1e* eRNA with an antisense oligonucleotide (ASO) (Supplementary Fig. 9a). Depletion of *TFF1e* eRNA abolished recruitment of MegaTrans components GATA3, RARα, and AP2γ to *TFF1* enhancer region in response to E_2, with no impact on the primary transcription factor, ERα (Fig 4.4a). This result is reminiscent of the disruption of the assembly of trans-recruited MegaTrans components, but not direct DNA binding of ERα, by 1,6-HD (Fig. 4.2 b,c,d) and supports a role for eRNAs in recruiting MegaTrans components. Moreover, E_2 stimulation of the eRNAdepleted cells failed to induce proximity between the *NRIP1* and *TFF1* regulatory regions (Fig. 4.4b and Supplementary Fig. 9b), suggesting that MegaTrans eRNAs are also required for E_2-induced proximity of MegaTrans enhancers.

To test whether eRNAs affect MegaTrans enhancers by altering the properties of phase-separated protein droplets, we mixed *in vitro* transcribed, fluorescently labeled *TFF1e* eRNA with purified ERα-MBP or GATA3-MBP fusion proteins, in the presence of 5% PEG and 200 mM NaCl. FRAP experiments revealed that *TFF1e* eRNA, but not control RNA, shortened the recovery time ($t_{1/2}$) of GATA3-MBP fusion protein droplets by ~50% (100±6s to 52±6s, comparable bleaching ROI) (Fig. 4.4c, Supplementary Fig. 9c, d). FRAP kinetics for ERα-MBP droplets also was reduced in the similar conditions (Fig. 4.4d, Supplementary Fig. 9e). These results suggest that the diffusion properties of phase-separated MegaTrans components are specifically affected by eRNAs transcribed from MegaTrans enhancers.

To further elucidate the interplay between eRNAs and MegaTrans enhancers, we directed our attention to condensins. This choice was motivated by previous report that both condensin I and II complexes, but not cohesin, are robustly recruited to ERα enhancers in an E_2-dependent manner in interphase MCF7 cells[31]. Here, analysis of ChIP-Seq data revealed a strong E_2-dependent recruitment of both NCAPG (a condensin I subunit) and NACAPH2 (a condensin II subunit) to MegaTrans enhancers, but only minimal recruitment to weak ERα-bound enhancers, non-ERα-bound enhancers (Supplementary Fig. 9f). Moreover, ChIP of condensin components following depletion of eRNAs from *TFF1* and *NRIP1* enhancers (Supplementary Fig. 9g) significantly reduced the recruitment of NCAPG and NCAPH2 to those enhancers (Fig. 4.4e), indicating that their recruitment to the MegaTrans enhancers is eRNA-dependent. Thus we asked whether condensins might serve as components of a phase-separated eRNP complex that induces

proximity of MegaTrans enhancers upon E_2 stimulation. Interestingly, SMC4, a component of the condensin complex, harbors an evolutionarily conserved IDR at its N-terminus (Supplementary Fig. 2a) and was precipitated by biotinylated isoxazole (Fig. 4.1b), supporting the potential participation of the condensin complex in phase separation events at MegaTrans enhancers. Moreover, following depletion of NCAPG or NCAPH2 (Supplementary Fig. 9h), FISH analysis revealed a significant reduction in E_2-induced proximity between *NRIP1e* and *TFF1e* (Fig. 4.4f and Supplementary Fig. 9i). In contrast, depletion of cohesin subunit RAD21 produced only minimal effects (Fig. 4.4f and Supplementary Fig. 9i), suggesting that selective condensin recruitment to MegaTrans enhancers may be required for longdistance homotypic association. These results are consistent with the recently established ability of condensin to multimerize[57]. Furthermore, analysis of previously reported GRO-seq data after depletion of either NCAPG or NCAPD3[31] revealed that eRNA synthesis was specifically reduced at MegaTrans enhancers (Fig. 4.4g), suggesting a feed-forward effect of condensins on eRNA expression. Thus, in addition to their known roles in mitosis and meiosis[58], gene regulation[59-61], and chromatin architecture[61,62], condensins also appear to facilitate long-distance homotypic enhancer association and cooperative activation of eRNP complexes at robust E_2-regulated enhancers.

Chronic stimulation by E_2 alters visco-elastic properties of MegaTrans enhancers and their effects on chromosomal architecture. The observation that disruption of transcription by 1,6-HD was restricted to signal-induced enhancers and did not affect constitutively active enhancers (Fig. 4.2 a, f, g and Supplementary Fig. 4b, third group in each panel) suggested a possible distinction in physicochemical

properties between acutely and chronically activated enhancers. To investigate this possibility, we reasoned that continuous stimulation of MegaTrans enhancers by E_2 for a prolonged period of time might impart those enhancers with biophysical properties resembling those of RNP complexes at constitutively active enhancers. We thus chronically activated MCF7 cells by culturing them in E_2-containing medium for 14-16 hrs. GRO-seq meta-analysis of cells treated with 2,5-HD or 1,6-HD after prolonged treatment with E_2 indicated that the active MegaTrans enhancers were no longer sensitive to 1,6-HD (Fig. 4.5a). Thus, chronic enhancer activation would appear to alter the biophysical properties of eRNPs at MegaTrans enhancers, compared to acute activation. These data, along with the lack of impact of 1,6-HD on constitutively active enhancers, also argue against an indiscriminate inhibition of transcription by 1,6-HD.

ChIP assays revealed a comparable level of recruitment of MegaTrans component RARα at *TFF1e* and *NRIP1e* enhancers after short-term (30 min) and long-term (14h) E_2 treatment (Supplementary Fig 10a). In contrast, GRO-seq data revealed that the level of induction of E_2 target genes by chronic E_2 treatment, although significantly higher than basal level, was lower than the induction by acute treatment of the ligand (Supplementary Fig. 10b). This suggests that 1,6-HDinsensitive MegaTrans assembly was not as transcriptionally competent as the complex assembled upon acute stimulation. To test the ligand responsiveness of complexes after long-term treatment, we treated the 14 hrs E_2-stimulated cells with one more dose of E_2 for 1hr. GRO-seq analysis between these two conditions revealed only minor differences in the transcription level (Supplementary Fig. 10c).

These data further support the idea that MegaTrans enhancers after long-term activation are not as transcriptionally competent as short-term activated enhancers.

This finding motivated us to explore the effects of prolonged E_2 stimulation on the biophysical properties of eRNP assembly. We induced ERα-Turquoise foci in MCF7 cells by short-term (30 min) and long-term (16 hrs) treatment with E_2. FRAP analysis revealed a significantly slower recovery of photo-bleached foci after long-term treatment in comparison to short-term treatment with E_2 (Fig. 4.5b and Supplementary Fig. 10d). The time constants derived from these two conditions were also significantly different (Fig. 4.5c), suggesting distinct physicochemical properties imparted by different activation regimen. We further examined the distinction between acute and chronic phase separation events *in vitro* by mixing GATA3, ERα, and *in vitro* transcribed *TFF1e* eRNA. The FRAP kinetics of the resulting droplets were then measured at 5 min, 90 min, and 180 min after the assembly. Consistent with the *in vivo* observations, the rapid FRAP kinetics observed upon immediate droplet formation of this ternary mixture *in vitro* was diminished at 90 min and dramatically slowed at 180 min (Fig. 4.5d). In addition, immediately assembled droplets were more sensitive to 1,6-HD when compared to the mature droplets (Supplementary Fig. 10e). These data are consistent with an alteration in the visco-elastic properties of eRNP condensates at MegaTans enhancers after long-term E_2 treatment and support a model in which the eRNP complex progressively transitions from a fluid to a more viscous gel-like or solid state.

We asked whether chronic E_2 stimulation might also affect induced enhancer proximity observed after acute stimulation. We determined the spatial proximity of

MegaTrans enhancer loci using DNA FISH probes targeting two different enhancer pairs, *TFF1e*/*NRIP1e* and *TIAM1e*/*DSCR3e*. We found that the spatial proximity observed after 50 min of E_2 treatment was no longer observed after 16 hrs treatment (Fig. 4.5e), indicating that chronic activation abolishes E_2-induced proximity of MegaTrans enhancers. This is consistent with the GRO-seq data indicating the attenuated transcriptional response after long-term E_2 stimulation (Supplementary Fig. 10c).

These data indicate the importance of the physicochemical properties of MegaTrans condensates in the functional behavior of ERα enhancers, highlighting the distinction between acute and chronic E_2 stimulation with respect to transcriptional activation and chromosomal architecture.

4.4 Discussion

Here, we provide evidence that acute enhancer activation by E_2 ligand and other signaling pathways results in eRNA-mediated RNP assembly displaying properties of phase-separated condensates at the most robust ERα enhancers. This assembly is apparently required for cooperative activation of these enhancers based on homotypic enhancer interactions spanning multiple TADs, altering chromosomal architecture. It has recently been discovered that phase separated condensates can exert forces on their associated chromatin, causing two distal telomere loci to be brought into close proximity[45]. We propose that the strongest Mega-Trans enhancers such as *NRIP1e* and *TFF1e* can bring their genomic loci into proximity with other Mega-Trans enhancers using a similar mechanism. Optimal cooperative activation of these enhancers is further augmented by the ability of the enhancer loci to interact

with ICGs, which are also membraneless RNP condensates[50,51] (Supplementary Fig. 8a,b), thereby potentially increasing local cofactor concentration and retention time. The observed effect of 1,6-HD on disruption of ligand-induced MegaTrans enhancer proximity and activation strongly suggests that the MegaTrans eRNP complex is also a condensate organized by hydrophobic interactions.

A striking observation in this context is that constitutively active enhancers or MegaTrans enhancers chronically stimulated by E_2 did not show comparable sensitivity to inhibition by 1,6-HD. This reduced sensitivity is consistent with less dynamic ERα foci *in vivo* and eRNP condensates *in vitro* after prolonged stimulation, suggesting an "ageing" mechanism that is reminiscent of the time- and concentration-dependent physicochemical transition observed with RNA-binding proteins[63,64]. The consequence of such an altered state is that chronically stimulated enhancers no longer exhibit ligand-induced spatial proximity and cooperativity across the chromosome. At a functional level, these enhancers are transcriptionally less active, compared to the acutely activated state, and are not responsive to further stimulation.

Drawing a parallel from recent findings on the surface tension driven coalescence of genomic loci[45], we speculate that the physical force driving the long-distance signal-induced enhancer proximity is the liquid surface tension of the MegaTrans condensates, a property that might be lost as condensates undergo transition to a more solid and less dynamic state over time. Interestingly, the liquid-to-solid transition of the RNA-binding protein FUS has been compared to the process of protein crystallization, whereby the metastable liquid phase triggers nucleation of a higher order assembly[64]. We also consider the possibility of a conformational

transition or the sampling of different conformations and interactions of the protein and RNA components over time. We therefore propose that ligand-activated, newly formed eRNP structures behave as metastable liquid droplets, governed by weak protein-protein, RNA-RNA, and protein-RNA interactions, which, upon prolonged activation, may mature to a thermodynamically favorable, less fluid, “hydrogel-like” state[33,63-65](Fig. 4.6).

An issue that has remained unresolved is how eRNAs might alter the physical properties of condensates assembled on enhancers. Intriguingly, in addition to its requirement for full assembly of MegaTrans enhancers, we have found that eRNA promotes a more dynamic liquid-like state in GATA3 condensates *in vitro* (Fig. 4c). We propose that this eRNA-dependent increase in fluidity may assist in the coalescence of phase separated enhancer condensates, not only across multiple TADs, but also with subnuclear structures such as ICGs. In summary, our model (Figure 6) features temporal changes for the physicochemical properties of ligand-dependent MegaTrans eRNP condensates: at first, these condensates exhibit dynamic cooperative spatial association, capable of altering chromosomal architecture at a global level, but they eventually solidify into independent, auto-regulatory transcriptional crucibles that have lost homotypic interaction properties.

4.5 Figures

Figure 4.1. Acutely active E_2-responsive MegaTrans enhancers concentrate a protein complex that can undergo phase transition. a. Schematic representation of the ERα/MegaTrans complex recruited to E_2-activated enhancers, which transcribe eRNAs and recruit the condensinI/II complexes. **b.** Western blot analyses showing that ERα, several MegaTrans components and condensin component SMC4 are precipitated by biotinylated isoxazole (b-isoxazole). FUS and GAPDH are used as a positive and negative control, respectively. **c,d.** FRAP data on phase-separated droplet formed in vitro by purified recombinant GATA3-MBP (**c**) and ERα-MBP (**d**). Top, charts show individual data points represented by dots, lines represent fitting to an exponential model to estimate the half-time of recovery. Bottom, representative images of in vitro droplets before and after photobleaching. **e.** Fluorescence microscopy images of a representative nucleus from MCF7 cells transfected with ERα-mCherry, before (-E_2) or after (+E_2, 5 or 15 minutes) E_2 treatment **f.** Mean intensity and photobleaching-normalized fluorescence of ERα-mTurquoise foci in E_2 treated MCF7 cells relative to pre-bleaching signal. Error bars represent S.E.M. of n ≥10 cells per time point. **g.** Levels of eRNA from indicated enhancers, measured by RT-PCR, from MCF7 cells depleted of endogenous GATA3 and expressing either WT or IDR-deleted GATA3 (GATA3-IDR mut), after 1h E_2 stimulation. shCTL indicates non-targeting control shRNA. The IDR (aa 2-250) is shown in schematics on top. Results are shown as individual data points (circles), mean ± s.d (lines). P-value calculated with unpaired Student's t-test. Data are representative of three independent experiments.

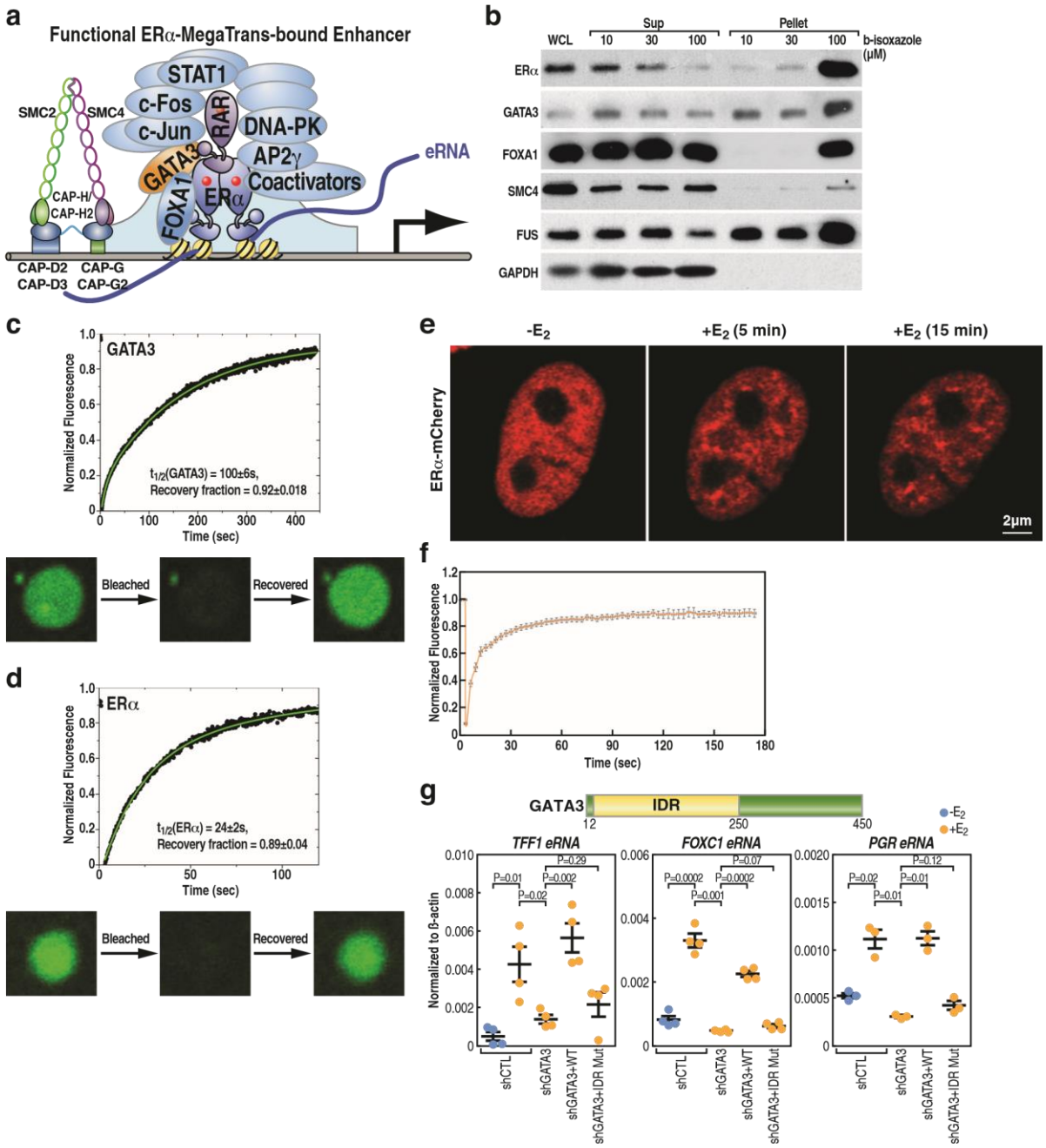
a
Functional ERα-MegaTrans-bound Enhancer
STAT1
c-Fos
c-Jun
RAR
DNA-PK
AP2γ
Coactivators
ERα
GATA3
FOXA1
SMC2
SMC4
CAP-H/
CAP-H2
CAP-D2
CAP-D3
CAP-G
CAP-G2
eRNA
b
Sup
Pellet
WCL
10
30
100
10
30
100
b-isoxazole (μM)
ERα
GATA3
FOXA1
SMC4
FUS
GAPDH
c
GATA3
Normalized Fluorescence
Time (sec)
t1/2(GATA3) = 100±6s,
Recovery fraction = 0.92±0.018
Bleached
Recovered
d
ERα
Normalized Fluorescence
Time (sec)
t1/2(ERα) = 24±2s,
Recovery fraction = 0.89±0.04
Bleached
Recovered
e
-E2
+E2 (5 min)
+E2 (15 min)
ERα-mCherry
2μm
f
Normalized Fluorescence
Time (sec)
g
GATA3
IDR
12
250
450
-E2
+E2
TFF1 eRNA
FOXC1 eRNA
PGR eRNA
Normalized to β-actin
P=0.01
P=0.02
P=0.002
P=0.29
P=0.0002
P=0.001
P=0.07
P=0.02
P=0.01
P=0.12
shCTL
shGATA3
shGATA3+WT
shGATA3+IDR Mut

Figure 4.2. Effect of phase-separation inhibition on acute enhancer transcriptional activation a. Meta-analysis of genome-wide GRO-seq data for enhancer activity in cells treated with 2,5-HD or 1,6-HD and E_2. Enhancers are classified as MegaTrans, weak ERα, and non ERα-bound enhancers **b-d.** Meta-analysis of ChIP-seq data representing the effect of 1,6-HD on chromatin recruitment of ERα (b), AP2γ (c) and GATA3 (d) on MegaTrans enhancers. **e.** Left, representative fluorescence microscopy images from MCF7 cells expressing ERα-Turquoise, showing loss of E_2-induced ERα foci upon 1,6-HD treatment. Right, quantification of foci number and intensity upon 1,6-HD treatment. Foci number data are shown in bar graphs, as mean and S.E.M. of n=3 cells. Foci intensity data are shown as box plots, in which boxes represent interquartile ranges (IQRs); whisker represents points in lower and upper quartiles within 1.5 IQR from lower and upper edges of IQR. The data are for n= 539, 446, and 436 ER foci for pre-, post-2 minute, and post-4 minute 1,6-HD timepoints, respectively. P-value calculated with two-tailed z-test. **f.** Meta-analysis of GRO-seq data showing impact of 1,6-HD on TNFα (1hr) activation of p65-bound enhancers in MCF7 cells **g.** Meta-analysis of GRO-seq data showing impact of 1,6-HD on KLA-stimulated (30min) enhancers in RAW264.7 cells.

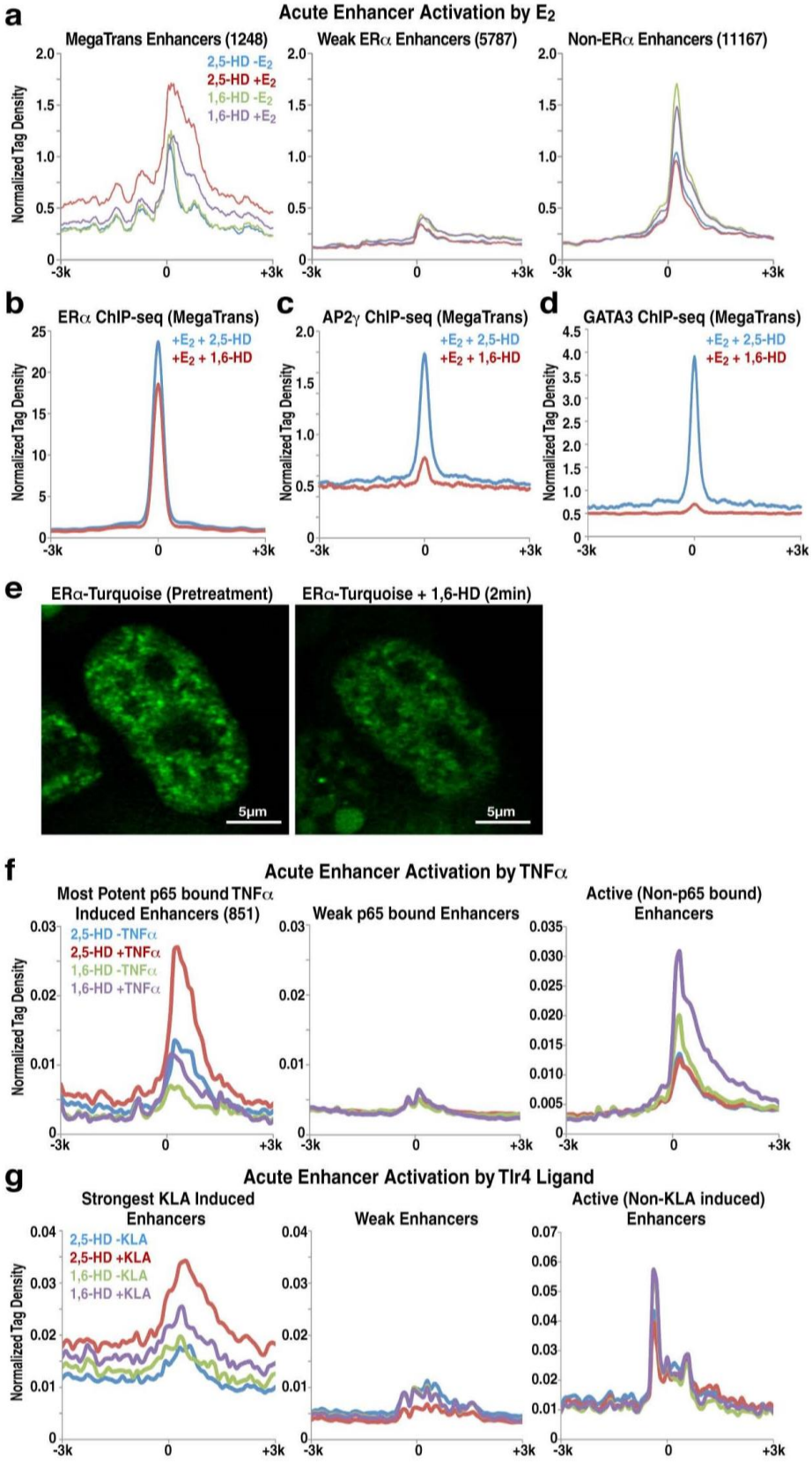
a
Acute Enhancer Activation by E2
MegaTrans Enhancers (1248)
Weak ERα Enhancers (5787)
Non-ERα Enhancers (11167)
2,5-HD -E2
2,5-HD +E2
1,6-HD -E2
1,6-HD +E2
Normalized Tag Density
-3k
0
+3k
b
ERα ChIP-seq (MegaTrans)
c
AP2γ ChIP-seq (MegaTrans)
d
GATA3 ChIP-seq (MegaTrans)
+E2 + 2,5-HD
+E2 + 1,6-HD
e
ERα-Turquoise (Pretreatment)
ERα-Turquoise + 1,6-HD (2min)
5μm
f
Acute Enhancer Activation by TNFα
Most Potent p65 bound TNFα Induced Enhancers (851)
Weak p65 bound Enhancers
Active (Non-p65 bound) Enhancers
2,5-HD -TNFα
2,5-HD +TNFα
1,6-HD -TNFα
1,6-HD +TNFα
g
Acute Enhancer Activation by Tlr4 Ligand
Strongest KLA Induced Enhancers
Weak Enhancers
Active (Non-KLA induced) Enhancers
2,5-HD -KLA
2,5-HD +KLA
1,6-HD -KLA
1,6-HD +KLA

Figure 4.3. Rapid ligand-induced interactions between distant MegaTrans enhancers. a. Schematic diagram of human Chr.21 showing enhancers with the highest levels of ERα binding and transcriptional activation in MCF7 cells following 1 hr E_2 stimulation[25,31]. Active transcription units are listed below. **b.** Representative DNA FISH images showing the E_2 induced proximity of indicated MegaTrans enhancer loci. Arrowhead points to the pair of loci in proximity. The *TFF1* and *DSCAM-AS1* loci are aneuploid in MCF7 cells, hence >2 FISH signals. **c.** Cumulative distribution of distances between indicated MegaTrans enhancers, with and without E_2 stimulation. Data pooled from >200 nuclei from at least two independent experiments. P-values were calculated using the Kolmogorov Smirnov test. **d.** Time course quantifying the fold changes in fractions of *TFF1*/*NRIP1* allele pairs with spatial separation <600 nm. Error bars are theoretical standard deviations and Pvalues were calculated using a bootstrap method (see Online Methods). For each time point, more than 650 distances were pooled from at least two independent experiments. **e.** RNA FISH using *NRIP1* and *TFF1* intronic mRNA probes after 15min of E_2 treatment, showing increased transcription from *NRIP1* allele in proximity to *TFF1* (indicated by arrow) compared to a allele that is spatially distant from *TIFF1* (indicated by arrowhead) **f.** Quantitation of RNA FISH signal intensity in relation to spatial distances between three different pairs of loci: *NRIP1* in relation to *TFF1* and to *DSCAM-AS1*; *DOPEY2* in relation to *TFF1*(A.U. = Arbitrary Unit). Boxes represent interquartile ranges (IQRs); whisker represents points in lower and upper quartiles within 1.5 IQR from lower and upper edges of IQR. For each pair of loci, at least 76 data points were pooled from two independent experiments. P-values were calculated using Wilcoxon Rank Sum test with continuity correction. **g.** Cumulative distribution of distances between *NRIP1* and *TFF1* enhancers in MCF7 cells after 50min E_2 stimulation, treated with 2,5-HD or 1,6-HD. P-value calculated using Kolmogorov Smirnov test. **h.** Cumulative frequency distribution of distances between E_2-induced ERα-Turquoise foci and SC-35-RFP (ICG marker).

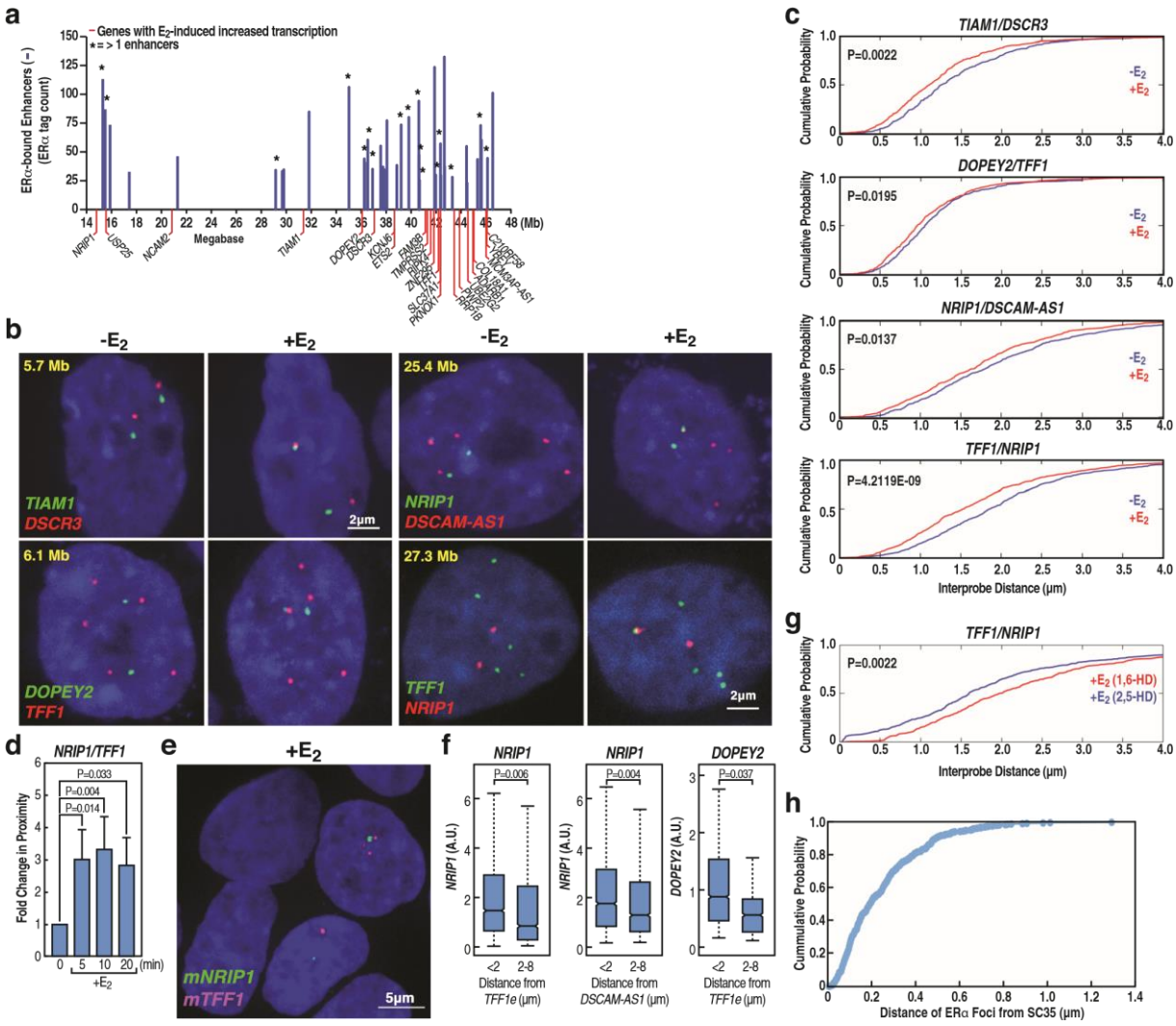
a
Genes with E2-induced increased transcription
* = > 1 enhancers
ERα-bound Enhancers (–)
(ERα tag count)
Megabase
48 (Mb)
NRIP1
USP25
NCAM2
TIAM1
DOPEY2
DSCR3
KCNJ6
ETS2
FAM83F
TMPRSS2
PIGP
ZNF295
PFKL
SLC37A1
PRDM14
RIPK4
IFNAR2
IFNAR1
COL18A1
SLC19A1
RIPK1
C21ORF58
DSCAM-AS1
b
-E2
+E2
-E2
+E2
5.7 Mb
TIAM1
DSCR3
2μm
25.4 Mb
NRIP1
DSCAM-AS1
6.1 Mb
DOPEY2
TFF1
27.3 Mb
TFF1
NRIP1
2μm
c
TIAM1/DSCR3
P=0.0022
DOPEY2/TFF1
P=0.0195
NRIP1/DSCAM-AS1
P=0.0137
TFF1/NRIP1
P=4.2119E-09
Cumulative Probability
-E2
+E2
Interprobe Distance (μm)
d
NRIP1/TFF1
P=0.033
P=0.004
P=0.014
Fold Change in Proximity
0 5 10 20 (min)
+E2
e
+E2
mNRIP1
mTFF1
5μm
f
NRIP1
P=0.006
NRIP1 (A.U.)
<2 2-8
Distance from TFF1e (μm)
NRIP1
P=0.004
NRIP1 (A.U.)
<2 2-8
Distance from DSCAM-AS1 (μm)
DOPEY2
P=0.037
DOPEY2 (A.U.)
<2 2-8
Distance from TFF1e (μm)
g
TFF1/NRIP1
P=0.0022
+E2 (1,6-HD)
+E2 (2,5-HD)
Cumulative Probability
Interprobe Distance (μm)
h
Cummulative Probability
Distance of ERα Foci from SC35 (μm)

Figure 4.4. Role of enhancer RNAs and condensins in E_2 induced chromosomal dynamics and eRNP assembly. a. ChIP data showing effect of *TFF1e* eRNA knockdown on recruitment of ERα, GATA3, RARα and AP2γ to the *TFF1e* enhancer following E_2 treatment. CTL-ASO indicates nontargeting oligo used as control. Data shown as individual values (circles), mean and s.d. (lines). Pvalues calculated with unpaired Student's t-test. Data are representative of 3 independent experiments. **b.** Fold changes in fractions of *NRIP1/TFF1* allele pairs with separation below the cutoff distance, showing that *TFF1e* eRNA knockdown abolishes E_2 induced proximity between *TFF1* and *NRIP1* enhancer loci. Error bars show theoretical sample standard deviations and p-values were calculated using a bootstrap method (see Online Methods). CTL-ASO indicates non-targeting oligo used as control. **c, d.** FRAP kinetics showing effect of *TFF1* eRNA (0.20 mg/ml) on GATA3-MBP (c) or ERα-MBP (d) fusion protein droplets *in vitro*. Data points shown as circles, lines represent fitting to an exponential model to estimate the half-time or recovery **e.** ChIP data showing effect of knocking down *TFF1* eRNA or NRIP1e eRNA on recruitment of condensin II subunit NCAPH2 (top) or condensin I subunit NCAPG (bottom) to the *TFF1e* and *NRIP1e* loci. CTL-ASO indicates non-targeting oligo used as control. Data shown are individual values (circles), mean and s.d. (lines). P-value calculated with unpaired Student's t-test. Data are representative of 3 independent experiments. **f.** Fractions of *NRIP1/TFF1* allele pairs with separation below the cut off distance in cells with knockdown of the indicated proteins. Error bars indicate theoretical sample standard deviations and P-values were calculated using a bootstrap method (see Online Methods). For each time point, more than 290 distances were pooled from at least two independent experiments. **g.** GRO-seq analyses showing effects of knockdown of *NCAPG* (Condensin I) or *NCAPD3* (Condensin II) on E_2-activated enhancer transcription. siCTL represent scrambled oligos used as control; results are grouped for MegaTrans, weak ERα enhancers and non- ERα-bound enhancers.

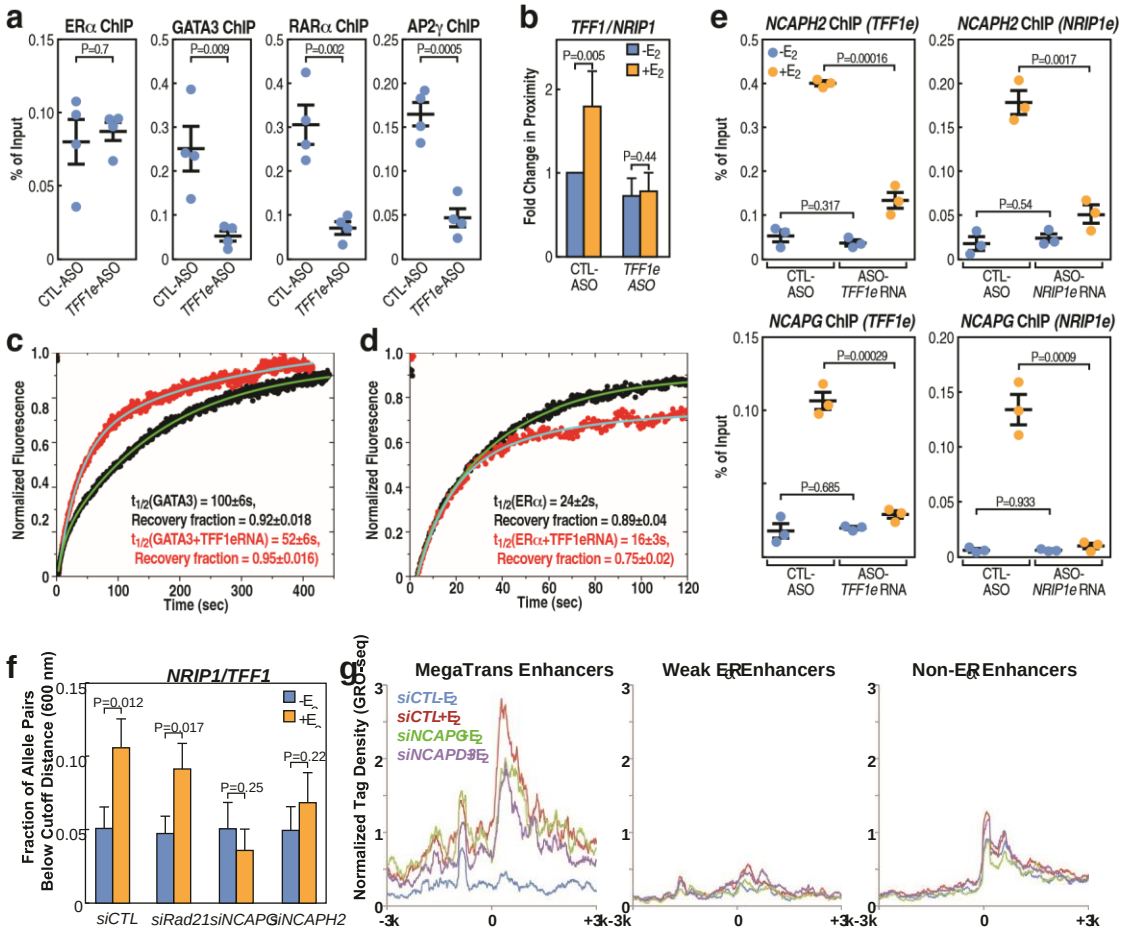
a
ERα ChIP
GATA3 ChIP
RARα ChIP
AP2γ ChIP
% of Input
P=0.7
P=0.009
P=0.002
P=0.0005
CTL-ASO
TFF1e-ASO
b
TFF1/NRIP1
Fold Change in Proximity
P=0.005
P=0.44
-E2
+E2
CTL-ASO
TFF1e ASO
c
Normalized Fluorescence
t1/2(GATA3) = 100±6s,
Recovery fraction = 0.92±0.018
t1/2(GATA3+TFF1eRNA) = 52±6s,
Recovery fraction = 0.95±0.016)
Time (sec)
d
Normalized Fluorescence
t1/2(ERα) = 24±2s,
Recovery fraction = 0.89±0.04
t1/2(ERα+TFF1eRNA) = 16±3s,
Recovery fraction = 0.75±0.02)
Time (sec)
e
NCAPH2 ChIP (TFF1e)
NCAPH2 ChIP (NRIP1e)
% of Input
P=0.00016
P=0.317
P=0.0017
P=0.54
CTL-ASO
ASO-TFF1e RNA
ASO-NRIP1e RNA
NCAPG ChIP (TFF1e)
NCAPG ChIP (NRIP1e)
P=0.00029
P=0.685
P=0.0009
P=0.933
f
NRIP1/TFF1
Fraction of Allele Pairs Below Cutoff Distance (600 nm)
P=0.012
P=0.017
P=0.25
P=0.22
siCTL
siRad21
siNCAPG
siNCAPH2
g
MegaTrans Enhancers
Weak ERα Enhancers
Non-ERα Enhancers
Normalized Tag Density (GRO-seq)
siCTL-E2
siCTL+E2
siNCAPG+E2
siNCAPD3+E2
-3k
0
+3k

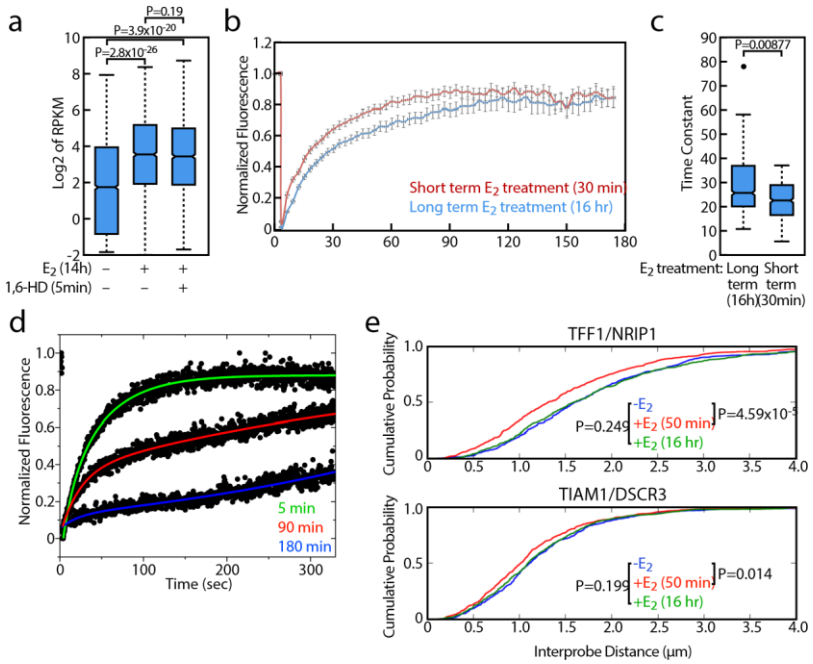

Figure 4.5. Chronic stimulation with E_2 causes a fluid to hydrogel-like transition at enhancers and prevents ligand-induced enhancer proximity. a. Box plots of GRO-seq analysis MCF7 cells not stimulated with E_2 and not treated with 1,6-Hexanediol (1,6-HD) or E_2 stimulation for 14 hrs with or without treatment with 1,6-HD for 5min. Central line shows median; boxes represent the 25th and 75th percentiles; whiskers extend 1.5× the interquartile range from the 25th and 75th percentiles. P-values denote statistical differences between treatment conditions. **b.** Fluorescent recovery of ERα-mTurquoise foci in MCF7 cells after short term (30 min) or long term (16 hrs) E_2 treatment. Each point represents the mean intensity and photobleaching-normalized fluorescence relative to pre-bleaching signal. Error bars represent S.E.M. of n = at least 10 cells per time point. **c.** Box plots showing time constants of FRAP recovery of ERα-mTurquoise foci in MCF7 cells treated with E_2 for long term (n=28) and short term (n=26). Boxes represent interquartile ranges (IQRs); whisker represents points in lower and upper quartiles within 1.5 IQR from lower and upper edges of IQR. P-value calculated with two-tailed z-test. **d.** FRAP analysis of i*n vitro* droplets formed by a ternary mixture of GATA3-MBP (7μM), ERα-MBP (7μM) and TFF1 eRNA (0.20 mg/ml), incubated for 5, 90 or 180 minutes. Data show a less rapid fluorescence recovery with increasing time of incubation. Data points are represented by dots, lines represent fitting to an exponential model **e.** Cumulative distribution of distances between indicated MegaTrans enhancer pairs after short term (50min) and long term (16 hrs) E_2 treatment, demonstrating that the E_2-induced spatial proximity is lost upon prolonged treatment. Data pooled from >150 nuclei examined in two independent experiments. P-values were calculated using the Kolmogorov Smirnov test.

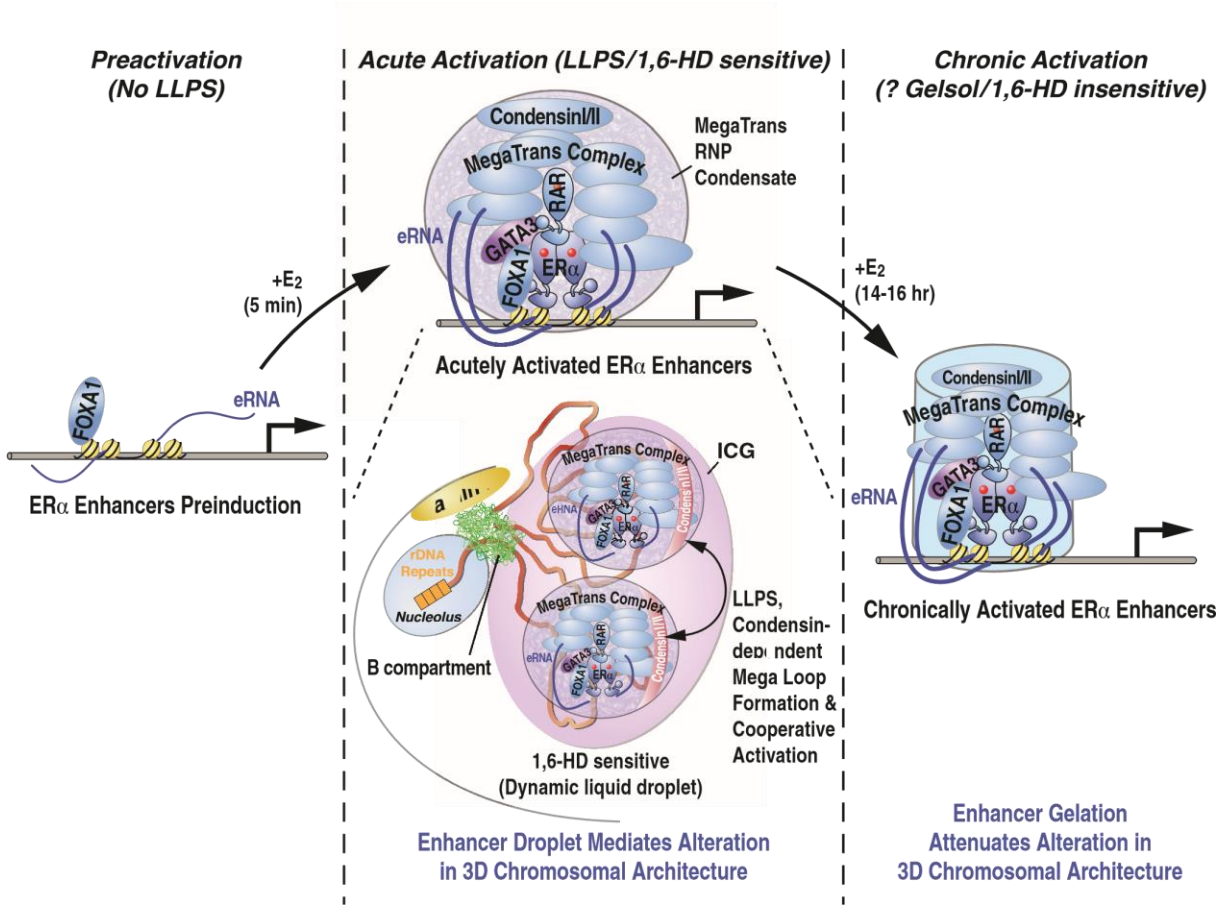

Figure 4.6. Model summary: MegaTrans enhancers are minimally active under unstimulated conditions. E_2 stimulation result in ERα dependent recruitment of MegaTrans complex, Condensin complex and eRNA transcription, causing "megaloops" of these enhancers. This results in an eRNAdependent RNP (eRNP) assembled by phase separation. Chronic stimulation alter the physicochemical properties of this complex to a "gelsol state" thus making them less sensitive to 1,6HD. Maximal enhancer activation occurs with colocalization of the enhancer on the ICG, apparently resulting in concentration of transcriptional machinery and increased transcriptional robustness of component enhancers. Association with other nuclear structures such as nucleolus and lamin-B represent a speculative model based on A/B compartments and rDNA locus in human Chr.21.

4.6 Methods

Antibodies, cell culture, molecular biology procedures, sequencing based assays. Antibodies, cell culture, molecular biology procedures (QRT-PCR, ChIP-seq and analyses; in vitro transcription; run-on sequencing; vector constructs), bioinformatics of enhancer characterization, generation of cell lines, protein purification, proximity calculation using microscopy data, In-situ HiC, Hi-C data analysis, 4C-seq and ATAC-seq are described in detail in Supplementary Note. Oligos, BAC and Fosmid clones are listed in Supplementary Table 4 and 5.

Treatment of cultured cells. Cells were cultured as described in supplementary note. For hexanediol treatment, cells were treated with 7.5- 8.5% 1,6-Hexanediol (1,6-HD) (Sigma, Cat#240117), 2,5-Hexanediol (2,5-HD) (Sigma, Cat # H11904) or 1,4-Butanediol (1,4-HD)(Sigma, Cat#493732) in phenol-red free DMEM with 5% charcoal stripped FBS (White medium) for 5 minutes. The chemical was washed away with white medium and was incubated with estrogen (100nM) or vehicle, for another 30 minutes at 37^0C before fixing with formaldehyde (for FISH), collecting RNA or nucleus for GRO-seq. In E_2 pretreatment experiments MCF7 cells were stimulated with E_2 for indicated time periods followed by treatment with 2,5-HD or 1,6-HD for 5 min. before collecting nucleus for GRO-seq. For TNFα stimulation, MCF7 cells were grown as described for E_2 stimulation and were treated with 8% 1,6-HD or 2,5Hexanediol for 5 min followed by stimulation by 100nM TNFα for 30 min before collecting nucleus for GROseq. For KLA treatment RAW264.7 cells were grown in DMEM media with 10% FBS. Cells were grown in medium with 0.5% serum

overnight before KLA stimulation. Cells were treated with 8.5% 1,6-HD for 5 min before stimulation with 100nM KLA for 30min.

Biotinylated Isoxazole-mediated precipitation. This assay was performed as described previously[33] with following modifications. MCF7 cells cultured in Phenol Red free media with charcoal stripped serum was stimulated with E_2 (100nM) for 50 min. ~15 million cells were scraped off with cell lifter and washed with ice cold PBS. Cell pellets were resuspended in 1ml lysis buffer (20mM Tris-HCl (pH.7.4), 300mM NaCl, 5mM MgCl2, 1% NP40, 10%Glycerol, 20mM β-mercaptoethanol, 1x Halt Protease/Phosphatase inhibitor cocktail (ThermoFisher, Cat#78440), 2mM Ribonucleoside vanadyl complexes (Sigma, Cat#R3380), 0.1mM phenylmethylsulfonylfluride (PMSF), 1:20 SuperaseIn (ThermoFisher, Cat#AM2696). Sonicated briefly on Bioruptor Pico (30sec on, 30 sec off, 5 cycles) and incubated with rotation at 4^0C for 30 min. Protein supernatant was collected by centrifugation at 4^0C, 16500 g for 15min. 5% lysates were saved for whole cell extract control and remaining were aliquoted equally and incubated with various concentrations (10, 30 and 100 µM) biotinylated isoxazole (Sigma, Cat#900572) at 4^0C for 1hr with rotation. Precipitates were isolated by centrifugation at 16500g for 15 minutes at 4^0C. Supernatant was saved and pellets were washed with lysis buffer with protease and RNAse inhibitor. Protein was denatured by heating at 98^0C for 5 minutes with Laemmli buffer with 0.1M dithiothreitol (DTT). Western blotting was performed by standard protocol.

Protein sequence analysis. Protein sequence from Uniprot database was analyzed using Predictor of Natural Disordered Region (PONDR), online analysis software. (Version:VL3).

In Vitro fluorescence labeling of proteins. The ERα-MBP and GATA3-MBP were fluorescently labeled with either Alexa488 or Alexa594 dyes (C5-maleimide derivative, Molecular Probes) using Cys-maleimide chemistry as described previously[35]. Both ERα (C381, C417, C447, C530) and GATA3 (C85, C183, C249, C375) contain four free cysteins, respectively, that were targeted for fluorescence labeling. The proteins containing MBP fusion tag, which lacks cysteine, and the dye mixtures (1:4) were incubated in 25 mM Tris buffer, 50 mM NaCl, pH 7.5 at 4 ^{o}C for ~12 hrs. The unreacted dye was removed using a 30 KDa MWCO spin filter. The labeling efficiency for all samples were observed to be ≥ 50% (UV-Vis absorption measurements), and no additional attempt was made to purify them further, given that only labeled protein is observed in the fluorescence microscopy experiments. For control experiments with MBP-alone sample, we used the same fluorescently tagged proteins for fluorescence microscopy experiments. Simultaneously, we performed bright-field microscopy to check droplet formation. Our results revealed that MBP-alone sample does not phase separated under similar experimental condition, which is consistent with a recent report[17].

Sample preparation for phase separation measurements. All of the protein samples were buffer exchanged in phase separation buffer (PS buffer: 25 mM Tris.HCl, pH 7.5 containing 200 mM NaCl) unless otherwise noted. Concentration measurements were performed using a NanoDrop oneC UV-Vis spectrophotometer

at room temperature. Variable amount of salt (NaCl) and PEG8000 were added from concentrated stocks as desired. For the microscopy experiments with using the MBP fusion proteins, the PS buffer containing either 5% or 8.75% PEG was used.

Confocal fluorescence microscopy. The fluorescence and DIC imaging were performed using a Zeiss LSM 710 laser scanning confocal microscope, equipped with a 63x oil immersion objective (Plan-Apochromat 63x/1.4 oil DIC M27) and a Zeiss Primovert inverted microscope. Samples were prepared and imaged using tween-coated (20% v/v) Nunc Lab-Tek Chambered Coverglass (ThermoFisher Scientific Inc) at room temperature (22±1^{o}C) unless otherwise noted, with ~ 1% labeled protein samples within the mixture of unlabeled materials. For salt induced phase separation of ERα and GATA3, appropriate amount of NaCl was either premixed in the buffer or injected into a 20 µl sample in the bulk phase while imaging was performed at the coverslip. Control experiments were also performed with injection of just buffer solutions without salt of identical volume, which produced no effect. All the samples were allowed to equilibrate in the chambered coverglass for 15-30 minutes before imaging. For Alexa488-labeled samples, the excitation and emission wavelengths were 488 nm/503-549 nm, and for Alexa594labeled samples, the excitation and emission wavelengths were 595 nm/602-632 nm. Fluorescence recovery after photobleaching (FRAP) experiments were performed using the same confocal set up. The bleaching ROI was ~ 1.0 µm^2 unless otherwise noted. The samples were bleached using either 5 or 10 iterative pulses of total time ~3.0-6.5 s utilizing 100% laser power. Analyses were performed using average fluorescence intensities from three regions of interrogation (ROI) corresponding to photobleaching,

reference, and background. The fluorescence signal of the protein droplet undergoing active photobleaching was corrected using the reference droplet signal to account for passive photobleaching during imaging. The fluorescence data were normalized and fitted with a two-exponential model[66]. Halftime of recovery was then obtained graphically. The images and data were analyzed using Fiji software[67] and the FRAP curves were plotted and analyzed using origin software (OriginPro 2016).

ERα foci formation assay. MCF7 cells were plated at 75% confluency 1 day prior to transfection. 0.75ug of pmCherry-ESR1 (ERα) plasmid was transfected using Lipofectamine 2000 (Thermo Fisher) per 24-well, and the cells were incubated in the transfection mixture for 6 hours. The cells were then washed and cultured in phenol-red free DMEM white medium (Life Technologies) supplemented with 5% charcoal stripped FBS. Transfected cells were re-plated into glass-bottom 96-wells (MatTek) the following day and cultured in DMEM white medium with 5% charcoal stripped FBS for another 24 hours prior to imaging. Zeiss LSM 880 Airyscan was equipped with a CO2 regulated incubation chamber (Incubator XL S1) where the ambient temperature was held at 37^0C. mCherry was excited using laser line DPSS at 561nm and images were acquired in FAST Airyscan mode. Z-stack of fluorescent MCF7 cells transfected with pmCherry-ESR1 were first imaged for 15 minutes at 5-minute intervals to acquire baseline readout of ERα expression. The cells were then immediately treated with 100nM 17β-estradiol (E_2) for estrogen stimulation and imaged consecutively for 1 hour at 5-minute intervals. Images acquired were compiled, processed, and edited with ZEN software (Zeiss). Intensity thresholds were set manually and uniformly to display nuclear signal and minimize background noise.

FRAP assay and analysis in live cells. MCF7 were transfected with pmTurqoise2-ESR1 and prepared for microscopy in identical conditions to those of the ERα Foci Formation Assay, with pmTurqoise2-ESR1 being used in place of pmCherry-ESR1. Prior to performing FRAP, cells were either untreated, pretreated with 16 hours of 100nM E_2, or were treated with 100nM E_2 immediately prior to FRAP. FRAP data for each condition was acquired over the course of approximately 1 hour, with the results being combined for each condition as no trend was observed between FRAP data acquired at the beginning versus the end of the hour. FRAP was performed on the Zeiss LSM 880 Airyscan, under the same incubation conditions as before. Bleaching of the pmTurqoise2-ESR1 signal was performed using the 405nm laser at maximum strength, with 2 identical size regions selected for bleaching per cell. Fluorescence signal was acquired through excitation using laser line Argon at 458nm, and mTurqoise2-ESR1 intensity was acquired in ZEN Black at the bleached regions, a control non-bleached region of the nucleus, a control region outside of the cells, and over the entirety of each cell. 2 baseline images were taken 3 seconds apart, which was followed by approximately 0.4 seconds of bleaching, and afterwards an image was taken immediately and then every 3 seconds until either a total of 60 images were acquired or the cell shifted planes dramatically.

Analysis of in vivo FRAP data. Analysis was performed by first normalizing the intensity of each bleached spot's average intensity at each time point to the maximum intensity of that spot at any point in the time series. This point of maximum intensity was one of the baseline points, and each time point was converted to a proportion of the original intensity. The total intensity of each cell at each time point

was normalized as a proportion of the maximum intensity of the total cell at any time point, thereby providing a value for the proportion of photobleaching of the total cell at each time point. The maximum intensity normalized value of each bleached region at each time point was then divided by the total cell photobleaching proportion at its respective cell and time point. These maximum-intensity and photo-bleaching normalized values were then either plotted or used to generate time constants. Mean graphs with error bars for these normalized values were generated by calculating mean and standard error over all overlapping time-points for all traces for each condition. Exponential rise curve plots contain each time-point from all traces combined for each condition, time 0 was set as the time-point acquired immediately after photo-bleaching, and the average intensity value of this new time-point 0 was subtracted from all intensity values for this condition to set the intensity offset to zero. These pooled points were fitted to an exponential rise curve with the formula $FRAP(t) = A(1-e^{-t/\tau})$, where FRAP(t) = fluorescent intensity at time t after photobleaching, A = amplitude, τ = time constant, and t = the time after photo-bleaching. The time constant and amplitude were optimized to fit the curve by subtracting the formula values from the actual values of each point, squaring this error value, summing the error of all the points for each condition, and optimizing for amplitude and the time constant using the Solver add-in in Microsoft Excel. Box plots comparing between FRAP time constants of short versus long-term 100nM E_2 treatment of ER-mTurqoise2 MCF7 cells were generated by calculating time constants for each individual trace. These calculations were performed as in the above plot, except traces were not pooled for each condition, and the intensity offset value subtracted

from each intensity value for each trace was the intensity value of each trace immediately after photo-bleaching. A p-value comparing between the short and long-term FRAP constants was generated by performing a 2-tailed z-test between the two samples for means. The apparent diffusion coefficient was calculated by the formula $D_{app} = r^2_{bleach}/\tau$, where D_{app} is the apparent diffusion coefficient, r^2_{bleach} is the radius of the bleached region in each FRAP experiment, and τ is the time constant calculated in the previous experiment. The radius of each bleached region for every FRAP experiment was set uniformly to 0.964 um.

SC35 co-localization calculation. MCF7 were co-transfected as before in the ERα foci formation assay, except 0.375µg pDsRed2SC35 and 0.375µg pmTurquoise2-ESR1 were used in place of 0.75µg pmCherry-ESR1. These transfected cells were prepared for and imaged under similar conditions as the ERα foci formation assay, with the 561 laser line being used for imaging pDsRed2-SC35 and 461 laser being used to visualize pmTurquoise2-ESR1. Imaging was begun on stripped, live, MCF7 cells, and was continued on the same live cells 30 after addition of 100nM E_2. After imaging, the FAST Airyscan images were again processed in the ZEN Black software package, but quantification of overlap was done by exporting the processed .czi from ZEN Black into Volocity software (Perkin Elmer, v6.0.1). In Volocity, these image stacks were cropped to each cells, and objects were identified using the identical “Automatic” setting for each cropped image in both the red (SC35) and green (ERα) channel. A representative single slice of a representative cell prior to and 30 minutes after 100nM E_2 treatment was presented, as extended focus of all z-slices would fail to show the distinct patterning present on each slice. Distances

between the centroid of each ERα foci object and the nearest SC35 object edge was calculated, as well as whether the ERα foci object had any overlap with any SC35 object. These “nearest distance” measurements for all ERα foci in all cells were then pooled together and plotted as the proportion of all ERα foci objects at or below the listed distance. The overlap measurements were similarly pooled for all ERα foci in all cells.

1,6-hexanediol (1,6-HD) treatments with ERα foci. MCF7 were transfected with pmTurqoise2-ESR1 and prepared for microscopy in identical conditions to those of the ERα foci formation Assay. MCF7 were pretreated with 100nM E_2 for 16 hrs prior to imaging. Cells were then imaged prior to 1,6-HD treatment to establish a baseline. 1,6HD was then added to cells at a final concentration of 5% in normal media, and images were again taken after 2 minutes of continuous treatment. A single representative and consistent slice of these image stacks were presented, as extended focus of all z-slices would fail to show the distinct ERα foci patterning on each slice.

DNA FISH. MCF7 cells were fixed with freshly made 4% paraformaldehyde in PBS for 8 min. Excess formaldehyde was quenched with 0.1M Tris-HCl (pH 7.4) for 5 min. Coverslips were washed with PBS and stored at 4^0C until used. Prior to hybridization coverslips were incubated in 0.1N HCl for 5min at room temperature. Washed twice with PBS. Coverslips were incubated in PBS containing 100µg/ml RNAse A for 1 hr. at 37^0C, followed by equilibration in 50% formamide/2XSSC for 1hr. 125ng of probe in equal volume mixture of formamide and 2X hybridization buffer mix (4XSSC/40%Dextran Sulphate) was used per coverslip. Coverslips on

glass slides were heated for 6 min on a hotplate with temperature set at 80^0C followed by overnight hybridization at 37^0C in a humidified dark chamber. The coverslips were then washed twice with pre-warmed buffer containing 50% formamide/2XSSC and twice with 2XSSC before being finally mounted with Vectashield antifade mounting medium with DAPI (Vector Laboratories). For ImmunoDNAFISH, cells were incubated first with PBS containing 0.5% Triton-X-100 and 5%BSA for 15 min at room temperature. Primary antibodies were used at a dilution of 1:50 in blocking buffer (0.1% Triton100/5% BSA in PBS) for 1 hr. at 37^0C. Washed 3 times in PBST (PBS containing 0.1% Triton X100). Incubated with appropriated fluorescent conjugated secondary antibody (1:1000) dilution for 30 min at room temperature. Cells were fixed for a second time with freshly prepared 2% paraformaldehyde for 10 min at room temperature followed by treatment with 0.1M Tris-HCl (pH 7.4) for 5 minutes. Washed twice in PBS and DNA FISH protocol described above was resumed FISH. All the probes used for DNA FISH experiment is provided in Supplementary Table 5.

RNA FISH. Cells containing coverslips were fixed in 4% freshly prepared paraformaldehyde. Washed twice with PBS with freshly added 2mM Ribonucleoside vanadyl complexes (Sigma-Aldrich, St. Louis, MO, USA). Cells were permeabilized and stored in 70% ethanol at 4^0C. Prior to probe hybridization coverslips were incubated with wash buffer (10% formamide/2XSSC) for 30 minutes at room temperature. RNA FISH probes were resuspended in hybridization buffer (10% formamide and 10% Dextran sulphate in 2XSSC). Coverslips were incubated with probes overnight at 37^0C in a humidification chamber. Post incubation washes were

done using pre-warmed wash buffer twice at 37^0C. Immuno RNA FISH were performed using the protocol described above with addition of primary antibody mixed along with the RNA FISH probes and incubated overnight. Probes and primary antibody was washed off using wash buffer at 37^0C followed by fluorescent conjugated secondary antibody incubation. Nuclei were counterstained by incubating in wash buffer containing Hoechst 33342 at a concentration of 1 g/ml for 15 min.

DNA and RNA FISH Probes. All the BAC based probes for DNA FISH were purchased in the fluorescent labeled from Empire Genomics (Buffalo, NY, USA). Fosmids were obtained from CHORI (Oakland, CA, USA). Fosmid based hybridization probes for DNA FISH were generated from 1 µg fosmid using Nick Translation kit (Abbot Molecular), Green 496, Orange 552 or Red 650 conjugate dUTP following manufacture recommended protocol. 125ng of each labeled probes, 4µg human Cot1 DNA (Thermo Fisher Scientific) and 10µg salmon testis DNA (Sigma-Aldrich) were used per coverslip. They were coprecipitated in ethanol and were resupsended in equal volume mixture of formamide and 2X hybridization buffer mix (4XSSC/40%Dextran Sulphate) prior to hybridization reaction. BAC and Fosmid clone ID used in this study are in Supplementary Table 5.

RNA FISH probes were designed using Stellaris Probe Designer tool (Biosearch Technologies). Repeat masked intronic sequences of TFF1, NRIP1 and DOPEY2 were used as template for probe design. The entire mRNA sequence of was used for generation of exonic probes. Probes were labeled with FAM, Quasar 570 or Quasar 670 dyes.

Microscopy for DNA and RNA FISH. Images were acquired using a Perkin Elmer Spinning Disk Confocal Microscope (100x Nikon Plane Apochromatic oil immersion objective, numerical aperture: 1.40). The microscope was equipped with a Piezo-Z drive and EMCCD Hamamatsu 14-bit 1Kx1K camera. Z-stack data was acquired at a step size of 150 nm.

Image analysis. 3D image stacks were initially analyzed using Volocity software (Perkin Elmer, v6.0.1). The functions “Find Object” and “Exclude Objects by Size” were combined for automatic detection of the FISH probe signals. For accurate and automated calculation of spatial distances between the probed loci, the 3D coordinates and raw intensity sums (without background subtraction) of FISH probe signals were exported to CSV files using the Volocity software and were analyzed using custom software implemented with Python, NumPy, and SciPy. To estimate the 3D distance distribution between any two genomic loci, the centroids of the FISH signals from those loci were used to calculate a number (see below) of shortest distances for each nucleus, and those distances were then pooled from all examined nuclei. This procedure assumed that each of the shortest distances obtained from each nucleus corresponded to loci located on the same chromosome. For experiments probing one diploid and one aneuploid locus, up to two shortest distances were obtained per nucleus. For experiments probing two aneuploid loci, the maximum number of shortest distances obtained per nucleus was equal to the smallest known copy number between the two loci in MCF-7 cells. The median distances between control and test conditions were compared using the Wilcoxon Rank Sum test with continuity correction. The empirical cumulative distributions of

distances were compared using the Kolmogorov-Smirnov test. To assess how the RNA-FISH signal from a given locus varies with 3D distance between that locus and a second locus, the raw intensity sums measured by Volocity software at the first locus were separated into two groups corresponding to distances ranging from 0 to 2 μm and from 2 μm to 8 μm. The median distances of the two groups were then compared using the Wilcoxon Rank Sum test with continuity correction. For calculation of median distances between RNA FISH foci and ERα cluster or ICG (SON antibody signal), distances calculated by Volocity, between edges of the closest of each signal, were used. Custom software used for this study is available upon request.

4.7 Acknowledgements

Chapter 4, in full, has been published in *Nature Structural and Molecular Biology*, 2019. “Phase separation of ligand-activated enhancers licenses cooperative chromosomal enhancer assembly.” Sree Nair, Lu Yang, Dario Meluzzi, Soohwan Oh, Feng Yang, Meyer Friedman, Susan Wang, Thomas Suter, Ibraheem Alshareedah, Amir Gamliel, Qi Ma, Jie Zhang, Yiren Hu, Yuliang Tan, Kenneth Ohgi, Ranveer Singh Jayani, Priya Banerjee, Aneel Aggarwal, and Michael Rosenfeld. The dissertation author is a coauthor of this paper.

4.9 References

48. Bulger, M. & Groudine, M. Functional and mechanistic diversity of distal transcription enhancers. *Cell* **144**, 327-339, doi:10.1016/j.cell.2011.01.024S0092-8674(11)00063-8 [pii] (2011).

49. Long, H. K., Prescott, S. L. & Wysocka, J. Ever-Changing Landscapes: Transcriptional Enhancers in Development and Evolution. *Cell* **167**, 1170-1187, doi:10.1016/j.cell.2016.09.018 (2016).

50. Lovén, J., Hoke, H. A., Lin, C. Y., Lau, A., Orlando, D. A., Vakoc, C. R., Bradner, J. E., Lee, T. I., & Young, R. A. (2013). Selective inhibition of tumor oncogenes by disruption of super-enhancers. Cell, 153(2), 320–334. https://doi.org/10.1016/j.cell.2013.03.036

51. Whyte, W. A., Orlando, D. A., Hnisz, D., Abraham, B. J., Lin, C. Y., Kagey, M. H., Rahl, P. B., Lee, T. I., & Young, R. A. (2013). Master transcription factors and mediator establish super-enhancers at key cell identity genes. Cell, 153(2), 307–319. https://doi.org/10.1016/j.cell.2013.03.035

52. Parker, S. C. J., Stitzel, M. L., Taylor, D. L., Orozco, J. M., Erdos, M. R., Akiyama, J. A., van Bueren, K. L., Chines, P. S., Narisu, N., NISC Comparative Sequencing Program, Black, B. L., Visel, A., Pennacchio, L. A., Collins, F. S., National Institutes of Health Intramural Sequencing Center Comparative Sequencing Program Authors, NISC Comparative Sequencing Program Authors., Becker, J., Benjamin, B., Blakesley, R., … Young, A. (2013). Chromatin stretch enhancer states drive cell-specific gene regulation and harbor human disease risk variants. Proceedings of the National Academy of Sciences, 110(44), 17921–17926. https://doi.org/10.1073/pnas.1317023110

53. Ji, X., Dadon, D. B., Powell, B. E., Fan, Z. P., Borges-Rivera, D., Shachar, S., Weintraub, A. S., Hnisz, D., Pegoraro, G., Lee, T. I., Misteli, T., Jaenisch, R., & Young, R. A. (2016). 3d chromosome regulatory landscape of human pluripotent cells. Cell Stem Cell, 18(2), 262–275. https://doi.org/10.1016/j.stem.2015.11.007

54. Kieffer-Kwon, K.-R., Tang, Z., Mathe, E., Qian, J., Sung, M.-H., Li, G., Resch, W., Baek, S., Pruett, N., Grøntved, L., Vian, L., Nelson, S., Zare, H., Hakim, O., Reyon, D., Yamane, A., Nakahashi, H., Kovalchuk, A. L., Zou, J., … Casellas, R. (2013). Interactome maps of mouse gene regulatory domains reveal basic principles of transcriptional regulation. Cell, 155(7), 1507–1520. https://doi.org/10.1016/j.cell.2013.11.039

55. Shin, H. Y., Willi, M., Yoo, K. H., Zeng, X., Wang, C., Metser, G., & Hennighausen, L. (2016). Hierarchy within the mammary STAT5-driven Wap super-enhancer. Nature Genetics, 48(8), 904–911. https://doi.org/10.1038/ng.3606

56. Hnisz, D., Shrinivas, K., Young, R. A., Chakraborty, A. K. & Sharp, P. A. A Phase Separation Model for Transcriptional Control. *Cell* **169**, 13-23, doi:10.1016/j.cell.2017.02.007 (2017).

57. Harlen, K. M. & Churchman, L. S. The code and beyond: transcription regulation by the RNA polymerase II carboxy-terminal domain. *Nat Rev Mol Cell Biol* **18**, 263-273, doi:10.1038/nrm.2017.10 (2017).

58. Alberti, S. Phase separation in biology. *Curr Biol* **27**, R1097-R1102, doi:10.1016/j.cub.2017.08.069 (2017).

59. Banani, S. F., Lee, H. O., Hyman, A. A. & Rosen, M. K. Biomolecular condensates: organizers of cellular biochemistry. *Nat Rev Mol Cell Biol*, doi:10.1038/nrm.2017.7 (2017).

60. Shin, Y. & Brangwynne, C. P. Liquid phase condensation in cell physiology and disease. *Science* **357**, doi:10.1126/science.aaf4382 (2017).

61. Cho, W.-K., Spille, J.-H., Hecht, M., Lee, C., Li, C., Grube, V., & Cisse, I. I. (2018). Mediator and RNA polymerase II clusters associate in transcription-dependent condensates. Science, 361(6400), 412–415. https://doi.org/10.1126/science.aar4199

62. Sabari, B. R., Dall'Agnese, A., Boija, A., Klein, I. A., Coffey, E. L., Shrinivas, K., Abraham, B. J., Hannett, N. M., Zamudio, A. V., Manteiga, J. C., Li, C. H., Guo, Y. E., Day, D. S., Schuijers, J., Vasile, E., Malik, S., Hnisz, D., Lee, T. I., Cisse, I. I., … Young, R. A. (2018). Coactivator condensation at super-enhancers links phase separation and gene control. Science, 361(6400), eaar3958. https://doi.org/10.1126/science.aar3958

63. Boija, A., Klein, I. A., Sabari, B. R., Dall'Agnese, A., Coffey, E. L., Zamudio, A. V., Li, C. H., Shrinivas, K., Manteiga, J. C., Hannett, N. M., Abraham, B. J., Afeyan, L. K., Guo, Y. E., Rimel, J. K., Fant, C. B., Schuijers, J., Lee, T. I., Taatjes, D. J., & Young, R. A. (2018). Transcription factors activate genes through the phase-separation capacity of their activation domains. Cell, 175(7), 1842-1855.e16. https://doi.org/10.1016/j.cell.2018.10.042

64. Boehning, M., Dugast-Darzacq, C., Rankovic, M., Hansen, A. S., Yu, T., Marie-Nelly, H., McSwiggen, D. T., Kokic, G., Dailey, G. M., Cramer, P., Darzacq, X., & Zweckstetter, M. (2018). RNA polymerase II clustering through carboxy-terminal domain phase separation. Nature Structural & Molecular Biology, 25(9), 833–840. https://doi.org/10.1038/s41594-018-0112-y

65. Chong, S., Dugast-Darzacq, C., Liu, Z., Dong, P., Dailey, G. M., Cattoglio, C., Heckert, A., Banala, S., Lavis, L., Darzacq, X., & Tjian, R. (2018). Imaging dynamic and selective low-complexity domain interactions that control gene

transcription. Science, 361(6400), eaar2555. https://doi.org/10.1126/science.aar2555

66. Kwon, I., Kato, M., Xiang, S., Wu, L., Theodoropoulos, P., Mirzaei, H., Han, T., Xie, S., Corden, J. L., & McKnight, S. L. (2013). Phosphorylation-regulated binding of rna polymerase ii to fibrous polymers of low-complexity domains. Cell, 155(5), 1049–1060. https://doi.org/10.1016/j.cell.2013.10.033

67. Lu, H., Yu, D., Hansen, A. S., Ganguly, S., Liu, R., Heckert, A., Darzacq, X., & Zhou, Q. (2018). Phase-separation mechanism for C-terminal hyperphosphorylation of RNA polymerase II. Nature, 558(7709), 318–323. https://doi.org/10.1038/s41586-018-0174-3

68. Boulay, G., Sandoval, G. J., Riggi, N., Iyer, S., Buisson, R., Naigles, B., Awad, M. E., Rengarajan, S., Volorio, A., McBride, M. J., Broye, L. C., Zou, L., Stamenkovic, I., Kadoch, C., & Rivera, M. N. (2017). Cancer-specific retargeting of baf complexes by a prion-like domain. Cell, 171(1), 163-178.e19. https://doi.org/10.1016/j.cell.2017.07.036

69. Carroll, J. S., Liu, X. S., Brodsky, A. S., Li, W., Meyer, C. A., Szary, A. J., Eeckhoute, J., Shao, W., Hestermann, E. V., Geistlinger, T. R., Fox, E. A., Silver, P. A., & Brown, M. (2005). Chromosome-wide mapping of estrogen receptor binding reveals long-range regulation requiring the forkhead protein foxa1. Cell, 122(1), 33–43. https://doi.org/10.1016/j.cell.2005.05.008

70. Li, W., Notani, D., Ma, Q., Tanasa, B., Nunez, E., Chen, A. Y., Merkurjev, D., Zhang, J., Ohgi, K., Song, X., Oh, S., Kim, H.-S., Glass, C. K., & Rosenfeld, M. G. (2013). Functional roles of enhancer RNAs for oestrogen-dependent transcriptional activation. Nature, 498(7455), 516–520. https://doi.org/10.1038/nature12210

71. Hah, N., Danko, C. G., Core, L., Waterfall, J. J., Siepel, A., Lis, J. T., & Kraus, W. L. (2011). A rapid, extensive, and transient transcriptional response to estrogen signaling in breast cancer cells. Cell, 145(4), 622–634. https://doi.org/10.1016/j.cell.2011.03.042

72. Liu, Z., Merkurjev, D., Yang, F., Li, W., Oh, S., Friedman, M. J., Song, X., Zhang, F., Ma, Q., Ohgi, K. A., Krones, A., & Rosenfeld, M. G. (2014). Enhancer activation requires trans-recruitment of a mega transcription factor complex. Cell, 159(2), 358–373. https://doi.org/10.1016/j.cell.2014.08.027

73. Pnueli, L., Rudnizky, S., Yosefzon, Y. & Melamed, P. RNA transcribed from a distal enhancer is required for activating the chromatin at the promoter of the gonadotropin α-subunit gene. *Proceedings of the National Academy of Sciences* **112**, 4369-4374, doi:10.1073/pnas.1414841112 (2015).

74. Kim, T.-K., Hemberg, M., Gray, J. M., Costa, A. M., Bear, D. M., Wu, J., Harmin, D. A., Laptewicz, M., Barbara-Haley, K., Kuersten, S., Markenscoff-Papadimitriou, E., Kuhl, D., Bito, H., Worley, P. F., Kreiman, G., & Greenberg, M. E. (2010). Widespread transcription at neuronal activity-regulated enhancers. Nature, 465(7295), 182–187. https://doi.org/10.1038/nature09033

75. Li, W., Notani, D. & Rosenfeld, M. G. Enhancers as non-coding RNA transcription units: recent insights and future perspectives. *Nat Rev Genet* **17**, 207-223, doi:10.1038/nrg.2016.4 (2016).

76. Dyson, H. J. & Wright, P. E. Intrinsically unstructured proteins and their functions. *Nature Reviews Molecular Cell Biology* **6**, 197, doi:10.1038/nrm1589 (2005).

77. Tantos, A., Han, K. H. & Tompa, P. Intrinsic disorder in cell signaling and gene transcription. *Mol Cell Endocrinol* **348**, 457-465, doi:10.1016/j.mce.2011.07.015 (2012).

78. Li, W., Hu, Y., Oh, S., Ma, Q., Merkurjev, D., Song, X., Zhou, X., Liu, Z., Tanasa, B., He, X., Chen, A. Y., Ohgi, K., Zhang, J., Liu, W., & Rosenfeld, M. G. (2015). Condensin i and ii complexes license full estrogen receptor α-dependent enhancer activation. Molecular Cell, 59(2), 188–202. https://doi.org/10.1016/j.molcel.2015.06.002

79. Bojcsuk, D., Nagy, G. & Balint, B. L. Inducible super-enhancers are organized based on canonical signal-specific transcription factor binding elements. *Nucleic Acids Res*, doi:10.1093/nar/gkw1283 (2016).

80. Kato, M., Han, T. W., Xie, S., Shi, K., Du, X., Wu, L. C., Mirzaei, H., Goldsmith, E. J., Longgood, J., Pei, J., Grishin, N. V., Frantz, D. E., Schneider, J. W., Chen, S., Li, L., Sawaya, M. R., Eisenberg, D., Tycko, R., & McKnight, S. L. (2012). Cell-free formation of rna granules: Low complexity sequence domains form dynamic fibers within hydrogels. Cell, 149(4), 753–767. https://doi.org/10.1016/j.cell.2012.04.017

81. Mitrea, D. M., Chandra, B., Ferrolino, M. C., Gibbs, E. B., Tolbert, M., White, M. R., & Kriwacki, R. W. (2018). Methods for physical characterization of phase-

separated bodies and membrane-less organelles. Journal of Molecular Biology, 430(23), 4773–4805. https://doi.org/10.1016/j.jmb.2018.07.006

82. Banerjee, P. R., Milin, A. N., Moosa, M. M., Onuchic, P. L. & Deniz, A. A. Reentrant Phase Transition Drives Dynamic Substructure Formation in Ribonucleoprotein Droplets. *Angew Chem Int Ed Engl* **56**, 11354-11359, doi:10.1002/anie.201703191 (2017).

83. Elbaum-Garfinkle, S., Kim, Y., Szczepaniak, K., Chen, C. C.-H., Eckmann, C. R., Myong, S., & Brangwynne, C. P. (2015). The disordered P granule protein LAF-1 drives phase separation into droplets with tunable viscosity and dynamics. Proceedings of the National Academy of Sciences, 112(23), 7189–7194. https://doi.org/10.1073/pnas.1504822112

84. Wang, J., Choi, J.-M., Holehouse, A. S., Lee, H. O., Zhang, X., Jahnel, M., Maharana, S., Lemaitre, R., Pozniakovsky, A., Drechsel, D., Poser, I., Pappu, R. V., Alberti, S., & Hyman, A. A. (2018). A molecular grammar governing the driving forces for phase separation of prion-like rna binding proteins. Cell, 174(3), 688-699.e16. https://doi.org/10.1016/j.cell.2018.06.006

85. Shin, Y., Berry, J., Pannucci, N., Haataja, M. P., Toettcher, J. E., & Brangwynne, C. P. (2017). Spatiotemporal control of intracellular phase transitions using light-activated optodroplets. Cell, 168(1–2), 159-171.e14. https://doi.org/10.1016/j.cell.2016.11.054

86. Nott, T. J., Petsalaki, E., Farber, P., Jervis, D., Fussner, E., Plochowietz, A., Craggs, T. D., Bazett-Jones, D. P., Pawson, T., Forman-Kay, J. D., & Baldwin, A. J. (2015). Phase transition of a disordered nuage protein generates environmentally responsive membraneless organelles. Molecular Cell, 57(5), 936–947. https://doi.org/10.1016/j.molcel.2015.01.013

87. Lin, Y., Mori, E., Kato, M., Xiang, S., Wu, L., Kwon, I., & McKnight, S. L. (2016). Toxic pr poly-dipeptides encoded by the c9orf72 repeat expansion target lc domain polymers. Cell, 167(3), 789-802.e12. https://doi.org/10.1016/j.cell.2016.10.003

88. Kato, M. & McKnight, S. L. A Solid-State Conceptualization of Information Transfer from Gene to Message to Protein. *Annu Rev Biochem*, doi:10.1146/annurev-biochem-061516-044700 (2017).

89. Franco, H. L., Nagari, A. & Kraus, W. L. TNFalpha signaling exposes latent estrogen receptor binding sites to alter the breast cancer cell transcriptome. *Mol Cell* **58**, 21-34, doi:10.1016/j.molcel.2015.02.001 (2015).

90. Kaikkonen, M. U., Spann, N. J., Heinz, S., Romanoski, C. E., Allison, K. A., Stender, J. D., Chun, H. B., Tough, D. F., Prinjha, R. K., Benner, C., & Glass, C. K. (2013). Remodeling of the enhancer landscape during macrophage activation is coupled to enhancer transcription. Molecular Cell, 51(3), 310–325. https://doi.org/10.1016/j.molcel.2013.07.010

91. Brangwynne, C. P., Mitchison, T. J. & Hyman, A. A. Active liquid-like behavior of nucleoli determines their size and shape in Xenopus laevis oocytes. *Proc Natl Acad Sci U S A* **108**, 4334-4339, doi:10.1073/pnas.1017150108 (2011).

92. Shin, Y., Chang, Y.-C., Lee, D. S. W., Berry, J., Sanders, D. W., Ronceray, P., Wingreen, N. S., Haataja, M., & Brangwynne, C. P. (2018). Liquid nuclear condensates mechanically sense and restructure the genome. Cell, 175(6), 1481-1491.e13. https://doi.org/10.1016/j.cell.2018.10.057

93. Brown, J. M., Green, J., das Neves, R. P., Wallace, H. A. C., Smith, A. J. H., Hughes, J., Gray, N., Taylor, S., Wood, W. G., Higgs, D. R., Iborra, F. J., & Buckle, V. J. (2008). Association between active genes occurs at nuclear speckles and is modulated by chromatin environment. Journal of Cell Biology, 182(6), 1083–1097. https://doi.org/10.1083/jcb.200803174

94. Shopland, L. S., Johnson, C. V., Byron, M., McNeil, J. & Lawrence, J. B. Clustering of multiple specific genes and gene-rich R-bands around SC-35 domains: evidence for local euchromatic neighborhoods. *J Cell Biol* **162**, 981-990, doi:10.1083/jcb.200303131 (2003).

95. Skowronska-Krawczyk, D., Ma, Q., Schwartz, M., Scully, K., Li, W., Liu, Z., Taylor, H., Tollkuhn, J., Ohgi, K. A., Notani, D., Kohwi, Y., Kohwi-Shigematsu, T., & Rosenfeld, M. G. (2014). Required enhancer–matrin-3 network interactions for a homeodomain transcription program. Nature, 514(7521), 257–261. https://doi.org/10.1038/nature13573

96. Quinodoz, S. A., Ollikainen, N., Tabak, B., Palla, A., Schmidt, J. M., Detmar, E., Lai, M. M., Shishkin, A. A., Bhat, P., Takei, Y., Trinh, V., Aznauryan, E., Russell, P., Cheng, C., Jovanovic, M., Chow, A., Cai, L., McDonel, P., Garber, M., & Guttman, M. (2018). Higher-order inter-chromosomal hubs shape 3d genome organization in the nucleus. Cell, 174(3), 744-757.e24. https://doi.org/10.1016/j.cell.2018.05.024

97. Marzahn, M. R., Marada, S., Lee, J., Nourse, A., Kenrick, S., Zhao, H., Ben-Nissan, G., Kolaitis, R., Peters, J. L., Pounds, S., Errington, W. J., Privé, G. G., Taylor, J. P., Sharon, M., Schuck, P., Ogden, S. K., & Mittag, T. (2016). Higher-order oligomerization promotes localization of SPOP to liquid nuclear speckles. The EMBO Journal, 35(12), 1254–1275. https://doi.org/10.15252/embj.201593169

98. Mitrea, D. M. & Kriwacki, R. W. Phase separation in biology; functional organization of a higher order. *Cell Commun Signal* **14**, 1, doi:10.1186/s12964-015-0125-7 (2016).

99. Ji, X., Zhou, Y., Pandit, S., Huang, J., Li, H., Lin, C. Y., Xiao, R., Burge, C. B., & Fu, X.-D. (2013). Sr proteins collaborate with 7sk and promoter-associated nascent rna to release paused polymerase. Cell, 153(4), 855–868. https://doi.org/10.1016/j.cell.2013.04.028

100. Pandit, S., Zhou, Y., Shiue, L., Coutinho-Mansfield, G., Li, H., Qiu, J., Huang, J., Yeo, G. W., Ares, M., & Fu, X.-D. (2013). Genome-wide analysis reveals sr protein cooperation and competition in regulated splicing. Molecular Cell, 50(2), 223–235. https://doi.org/10.1016/j.molcel.2013.03.001

101. Lai, F. & Shiekhattar, R. Enhancer RNAs: the new molecules of transcription. *Curr Opin Genet Dev* **25**, 38-42, doi:10.1016/j.gde.2013.11.017 (2014).

102. Hah, N., Murakami, S., Nagari, A., Danko, C. G. & Kraus, W. L. Enhancer transcripts mark active estrogen receptor binding sites. *Genome Res* **23**, 1210-1223, doi:10.1101/gr.152306.112 (2013).

103. Mittag, T. & Parker, R. Multiple Modes of Protein-Protein Interactions Promote RNP Granule Assembly. *J Mol Biol*, doi:10.1016/j.jmb.2018.08.005 (2018).

104. Keenholtz, R. A., Dhanaraman, T., Palou, R., Yu, J., D'Amours, D., & Marko, J. F. (2017). Oligomerization and ATP stimulate condensin-mediated DNA compaction. Scientific Reports, 7(1), 14279. https://doi.org/10.1038/s41598-017-14701-5

105. Hirano, T. Capturing condensin in chromosomes. *Nat Genet* **49**, 1419-1420, doi:10.1038/ng.3962 (2017).

106. D'Ambrosio, C., Schmidt, C. K., Katou, Y., Kelly, G., Itoh, T., Shirahige, K., & Uhlmann, F. (2008). Identification of cis-acting sites for condensin loading onto

budding yeast chromosomes. Genes & Development, 22(16), 2215–2227. https://doi.org/10.1101/gad.1675708

107. Haeusler, R. A., Pratt-Hyatt, M., Good, P. D., Gipson, T. A. & Engelke, D. R. Clustering of yeast tRNA genes is mediated by specific association of condensin with tRNA gene transcription complexes. *Genes Dev* **22**, 2204-2214, doi:10.1101/gad.1675908 (2008).

108. Wood, A. J., Severson, A. F. & Meyer, B. J. Condensin and cohesin complexity: the expanding repertoire of functions. *Nat Rev Genet* **11**, 391-404, doi:10.1038/nrg2794 (2010).

109. Crane, E., Bian, Q., McCord, R. P., Lajoie, B. R., Wheeler, B. S., Ralston, E. J., Uzawa, S., Dekker, J., & Meyer, B. J. (2015). Condensin-driven remodelling of X chromosome topology during dosage compensation. Nature, 523(7559), 240–244. https://doi.org/10.1038/nature14450

110. Lin, Y., Protter, D. S., Rosen, M. K. & Parker, R. Formation and Maturation of Phase-Separated Liquid Droplets by RNA-Binding Proteins. *Mol Cell* **60**, 208-219, doi:10.1016/j.molcel.2015.08.018 (2015).

111. Patel, A., Lee, H. O., Jawerth, L., Maharana, S., Jahnel, M., Hein, M. Y., Stoynov, S., Mahamid, J., Saha, S., Franzmann, T. M., Pozniakovski, A., Poser, I., Maghelli, N., Royer, L. A., Weigert, M., Myers, E. W., Grill, S., Drechsel, D., Hyman, A. A., & Alberti, S. (2015). A liquid-to-solid phase transition of the als protein fus accelerated by disease mutation. Cell, 162(5), 1066–1077. https://doi.org/10.1016/j.cell.2015.07.047

112. Molliex, A., Temirov, J., Lee, J., Coughlin, M., Kanagaraj, A. P., Kim, H. J., Mittag, T., & Taylor, J. P. (2015). Phase separation by low complexity domains promotes stress granule assembly and drives pathological fibrillization. Cell, 163(1), 123–133. https://doi.org/10.1016/j.cell.2015.09.015